

Synthesis, Characterisation and Biological Evaluation of Novel *N*-Ferrocenyl
Naphthoyl Amino Acid and Dipeptide Derivatives as Potential Anti-Cancer
Agents

by

Áine Mooney B. A. (Mod.)

A thesis presented for the degree of Doctor of Philosophy

at

Dublin City University

Under the supervision of Dr. Peter T. M. Kenny



OllScoil Chathair Bhaile Átha Cliath

School of Chemical Sciences

September 2010

Dedicated to Mum, Dad and Claire

I hereby certify that this material, which I now submit for assessment on the programme of study leading to the award of Ph.D. is entirely my own work, that I have exercised reasonable care to ensure that the work is original, and does not to the best of my knowledge breach any law of copyright, and has not been taken from the work of others save and to the extent that such work has been cited and acknowledged within the text of my work.

Signed: _____

Áine Mooney

ID No. _____

Date: _____

Acknowledgements

First and foremost, I would like to extend my deepest thanks to Dr. Peter T. M. Kenny for giving me the opportunity to conduct research under his supervision, and for his constant support, encouragement and enthusiasm throughout the past couple of years.

I would also like to express my gratitude to:

The Irish Research Council for Science, Engineering and Technology (IRCSET), who generously provided the funding that allowed me to conduct my research, in the form of a scholarship under the Embark Initiative.

Dr. Norma O'Donovan and Dermot O'Sullivan in the National Institute of Cellular Biotechnology (NICB) for their invaluable assistance with the *in vitro* biological screening.

Dr. Thamir Maghoub in the NICB for conducting the biological studies in the melanoma cell line, and for all of his advice and assistance with the cell cycle analysis.

Dr. Dilip K. Rai in Teagasc, for obtaining the tandem MS spectra.

Prof. Sylvia Draper in Trinity College Dublin for obtaining the X-ray crystallographic data.

Dr. John O'Brien in Trinity College Dublin for his assistance in obtaining and interpreting the NMR spectra of the *N*-methylated derivatives.

Dr. Mary Pryce of the School of Chemical Sciences for the use of her potentiostat and PC; Emma Harvey for her assistance in performing the cyclic voltammetry experiments, and Dr. Yvonne Halpin for her advice in relation to the setup of these experiments.

The entire technical staff of the School of Chemical Sciences and the NICB, especially, Damien McGuirk, John McLoughlin, Ambrose May, Veronica Dobbin, Vinny Hooper, Mary Ross, Catherine Keogh and Mick Henry.

A special thanks goes to my PKRG (Peter Kenny Research Group) colleagues, Alok, Will, Andy, Rachel and especially Alan, Brian Moran and Paula.

On a personal note, I want to say a big thank you to all of the many postgraduates in the School of Chemical Sciences, especially Debbie (my peptide buddy), Saibhy, Dan, Shelly, Sonia, Sharon, Mags, Brian Deegan, Ewa, Neil, Tom, and Emma; thank you so much for welcoming me to DCU and for your friendship over the past couple of years, I will always remember and cherish the good times we've had together...here's to many more!!! Thanks also to the gang in the NICB; Thamir and everyone who worked in G117 through the years, especially Dermot, Laura, Naomi, Sandra, Gráinne, and Fiona.

An important thank you goes to Brian Murphy, I know I haven't been much fun recently, so thank you for sticking by me, and more importantly, thanks for all the hugs, chocolate, cups of tea, baileys coffees, and glasses of wine!! I also want to thank my friends, especially Gemma, Leanne, Niamh, and Elizabeth, who have put up with my absences the last couple of years, but who were always happy to be called on when a de-stressing night off was needed. Thank you!

A huge thank you also goes to Claire, the best sister a girl could ever ask for, and Ronan, my sort-of brother-in-law, thanks for always being there for me. And last, but most importantly not least, a huge thank you to my parents, Maria and Tony, for their constant and unending support and belief in me - I hope I've made you proud.

Abstract

The aim of this research thesis was to explore the structure-activity relationship (SAR) of ferrocenyl-peptide bioconjugates, a novel class of potential anti-cancer agents. A series of *N*-(ferrocenyl)naphthoyl amino acid and dipeptide derivatives were synthesised by coupling 3-ferrocenylnaphthalene-2-carboxylic acid and 6-ferrocenylnaphthalene-2-carboxylic acid to α -amino acid ethyl esters and dipeptide ethyl esters in the presence of *N*-(3-dimethylaminopropyl)-*N'*-ethylcarbodiimide hydrochloride (EDC) and 1-hydroxybenzotriazole (HOBt). The compounds were fully characterised by a wide range of spectroscopic techniques, including ^1H and ^{13}C NMR, IR, UV-Vis, MS and CV. X-ray crystallographic studies of intermediate compounds were also performed.

Biological evaluation of the *N*-(ferrocenyl)naphthoyl amino acid and dipeptide derivatives was performed *in vitro*. These novel derivatives exhibited a strong anti-proliferative effect in the H1299 non-small cell lung cancer cell line, whilst the Sk-Mel-28 melanoma cell line was slightly more resistant to these compounds. *N*-(6-ferrocenyl-2-naphthoyl)-glycine-L-alanine ethyl ester and *N*-(6-ferrocenyl-2-naphthoyl)-glycine-glycine ethyl ester were identified as the most potent compounds. In particular, a remarkable inhibitory effect on H1299 cell proliferation was observed for *N*-(6-ferrocenyl-2-naphthoyl)-glycine-glycine ethyl ester ($\text{IC}_{50} = 0.13 \pm 0.02 \mu\text{M}$).

Based on these findings, a secondary SAR study was undertaken. The focus of this study was directed to the peptide chain, whereby isosteric replacements were employed to generate an additional series of *N*-(ferrocenyl)naphthoyl dipeptide derivatives. In addition, *N*-naphthoyl analogues of the two most potent compounds and a homologous series of *N*-(ferrocenyl)naphthoyl amino acid derivatives were prepared. The compounds were fully characterised and biological evaluation identified three more compounds that displayed a potent anti-proliferative effect in both cell lines: *N*-(6-ferrocenyl-2-naphthoyl)-sarcosine-glycine ethyl ester, *N*-(6-ferrocenyl-2-naphthoyl)-glycine-D-alanine ethyl ester and *N*-(6-ferrocenyl-2-naphthoyl)- γ -aminobutyric acid ethyl ester. The *N*-naphthoyl analogues were shown to be inactive.

In total, the five most active compounds have an equivalent or more potent anti-proliferative effect in the H1299 cell line than cisplatin. Furthermore, four of these compounds possess IC₅₀ values that lie in the nanomolar range. In the Sk-Mel-28 cell line, significant IC₅₀ values ranging from 1.06 ± 0.05 to 3.74 ± 0.37 μM were determined for the five compounds. Cell cycle analysis in the H1299 cell line has shown *N*-(6-ferrocenyl-2-naphthoyl)-glycine-glycine ethyl ester and *N*-(6-ferrocenyl-2-naphthoyl)-sarcosine-glycine ethyl ester to cause a significant increase in the sub-G0/G1 peak, which is suggestive of apoptosis.

Table of Contents

Title page.....	i
Declaration.....	iii
Acknowledgements.....	iv
Abstract	vi
Table of Contents.....	viii
Chapter 1	1
Cancer, chemotherapy and bioorganometallic anti-cancer agents	1
1.1. Cancer and cancer chemotherapy	1
1.1.1. Introduction.....	1
1.1.2. Lung cancer.....	3
1.1.3. Melanoma	4
1.1.4. Cancer chemotherapy	4
1.1.4.1. Platinum agents	6
1.1.4.2. Alkylating agents.....	7
1.1.4.3. Anti-microtubule agents.....	8
1.1.4.4. Anti-metabolites	9
1.1.4.5. DNA topoisomerase inhibitors.....	10
1.2. Bioorganometallic anti-cancer agents	10
1.2.1. Introduction.....	10
1.2.2. Ferricenium salts	12
1.2.3. Metallocene-based selective estrogen receptor modulators (SERMs) and anti-androgens.....	15
1.2.4. Ferrocenyl-peptide conjugates	30
1.2.5. Other metallocene complexes as anti-cancer agents	35
1.3. Conclusions	40
References	41
Chapter 2.....	45
Synthesis and structural characterisation of <i>N</i> -(ferrocenyl)naphthoyl amino acid and dipeptide derivatives which contain α -amino acids.....	45

2.1. Introduction	45
2.2. The synthesis of <i>N</i> -(ferrocenyl)naphthoyl amino acid and dipeptide derivatives which contain α -amino acids	49
2.2.1. The preparation of methyl ferrocenylnaphthalene-2-carboxylate.....	51
2.2.2. The preparation of ferrocenylnaphthalene-2-carboxylic acid.....	53
2.2.3. Amino acids	53
2.2.4. Carboxyl protecting groups	53
2.3. Amide Bond Formation.....	54
2.3.1. Acyl chlorides	55
2.3.2. Anhydrides	55
2.3.3. Phosphonium Reagents.....	57
2.3.4. Carbodiimides	58
2.4. Purification and yields of <i>N</i> -(ferrocenyl)naphthoyl amino acid and dipeptide derivatives	61
2.5. ¹ H NMR studies of <i>N</i> -(ferrocenyl)naphthoyl amino acid and dipeptide derivatives	63
2.5.1. ¹ H NMR study of <i>N</i> -(3-ferrocenyl-2-naphthoyl)-glycine-L-alanine ethyl ester (85)	66
2.5.2. ¹ H NMR study of <i>N</i> -(6-ferrocenyl-2-naphthoyl)-glycine-L-alanine ethyl ester (51)	67
2.6. ¹³ C and DEPT 135 NMR studies of <i>N</i> -(ferrocenyl)naphthoyl amino acid and dipeptide derivatives	69
2.6.1. ¹³ C and DEPT 135 NMR study of <i>N</i> -(6-ferrocenyl-2-naphthoyl)-glycine-L-leucine ethyl ester (97)	70
2.7. HMQC study of <i>N</i> -(6-ferrocenyl-2-naphthoyl)-L-alanine-glycine ethyl ester (99)	72
2.8. Infra red studies of <i>N</i> -(ferrocenyl)naphthoyl amino acid and dipeptide derivatives	75
2.9. UV-Vis studies of <i>N</i> -(ferrocenyl)naphthoyl amino acid and dipeptide derivatives	77
2.10. Cyclic voltammetry studies of <i>N</i> -(ferrocenyl)naphthoyl amino acid and dipeptide derivatives	79
2.11. Mass spectrometric studies of <i>N</i> -(ferrocenyl)naphthoyl amino acid and dipeptide derivatives	82

2.11.1. Tandem Mass Spectrometry (MS/MS).....	83
2.12. X-ray crystallography study of methyl ferrocenylnaphthalene-2-carboxylate.....	85
2.13. Conclusions	90
Experimental Procedures	92
References	121
Chapter 3.....	123
Biological Evaluation of <i>N</i> -(ferrocenyl)naphthoyl amino acid and dipeptide derivatives which contain α -amino acids.....	123
3.1. Introduction	123
3.1.1. Miniaturised <i>in vitro</i> methods.....	123
3.1.1.1. MTT assay.....	124
3.1.1.2. Neutral red assay	125
3.1.1.3. Protein staining assays	125
3.1.1.4. Acid phosphatase assay.....	126
3.2. Preliminary <i>in vitro</i> study of selected <i>N</i> -(ferrocenyl)naphthoyl dipeptide derivatives	127
3.3. <i>In vitro</i> evaluation in the H1299 cell line and the Sk-Mel-28 cell line.....	129
3.3.1. Methyl ferrocenylnaphthalene-2-carboxylate.....	131
3.3.2. <i>N</i> -(ferrocenyl)naphthoyl amino acid derivatives	131
3.3.3. <i>N</i> -(ferrocenyl)naphthoyl dipeptide derivatives	133
3.3.4. IC ₅₀ value determination.....	135
3.4. Structure-activity relationship of <i>N</i> -(ferrocenyl)naphthoyl amino acid and dipeptide derivatives	137
3.5. Conclusions	139
Materials and Methods.....	141
References	144
Chapter 4.....	145
Synthesis and structural characterisation of <i>N</i> -naphthoyl dipeptide derivatives and <i>N</i> - (ferrocenyl)naphthoyl amino acid and dipeptide derivatives which contain unusual amino acids	145
4.1. Introduction	145

4.2. Protection of the amino terminus of an amino acid	147
4.2.1. <i>t</i> -Butoxycarbonyl (Boc) protecting group	148
4.3. The synthesis of <i>N</i> -naphthoyl dipeptide derivatives and <i>N</i> -(ferrocenyl)naphthoyl amino acid and dipeptide derivatives which contain unusual amino acids	149
4.3.1. <i>N</i> -(ferrocenyl)naphthoyl dipeptide derivatives	149
4.3.2. <i>N</i> -naphthoyl dipeptide derivatives and <i>N</i> -(ferrocenyl)naphthoyl amino acid derivatives.....	151
4.4. ¹ H and ¹³ C NMR studies of <i>N</i> -(ferrocenyl)naphthoyl dipeptide derivatives which contain <i>N</i> -methyl amino acids	153
4.4.1. ¹ H NMR studies of <i>N</i> -(ferrocenyl)naphthoyl dipeptide derivatives which contain <i>N</i> -methyl amino acids	154
4.4.2. ¹³ C NMR and DEPT 135 studies of <i>N</i> -(ferrocenyl)naphthoyl dipeptide derivatives which contain <i>N</i> -methyl amino acids.....	156
4.4.3. ¹ H and ¹³ C NMR study of <i>N</i> -(3-ferrocenyl-2-naphthoyl)-sarcosine-glycine ethyl ester (116).....	157
4.4.4. Variable temperature ¹ H NMR study of <i>N</i> -(3-ferrocenyl-2-naphthoyl)-sarcosine-sarcosine ethyl ester (117).....	161
4.5. ¹ H NMR studies of <i>N</i> -naphthoyl dipeptide derivatives and <i>N</i> -(ferrocenyl)naphthoyl amino acid and dipeptide derivatives.....	164
4.5.1. ¹ H NMR study of <i>N</i> -(3-ferrocenyl-2-naphthoyl)- γ -aminobutyric acid ethyl ester (136).....	166
4.6. ¹³ C NMR and DEPT 135 studies of <i>N</i> -naphthoyl dipeptide derivatives and <i>N</i> -(ferrocenyl)naphthoyl amino acid and dipeptide derivatives	167
4.6.1. ¹³ C and DEPT 135 NMR study of <i>N</i> -(6-ferrocenyl-2-naphthoyl)- δ -amino-n-valeric acid ethyl ester (140).....	169
4.7. COSY study of <i>N</i> -(6-ferrocenyl-2-naphthoyl)-glycine- γ -aminobutyric acid ethyl ester (131).....	171
4.8. Infra red studies of <i>N</i> -naphthoyl dipeptide derivatives and <i>N</i> -(ferrocenyl)naphthoyl amino acid and dipeptide derivatives.....	173
4.9. UV-Vis studies of <i>N</i> -(ferrocenyl)naphthoyl amino acid and dipeptide derivatives	174

4.10. Cyclic voltammetry studies of <i>N</i> -(ferrocenyl)naphthoyl amino acid and dipeptide derivatives	175
4.11. Conclusions	176
Experimental Procedures	178
References	211
Chapter 5	212
Biological Evaluation of <i>N</i> -naphthoyl dipeptide derivatives and <i>N</i> -(ferrocenyl)naphthoyl amino acid and dipeptide derivatives which contain unusual amino acids.....	212
5.1. <i>In vitro</i> evaluation in the H1299 cell line and the Sk-Mel-28 cell line.....	212
5.1.1. <i>N</i> -(ferrocenyl)naphthoyl dipeptide derivatives	212
5.1.2. <i>N</i> -naphthoyl dipeptide derivatives	216
5.1.3. <i>N</i> -(ferrocenyl)naphthoyl amino acid derivatives	217
5.1.4. IC ₅₀ value determination.....	218
5.2. Structure-activity relationship of <i>N</i> -(ferrocenyl)naphthoyl amino acid and dipeptide derivatives	219
5.3. Cell cycle analysis of <i>N</i> -(6-ferrocenyl-2-naphthoyl)-glycine-glycine ethyl ester (96) and <i>N</i> -(6-ferrocenyl-2-naphthoyl)-sarcosine-glycine ethyl ester (120)	221
5.4. Conclusions	227
Materials and Methods.....	229
References	230
Appendix I-Abbreviations and Units	231
Appendix II-Publications	243

Chapter 1

Cancer, chemotherapy and bioorganometallic anti-cancer agents

1.1. Cancer and cancer chemotherapy

1.1.1. Introduction

The term “cancer” is used to describe a disease distinguishable by the abnormal growth of cells which ultimately evolves into a population of cells that can invade tissues and spread to other parts of the body. It is a Latin term, literally translated from the Greek “Karkinos” meaning crab, which refers to the metaphorical claws reaching out to invade surrounding tissues. At a molecular level, cancer cells are characterised by numerous alterations in multiple gene expression which leads to deviation from the normal program for cell division and cell differentiation.¹ The growth of the tumour cell population is promoted by an imbalance between cell replication and cell death. Over time, this aberrant growth of cancer cells progresses to form a malignant tumour capable of invading locally, spreading to regional lymph nodes and metastasising to distant organs within the body. Thus, if cancer cell growth is allowed to continue unchecked over a prolonged period, this disease can prove to be life threatening and even fatal to the patient.

Cancers arise from a single cell which undergoes mutation; consequently, cancer may develop in any region within the body. In terms of nomenclature, it is common practice to name cancers according to the location of the tumour growth and the type of cell from which they were originally derived *e.g.* lung carcinoma. Carcinoma refers to cancers that begin in the skin or in tissues that line or cover internal organs. Similarly, cancers that originate in bone, cartilage, fat, muscle, blood vessels or other connective tissues are sarcomas. Lymphoma and multiple myeloma arise from cells of the immune system. Lastly, leukaemia develops from blood-forming tissue such as the bone marrow, causing large numbers of abnormal blood cells to be produced and enter the blood.

Cancer is a major cause of death and disease worldwide. It is estimated that in 2002 alone, there were 10.9 million new cases of cancer and 6.7 million deaths from cancer.² In Ireland there were over 21,000 new cases of cancer reported each year up to 2004 and over 11,261

cancer deaths annually.³ Although incidence rates have increased between 1994 and 2004, cancer death rates have fallen during this period, indicating an improvement in cancer survival either through early detection, improved treatment or both. Cancer is more common with increasing age; half of the patients diagnosed in Ireland between 2000 and 2004 were over 68 years of age.³ Given the fact that more and more people are living beyond 65 years, the number of cancer cases is sure to continue to rise.

The possibility of developing cancer is dependent on a number of risk factors which can vary according to the tumour location *e.g.* there is an increased risk of developing melanoma following over-exposure to ultraviolet (UV) radiation. Tobacco is the greatest risk factor in the development of many cancers (lung, larynx, oesophagus, stomach, pancreas, kidney, liver and bladder). Other factors include genetic predisposition, lack of balanced diet and physical activity, obesity, alcohol consumption, exposure to certain chemicals and gases (asbestos, benzene and radon gas), exposure to ultraviolet or ionising radiation, infections such as the human papillomavirus (HPV) and treatments such as exposure to estrogen through Hormone Replacement Therapy (HRT).⁴

In Ireland, the most common forms of cancer in males are cancers of the prostate, colon, lung and lymphoma whereas among women cancers of the breast, colon, lung and ovaries are the most common.³ Five-year survival rates can be used to gain a more accurate picture of the most lethal forms of cancer that affect the Irish population. Survival rates are primarily dependent on the location of the tumour, since this influences the ease with which the tumour can be detected, which in turn aids detection and treatment at an early stage. As a consequence, survival rates for the many distinct forms of cancer show a large variation. Perhaps the most striking example is the survival rate for males diagnosed with pancreatic cancer (5.4%) compared to that observed for males diagnosed with testicular cancer (96.9%).³ Lung cancer and advanced metastatic melanoma are two forms of cancer for which survival rates remain critically low. Consequently, the research within this project is focussed on the synthesis of *N*-(ferrocenyl)naphthoyl amino acid and dipeptide derivatives and their biological evaluation as potential chemotherapeutic agents for the treatment of lung cancer and advanced melanoma.

1.1.2. Lung cancer

Lung cancer is a devastating disease and has been the most common cancer in the world since 1985. Approximately 1.35 million new cases of lung cancer (12.4% of total cancers) occur worldwide every year.² Lung cancer is the leading cause of cancer mortality both worldwide and in Europe.⁵ In Ireland, lung cancer is the 3rd most common cancer in men and women, is responsible for 20.8% of all cancer-related deaths and has a five-year relative survival of only 10.4% for patients diagnosed between 2000 and 2004.⁴ Such low survival rates can be attributed to poor detection at the early stage of the disease, which severely hinders treatment. In 2001, 47.6% of Irish patients diagnosed with lung cancer, presented at an advanced stage (III/IV) and almost the same percentage of patients (46.3%) only received palliative treatment.⁴

Cigarette smoke is the primary environmental cause of lung cancer and is responsible for 85% of all cases in men and 47% of all cases in women worldwide. However, in Europe and North America this figure rises to as high as 90-95% and 74-85% of all cases in men and women, respectively.² Other causes include exposure to chemicals such as asbestos as well as the naturally occurring radioactive gas, radon.

Lung cancer is divided into two major types based on histological appearance: small cell lung cancer (SCLC) and non-small cell lung cancer (NSCLC). Approximately 20% of all lung cancers are SCLC, which is a very aggressive form of cancer due to early metastasis (both local and distant).⁶ Chemotherapy is the most common treatment for SCLC because of early metastatic spread. However, even with treatment, long-term survival remains poor. The remaining 80% of all lung cancers are NSCLC, comprising adenocarcinomas, squamous cell and large cell carcinomas.⁷ Surgery is generally regarded as the best treatment option for NSCLC. However, 75% of NSCLC tumours are inoperable at the time of diagnosis.⁷ A further 20% of patients with locally advanced disease receive radiotherapy. In these cases, chemotherapy following standard treatment has been shown to help patients live longer.⁸

1.1.3. Melanoma

Worldwide, malignant melanoma of the skin accounts for 160,000 new cases annually, with slightly more cases occurring in women than in men.² Over the past two decades, European National Cancer Registries show a rising incidence of melanoma.⁹ In Ireland, the number of melanoma cases rose by approximately 50% between 1994 and 2004, making this the fastest rising preventable cancer.³ Relative survival figures from malignant melanoma are relatively high, with 86.3% of patients surviving five years.⁴ This is primarily due to increased awareness and detection at an early stage, which is crucial for surgical resection of the tumour.

The principal risk factor associated with melanoma is exposure to UV radiation from sunshine or UV-emitting tanning devices. The level of risk of developing melanoma through over-exposure to UV radiation depends upon skin type; those with fairer skin that sunburns easily are more at risk.⁴ Recently, UV-emitting tanning devices have been classified as “carcinogenic to humans” following studies that showed the risk of developing melanoma increases by 75% when the use of tanning devices starts before 30 years of age.¹⁰

Malignant melanoma has the potential to metastasise to any organ within the body, and common sites of dissemination include the skin, lymph nodes, liver, bone, lungs and brain.¹¹ Patients with advanced disease such as those with distant metastasis have a poor prognosis, with a one-year survival rate of less than 5%. Advanced metastatic melanoma is almost uniformly fatal, with the median survival standing at only nine months. This poor prognosis is due, at least in part, to the fact that metastatic melanoma is notoriously resistant to all current forms of treatment.

1.1.4. Cancer chemotherapy

Chemotherapy is the most effective treatment for metastatic tumours. It is the treatment of choice for patients who have cancers that do not respond to surgery or radiation. Chemotherapy impedes the growth and spread of the tumour by utilising drugs that are capable of killing cancer cells. Most conventional chemotherapeutic drugs are cytotoxic

agents; they elicit cancer cell death by interfering with the cell replication process. This can be accomplished by disrupting the function of DNA, either by acting directly on DNA or by inhibiting the enzymes involved in DNA synthesis *e.g.* topoisomerase II.¹² Alternatively, drugs may act by interfering with the mechanics of cell division *e.g.* by binding to microtubules.¹³ Cytotoxic agents aim to target cancer cells in a selective manner. Their selectivity is based primarily on the fact that cancer cells divide more rapidly than normal cells. Unfortunately, there are also cells in the bone marrow, digestive tract and hair follicles that divide rapidly under normal circumstances. Most cytotoxic agents also act on these cells and for this reason myelosuppression (decreased production of blood cells), mucositis (inflammation of lining of the digestive tract) and hair loss are all common side effects.

The appearance of cancer cells resistant to a range of cytotoxic drugs is also a serious problem in cancer chemotherapy. Clinical drug resistance represents a major barrier to be overcome before chemotherapy can become curative for patients presenting with metastatic cancer. There are two main types of cancer resistance. Intrinsic drug resistance is present at the time of diagnosis in tumours that fail to respond to first-line chemotherapy. In contrast, acquired drug resistance occurs in tumours that can often be highly responsive to initial treatment, but present with strong resistance to the original treatment upon tumour recurrence.¹² In such cases, the tumour becomes resistant to previously used drugs, as well as new agents that possess both different structures and modes of action. A number of specific resistance mechanisms that occur at a molecular level have been described *in vivo* and *in vitro*. The three main proposed mechanisms include the reduction of intracellular accumulation of anti-cancer drugs by increased drug efflux (MDR), alterations in drug targets (topoisomerase II) or activation of detoxifying systems (glutathione-S-transferases). To this day, traditional cytotoxic drugs form the cornerstone of clinical chemotherapy for lung cancer and melanoma patients. This is despite the inherent problems associated with these agents, including their toxicity, harsh side effects and acquired drug resistance. A brief overview of the main anti-cancer agents employed in the treatment of lung cancer and melanoma follows.

1.1.4.1. Platinum agents

Cisplatin **1** is a very effective, but highly toxic, anti-tumour drug. Its clinical use was initiated in the early 1970s, and it is one of the most widely employed anti-cancer agents, useful in ovarian, testicular, small cell lung and other cancers.¹⁴ It is a square-planar complex containing two relatively inert ammonia molecules and two labile chloride ions coordinated to the central Pt(II) atom in a *cis* configuration. The *in vivo* anti-cancer activity of cisplatin is due to the replacement of the chloride ligands by neutral water ligands to give reactive positively charged species (Figure 1.1).¹² This process is facilitated within the cell by the relatively low cellular concentration of chloride ions.¹⁵ The platinum atom of these positively charged species binds strongly to DNA, forming covalent bonds with the N-7 positions of purine bases to yield 1,2- and 1,3-intrastrand DNA crosslinks.

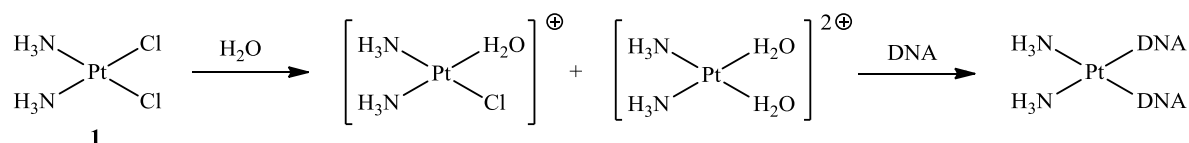
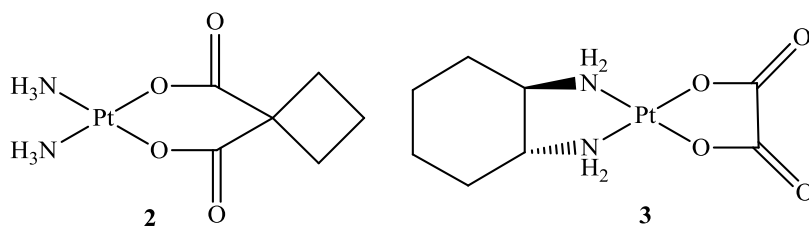


Figure 1.1 Cellular activation of cisplatin ¹².

The 2nd and 3rd generation platinum drugs carboplatin **2** and oxaliplatin **3** were developed in later years to address the severe side effects (nephrotoxicity, neurotoxicity and emetogenesis) associated with cisplatin. These derivatives contain different leaving groups (cyclobutane-1,1-dicarboxylate and oxalate in the cases of **2** and **3**, respectively) in place of the chloride ions which aid solubility, increase stability and reduce toxicity.



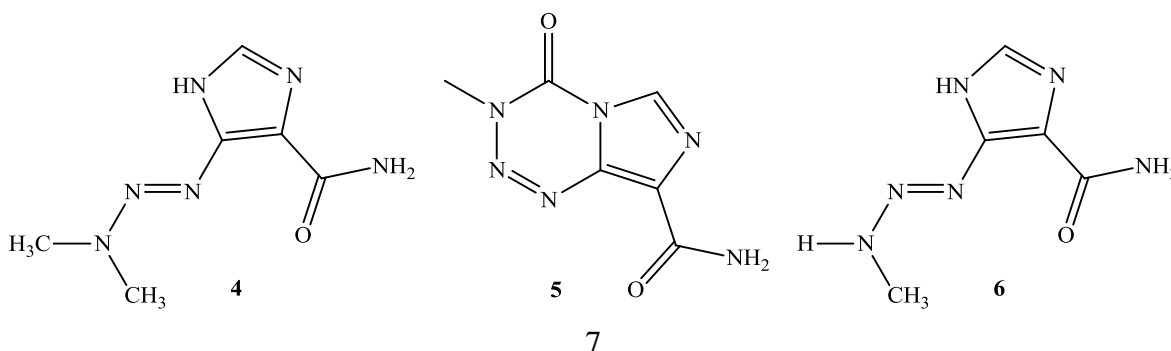
The platinum agents are some of the most frequently employed anti-cancer agents. Chemotherapy with platinum agents is widely used and is regarded as a first line treatment for SCLC, either as a single agent or in combination with etoposide.⁶ The standard therapy for patients with NSCLC is a platinum agent in combination with a second agent, typically

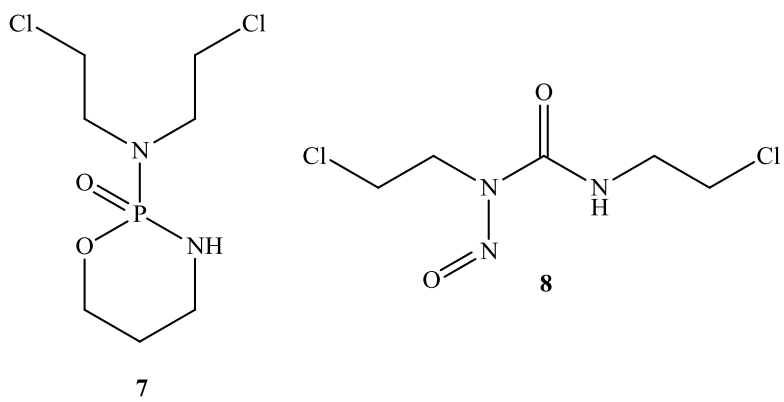
gemcitabine, paclitaxel, vinorelbine, and docetaxel.¹⁶ This is despite the fact that NSCLC is known to be inherently resistant to platinum therapy.¹⁷ Platinum agents are also used as single agents for the chemotherapy of metastatic melanoma, although studies have shown cisplatin to induce only a 15% response rate.¹⁸ Another accepted treatment for melanoma includes a platinum agent in combination with vinblastine **9** and dacarbazine **4**.

1.1.4.2. Alkylating agents

Alkylating agents are highly electrophilic compounds that attach alkyl groups to DNA by reacting at the nucleophilic sites present in the DNA bases. The main nucleophilic sites are the N-1 and N-3 of adenine, N-3 of cytosine and in particular, the N-7 of guanine.¹² Some alkylating agents possess two alkylating groups so that following initial reaction with a DNA base, the remaining alkylating group can react with another base contained either within the same DNA strand or within the complementary DNA strand. Thus, alkylation prevents DNA replication and RNA transcription from the affected DNA. It also leads to the fragmentation of DNA by hydrolytic reactions and by the action of repair enzymes that attempt to remove the modified bases. In addition, alkylation can lead to the mispairing of DNA nucleotides, since the normal hydrogen bonding pattern between bases becomes altered.

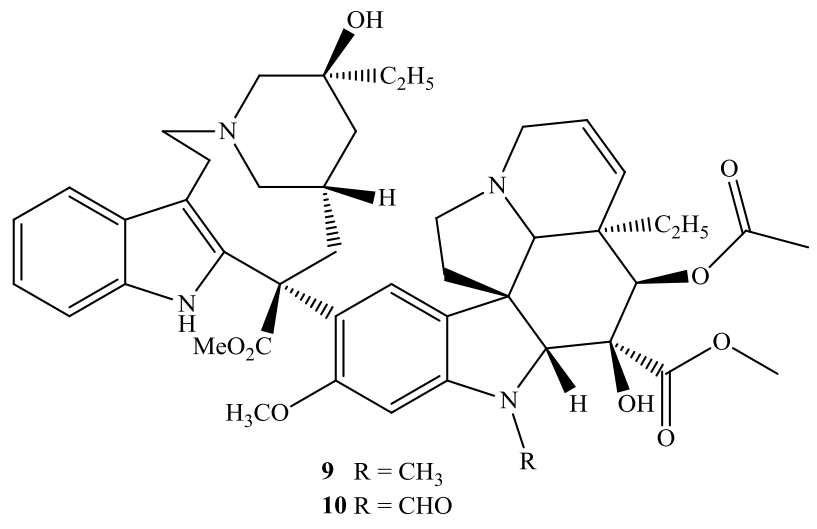
Dacarbazine **4** and temozolomide **5** are two structurally related prodrugs; both drugs are metabolised *in vivo* to MTIC **6**, which spontaneously degrades to form diazomethane, a potent alkylating agent. The single-agent chemotherapy of metastatic melanoma depends primarily on these two drugs which typically produce response rates that range from 15% to 25%.¹⁸ Other examples of alkylating agents sometimes used in the treatment of SCLC and melanoma are cyclophosphamide **7** and carmustine **8**.

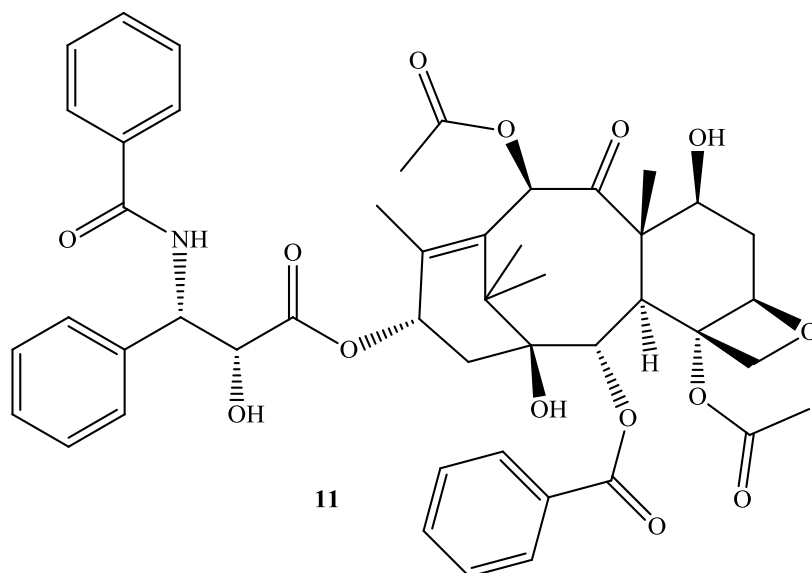




1.1.4.3. Anti-microtubule agents

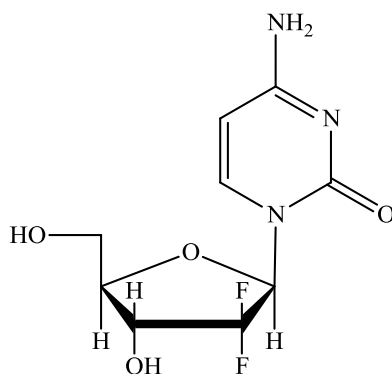
Anti-microtubule agents prevent cell mitosis by interfering with the formation of the mitotic spindle required for cell division. The main cellular target of these compounds is the structural protein tubulin. During mitosis, tubulin undergoes polymerisation to form the mitotic spindle. The vinca alkaloids, of which vinblastine **9**, vincristine **10** and vinorelbine are the main examples, bind to tubulin and prevent polymerisation from occurring. Taxanes, such as paclitaxel **11** and docetaxel, bind to the β -subunit of tubulin, accelerating polymerisation and stabilising the resultant microtubules to prevent depolymerisation.¹² Both classes of compounds are frequently used in combination therapies for the treatment of lung cancer and melanoma.





1.1.4.4. Anti-metabolites

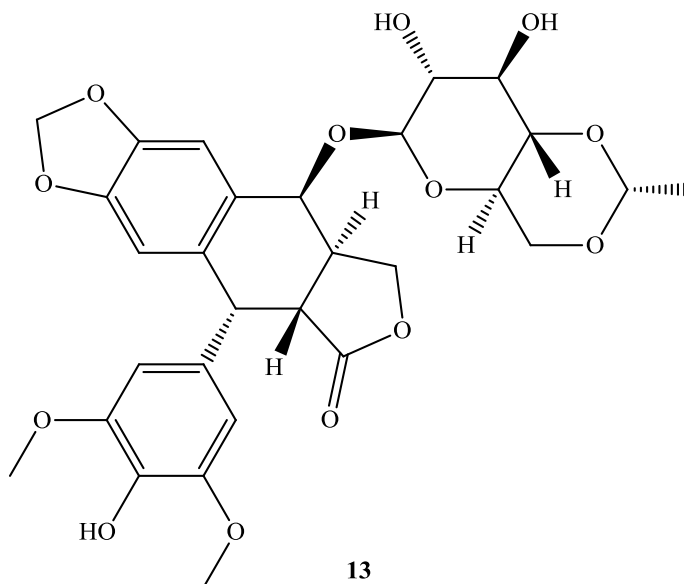
Anti-metabolites are agents which inhibit the enzymes involved in the synthesis of DNA or its building blocks. Gemcitabine **12** is a pyrimidine based anti-metabolite prodrug; it is a fluorinated analogue of the natural DNA building block 2-deoxycytidine. Inside the cell, the active triphosphate analogue is formed following several enzymatic reactions. The cytotoxicity of gemcitabine results from the incorporation of this active triphosphate derivative into a growing DNA chain, which causes the addition of a single deoxynucleotide and chain termination.¹⁹



12

1.1.4.5. DNA topoisomerase inhibitors

Etoposide **13** is a semi-synthetic derivative of the naturally occurring podophyllotoxins, and exerts its anti-cancer activity by stabilising the DNA-topoisomerase II complex, preventing the resealing of DNA strands which have been cleaved by the enzyme.¹²



1.2. Bioorganometallic anti-cancer agents

1.2.1. Introduction

Interest in metal complexes with biological applications has grown at a phenomenal rate since the serendipitous discovery of the inhibition of cell division by Pt complexes in 1965, and the subsequent identification of cis-dichlorodiamineplatinum(II) or cisplatin **1** as an effective anti-cancer drug.^{20,21} Research in this area is thriving; so much so that Gainferrara *et al* have recently proposed a system of categorising the diverse range of metal anti-cancer compounds according to their mode of action.²² Five distinct categories have been proposed for these compounds wherein:

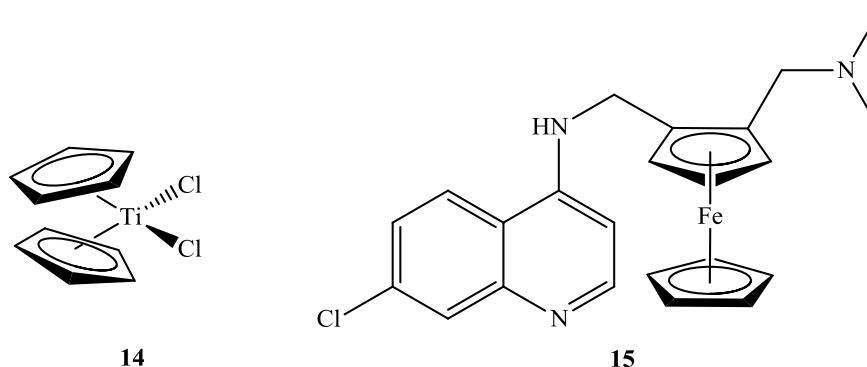
- The metal has a functional role *i.e.* the activity is derived from direct binding of the metal fragment to the biological target.

- The metal has a structural role *i.e.* it is important in determining the shape of the compound and binding to the biological target occurs through non-covalent interactions.
- The metal is a carrier for active ligands that are delivered *in vivo*.
- The metal compound behaves as a catalyst *in vivo e.g.* through the production of reactive oxygen species (ROS) that cause cell damage.
- The metal compound is photoactive and behaves as a photosensitiser.

Some of the most promising novel non-platinum metal anti-cancer agents are emerging from the field of bioorganometallic chemistry. “Bioorganometallic chemistry” is a term first coined by Gérard Jaouen in 1985 to describe the discipline dedicated to the study of biomolecules or biologically active molecules that contain at least one direct metal-carbon bond.²³ Organometallic complexes have received much attention, due to the large diversity of structure and bonding modes on offer (e.g. π -coordination, multiple M-C bonds).²⁴ Organometallic compounds containing transition metals, such as Co, Cu, Fe, Ga, Ge, Mo, Pt, Sn, Rh, Ru, Ti and V are known to have anti-proliferative (*in vitro*) and anti-neoplastic (*in vivo*) activities.²⁵ In particular, early transition metal compounds belonging to a group of metallocene dichlorides (Cp_2MCl_2) with M = Ti, V, Nb, Mo, have all showed remarkable anti-tumour activity.²⁶ These derivatives were originally investigated in the hope that the *cis*- MCl_2 motif would react with DNA in a similar manner to cisplatin.²⁴ In fact, these complexes bind only weakly to DNA and more strongly to the phosphate backbone, and there is no evidence that they exhibit similar mechanisms of action. The most noteworthy of these metallocene compounds is titanocene dichloride **14**; the first non-platinum organometallic compound to enter clinical trials in 1993. Unfortunately, Phase II clinical trials of titanocene dichloride were abandoned when its efficacy as an anti-cancer therapeutic against metastatic renal cell carcinoma and metastatic breast cancer proved too low to warrant further trials.²⁷

Ferrocene is perhaps the quintessential organometallic molecule, and indeed was the first example of the well known “metallocene” compounds to be discovered.^{28,29} The elucidation of this novel π -complexed “sandwich” structure revolutionised the field of organometallic

chemistry and resulted in the Nobel Prize in Chemistry being awarded to G. Wilkinson and E. O. Fischer in 1973. There now exists an entire class of metallocenes containing various transition metals such as V(II), Cr(II), Mn(II), Co(II), Ru(II) and Ni(II), however ferrocene is still the main focus of research primarily due to its remarkable stability and ease of preparation.³⁰ Ferrocene is also a particularly attractive candidate for incorporation into biomolecules and biologically active compounds due to its aromatic character, redox properties and low toxicity. The medicinal application of ferrocene derivatives is currently a thriving area of research, with countless reports showing their activity *in vitro* and *in vivo* and potential as anti-cancer, anti-malarial, anti-fungal, anti-viral and anti-bacterial agents.³¹ Most promisingly, phase II clinical trials have commenced with the anti-malarial compound ferroquine **15** (SR97193) in combination with artesunate as recommended by the World Health Organisation (WHO).³²



1.2.2. Ferricenium salts

One of the most important properties of ferrocene is the ease by which it undergoes oxidation to form the ferricenium cation ($\text{Fc} \rightarrow \text{Fc}^+$). This occurs in a reversible manner and is demonstrated in Figure 1.2. Oxidation/reduction is accommodated readily by the loss/gain of an electron from a high energy, non-bonding orbital and can occur both chemically and electrochemically. The oxidation potential of ferrocene is sensitive to the nature of its substituents: electron donating substituents such as alkyl groups tend to aid oxidation, whereas electron withdrawing substituents such as aryl groups tend to hinder oxidation.³⁰

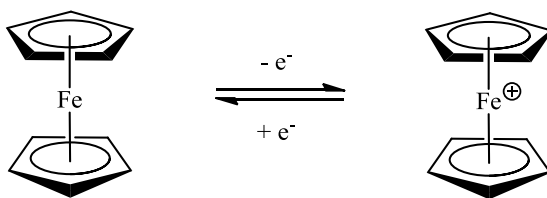
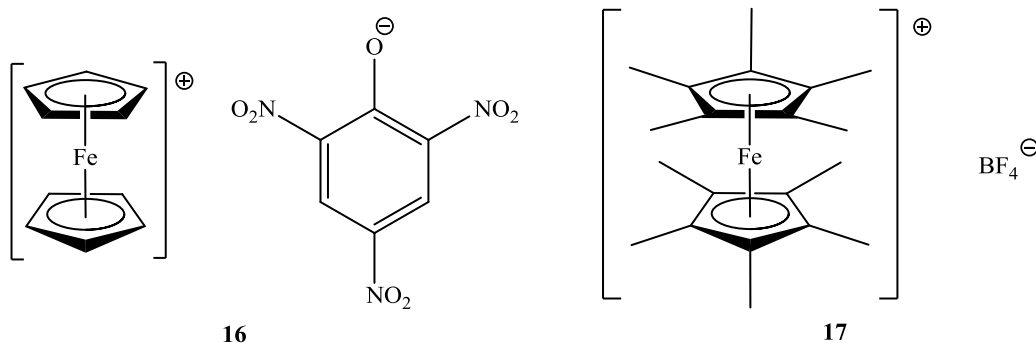


Figure 1.2 Oxidation/reduction of ferrocene.

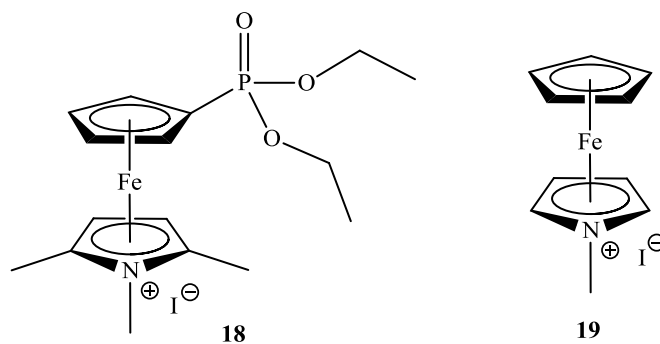
The redox properties of ferrocene have often been implicated in its cytotoxicity.²⁵ The anti-tumour properties of ferricenium salts were first reported by Kopf-Maier *et al* in 1984.³³ These ionic, water soluble complexes were found to exhibit high cure rates in tests against fluid Ehrlich ascites tumour. Ferricenium picrate **16** and trichloroacetate salts were found to elicit 100% cure rates using an optimal dose of 220-300 mg kg⁻¹.

In vivo studies were conducted by Osella *et al* to assess the ability of ferricenium salts, *e.g.* [FcCOOH]⁺[PF₆]⁻, to inhibit the growth of Ehrlich ascites tumours.³⁴ It was observed that only Fe(III) ferricenium salts inhibited tumour cell growth; the corresponding Fe(II) ferrocene derivatives, *e.g.* FcCOOH, failed to display any inhibitory activity. Thus, inhibitory activity is independent of redox potential, at least in the range 175 to 330 mV. It was also observed that ferricenium species do not undergo intercalation with DNA. ¹H and ³¹P NMR studies suggest that interaction with DNA occurs primarily *via* an electrostatic interaction with the phosphate backbone. Using electron spin resonance (ESR) experiments, it was proposed that the ferricenium salts produced hydroxyl radicals (HO[•]) under physiological conditions, which in turn resulted in DNA damage. Subsequent studies were conducted wherein different ferricenium salts were prepared and evaluated *in vitro* in the MCF-7 breast cancer cell line.³⁵ Decamethylferricenium tetrafluoroborate **17** was revealed as the most active of these salts, displaying an IC₅₀ value of 37 μM.



ESR experiments confirmed that reactive oxygen species (ROS) are produced when compound **17** is dissolved in aqueous media. From the ESR pattern it is suggested that this occurs *via* a Haber-Weiss like process, followed by a Fenton reaction to yield the hydroxyl radical. Fluorescence Activated Cell Sorting (FACS) measurements of 8-oxo-7,8-dihydroguanine (8-oxo-Gua), the biomarker for oxidative stress on DNA, also revealed that compound **17** was able to increase the 8-oxo-Gua level and induce oxidative stress in cells in a dose-dependent manner.

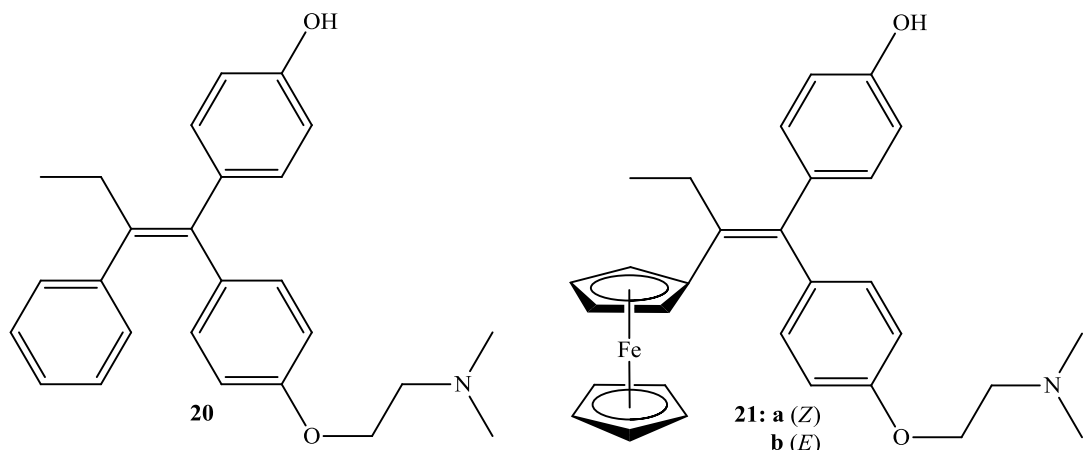
Preliminary studies by Kowalski *et al* demonstrated the *in vitro* cytotoxic activity of azaferrocenes in the HeLa cervical cancer cell line.³⁶ In particular, compound **18** was found to show selectivity for the cancerous HeLa cell line over the non-cancerous NIH 3T3 cell line. Although in this study the compounds were evaluated at millimolar concentrations, these results were adequate to warrant further investigation of azaferrocene derivatives. Subsequent studies showed that azaferrocenes such as compound **19** can induce DNA scission, mainly by causing single strand DNA breaks.³⁷ Even at the lowest concentrations tested, namely 6.25 μM , compound **19** caused complete degradation of the DNA plasmid. ESR experiments suggest a free radical mechanism of DNA scission by azaferrocenes. The strength of the iron-heteroatom ring bonding and the release of redox active metal cations that can generate ROS were found to be important in DNA scission.



1.2.3. Metallocene-based selective estrogen receptor modulators (SERMs) and anti-androgens

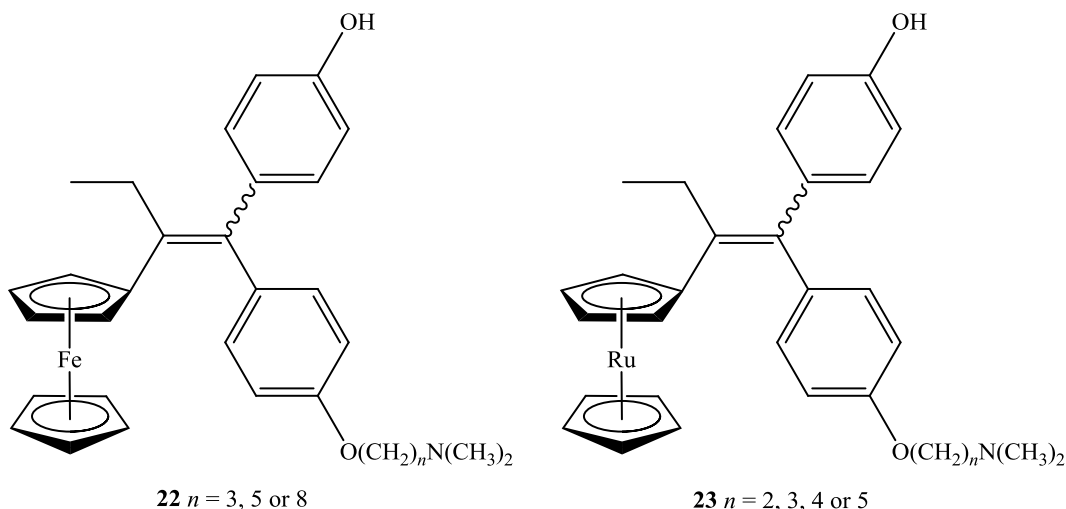
Tamoxifen is a widely prescribed selective estrogen receptor modulator (SERM). It is employed in the treatment of hormone-dependent breast cancer, where the estrogen receptor (ER) is present. These are known as ER positive cells, ER(+).³⁸ SERMs are capable of interacting with the estrogen binding sites, despite their non-steroidal structure. The anti-proliferative effect of tamoxifen is due to the hydroxylated form **20** produced *in vivo*. 4-Hydroxytamoxifen **20** binds competitively to the estrogen receptor binding site, to produce an anti-estrogenic effect.³⁹ However, some breast cancer cells do not express ER. These are referred to as ER negative cells, ER(-) and are resistant to tamoxifen. Also, some cells may develop resistance to tamoxifen following prolonged exposure.³⁸

Over the past decade, Jaouen *et al* have extensively studied a series of ferrocene substituted tamoxifen derivatives. The first of these derivatives, ferrocenyl hydroxytamoxifen (hydroxyferrocifen) **21**, was reported in 1996 by Top *et al*.⁴⁰ It was postulated that the replacement of the β -aromatic ring of 4-hydroxytamoxifen **20** with ferrocene could produce a single molecule possessing both anti-estrogenic and anti-tumour properties. The target compound **21** was synthesised as a mixture of (*Z*)- **21a** and (*E*)- **21b** isomers, which were separated prior to biological testing. The anti-proliferative effect of both isomers was evaluated in the ER(+) MCF-7 breast cancer cell line. IC₅₀ values of 3.4 and 4.9 μ M were obtained for **21a** and **21b**, respectively. Tamoxifen was found to exhibit an IC₅₀ of 6.4 μ M under the same conditions. A DNA damage assay indicated that the ferrocenic compounds show genotoxic activity at low micromolar concentrations, whilst tamoxifen does not have any effect.



Altering the length of the dimethylamino side chain was found not to dramatically influence the anti-proliferative activity of ferrocenyl tamoxifen compounds.⁴¹ Compounds such as **21** and **22** ($n=3, 5$ or 8) displayed a strong anti-proliferative effect in the MCF-7 cell line when tested at a concentration of $1\ \mu\text{M}$. However, this effect does weaken when the chain is lengthened to $n=8$. Extending the biological evaluation to include the ER(-) MDA-MB231 breast cancer cell line revealed some interesting results. At $1\ \mu\text{M}$, compound **20** had no effect on cell proliferation, whereas the ferrocenyl tamoxifen derivatives **21** and **22** showed a strong anti-proliferative effect, except for when $n=8$.

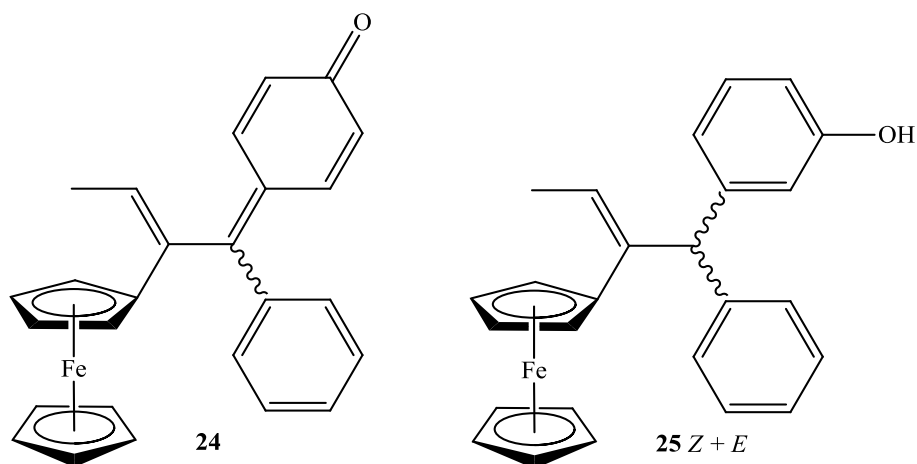
Pigeon *et al* prepared the ruthenocene analogue of hydroxytamoxifen, compound **23**. *In vitro*, compound **23** displays an anti-proliferative effect similar to compound **20** on ER(+) MCF-7 cells, whilst these compounds have no effect on the ER(-) MDA-MB231 cell line.⁴² Thus, these compounds act in an anti-estrogenic manner similar to compound **20**. These results contrast surprisingly with those observed for the ferrocenyl derivatives. Electrochemical experiments revealed that oxidation leads to rapid decomposition of the ruthenocene radical cation. This is a possible explanation for the difference in activity between the two analogues, **22** and **23**.



The activity of compound **21** had been attributed to intracellular oxidation to the ferricenium ion, leading to hydroxyl radical formation and oxidative stress. Thus, the ability of **21** to induce oxidative stress *via* the Fenton reaction was investigated by Osella and Jaouen.⁴³ The level of oxidative stress was assessed by measuring the production of 8-oxo-Gua, the first product of oxidative attack to DNA and hence, a marker for nucleobase oxidative damage. Interestingly, compound **21** did not significantly increase 8-oxo-Gua levels, in either hormone-dependent or hormone-independent cells and thus the growth inhibition observed cannot be attributed to oxidative stress.

Hillard *et al* used cyclic voltammetry to propose another possible mechanism of cytotoxicity for the ferrocenyl tamoxifen derivatives.⁴⁴ Cyclic voltammograms of several derivatives were obtained in methanol, and then pyridine was added to determine the reactivity of the electrochemically generated cations towards nucleophiles. Addition of pyridine caused two major changes to the voltammograms. The Fc/Fc⁺ couple became irreversible, indicating that the Fc⁺ was scavenged chemically and the Fc oxidation wave increased, indicating a secondary electron transfer. Any phenol-oxidation waves also underwent a dramatic cathodic shift. They proposed that following oxidation to Fc⁺, the electron becomes delocalised over the π -system, imparting a slight positive charge on the hydroxyl group. The acidified hydroxyl proton is easily abstracted in the presence of pyridine. The resulting phenoxy radical can then be oxidised. Another proton abstraction, this time from the ethyl group, results in the formation of a quinone methide. In the presence of basic species like DNA, the quinone methide species **24** will be formed which

in turn will lead to cell death. The oxidation of tamoxifen and other SERMs to quinoids is also a recognised pathway for their cytotoxicity.⁴⁵

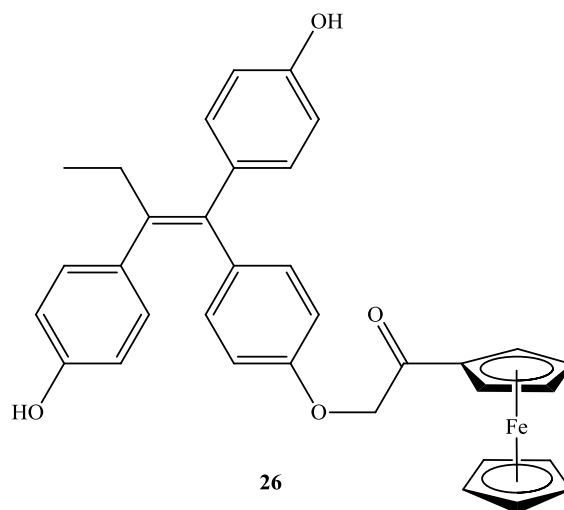


This mechanism of action was further validated by studies of derivatives bearing a hydroxyl group in the *meta*-position of the phenol.⁴⁶ For example, compound **25** maintains the ferrocene- π -system-phenol motif but the *m*-phenol prevents quinone methide formation. Cyclic voltammograms of **25** show no electrochemical changes upon addition of pyridine to solution. In addition, the IC₅₀ value of **25** against MDA-MB231 cells (hormone-independent) is more than twice that of the *p*-phenol analogue.

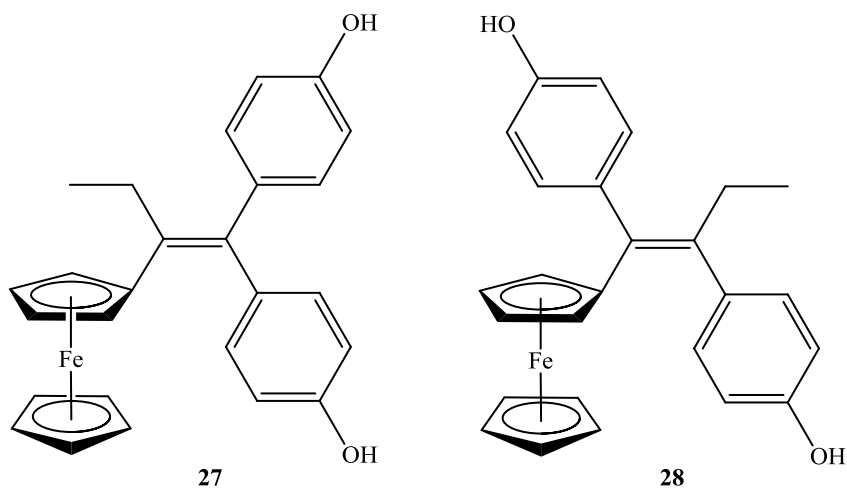
Nguyen *et al* have prepared further ferrocenyl tamoxifen derivatives. Compound **26** maintains the three aromatic rings of the hydroxytamoxifen skeleton, however, a lipophilic ferrocenyl group has been appended to this skeleton in place of the dimethyl amino side chain.⁴⁷ The IC₅₀ value of compound **26** was 10.4 μ M when tested in the ER(+) MCF-7 cell line. Interestingly, compound **26** also showed activity in the ER(-) PC-3 prostate cancer cell line (IC₅₀ value = 8.9 μ M). This suggests that the cytotoxic character of the ferrocenyl group is responsible for the observed anti-proliferative activity as the generation of a quinone methide species is impossible.

The structure-activity relationship (SAR) of compound **26** was investigated by varying three parameters: the length of the side chain, the presence of one or two phenolic groups, and the presence or absence of a ketone group adjacent to the ferrocene moiety.⁴⁸ Removal of the ketone functionality and variation of the side chain from one carbon to four carbons in length had little effect on the anti-proliferative activity in the PC-3 cell line; IC₅₀ values were found to be around 10 μ M for each derivative. Conversely, in the MCF-7 cell line

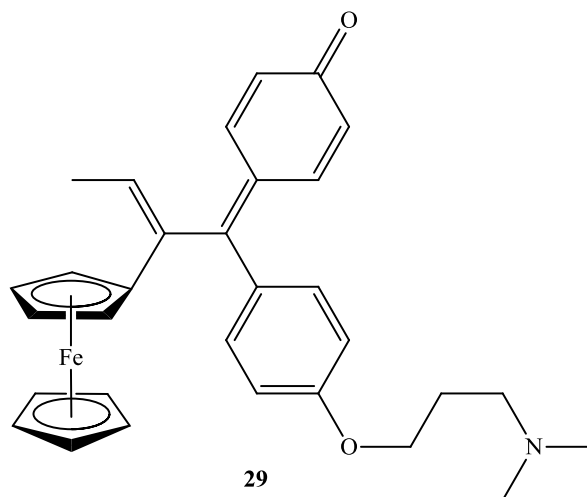
each derivative displayed a proliferative effect. Derivatives that possessed only one phenolic group and lacked the ketone functionality, showed a proliferative effect in the MCF-7 cell line, and had little effect in the PC-3 cell line, when tested at 10 μM . The loss of one of the phenolic groups from compound **26** was also found to significantly weaken the cytotoxic activity.



Vessières *et al* have prepared a series of diphenolic compounds derivatised with ferrocene and studied their anti-cancer activity in both hormone dependent and independent breast cancer cell .⁴⁹ Derivative **27** was found to show strong anti-proliferative activity against MCF-7 and MDA-MB231 cell lines, with IC_{50} values of 0.7 μM and 0.6 μM , respectively. Conversely, compound **28**, which is a regioisomer of compound **27**, displays only modest activity against both cell lines.



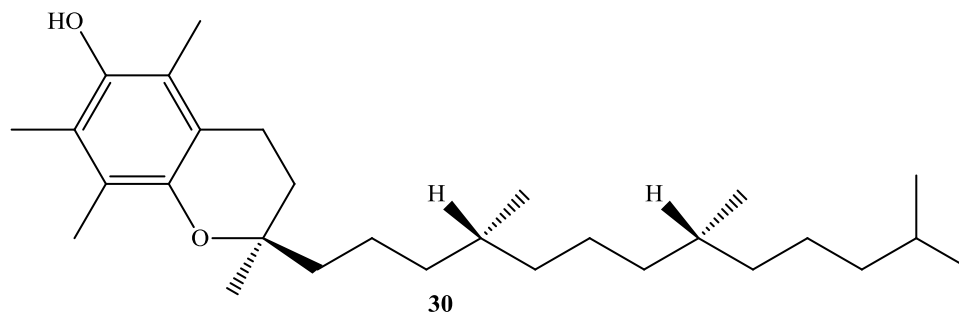
In terms of structure, there are two main differences between compound **27** and **28**. In compound **27** one of the two phenol groups is always oriented *trans* to the ferrocenyl group, whereas in compound **28** there is a *cis* relationship between the ferrocenyl and phenol groups. Secondly, in compound **27** the two phenol rings are bonded to the same carbon of the alkene, whereas in compound **28** each carbon of the alkene is attached to a phenol ring. The difference in biological activity of these two compounds indicates that the ferrocene moiety is not solely responsible for cytotoxicity. The relationship between the ferrocenyl group and the rest of the molecule must also be taken into consideration. Derivatives of **27** and **28**, where one -OH group has been replaced by an -OMe group, were studied by cyclic voltammetry.⁴⁴ Only the compound in which the ferrocene and ethyl groups were attached to the same carbon showed irreversible redox activity upon addition of pyridine to solution. Therefore, the position of the ferrocenyl group in relation to the ethyl group is essential for formation of a quinone methide species.



The *in vitro* formation of quinone methide species from ferrocenyl phenol derivatives was investigated by Hamels *et al.*⁵⁰ Rat liver microsomes, which contain the main enzymes involved in xenobiotic metabolism, were incubated with either compound **22** or **27**. Analysis by HPLC-MS of a sample taken following incubation for 30 minutes, demonstrated the formation of the corresponding quinone methide species as the major product of metabolism. The quinone methide species **29** formed from compound **22** ($n=3$), was prepared by chemical oxidation and tested in the ER(-) MDA-MB231 cell line. An IC₅₀ value of $4.2 \pm 1 \mu\text{M}$ was determined for compound **29**. This value is higher than that of

compound **22** (IC_{50} value = 0.5 μ M), although this may be due to the instability in the incubation medium.

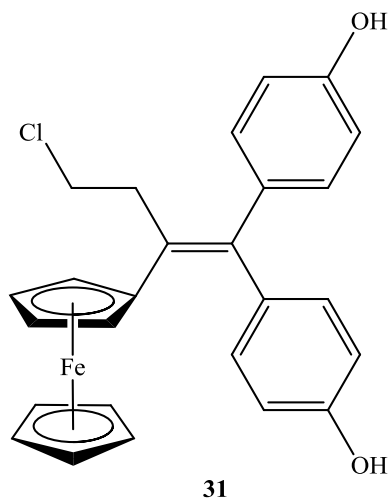
Compounds **26** and **27** have been successfully incorporated into two types of nanoparticles, namely nanocapsules and PEG/PLA (polyethyleneglycol/poly-D-lactic acid) nanospheres with the aim of finding an *in vivo* drug delivery model.⁵¹ These nanoparticles can improve the bioavailability of these compounds by protecting them from hydrolysis, oxidation and degradation. Cell cycle analysis revealed that compounds **26** and **27** both increase apoptosis in MCF-7 cells when administered freely at a concentration of 10 μ M. Upon entrapment in PEG/PLA nanospheres, this ability to induce apoptosis is enhanced. At a concentration of 1 μ M, whether free or encapsulated in nanocapsules, compound **27** causes an arrest in S-phase of the cell cycle, and to a more limited extent in the G2/M phase. No significant effect was observed for compound **26** at this low concentration. Further studies performed in the presence of α -tocopherol **30**, a well known anti-oxidant, showed a decrease in the levels of apoptotic cells found in the sub-G0/G1 phase. These results suggest that the anti-oxidant may prevent oxidation of ferrocene to the ferricenium ion and therefore prevent the formation of the quinone methide species, leading to a loss in anti-proliferative effect.



Lipid nanocapsules and swollen micelles containing compound **27** have been prepared by Allard *et al* and studied as a treatment for malignant gliomas.⁵² *In vitro* survival assays were performed on 9L glioma cell and on newborn rat astrocyte primary cultures. An IC_{50} value of 0.5 μ M was determined for compound **27** when tested in the 9L glioma cells, whereas the IC_{50} value for hydroxytamoxifen **20** was 35 μ M and ferrocene was totally inactive. Encapsulation in lipid nanocapsules did not alter the anti-proliferative activity of compound **27**. In contrast, the micelles loaded with compound **27** showed only a toxicity related to the nanocarrier, implying inefficient release of the compound to the surrounding

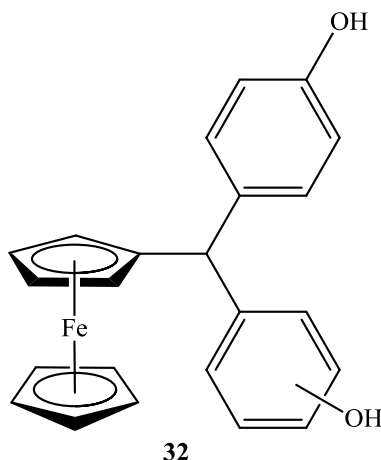
environment. When tested on astrocytes, either freely or bound within lipid nanocapsules, compound **27** was found to be much less cytotoxic, suggesting selectivity towards cancer cells alone. *In vivo* studies conducted on a 9L subcutaneous glioma model in rats showed a significant reduction in tumour mass following treatment with the loaded lipid nanocapsules.

The importance of the ferrocenyl group to the activity of this series of compounds was demonstrated by Hillard *et al.* A series of organometallic analogues of compound **27** were prepared wherein the ferrocenyl moiety was replaced by pentamethylferrocene, ruthenocene, cyclopentadienyl rhenium tricarbonyl and cyclopentadienyl manganese tricarbonyl units.⁵³ Incorporation of these units resulted in the loss of anti-proliferative effect in the ER(-) MDA-MB231 cell line and an estrogenic effect in the ER(+) MCF-7 cell line. Substitution of the ethyl group of compound **27** with chlorine to give compound **31** decreased the anti-proliferative effect slightly, with the IC₅₀ value increasing to 1 μ M against MDA-MB231 cells. Cyclic voltammetry experiments indicate that the chloro substituent increases the ferrocene redox potential by +40 mV in methanol and +73 mV upon addition of pyridine.

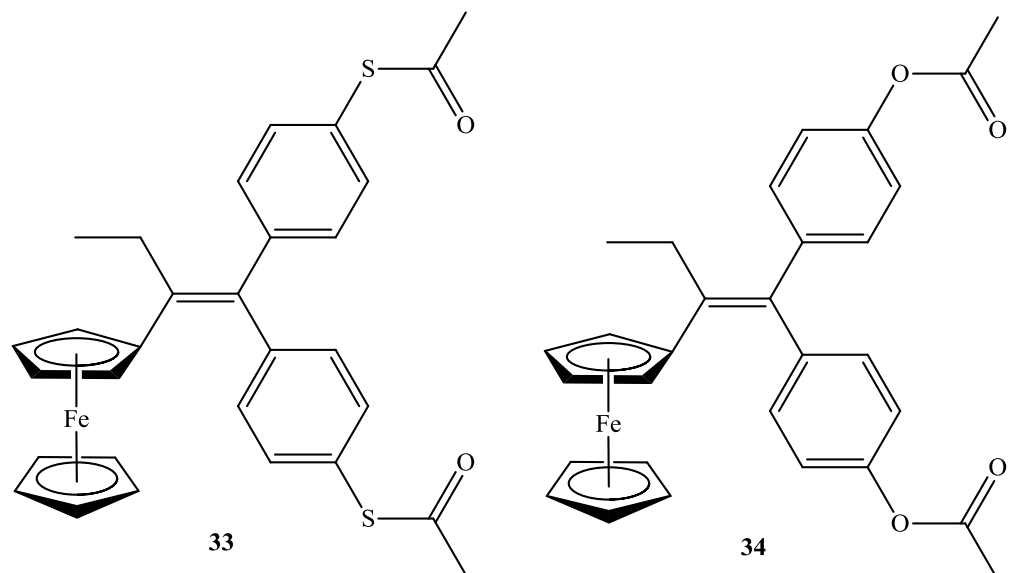


The importance of conjugation to the activity of these compounds is evident from the biological results obtained for a series of unconjugated ferrocenyl phenols, for example compound **32**.⁵⁴ IC₅₀ values were determined for compound **32** in ER(-) MDA-MB231 and PC-3 cell lines and averaged around 3-3.5 μ M. Activity was best when the hydroxyl group was in the *para*-position. In comparison to compound **27**, these derivatives are around five

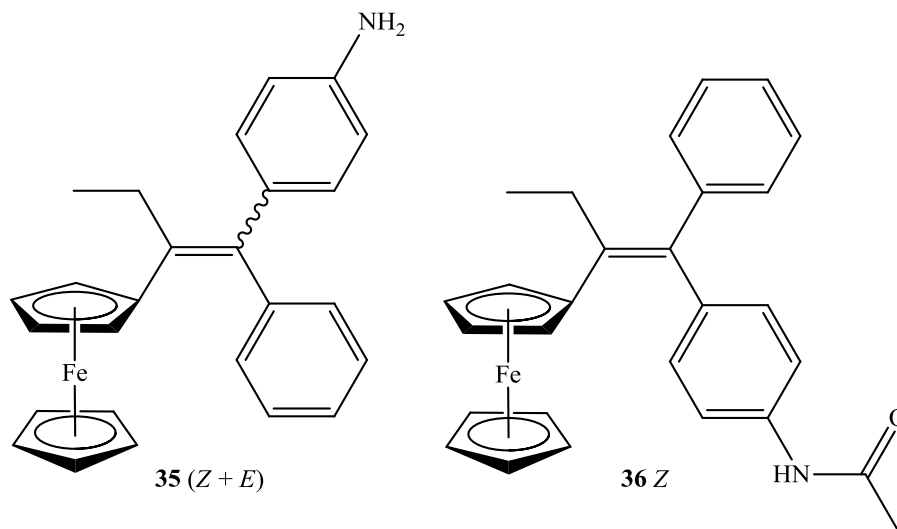
to seven times less cytotoxic. Cyclic voltammetry experiments revealed no major change in the ferrocene/ferricenium redox couple upon addition of pyridine to a solution of compound **32**. These results indicate that conjugated π -system of compound **27** facilitates the generation of a reactive quinone methide species. Due to the absence of a π -system in compound **32** it is unable to mediate electron transfer. However, the significant IC_{50} values obtained for this compound indicates that Fenton chemistry may be responsible for the observed cytotoxicity.



The importance of the phenol groups of this class of compounds was investigated in a number of studies. Initially, Heilmann *et al* prepared thioether and thioester analogues of compound **27**, for example compound **33**.⁵⁵ When tested at 1 μ M, these compounds displayed a strong proliferative effect in the ER(+) MCF-7 cell line, and failed to show any anti-proliferative effect in the ER(-) MDA-MB231 cell line. The ester analogue of compound **33** was also prepared, namely compound **34**. At 1 μ M, compound **34** displayed an anti-proliferative effect equalling that of compound **27**. This suggests that the ester moiety is hydrolysed by enzymes to generate compound **27** *in situ*. Since thioesterases are known to be present in breast cancer cells, it can be expected that hydrolysis also occurs for compound **33**. The lack of anti-proliferative activity for compound **33** suggests that the corresponding ferrocenyl thiophenol is also not cytotoxic.

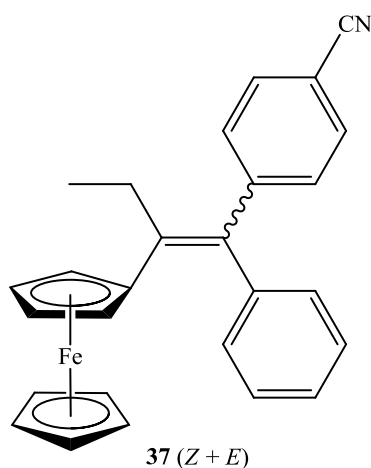


Pigeon *et al* have replaced the phenol group with an aniline or acetanilide group to give compounds **35** and **36**, respectively.⁵⁶ Both compounds were found to show a strong anti-proliferative effect in the ER(-) MDA-MB231 cell line, with IC₅₀ values of 0.8 μM for compound **35** and 0.65 μM for compound **36**. Cyclic voltammetry experiments indicate that both compounds can be transformed into oxidised products *via* the ferricenium-mediated proton-coupled electron transfer mechanism. It is likely that the reactive species generated is an imino methide species, which has been implicated in cytotoxic processes.



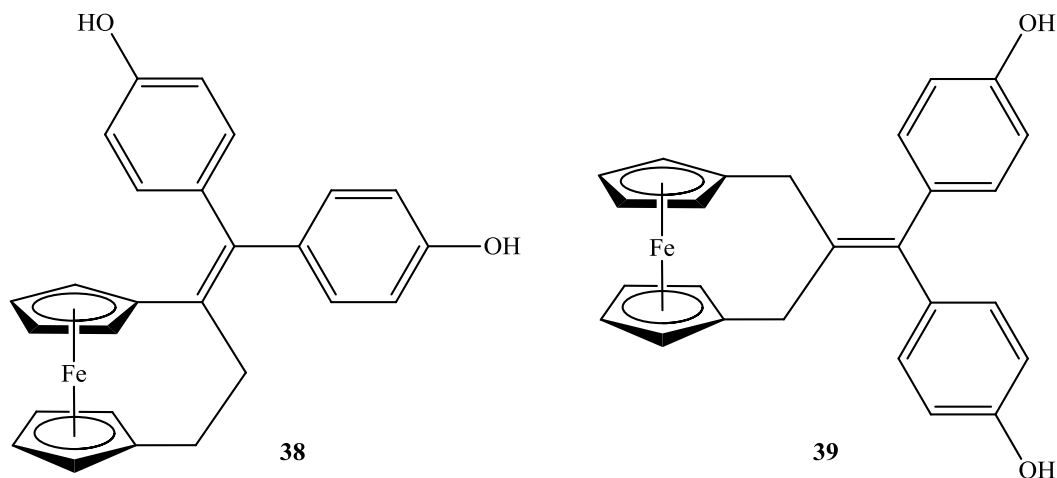
Zekri *et al* studied the effect of incorporating Br, Cl, CF₃ and CN groups in place of the amino group of compound **35**.⁵⁷ No anti-proliferative effect was observed for the Br, Cl and CF₃ derivatives when tested at a concentration of 10 μM in the ER(-) MDA-MB231 cell

line. The cyano analogue **37** of compound **35**, was the only derivative to show an anti-proliferative effect in this cell line. IC_{50} values of 11 and 60 μM were determined for the (*Z*)- and (*E*)- isomers of compound **37**, respectively. Cyclic voltammograms obtained for each derivative lack any features other than the reversible ferrocene/ferricenium redox wave. The absence of other oxidation waves indicates the inability of these compounds to undergo ferricenium-mediated proton-coupled electron transfer. QSAR studies reveal that the cytotoxicity observed for this class of compounds is primarily dependent on the presence of a protic substituent in the *para*-position of the phenyl ring. The resonance donating ability of this substituent may also be important for cytotoxicity.

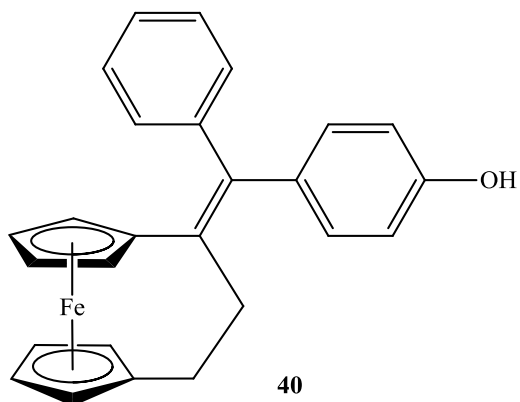


Evaluation of the two lead ferrocenyl phenol compounds in primary and metastatic melanoma cell lines was conducted by Michard *et al.*⁵⁸ Compound **22** ($n=3$) and **27** were tested in a panel of four cell lines, a normal cell line (NHEM), two primary melanoma cell lines (WM35 and WM793) and one metastatic melanoma cell line (WM9). At a concentration of 1 μM , compound **22** displayed selectivity towards the three melanoma cell lines, inducing a strong anti-proliferative effect whilst the normal melanocytes remained relatively unharmed. Compound **27** also displayed selectivity for cancerous cells and inhibited the growth of the primary melanoma cell lines at a concentration of 0.1 μM . However, it was ineffective in the metastatic cell line. Increasing the concentration of compound **27** to 1 μM increased the anti-proliferative effect in all four cell lines. An assay using the $\text{H}_2\text{DCF-DA}$ fluorescent probe to monitor the production of reactive oxygen species (ROS) showed that neither compound induced ROS production in any cell line.

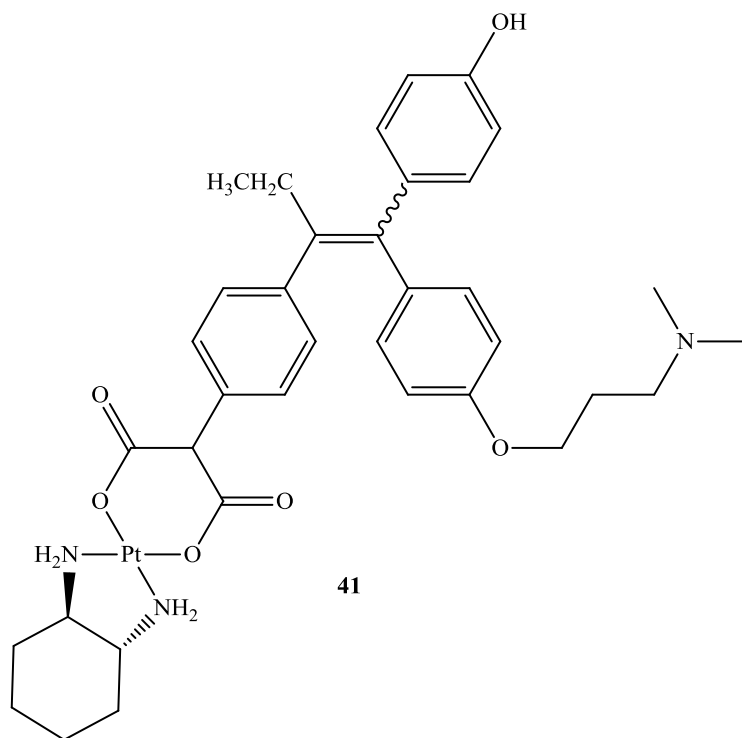
Compounds **38** and **39**, which possess the [3]ferrocenophane motif incorporated into the ferrocenyl phenol structure were prepared and studied by Plazuk *et al.*⁵⁹ In the ER(+) MCF-7 cell line, compounds **38** and **39** exhibited IC₅₀ values of 4 μM and 1 μM, respectively. In the ER(-) MDA-MB231 and PC-3 cell lines, the anti-proliferative effect of compound **38** increases dramatically, with an IC₅₀ value of 0.09 μM. This compound is ten times more active than compound **39**, for which IC₅₀ values of around 1 μM were obtained in both cell lines. Conjugation between the ferrocenyl and phenol groups is absent from compound **39**, which may explain the difference in cytotoxicity. Cyclic voltammetry experiments performed in the presence of imidazole show the formation of a quinone methide species from both compounds **38** and **39**. In the case of compound **39**, the required intramolecular electron transfer may proceed either “through space” or *via* the formation of an intermediate α -methylene radical, which can delocalise over the π -system and undergo an additional oxidation step to yield the quinone methide species.



Gormen *et al* prepared the monophenol analogue of compound **38**, namely compound **40**.⁶⁰ In the ER(-) MDA-MB231 cell line the IC₅₀ value was determined to be 0.47 ± 0.01 μM, corresponding to a five-fold decrease in activity. Replacement of the phenol group with an acetanilide group does not alter the IC₅₀ value however replacement with an aniline group reduces the IC₅₀ value to 0.21 ± 0.03 μM.

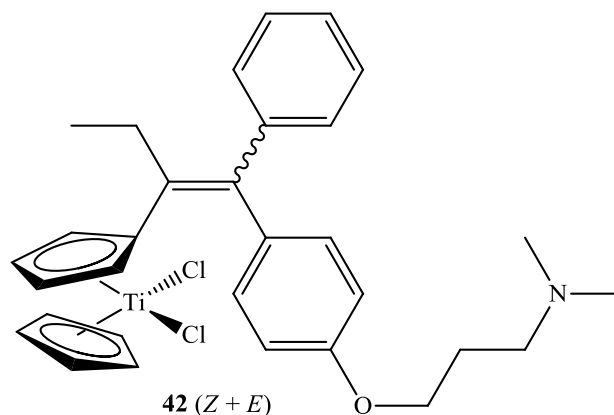


Tamoxifen has also been appended to other known cytotoxic compounds. For example, the cytotoxic (DACH)Pt fragment of oxaliplatin **3** has been attached to the β -aromatic ring of tamoxifen molecule *via* a malonato moiety to give compound **41**.⁶¹ In the ER(+) MCF-7 cell line, compound **41** had an IC_{50} value of 4.0 μ M, whereas oxaliplatin had an IC_{50} value of 7.4 μ M. Therefore the anti-proliferative effect of **41** is similar to that observed for the parent platinum complex.

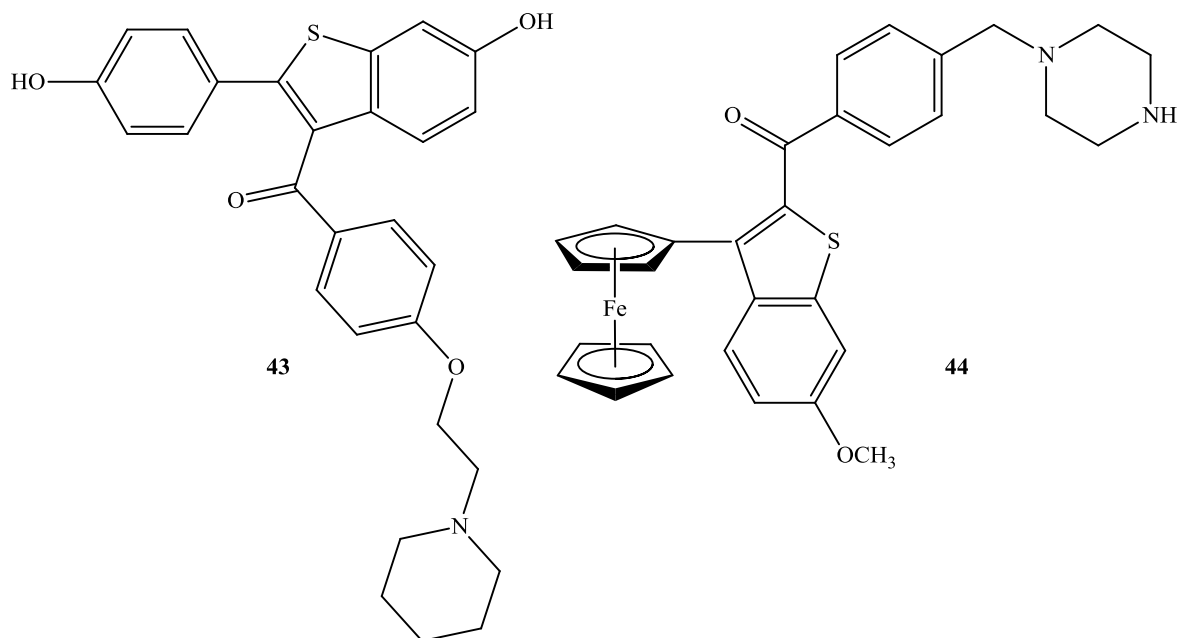


Top *et al* also selected titanocene dichloride **14** for attachment to the tamoxifen skeleton.⁶² However, the most important finding of this study was that the resulting compound **42** exerted a powerful estrogenic effect on MCF-7 cells. Compound **14** was also found to exert

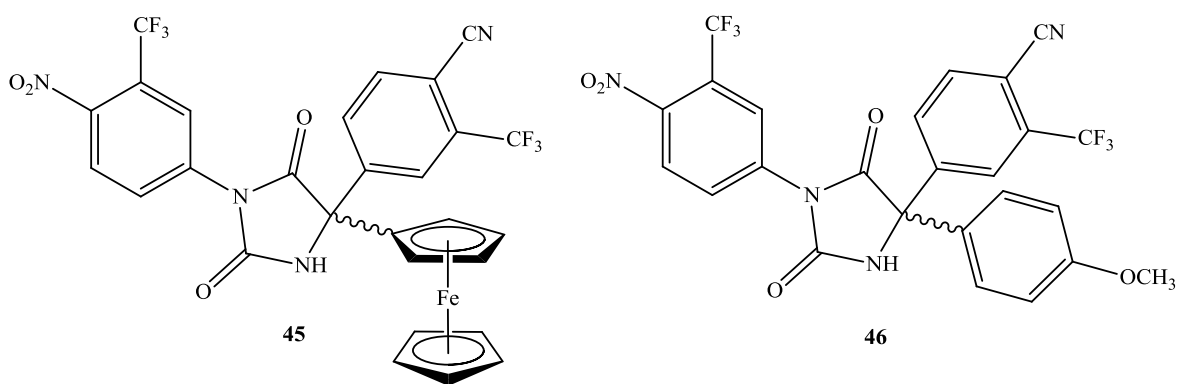
an estrogenic effect, which implies that any anti-proliferative effect due to the tamoxifen fragment of **42** is concealed by the strength of the estrogenic effect. The proliferative effect caused by **14** has been attributed to the Ti(IV) ion. The parent molecule undergoes hydrolysis of the chloride ligands and the cyclopentadienyl groups leading to the complete release of Ti(IV). A molecular modelling study indicated that the Ti(IV) ion had a similar effect to estradiol on the estrogen receptor (ER).



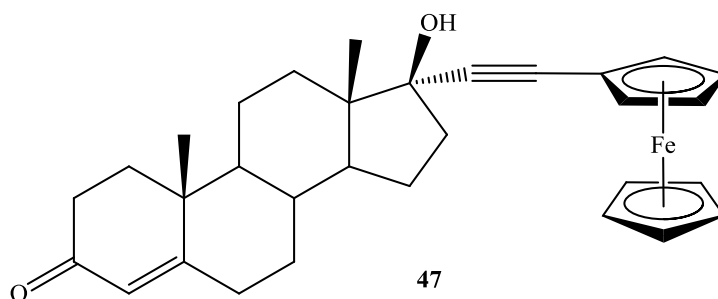
Raloxifene **43** is a SERM approved for the treatment of postmenopausal osteoporosis. Whilst compound **43** is an estrogen agonist in bone tissue, it acts as an anti-estrogen in mammary tissue, and has been found to decrease breast cancer risk in postmenopausal women. Ferreira *et al* have prepared a series of organometallic benzo[*b*]thiophene derivatives inspired by the structure of **43**.⁶³ These 2-benzoyl-3-ferrocenylbenzo[*b*]thiophene compounds contain various tertiary alkylamino groups substituted at the *para*-position of the benzoyl moiety. The anti-proliferative activity of this series was evaluated *in vitro* in a panel of human tumour cell lines containing examples of ovarian (2008, C13*, RH4), cervical (A431), lung (A549), colon (HCT-15), and breast (MCF-7, MCF-7 ADR) cancers. The piperazinyll derivative **44** showed the greatest anti-proliferative effect across the panel of cell lines, with IC₅₀ values ranging from 0.74 to 3.85 μM. The anti-proliferative effect of compound **44** was more marked against the breast, cervical and ovarian cell lines. A correlation between anti-proliferative effect and redox potential of the ferrocene/ferricenium couple is observed for this series of compounds, with compound **44** being the most easily oxidised member of the series.



Payen *et al* have prepared ferrocenyl derivatives of the non-steroidal anti-androgen nilutamide, used in the treatment of prostate cancer.⁶⁴ Analogues of nilutamide were prepared where the C-5 position of the hydantoin ring was substituted with ferrocene **45** and a *para*-anisyl group, **46**. Both analogues showed negligible binding affinity for the androgen receptor (AR), which is claimed to play a vital role in cancer development. The *in vitro* anti-proliferative effect of both compounds was strongest in the hormone independent PC-3 prostate cancer cell line. IC₅₀ values of 5.4 ± 0.5 μM and 5.6 ± 0.4 μM were obtained for compounds **45** and **46**, respectively. These results indicate that any anti-proliferative effect is due solely to the aromatic character of ferrocene and is independent of its organometallic nature.



Organometallic derivatives of the steroidal androgens, testosterone and dihydrotestosterone (DHT), have been prepared by Top *et al.*⁶⁵ Substitution with an ethynylferrocene group was carried out at the 17 α position of the steroid, to give compounds such as **47**. All of the compounds were found to show only a negligible binding affinity for the androgen receptor (AR). In the hormone independent PC-3 cell line, compound **47** and the corresponding DHT derivative displayed a strong anti-proliferative effect, with IC₅₀ values of 4.7 and 8.3 μ M, respectively. As expected, both testosterone and DHT had no effect in this AR negative cell line.

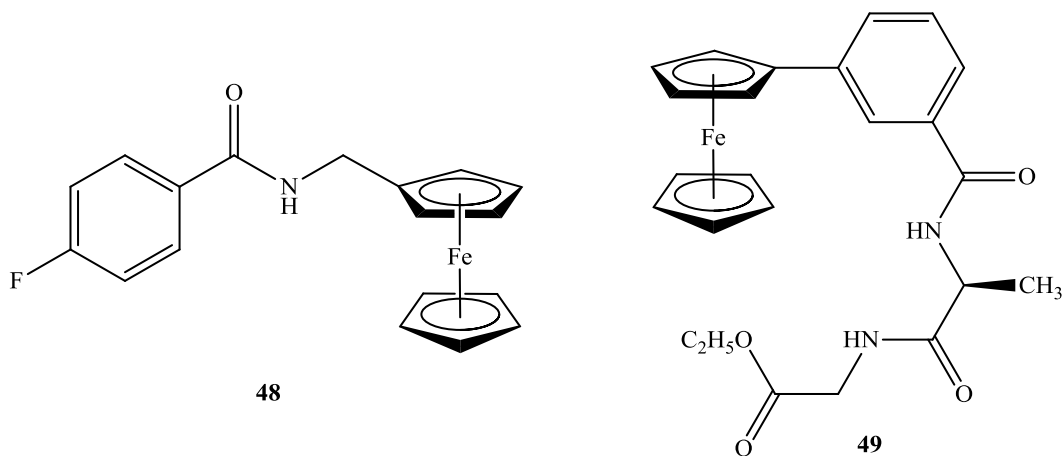


1.2.4. Ferrocenyl-peptide conjugates

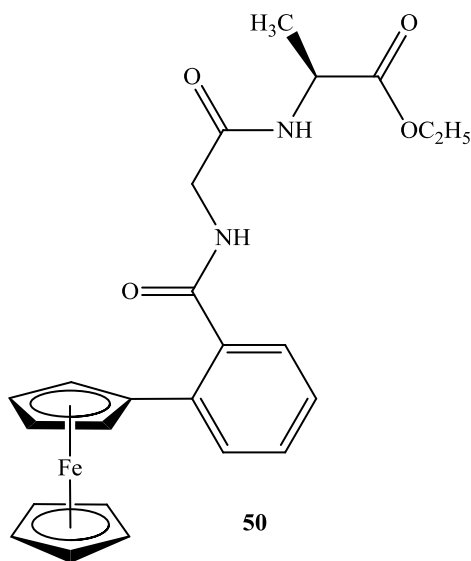
A series of *N*-(ferrocenylmethyl)fluorobenzene-carboxamide derivatives were prepared by Kelly *et al* using standard peptide coupling procedures.⁶⁶ The strategic replacement of hydrogen with fluorine is a recognised strategy in the development of various drug types. *In vitro* evaluation in the ER(-) MDA-MB-435-S-F breast cancer cell line revealed the 4-fluoro derivative **48** as the compound showing the strongest anti-proliferative effect. An IC₅₀ value of between 11 and 14 μ M was determined for compound **48**. As the concentration of **48** increased, the anti-proliferative effect increased, indicating a dose-dependent relationship.

N-(ferrocenyl)benzoyl dipeptide esters have also been shown to be highly active *in vitro*.^{67,68,69} Initially, *N*-{*ortho*-(ferrocenyl)-benzoyl}-glycine ethyl ester was tested for *in vitro* anti-proliferative activity in the H1299 non-small cell lung cancer (NSCLC) cell line. This compound was found to be cytotoxic, with an IC₅₀ value of 48 μ M, whilst the starting material, *ortho*-ferrocenyl ethyl benzoate, was completely inactive in this cell line. Therefore, other derivatives were evaluated for their anti-proliferative effect in the H1299

cell line. Savage *et al* prepared a series of *N*-{*meta*-(ferrocenyl)-benzoyl} dipeptide derivatives containing L-alanine as the first α -amino acid in the peptide chain.⁶⁷ The L-alanine-glycine ethyl ester derivative **49** was found to have an IC₅₀ value of 26 μ M in the H1299 cell line, whilst an IC₅₀ value of 21 μ M was calculated for the corresponding *ortho*-analogue.



A series of *N*-{*ortho*-(ferrocenyl)-benzoyl} dipeptide derivatives containing glycine as the first α -amino acid in the peptide chain were prepared by Corry *et al*.⁶⁸ The glycine-L-alanine ethyl ester derivative **50** was shown to exhibit a strong anti-proliferative effect in the H1299 cell line, with an IC₅₀ value of 5.3 μ M. Subsequently, the *in vitro* anti-proliferative effect of the *meta*- and *para*- analogues of **50** was investigated, and the IC₅₀ values determined were 4.0 and 6.6 μ M, respectively.⁶⁹ These results indicate that orientation around the central benzoyl moiety is not a crucial factor for biological activity. However, the order of the α -amino acids in the dipeptide chain was found to influence the biological activity. *N*-(ferrocenyl)benzoyl dipeptide derivatives that contained glycine as the *N*-terminal amino acid had a greater anti-proliferative effect in the H1299 cell line than derivatives that contained L-alanine as the *N*-terminal amino acid.

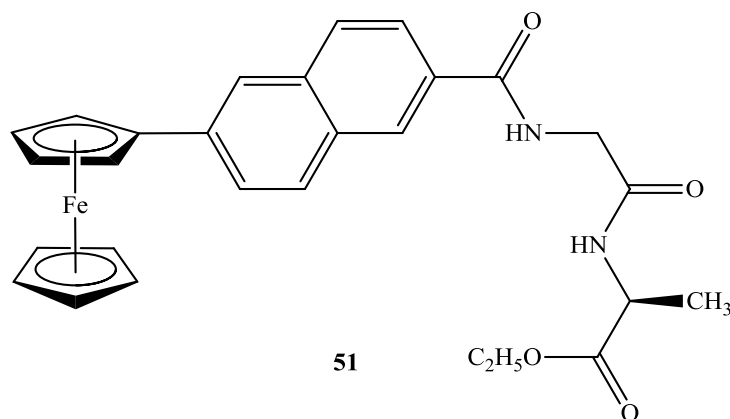


The biological activity of these compounds is possibly due to their low redox potentials and their ability to form reactive oxygen species (ROS) under physiological conditions. The anti-proliferative effect of **50** is not solely due to ferrocene so it is plausible that the peptide chain is involved in a secondary mode of action.⁶⁷ Cell cycle analysis was performed on a control sample and on cells treated with *N*-{*ortho*-(ferrocenyl)-benzoyl}-glycine-L-alanine ethyl ester (compound **50**) at concentrations of 5 μM , 10 μM , 20 μM and 40 μM . As the concentration of compound **50** increases, the percentage of cells in the G1 phase of the cell cycle decreases, suggesting a block in the G2/M phase, preventing the cells re-entering the G1 phase.⁶⁹

Corry *et al* prepared a *N*-(ferrocenyl)benzoyl tripeptide and tetrapeptide ethyl ester derivatives, using standard peptide coupling procedures.⁷⁰ The *N*-{*ortho*-(ferrocenyl)-benzoyl}-glycine-glycine-glycine ethyl ester was tested *in vitro* for anti-proliferative effect in the H1299 cell line and an IC_{50} value of 63 μM was determined. The tetra-glycine analogue was also tested, however, it did not register an IC_{50} value in the concentration range tested (1-100 μM). Thus, it can be concluded that a dipeptide chain is required for optimum activity.

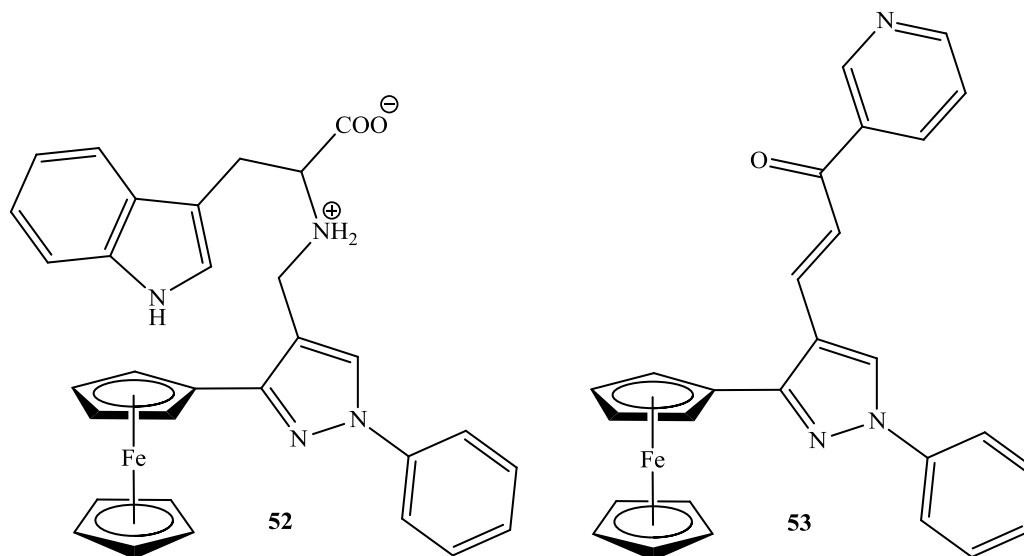
The importance of the benzoyl linker in this series of compounds was investigated by Mooney *et al*.⁷¹ The benzoyl unit that links the redox active ferrocene group to the peptide chain was replaced by a naphthoyl unit to give a series of *N*-(ferrocenyl)naphthoyl dipeptide ethyl esters. The naphthoyl unit employed contained the dipeptide chain

substituted in the 2-position and the ferrocene moiety substituted in either the 3- or 6-position. Assessment of *in vitro* anti-proliferative effect in the H1299 cell line, revealed this series of compounds to be more potent than the benzoyl analogues, with IC₅₀ values below 10 μM determined for each compound. The *N*-(6-ferrocenyl-2-naphthoyl)-glycine-L-alanine ethyl ester **51** exhibited the strongest anti-proliferative effect, with an IC₅₀ value of 1.3 ± 0.1 μM. Cisplatin **1** was found to have an IC₅₀ value of 1.5 ± 0.1 μM, thus compound **1** and **51** are equipotent in this cell line.

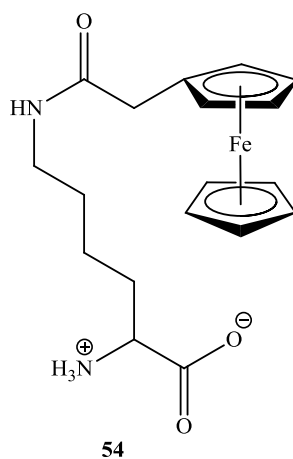


Joksović *et al* appended a ferrocenyl pyrazole unit to the *N*-terminal of α-amino acids.⁷² The *in vitro* anti-proliferative effect of these modified amino acids was evaluated in cervix adenocarcinoma (HeLa), melanoma (Fem-x) cells and myelogenous leukaemia (K562) cell lines. IC₅₀ values were found to vary from >60 μM to around 6 μM across the range of cell lines. The L-tryptophan derivative **52** showed the strongest overall anti-proliferative effect, with IC₅₀ values of 7.95 ± 1.42 μM, 9.78 ± 0.27 μM and 6.34 ± 1.24 μM for each respective cell line.

Subsequently, Ratković *et al* prepared a series of compounds wherein the ferrocenyl pyrazole unit was appended to various chalcones.⁷³ *In vitro* evaluation in the same three cell lines (HeLa, Fem-x and K562) revealed compound **53** to be the most active ferrocenyl chalcone. The strongest anti-proliferative effect for **53** was observed in the myelogenous leukaemia K562 cell line. An IC₅₀ value of 5.42 ± 0.53 μM was determined for **53**, and is comparable with cisplatin in this cell line (IC₅₀ value = 5.90 ± 0.20 μM).

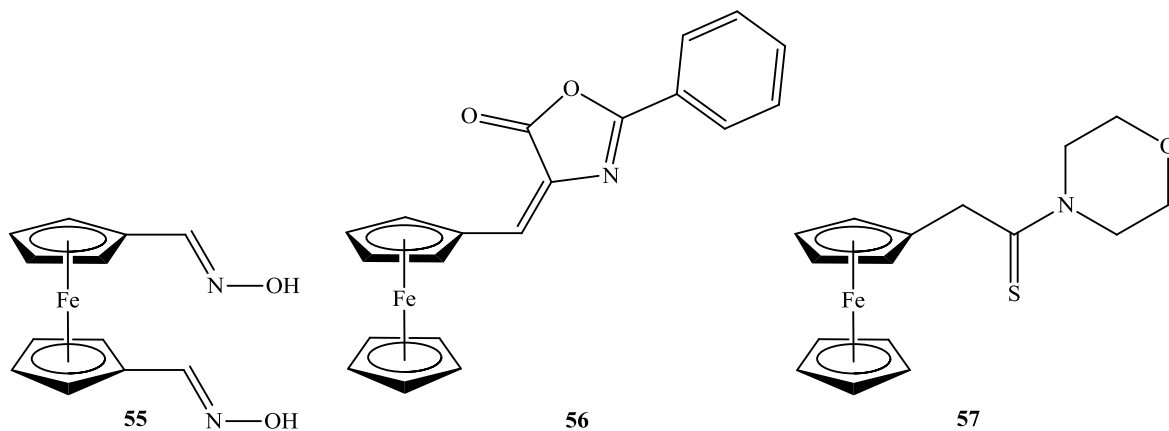


Working towards the aim of incorporating an unnatural ferrocene amino acid into a nucleic-acid-binding protein in order to confer nucleolytic activity, Gellett *et al* prepared a N^α - N^ϵ -(ferrocene-1-acetyl)-L-lysine conjugate **54**.⁷⁴ The ability of this ferrocene amino acid to cleave DNA was studied by incubation of **54** with supercoiled pUC19 DNA. At low concentrations, compound **54** predominantly induced single strand cleavage to give circular nicked DNA. At higher concentrations, the levels of double strand cleavage were found to increase to give 47% linear DNA. In contrast, assays performed with ferroceneacetic acid showed no DNA cleavage. It is possible that the amine group of the lysine zwitterion present in compound **54** may bring the redox centre of the ferrocene moiety into close proximity of the negatively charged DNA backbone.

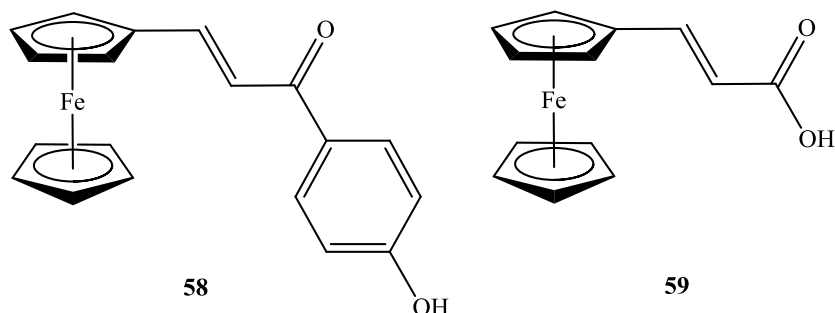


1.2.5. Other metallocene complexes as anti-cancer agents

Topoisomerases are enzymes that are crucial in DNA replication, transcription and repair. They can be divided into two categories, topoisomerase I and topoisomerase II. Due to their crucial role in DNA function, topoisomerase I and topoisomerase II inhibitors have become important targets for researchers. Several ferrocenyl derivatives have been prepared as topoisomerase II inhibitors. The carboxaldoxime derivative **55** had a strong anti-proliferative effect when tested *in vitro* in the Colo-205 colon carcinoma cell line.⁷⁵ It is proposed that complexation with the topoisomerase II enzyme is as a result of nitrogen and oxygen interaction between **55** and the topoisomerase. The azalactone derivative **56** allows ATP binding to the topoisomerase enzyme and induces the formation of cleavable complexes, while thiomorpholide amido methyl ferrocene **57** competes with ATP binding and inhibits the catalytic activity of the enzyme.⁷⁶ The exact role of ferrocene in these examples is unclear.

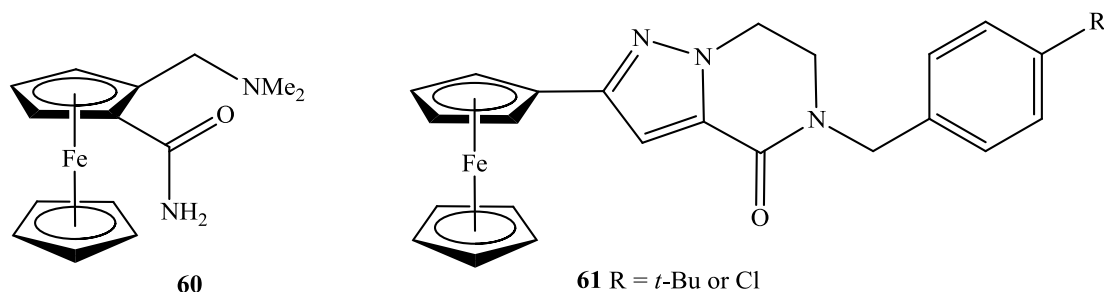


A series of ferrocenyl-aryl-chalcones were prepared by Zsoldos-Mády *et al* and evaluated *in vitro* in the human leukaemia (HL-60) cell line.⁷⁷ Compound **58** showed the strongest anti-proliferative effect (IC_{50} value = 1.75 μ M). Substitution of the phenolic hydroxyl group of **58** with either an acetyl or methyl group did not alter the anti-proliferative effect significantly. Neither did the attachment of a bulky acetylated glucose or galactose moiety. Removal of the phenyl ring to give the acrylic acid derivative **59** resulted in a decrease in anti-proliferative effect. Compound **59** was found to display an IC_{50} value of 9.4 ± 3 μ M in the HL-60 cell line.⁷⁸



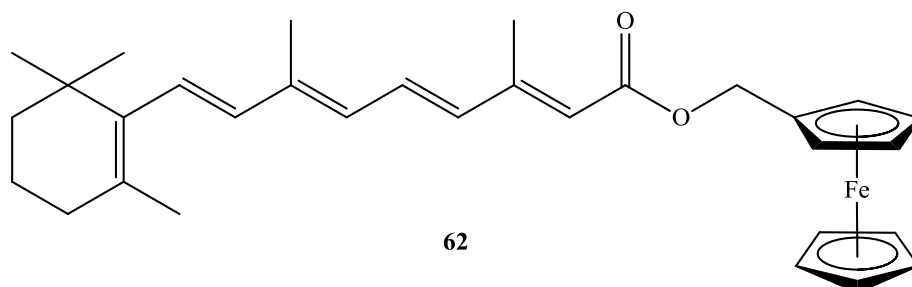
Cyclodextrin (CD) inclusion complexes have been shown to be useful in enhancing the solubility, stability and bioavailability of drug molecules. Petrovski *et al* have studied the effect of CD inclusion complexes on the *in vitro* anti-proliferative activity of a group of 1,2-disubstituted ferrocenes in the Ehrlich ascites tumour (EAT) cell line.⁷⁹ Compound **60** was found to display an IC_{50} value of $71.2 \pm 1.1 \mu\text{M}$. Upon inclusion in TRIMEB and HP β CD, the IC_{50} value decreases to $25.2 \pm 1.0 \mu\text{M}$ and $20.0 \pm 1.1 \mu\text{M}$, respectively.

Xie *et al* prepared a series of novel 5-alkyl-2-ferrocenyl-6,7-dihydropyrazolo[1,5-*a*]pyrazin-4(5*H*)-one derivatives.⁸⁰ *In vitro* evaluation in the A549 lung cancer cell line, revealed compound **61** to be the most active derivative, with an IC_{50} value of $10 \mu\text{M}$ after 48 hours of treatment. Examination of cells treated with $20 \mu\text{M}$ of compound **61** under a phase contrast microscope, revealed the occurrence of morphological changes associated with apoptosis, particularly when $R = t\text{-Bu}$.⁸¹ Compound **61** was also found to significantly increase the levels of intracellular reactive oxygen species (ROS).

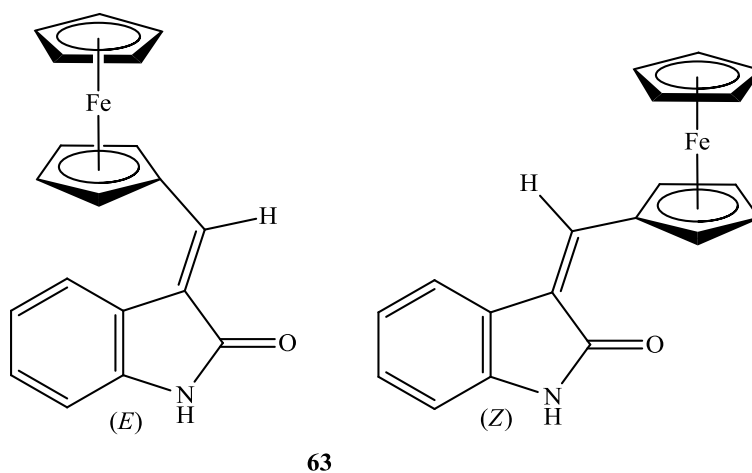


13-*cis*-Retinoic acid possesses potential as a chemotherapeutic agent, but harsh side effects at the therapeutically required dosage levels prevent it from being of practical value. Long *et al* have prepared a series of organometallic derivatives consisting of 13-*cis*-retinoic acid appended to a ferrocenyl group *via* either alkyl or aryl linkers.⁸² These derivatives were evaluated *in vitro* for anti-proliferative activity against three cancer cell lines: lung (A549),

liver (BEL7404) and tongue (Tca). All the compounds tested were found to have moderate anti-cancer activity, with IC_{50} values typically varying from 42 μM to 18.6 μM . Compound **62** showed the best anti-proliferative effect, with IC_{50} values in the range of 18.6 to 22.3 μM against all cell lines.

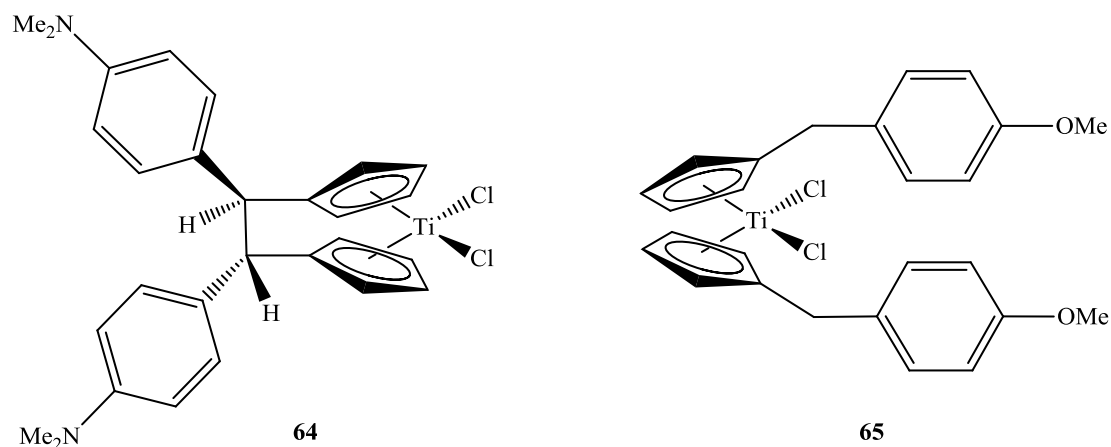


The methyldiene-1,3-dihydro-2H-indol-2-one (oxindole) skeleton is found in a number of compounds with promising anti-cancer activity. It was therefore of interest to Spencer *et al.* to investigate the anti-cancer potential of a ferrocene-substituted oxindole, compound **63**.⁸³ Both the (*Z*)- and (*E*)- isomers of compound **63** were evaluated against B16 (Murine Melanoma) and Vero (African Green Monkey Kidney Epithelia) cell lines and were found to exhibit strong anti-proliferative activities. An IC_{50} value of $0.7 \pm 0.2 \mu M$ was obtained for the (*Z*)-isomer in both cell lines and IC_{50} values of $0.9 \pm 0.05 \mu M$ and $1.2 \pm 0.3 \mu M$ were obtained for the (*E*)-isomer in each cell line, respectively.

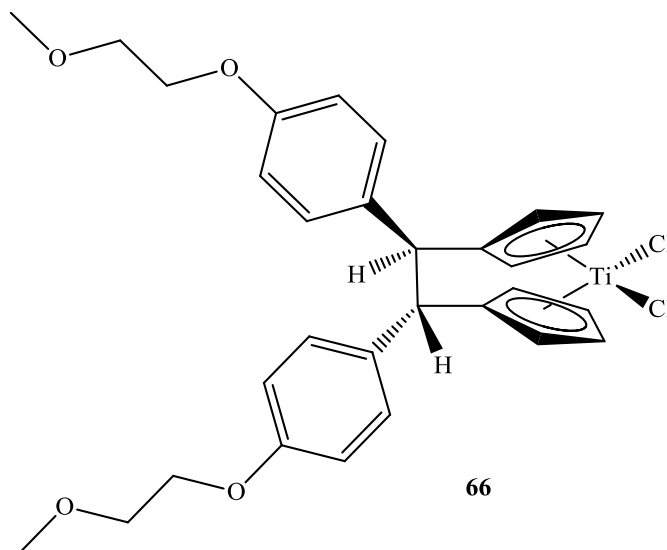


Metallocene dichlorides with Ti, V and Nb metal centres have also shown anti-tumour activity.⁸⁴ Titanocene dichloride **14** reached phase II clinical trials for patients with renal cell carcinoma and metastatic breast cancer. Substituted titanocene dichlorides have been prepared by Tacke *et al* as potential anti-cancer drugs.²⁷ The anti-proliferative activity of

these derivatives has been consistently evaluated in the pig kidney cell line LLC-PK. In addition, the two most promising compounds **64** and **65** have been evaluated in 36 human tumour cell lines.⁸⁴

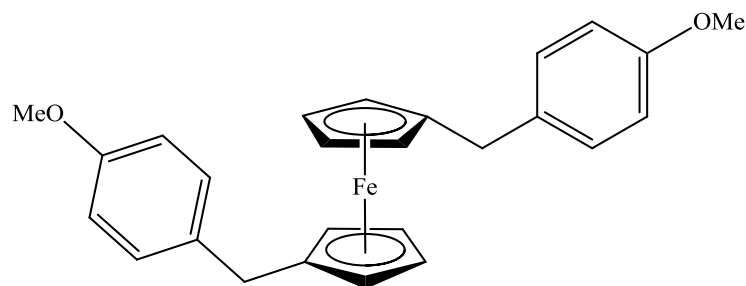


Prostate, cervix and renal cell cancer were all shown to be prime targets for these novel titanocenes. *In vivo* experiments with these two derivatives showed the successful treatment of xenografted Caki-1 tumours and xenografted Ehrlich's ascites tumour in mice. Surprisingly, a change in the substitution pattern of titanocenes can also lead to proliferative effects, as observed by Strohfeldt *et al* for compound **66**.⁸⁵



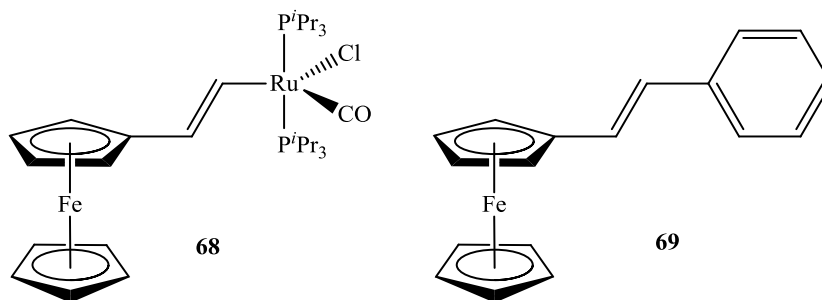
Considering that Top *et al* had previously observed a strong estrogenic/proliferative effect for the titanocene dichloride tamoxifen derivative **42**, compounds **65** and **66** were evaluated *in vitro* in the ER(+) MCF-7 breast cancer cell line.⁸⁶ Compound **66** exhibited a strong proliferative effect in this cell line when tested at 10 μ M. On the other hand, compound **65**

does not exhibit a significant effect at 10 μM , suggesting that this molecule is more stable to total hydrolysis than compound **66**. The ferrocenyl analogue **67** of compound **65** was also prepared as part of this study and evaluated *in vitro* in both the ER(+) MCF-7 cell line and the ER(-) MDA-MB231 cell line. At a concentration of 10 μM , compound **67** shows a slight anti-proliferative effect in the MCF-7 cell line. In the MDA-MB231 cell line, an IC_{50} value of 95 μM was determined for **67**.



67

Mixed binuclear ferrocene/ruthenium organometallic species, for example compound **68**, have been shown to exhibit anti-proliferative effects in colon carcinoma (HT-29) and breast cancer (MCF-7) cell lines.⁸⁷ The PF_6^- salt of compound **68** displayed a slightly stronger anti-proliferative effect compared to **68**, with IC_{50} values of $9.2 \pm 0.4 \mu\text{M}$ and $4.8 \pm 0.2 \mu\text{M}$ in the HT-29 and MCF-7 cell line, respectively. The mononuclear analogue **69** was completely inactive in the HT-29 cell line and displayed only a weak anti-proliferative effect in the MCF-7 cell line, with an IC_{50} value of $54.8 \pm 14.5 \mu\text{M}$. These results suggest that the presence of the ruthenium centre may play an important role in triggering anti-proliferative effect.



1.3. Conclusions

Cancer is a devastating disease that can affect any part of the human anatomy. Lung cancer and metastatic melanoma are two forms of cancer for which survival rates remain critically low. The current chemotherapeutic treatments for these diseases are largely ineffective, due to their reliance on traditional chemotherapeutic drugs, for which there are widespread resistance problems and severe toxic side effects.

Research in the area of metal anti-cancer drugs is flourishing, with metallocenes receiving much attention. Ferrocene is the archetypal metallocene; it is a small, rigid, lipophilic molecule that can easily penetrate the cell membrane. Over the past decade, ferrocene derivatives have shown great promise in the area of medicinal organometallic chemistry. For example, ferroquine (SR97193), a unique anti-malarial drug candidate has commenced phase II clinical trials in combination with artesunate.³² Biologically active ferrocene derivatives can be divided into two groups, namely, novel ferrocenyl derivatives found to exert a biological effect and ferrocenyl analogues of known drugs. In the second case, ferrocene is frequently used as a bioisostere for a phenyl ring contained in the original drug molecule. This strategy was devised to overcome problems related to drug resistance and the ferrocifens (ferrocenyl tamoxifen derivatives) represent the most successful application of this approach in cancer research. Ferrocifens have shown promising results *in vitro* in both ER(+) and ER(-) breast cancer cell lines, whereas the parent molecule tamoxifen only expresses an anti-proliferative effect in ER(+) cells.

The reversible redox properties of ferrocene have been strongly associated with the biological activity of ferrocenyl compounds. Ferricenium salts known to inhibit tumour growth have been shown to produce hydroxyl radicals (HO[•]) *via* the Fenton reaction under physiological conditions. Ferrocenyl derivatives have also been shown to significantly increase the levels of intracellular reactive oxygen species (ROS) *in vitro*. High levels of intracellular ROS can lead to oxidative damage to DNA and subsequent cell death.

References

1. R. W. Ruddon, *Cancer Biology*, Oxford University Press, **2007**.
2. D. M. Parkin, F. Bray, J. Ferlay and P. Pisani, *Ca-a Cancer Journal for Clinicians*, 2005, **55**, 74-108.
3. D. W. Donnelly, Gavin, A. T., Comber, H. "Cancer in Ireland: A summary report," 2009.
4. D. W. Donnelly, Gavin, A. T., Comber, H. "Cancer in Ireland 1994-2004: A comprehensive report," 2009.
5. J. Ferlay, P. Autier, M. Boniol, M. Heanue, M. Colombet and P. Boyle, *Annals of Oncology*, 2007, **18**, 581-592.
6. U. Amarasena Isuru, A. E. Walters Julia, R. Wood-Baker and K. Fong In *Cochrane Database of Systematic Reviews*; John Wiley & Sons, Ltd: Chichester, UK, 2008.
7. S. Burdett, L. Stewart and L. Rydzewska In *Cochrane Database of Systematic Reviews*; John Wiley & Sons, Ltd: Chichester, UK, 2007.
8. N.-S. C. L. C. C. Group In *Cochrane Database of Systematic Reviews*; John Wiley & Sons, Ltd: Chichester, UK, 2000.
9. R. M. MacKie, A. Hauschild and A. M. M. Eggermont, *Annals of Oncology*, 2009, **20**, 1-7.
10. F. El Ghissassi, R. Baan, K. Straif, Y. Grosse, B. Secretan, V. Bouvard, L. Benbrahim-Tallaa, N. Guha, C. Freeman, L. Galichet and V. Coglianò, *The Lancet Oncology*, 2009, **10**, 751-752.
11. P. Mohr, A. M. M. Eggermont, A. Hauschild and A. Buzaid, *Annals of Oncology*, 2009, **20**, 14-21.
12. G. L. Patrick, *An Introduction to Medicinal Chemistry*, 3rd ed., Oxford University Press, **2005**.
13. S. Neidle, *Cancer Drug Design and Discovery*, Elsevier Academic Press, **2008**.
14. C. Avendaño and J. C. Menéndez, *Medicinal Chemistry of Anticancer Drugs*, Elsevier, **2008**.
15. D. Wang and S. J. Lippard, *Nature Reviews Drug Discovery*, 2005, **4**, 307-320.
16. T. E. Stinchcombe and M. A. Socinski, *Proc Am Thorac Soc*, 2009, **6**, 233-241.
17. G. Giaccone, *Drugs*, 2000, **59**, 9-17.
18. H. J. Gogas, J. M. Kirkwood and V. K. Sondak, *Cancer*, 2007, **109**, 455-464.
19. H. Achiwa, T. Oguri, S. Sato, H. Maeda, T. Niimi and R. Ueda, *Cancer Science*, 2004, **95**, 753-757.
20. B. Rosenberg, L. Vancamp and T. Krigas, *Nature*, 1965, **205**, 698-&.
21. B. Rosenberg, L. Vancamp, J. E. Trosko and V. H. Mansour, *Nature*, 1969, **222**, 385-&.
22. T. Gianferrara, I. Bratsos and E. Alessio, *Dalton Transactions*, 2009, 7588-7598.
23. C. G. Hartinger and P. J. Dyson, *Chemical Society Reviews*, 2009, **38**, 391-401.
24. Y. K. Yan, M. Melchart, A. Habtemariam and P. J. Sadler, *Chemical Communications*, 2005, 4764-4776.
25. E. W. Neuse, *Journal of Inorganic and Organometallic Polymers and Materials*, 2005, **15**, 3-32.
26. P. Kopfmaier and H. Kopf, *Chemical Reviews*, 1987, **87**, 1137-1152.

27. K. Strohfeltd and M. Tacke, *Chemical Society Reviews*, 2008, **37**, 1174-1187.
28. T. J. Kealy and P. L. Pauson, *Nature*, 1951, **168**, 1039-1040.
29. S. A. Miller, J. A. Tebboth and J. F. Tremaine, *Journal of the Chemical Society*, 1952, 632-635.
30. N. J. Long, *Metallocenes : An Introduction to Sandwich Complexes*, Blackwell Science, **1998**.
31. M. F. R. Fouda, M. M. Abd-Elzaher, R. A. Abdelsamaia and A. A. Labib, *Applied Organometallic Chemistry*, 2007, **21**, 613-625.
32. D. Dive and C. Biot, *Chemmedchem*, 2008, **3**, 383-391.
33. P. Kopfmaier, H. Kopf and E. W. Neuse, *Journal of Cancer Research and Clinical Oncology*, 1984, **108**, 336-340.
34. D. Osella, M. Ferrali, P. Zanello, F. Laschi, M. Fontani, C. Nervi and G. Cavigiolio, *Inorganica Chimica Acta*, 2000, **306**, 42-48.
35. G. Tabbi, C. Cassino, G. Cavigiolio, D. Colangelo, A. Ghiglia, I. Viano and D. Osella, *Journal of Medicinal Chemistry*, 2002, **45**, 5786-5796.
36. K. Kowalski, J. Zakrzewski, N. J. Long, N. Suwaki, D. J. Mann and A. J. P. White, *Dalton Transactions*, 2006, 571-576.
37. K. Kowalski, N. Suwaki, J. Zakrzewski, A. J. P. White, N. J. Long and D. J. Mann, *Dalton Transactions*, 2007, 743-748.
38. G. Jaouen, *Bioorganometallics : Biomolecules, Labeling, Medicine*, Wiley-VCH, **2006**.
39. V. C. Jordan, *Journal of Medicinal Chemistry*, 2003, **46**, 883-908.
40. S. Top, J. Tang, A. Vessieres, D. Carrez, C. Provot and G. Jaouen, *Chemical Communications*, 1996, 955-956.
41. S. Top, A. Vessieres, G. Leclercq, J. Quivy, J. Tang, J. Vaissermann, M. Huche and G. Jaouen, *Chemistry-a European Journal*, 2003, **9**, 5223-5236.
42. P. Pigeon, S. Top, A. Vessieres, M. Huche, E. A. Hillard, E. Salomon and G. Jaouen, *Journal of Medicinal Chemistry*, 2005, **48**, 2814-2821.
43. D. Osella, H. Mahboobi, D. Colangelo, G. Cavigiolio, A. Vessieres and G. Jaouen, *Inorganica Chimica Acta*, 2005, **358**, 1993-1998.
44. E. Hillard, A. Vessieres, L. Thouin, G. Jaouen and C. Amatore, *Angewandte Chemie-International Edition*, 2006, **45**, 285-290.
45. P. W. Fan, F. G. Zhang and J. L. Bolton, *Chemical Research in Toxicology*, 2000, **13**, 45-52.
46. E. A. Hillard, P. Pigeon, A. Vessieres, C. Amatore and G. Jaouen, *Dalton Transactions*, 2007, 5073-5081.
47. A. Nguyen, S. Top, A. Vessières, P. Pigeon, M. Huché, E. A. Hillard and G. Jaouen, *Journal of Organometallic Chemistry*, 2007, **692**, 1219-1225.
48. A. Nguyen, S. Top, P. Pigeon, A. Vessieres, E. A. Hillard, M. A. Plamont, M. Huche, C. Rigamonti and G. Jaouen, *Chemistry-a European Journal*, 2009, **15**, 684-696.
49. A. Vessieres, S. Top, P. Pigeon, E. Hillard, L. Boubeker, D. Spera and G. Jaouen, *Journal of Medicinal Chemistry*, 2005, **48**, 3937-3940.

50. D. Hamels, Patrick M. Dansette, Elizabeth A. Hillard, S. Top, A. Vessières, P. Herson, G. Jaouen and D. Mansuy, *Angewandte Chemie International Edition*, 2009, **48**, 9124-9126.
51. A. Nguyen, V. Marsaud, C. Bouclier, S. Top, A. Vessieres, P. Pigeon, R. Gref, P. Legrand, G. Jaouen and J. M. Renoir, *International Journal of Pharmaceutics*, 2008, **347**, 128-135.
52. E. Allard, C. Passirani, E. Garcion, P. Pigeon, A. Vessieres, G. Jaouen and J. P. Benoit, *Journal of Controlled Release*, 2008, **130**, 146-153.
53. E. A. Hillard, A. Vessières, S. Top, P. Pigeon, K. Kowalski, M. Huché and G. Jaouen, *Journal of Organometallic Chemistry*, 2007, **692**, 1315-1326.
54. E. Hillard, A. Vessieres, F. Le Bideau, D. Plazuk, D. Spera, M. Huche and G. Jaouen, *Chemmedchem*, 2006, **1**, 551-559.
55. J. B. Heilmann, E. A. Hillard, M. A. Plamont, P. Pigeon, M. Bolte, G. Jaouen and A. Vessieres, *Journal of Organometallic Chemistry*, 2008, **693**, 1716-1722.
56. P. Pigeon, S. Top, O. Zekri, E. A. Hillard, A. Vessières, M.-A. Plamont, O. Buriez, E. Labbé, M. Huché, S. Boutamine, C. Amatore and G. Jaouen, *Journal of Organometallic Chemistry*, 2009, **694**, 895-901.
57. O. Zekri, E. A. Hillard, S. Top, A. Vessieres, P. Pigeon, M. A. Plamont, M. Huche, S. Boutamine, M. J. McGlinchey, H. Muller-Bunz and G. Jaouen, *Dalton Transactions*, 2009, 4318-4326.
58. Q. Michard, G. Jaouen, A. Vessieres and B. A. Bernard, *Journal of Inorganic Biochemistry*, 2008, **102**, 1980-1985.
59. D. Plazuk, A. Vessieres, E. A. Hillard, O. Buriez, E. Labbe, P. Pigeon, M. A. Plamont, C. Amatore, J. Zakrzewski and G. Jaouen, *Journal of Medicinal Chemistry*, 2009, **52**, 4964-4967.
60. M. Gormen, D. Plazuk, P. Pigeon, E. A. Hillard, M.-A. Plamont, S. Top, A. Vessières and G. Jaouen, *Tetrahedron Letters*, 2010, **51**, 118-120.
61. S. Top, E. B. Kaloun, A. Vessieres, G. Leclercq, I. Laios, M. Ourevitch, C. Deuschel, M. J. McGlinchey and G. Jaouen, *Chembiochem*, 2003, **4**, 754-761.
62. S. Top, E. B. Kaloun, A. Vessieres, I. Laios, G. Leclercq and G. Jaouen, *Journal of Organometallic Chemistry*, 2002, **643**, 350-356.
63. A. P. Ferreira, J. L. F. da Silva, M. T. Duarte, M. F. M. da Piedade, M. P. Robalo, S. G. Harjivan, C. Marzano, V. Gandin and M. M. Marques, *Organometallics*, 2009, **28**, 5412-5423.
64. O. Payen, S. Top, A. Vessieres, E. Brule, M. A. Plamont, M. J. McGlinchey, H. Muller-Bunz and G. Jaouen, *Journal of Medicinal Chemistry*, 2008, **51**, 1791-1799.
65. S. Top, C. Thibaudeau, A. Vessieres, E. Brule, F. Le Bideau, J. M. Joerger, M. A. Plamont, S. Samreth, A. Edgar, J. Marrot, P. Herson and G. Jaouen, *Organometallics*, 2009, **28**, 1414-1424.
66. P. N. Kelly, A. Prêtre, S. Devoy, I. O'Rielly, R. Devery, A. Goel, J. F. Gallagher, A. J. Lough and P. T. M. Kenny, *Journal of Organometallic Chemistry*, 2007, **692**, 1327-1331.
67. A. Goel, D. Savage, S. R. Alley, P. N. Kelly, D. O'Sullivan, H. Mueller-Bunz and P. T. M. Kenny, *Journal of Organometallic Chemistry*, 2007, **692**, 1292-1299.

68. A. J. Corry, A. Goel, S. R. Alley, P. N. Kelly, D. O'Sullivan, D. Savage and P. T. M. Kenny, *Journal of Organometallic Chemistry*, 2007, **692**, 1405-1410.
69. A. J. Corry, N. O'Donovan, Á. Mooney, D. O'Sullivan, D. K. Rai and P. T. M. Kenny, *Journal of Organometallic Chemistry*, 2009, **694**, 880-885.
70. A. J. Corry, A. Mooney, D. O'Sullivan and P. T. M. Kenny, *Inorganica Chimica Acta*, 2009, **362**, 2957-2961.
71. Á. Mooney, A. J. Corry, D. O'Sullivan, D. K. Rai and P. T. M. Kenny, *Journal of Organometallic Chemistry*, 2009, **694**, 886-894.
72. M. D. Joksovic, V. Markovic, Z. D. Juranic, T. Stanojkovic, L. S. Jovanovic, I. S. Damljanovic, K. M. Szecsenyi, N. Todorovic, S. Trifunovic and R. D. Vukicevic, *Journal of Organometallic Chemistry*, 2009, **694**, 3935-3942.
73. Z. Ratkovic, Z. D. Juranic, T. Stanojkovic, D. Manojlovic, R. D. Vukicevic, N. Radulovic and M. D. Joksovic, *Bioorganic Chemistry*, 2010, **38**, 26-32.
74. A. M. Gellett, P. W. Huber and P. J. Higgins, *Journal of Organometallic Chemistry*, 2008, **693**, 2959-2962.
75. Y. N. V. Gopal, D. Jayaraju and A. K. Kondapi, *Archives of Biochemistry and Biophysics*, 2000, **376**, 229-235.
76. A. D. S. Krishna, G. Panda and A. K. Kondapi, *Archives of Biochemistry and Biophysics*, 2005, **438**, 206-216.
77. V. Zsoldos-Mady, A. Csampai, R. Szabo, E. Meszaros-Alapi, J. Pasztor, F. Hudecz and P. Sohar, *Chemmedchem*, 2006, **1**, 1119-1125.
78. Z. Miklán, R. Szabó, V. Zsoldos-Mády, J. Reményi, Z. Bánóczi and F. Hudecz, *Peptide Science*, 2007, **88**, 108-114.
79. Z. Petrovski, M. de Matos, S. S. Braga, C. C. L. Pereira, M. L. Matos, I. S. Goncalves, M. Pillinger, P. M. Alves and C. C. Romao, *Journal of Organometallic Chemistry*, 2008, **693**, 675-684.
80. Y. S. Xie, X. H. Pan, B. X. Zhao, J. T. Liu, D. S. Shin, J. H. Zhang, L. W. Zheng, J. Zhao and J. Y. Miao, *Journal of Organometallic Chemistry*, 2008, **693**, 1367-1374.
81. X. H. Pan, X. Liu, B. X. Zhao, Y. S. Xie, D. S. Shin, S. L. Zhang, J. Zhao and J. Y. Miao, *Bioorganic & Medicinal Chemistry*, 2008, **16**, 9093-9100.
82. B. H. Long, S. Z. Liang, D. C. Xin, Y. B. Yang and J. N. Xiang, *European Journal of Medicinal Chemistry*, 2009, **44**, 2572-2576.
83. J. Spencer, A. P. Mendham, A. K. Kotha, S. C. W. Richardson, E. A. Hillard, G. Jaouen, L. Male and M. B. Hursthouse, *Dalton Transactions*, 2009, 918-921.
84. C. Pampillón, N. J. Sweeney, K. Strohfeltd and M. Tacke, *Journal of Organometallic Chemistry*, 2007, **692**, 2153-2159.
85. K. Strohfeltd, H. Muller-Bunz, C. Pampillon, N. J. Sweeney and M. Tacke, *European Journal of Inorganic Chemistry*, 2006, 4621-4628.
86. A. Vessières, M.-A. Plamont, C. Cabestaing, J. Claffey, S. Dieckmann, M. Hogan, H. Müller-Bunz, K. Strohfeltd and M. Tacke, *Journal of Organometallic Chemistry*, 2009, **694**, 874-879.
87. I. Ott, K. Kowalski, R. Gust, J. Maurer, P. Mücke and R. F. Winter, *Bioorganic & Medicinal Chemistry Letters*, 2010, **20**, 866-869.

Chapter 2

Synthesis and structural characterisation of *N*-(ferrocenyl)naphthoyl amino acid and dipeptide derivatives which contain α -amino acids

2.1. Introduction

Amino acids are one of nature's most essential building blocks; they are naturally occurring organic compounds with an amino group at one terminus and a carboxylic acid group at the other. In nature, individual α -amino acid units are linked together by an amide bond to form peptides, and much larger macromolecules known as proteins. Peptides and proteins form an essential part of any biological system and are involved in many diverse processes *e.g.* proteins known as enzymes are responsible for catalysing a vast range of specific chemical reactions within the cell. This remarkable variety in protein function is due to the versatile nature of α -amino acids; there are 20 "essential" α -amino acids, each containing a side chain functional group that varies in size, shape, charge, hydrogen-bonding capacity, hydrophobic character, and chemical reactivity.¹

The α -amino acids L-tryptophan and L-tyrosine are also key precursors in the biosynthesis of many important neurotransmitters and hormones. Clearly, this group of basic building blocks is indispensable in nature. The increasing volume of drug molecules that contain α -amino acids and peptide-based drugs on the market is a testament to the utility of these multifunctional units (Figure 2.1).

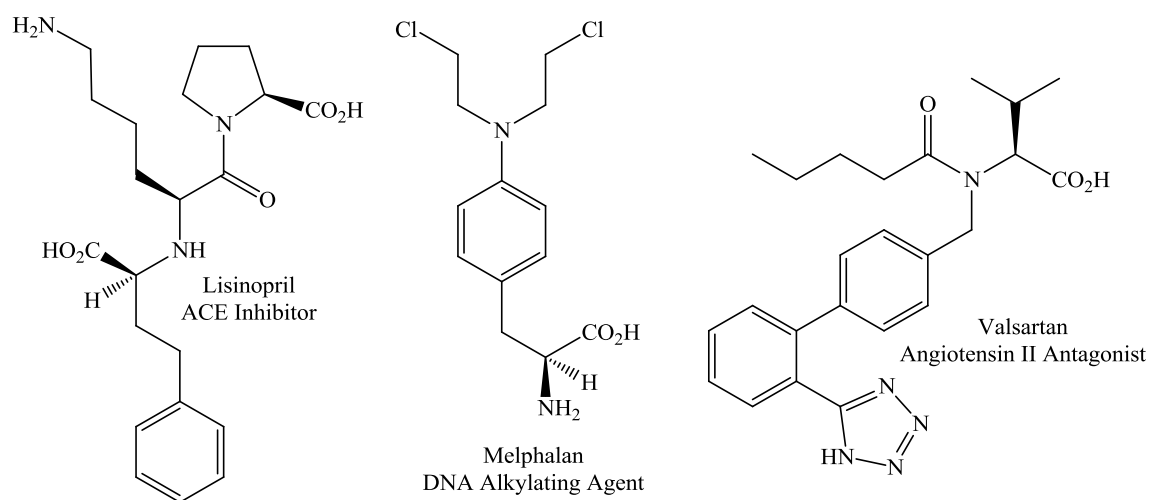


Figure 2.1 Drug molecules that contain α -amino acids currently on the market.

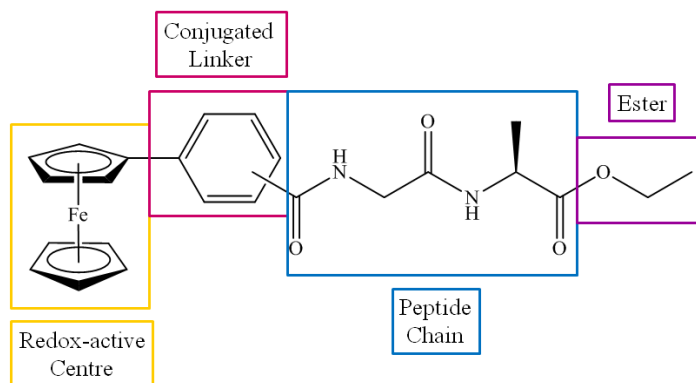
Organometallic compounds are versatile species due to the range of both structure and bonding modes that are accessible. As a consequence, they have been incorporated in a wide variety of materials that have diverse applications. Ferrocene is a particularly useful organometallic compound for biological applications since it is stable in aqueous and aerobic media, is easy to use and exhibits interesting spectroscopic and electrochemical properties. Bioconjugates of ferrocene with amino acids and peptides have been the subject of much research towards the development of novel sensor compounds, peptide mimetic models, and unnatural drugs.² Ferrocenyl-peptide bioconjugates have been investigated as anti-bacterial agents, however only a limited toxicity was observed.^{3,4} *N*-benzoyl peptides have been shown to have a wide range of biological activity that includes the treatment of diabetes⁵ and rheumatoid arthritis.^{6,7} The benzylation of an *N*-terminal amino acid increases the lipophilicity of the amino acid and substitution on such a group is often crucial for its biological activity. Appending a ferrocenyl unit to *N*-benzoyl peptides is an appealing approach in the design of ferrocenyl-peptide bioconjugates that act as unnatural drugs. Not only will the combination of both aromatic moieties aid in increasing the lipophilicity of the peptide, the presence of the benzoyl unit between the ferrocene and the peptide should lower the redox potential of these bioconjugates, thereby making them easier to oxidise. Ferricenium salts known to inhibit tumour growth have been shown to produce hydroxyl radicals under physiological conditions, leading to oxidatively damaged DNA.⁸ Thus, ferrocenyl derivatives that possess redox potentials which fall within the range of biologically accessible potentials offer an attractive and alternative method to target and kill cancer cells.

Previous work in this laboratory has shown this approach to be particularly fruitful. A series of novel *N*-(ferrocenyl)benzoyl peptide derivatives were synthesised and selected compounds were tested for *in vitro* anti-cancer activity in the non-small cell lung cancer (NSCLC) derived H1299 cell line. The effect of these compounds on cell proliferation was expressed as an IC₅₀ value, which corresponds to the concentration of the drug required for 50% inhibition of cell growth (Table 2.1). The *N*-*ortho*, *N*-*meta* and *N*-{*para*-(ferrocenyl)-benzoyl}-glycine-L-alanine ethyl esters were identified as the most potent members of this series, with a remarkable anti-proliferative effect of on average 5.3 μM.

Table 2.1 IC₅₀ values for *N*-(ferrocenyl)benzoyl peptide derivatives in the H1299 cell line.

Compound	IC ₅₀ value (μM)
<i>N</i> -{ <i>ortho</i> -(ferrocenyl)-benzoyl}-Gly-OEt ⁹	48
<i>N</i> -{ <i>meta</i> -(ferrocenyl)-benzoyl}-L-Ala-Gly-OEt ⁹	26
<i>N</i> -{ <i>ortho</i> -(ferrocenyl)-benzoyl}-L-Ala-Gly-OEt ⁹	21
<i>N</i> -{ <i>ortho</i> -(ferrocenyl)-benzoyl}-Gly-L-Ala-OEt ¹⁰	5.3
<i>N</i> -{ <i>meta</i> -(ferrocenyl)-benzoyl}-Gly-L-Ala-OEt ¹¹	4.0
<i>N</i> -{ <i>para</i> -(ferrocenyl)-benzoyl}-Gly-L-Ala-OEt ¹¹	6.6
<i>N</i> -{ <i>meta</i> -(ferrocenyl)-benzoyl}-Gly-L-2-aminobutyric acid-OEt ¹¹	10.5
<i>N</i> -{ <i>meta</i> -(ferrocenyl)-benzoyl}-Gly-L-norvaline-OEt ¹¹	19.1
<i>N</i> -{ <i>meta</i> -(ferrocenyl)-benzoyl}-Gly-L-norleucine-OEt ¹¹	18.9
<i>N</i> -{ <i>ortho</i> -(ferrocenyl)-benzoyl}-Gly-Gly-OEt ¹²	20
<i>N</i> -{ <i>ortho</i> -(ferrocenyl)-benzoyl}-Gly-Gly-Gly-OEt ¹²	63
<i>N</i> -{ <i>ortho</i> -(ferrocenyl)-benzoyl}-Gly-Gly-Gly-Gly-OEt ¹²	>100

The primary objective of this research thesis is to explore the structure-activity relationship (SAR) of these novel ferrocenyl-peptide bioconjugates in order to enhance their *in vitro* anti-proliferative effect. Since the precise biological target of these compounds is unknown at this point in time, the best approach is to perform enough syntheses to identify the molecular features which are favourable and those which are detrimental to the activity. With this in mind, the lead compound was divided into four distinct regions for SAR evaluation (Figure 2.2).

**Figure 2.2** SAR regions of *N*-(ferrocenyl)benzoyl-glycine-L-alanine ethyl ester.

The first region consists of the ferrocene electroactive core, which could be varied by replacing ferrocene with an alternative metallocene. The most common approach reported in the literature is the incorporation of ruthenocene in place of ferrocene.^{13,14} This would be a logical step since in this case, a low oxidation potential is believed to be important for anti-proliferative effect and ruthenocene undergoes electrochemical oxidation more readily than ferrocene. Nonetheless, there is some controversy surrounding the oxidation of ruthenocene, as some reports suggest a one-electron oxidation process, whilst other studies have indicated that ruthenocene undergoes a two-electron irreversible oxidation process.¹⁵ Studies conducted by Jaouen *et al* concerning organometallic tamoxifen derivatives reported a loss of activity in the ER(-) breast cancer cell line when the ferrocenyl group was replaced with ruthenocene.¹³ Since the reversible redox properties displayed by the *N*-(ferrocenyl)benzoyl peptide derivatives are believed to play an integral role in the mode of action of these novel drugs, it was concluded that any ruthenocenyl analogues would not display the same biological activity.

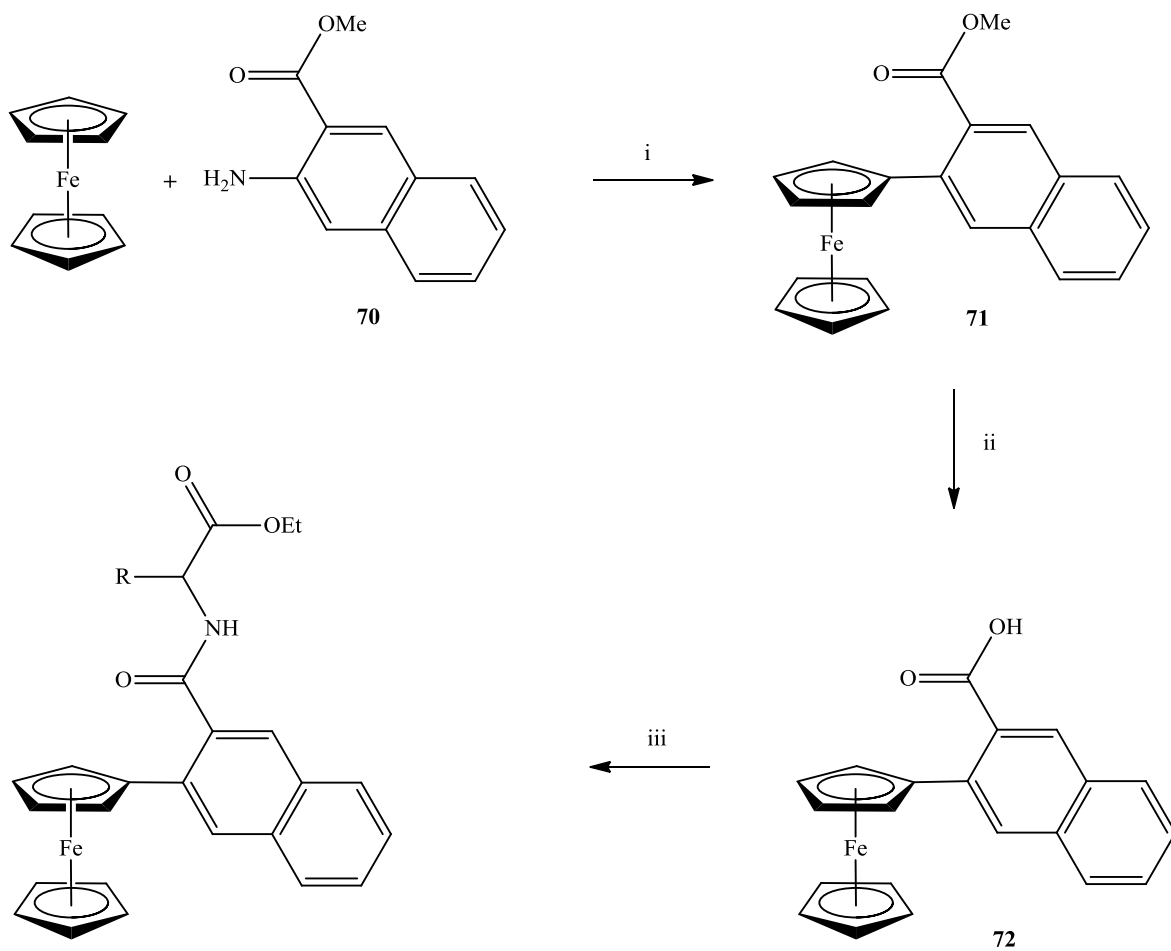
The three remaining regions all offer excellent starting points for introducing diversity into this series of ferrocenyl-peptide bioconjugates. The conjugated linker was considered to be the most fundamental region that may be altered, since the conjugating ability of the linker is important in determining the redox potential of the derivative. There is an abundance of aromatic and hetero-aromatic ring systems that could potentially be incorporated in place of the benzene ring. Perhaps the simplest alteration is to employ a naphthalene ring as the conjugated linker. Following a search of commercially available chemicals, two disubstituted naphthalene compounds were selected for this purpose: 3-amino-2-naphthoic acid and 6-amino-2-naphthoic acid. These compounds are amenable to the synthetic route employed in the synthesis of the *N*-(ferrocenyl)benzoyl peptide derivatives, which should allow for the facile synthesis of a series of *N*-(ferrocenyl)naphthoyl analogues.

In relation to the peptide chain, limiting the amino acids at this point in time to the 20 essential α -amino acids still provides a great assortment of side chain functional groups. Since the IC₅₀ values determined for the selected *N*-(ferrocenyl)benzoyl peptide derivatives indicate that the presence of either a tripeptide or tetrapeptide chain has a negative effect on biological activity, the peptide chain length was limited to dipeptides and single α -amino

acids for this study. Even by imposing these restrictions, there are still a substantial number of derivatives that could be synthesised, since it is possible to form 400 different dipeptide chains from the 20 essential α -amino acids. The previous study indicated that anti-proliferative effect is best when the small, neutral α -amino acids glycine and L-alanine are present in the peptide chain. However, the effect of branched alkyl groups and aromatic groups on biological activity has never been investigated. For this reason, L-leucine and L-phenylalanine were also selected from the 20 essential α -amino acids for this initial study. There is a variety of different alkyl and aromatic groups that could be introduced in the ester functionality. However, alteration of the ester group is more of a concern at the later stages of drug design and development, when factors such as oral absorption and biodistribution are being taken into consideration. Since this is a primary SAR exploration, the ester group was unaltered during these studies.

2.2. The synthesis of *N*-(ferrocenyl)naphthoyl amino acid and dipeptide derivatives which contain α -amino acids

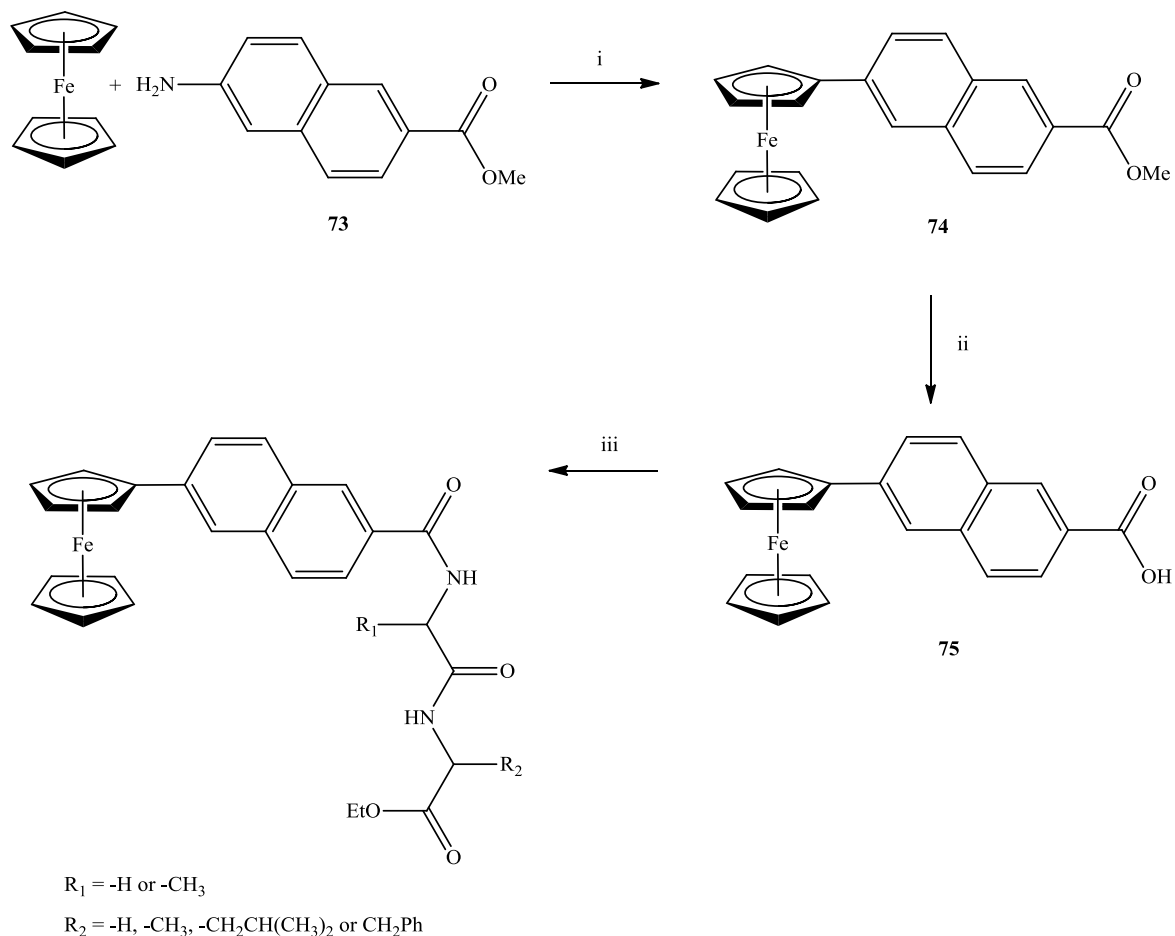
Peptide coupling reactions allow the facile introduction of the ferrocenyl naphthoyl group onto an amino acid or dipeptide. Thus, the ferrocenyl naphthoyl moiety was appended to a series of amino acid and dipeptide ethyl esters under solution phase peptide coupling conditions. A solution of ferrocenylnaphthalene-2-carboxylic acid in dichloromethane at 0°C, was treated with *N*-(3-dimethylaminopropyl)-*N'*-ethylcarbodiimide hydrochloride (EDC), 1-hydroxybenzotriazole (HOBt) and triethylamine (Et₃N). An equimolar amount of the required amino acid ethyl ester hydrochloride or the dipeptide ethyl ester hydrochloride was then added to this stirred solution. The procedure is similar to that used for the synthesis of the *N*-(ferrocenyl)benzoyl peptide derivatives.¹⁶ Scheme 2.1 outlines the synthetic route employed in the synthesis of the *N*-(3-ferrocenyl-2-naphthoyl) amino acid derivatives, whilst Scheme 2.2 outlines the synthetic route employed in the synthesis of the *N*-(6-ferrocenyl-2-naphthoyl) dipeptide derivatives.



R = -H, -CH₃, -CH₂CH(CH₃)₂ or -CH₂Ph

(i) NaNO₂, HCl, 5 °C; (ii) NaOH/MeOH, H₂O; (iii) EDC, HOBT, Et₃N, amino acid ethyl ester.

Scheme 2.1 The general reaction scheme for the synthesis of *N*-(3-ferrocenyl-2-naphthoyl) amino acid derivatives.



(i) NaNO_2 , HCl , $5\text{ }^\circ\text{C}$; (ii) NaOH/MeOH , H_2O ; (iii) EDC , HOBT , Et_3N , dipeptide ethyl ester.

Scheme 2.2 The general reaction scheme for the synthesis of *N*-(6-ferrocenyl-2-naphthoyl) dipeptide derivatives.

2.2.1. The preparation of methyl ferrocenylnaphthalene-2-carboxylate

Ferrocene reacts 3×10^6 times faster than benzene towards electrophilic substitution, hence, this class of reactions dominates the chemistry of ferrocene.¹⁵ Thus, the arylation of ferrocene is readily achieved by reacting ferrocene with an aryl diazonium salt. In this case, the appropriate methyl aminonaphthalene-2-carboxylate was treated with sodium nitrite in the presence of hydrochloric acid at a temperature below $5\text{ }^\circ\text{C}$ to yield the diazonium salt. Above $5\text{ }^\circ\text{C}$ the diazonium salt decomposes resulting in the formation of an aryl carbocation

and evolution of nitrogen gas. Ferrocene present *in situ* reacts with this unstable aryl cation *via* electrophilic aromatic substitution to furnish the methyl ferrocenylnaphthalene-2-carboxylate as an orange/red solid.

There is still debate as to the mechanism by which ferrocene undergoes electrophilic aromatic substitution. A reaction mechanism where the initial interaction occurs between the electrophile and the weakly bonding electrons of the iron atom was proposed by Rosenblum *et al* in 1963.¹⁷ This initial interaction is followed by a transfer of the electrophile to the *endo* face of the η^5 -C₅H₅ *i.e.* the side nearest the iron atom. Subsequent proton elimination gives the substituted product (Figure 2.3). Alternatively, it has been proposed that the electrophile can react directly with the cyclopentadienyl ring and does not have any direct interaction with the iron atom. In this case the electrophile can be added to either the *exo* or *endo* face of the ferrocene molecule (Figure 2.4).

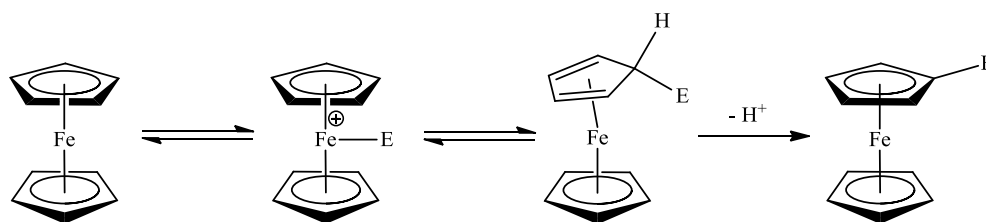


Figure 2.3 Possible reaction mechanism that proceeds *via* the transition states in which the electrophile is bonded to the iron atom.¹⁵

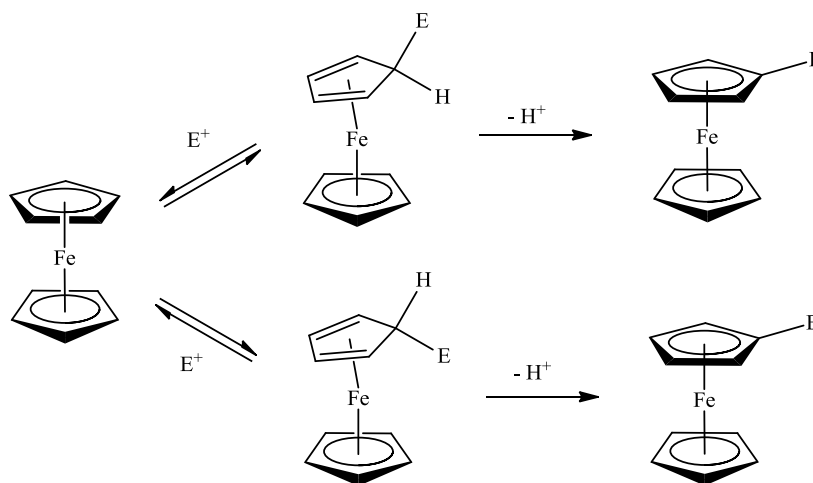


Figure 2.4 Possible reaction mechanism for the electrophilic substitution of ferrocene where the electrophile reacts directly with the cyclopentadienyl ring *via* the *exo* or *endo* transition state.

2.2.2. The preparation of ferrocenylnaphthalene-2-carboxylic acid

Hydrolysis of methyl ferrocenylnaphthalene-2-carboxylate in 10% sodium hydroxide solution effectively removes the ester group to produce ferrocenylnaphthalene-2-carboxylic acid. In the ^1H NMR spectra a broad singlet between δ 12.7 to δ 13 indicates the presence of the carboxylic acid proton. Hydrolysis can also be monitored by the disappearance of the methyl ester peak from the ^1H and ^{13}C NMR spectra.

2.2.3. Amino acids

Proteins and peptides are comprised of individual amino acids linked together *via* an amide or peptide bond. The synthetic value of amino acids as building blocks stems from the fact that they can be linked together by an amide bond to form peptide chains or linked to other suitable compounds *e.g.* ferrocenylnaphthalene-2-carboxylic acid. In the formation of an amide bond between two amino acids protection of the *N*-terminus of one amino acid and the *C*-terminus of the other amino acid is required to ensure regiospecific coupling. For this reason, it was necessary to protect the *C*-terminus of the amino acids and dipeptides prior to condensation with ferrocenylnaphthalene-2-carboxylic acid.

2.2.4. Carboxyl protecting groups

The most typical means of protection is esterification, which not only aids solubility in organic solvents but also ensures that (i) an amide bond and not an anhydride is formed and (ii) that only the product of mono-addition is formed.¹⁸ Thus, conversion of the carboxylic acid group to the ester was achieved by treatment of the amino acid or peptide with thionyl chloride and ethanol to give the corresponding ethyl ester hydrochloride salt (Figure 2.5). The hydrochloride salts can be neutralised to give the corresponding free bases, however these decompose quite rapidly at room temperature. The free base forms are therefore generated *in situ* only when required, by neutralisation with a tertiary amine such as triethylamine.¹⁹ The hydrochloride salt can be easily identified in the ^1H NMR spectrum as a broad singlet integrating for three protons. In $\text{DMSO-}d_6$ this peak is present between δ 8 and δ 9.

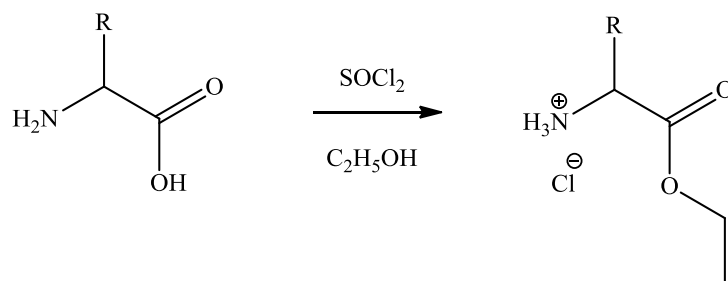


Figure 2.5 The protection of the carboxyl terminus of an amino acid by conversion to an ethyl ester.

Ethyl esters are completely stable towards HBr, acetic acid, trifluoroacetic acid (TFA) or catalytic hydrogenolysis and therefore the selective removal of amino protecting groups from peptide ethyl ester derivatives presents no difficulties. Due to the stability of the ethyl ester protecting group, its own removal may present difficulties. Saponification is sometimes satisfactory however the base that is required for this process may cause racemisation (Figure 2.6).

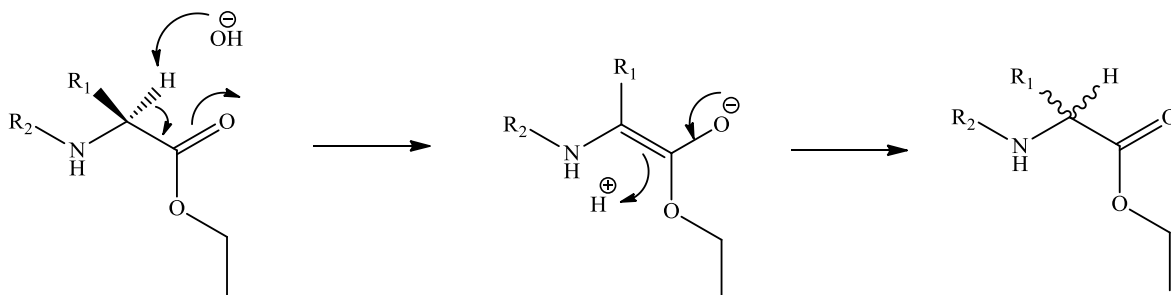


Figure 2.6 The process of racemisation that may occur instead of the desired cleavage reaction due to the presence of base required for saponification.

2.3. Amide Bond Formation

The key step in peptide synthesis is the condensation of distinct carboxylic acid and amine moieties to form the amide bond. For this purpose, it is necessary to activate the carboxylic acid, since (i) carboxylic acids simply form salts with amines at ambient temperatures¹⁹ and (ii) high temperature (> 200 °C) reaction conditions are typically detrimental to the integrity of the substrates. The activation process occurs by converting the –OH of the acid into a

good leaving group prior to treatment with the amine.²⁰ This is achieved by employing peptide coupling reagents.

2.3.1. Acyl chlorides

The most simple and straightforward way to activate a carboxylic acid is to convert it into its corresponding acyl chloride prior to coupling to the amine. However, acyl chlorides have a limited value in peptide coupling due to the danger of hydrolysis, racemisation, cleavage of protecting groups and other side reactions.²¹ Harsh reagents such as thionyl chloride (SOCl₂) or phosphorous pentachloride (PCl₅) are commonly used to generate acyl chlorides. These reagents have proven to be too vigorous for some substrates and in particular, are not compatible with acid-sensitive substrates. Coupling to the amine moiety is typically performed under basic conditions to trap any HCl formed and thus avoid the conversion of the amine into its unreactive HCl salt. Unfortunately, acyl chlorides display a tendency to racemise under such basic conditions, *via* the formation of a ketene (Figure 2.7). The ketene may react with a nucleophile such as an amine to yield the corresponding addition product with an obvious loss of chiral integrity.²¹

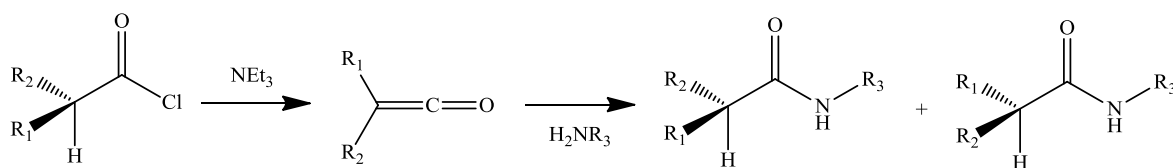


Figure 2.7 Potential racemisation under basic conditions *via* ketene formation.

2.3.2. Anhydrides

Symmetric anhydrides can be prepared from the corresponding carboxylic acid by reacting two molecules of acid in the presence of one equivalent of 1,3-dicyclohexylcarbodiimide (DCC) under mild conditions. In a second step the anhydride is reacted with the appropriate amine to form the required amide. The main limitation of this method is that only half of the acid used is effectively incorporated into the product. To overcome this problem, mixed anhydrides were developed where the second carboxylic moiety is cheap and easy to couple onto the acid.²¹ Mixed pivalic anhydrides are the most favoured, as the presence of the

bulky *t*-Bu group directs the attack of the amine to the required carboxy component (Figure 2.8).

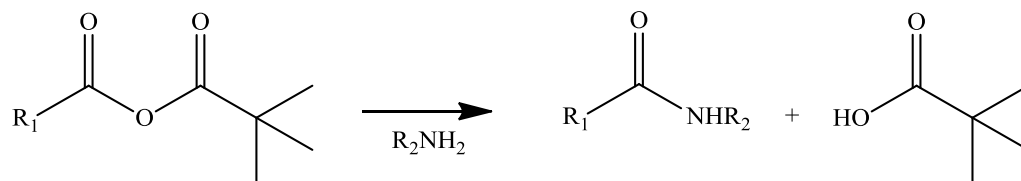


Figure 2.8 Amide bond formation *via* a mixed pivalic anhydride.

An alternative strategy involves the generation and aminolysis of a carboxylic-carbonic anhydride *e.g.* ethoxycarbonyl anhydrides. Since one of the carbonyl groups in the activated intermediate is bonded to two oxygen atoms, its reactivity is diminished and nucleophilic attack is directed towards the other more reactive carbonyl.¹⁹ Ethoxycarbonyl anhydrides can be generated using ethyl chloroformate or 2-ethoxy-1-ethoxycarbonyl-1,2-dihydroquinoline **76** (EEDQ) (Figure 2.9).

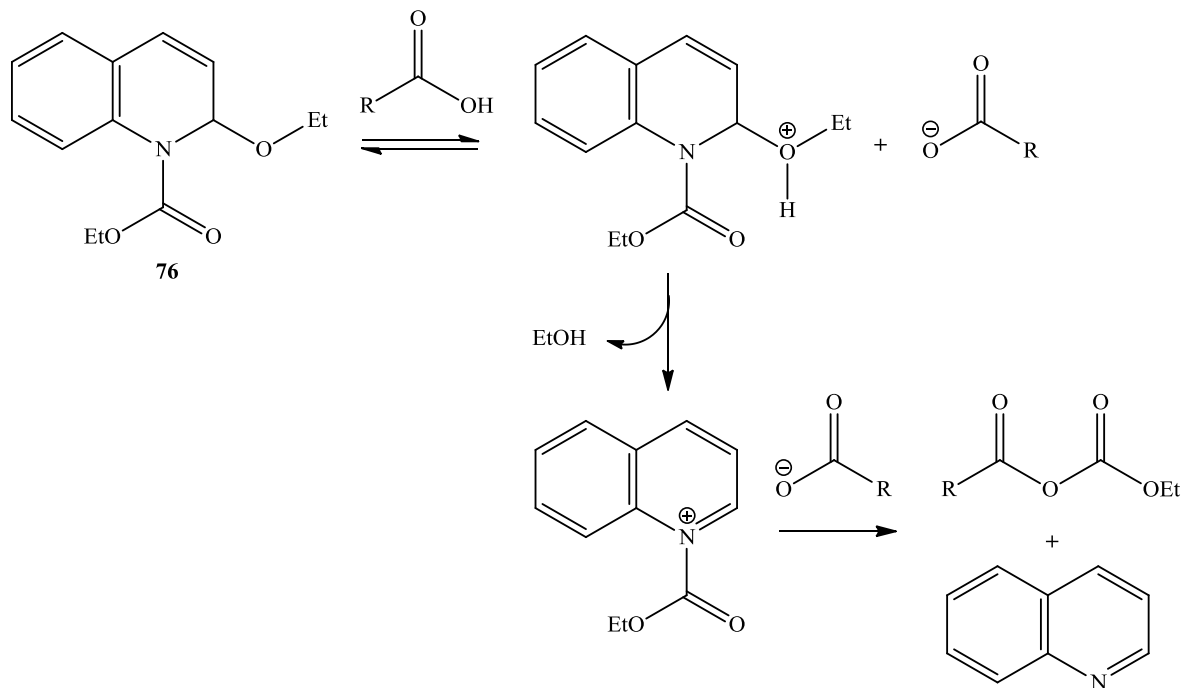
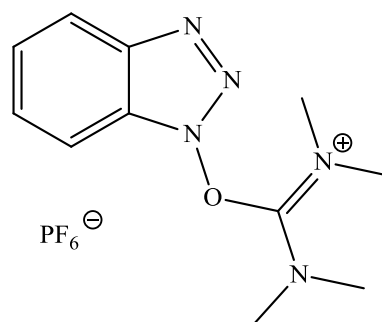
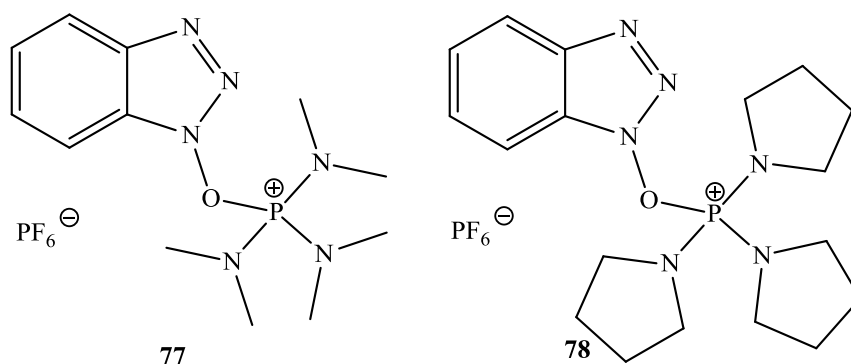


Figure 2.9 Ethoxycarbonyl anhydride preparation using EEDQ **76**.

2.3.3. Phosphonium Reagents

Phosphonium cations may undergo attack from carboxylate anions to form acyloxyphosphonium species, which can react readily with nucleophiles at the acyl carbon.¹⁹ Since these phosphonium cations hold promise as direct coupling reagents, a number of phosphonium salts have been developed for this purpose. Benzotriazol-1-yl-oxy-tris-(dimethylamino)-phosphonium hexafluorophosphate **77** (BOP) was the first of these reagents to be introduced. The BOP reagent reacts with the carboxylate anion to generate both the activated acylphosphonium species and HOBt. HOBt reacts with the activated acid to give a reactive benzotriazole ester that readily undergoes aminolysis (Figure 2.10). However, the use of BOP has been limited due to the carcinogenicity and respiratory toxicity associated with the by-product hexamethylphosphoramide (HMPA).²⁰ Phosphonium derivatives that generate less toxic by-products e.g. benzotriazol-1-yl-oxy-tris-pyrrolidino-phosphonium hexafluorophosphate **78** (PyBop) have been developed, although the success of these reagents is now overshadowed by reagents such as *O*-(1*H*-benzotriazol-1-yl)-*N,N,N',N'*-tetramethyluronium hexafluorophosphate **79** (HBTU).



79

57

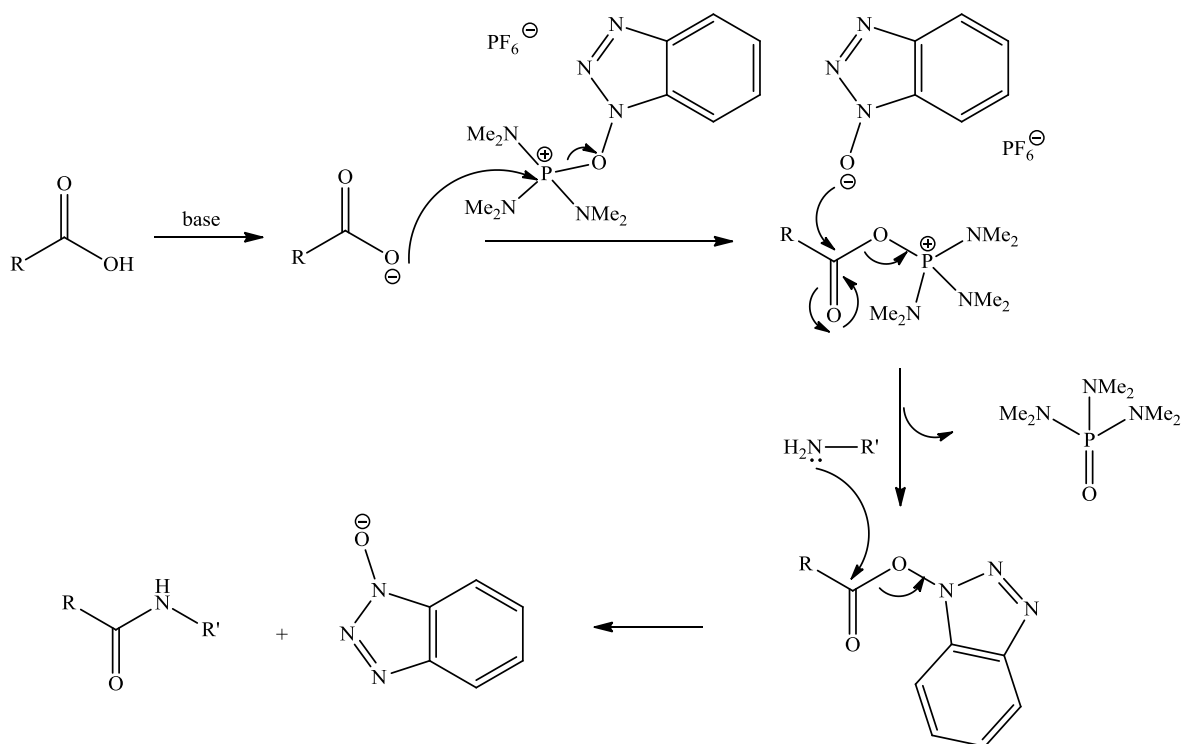


Figure 2.10 Amide bond formation using BOP reagent.

2.3.4. Carbodiimides

The use of carbodiimides as efficient peptide coupling reagents is commonplace ever since Hess and Sheehan first demonstrated the usefulness of 1,3-dicyclohexylcarbodiimide (DCC) in activating carboxyl groups towards nucleophilic attack. The first step towards peptide coupling involves addition of the carboxyl group to the carbodiimide to give an *O*-acylisourea intermediate. This is a potent acylating agent, and will react rapidly to form the required peptide product either through direct aminolysis or *via* a symmetrical anhydride intermediate (Figure 2.11).¹⁹

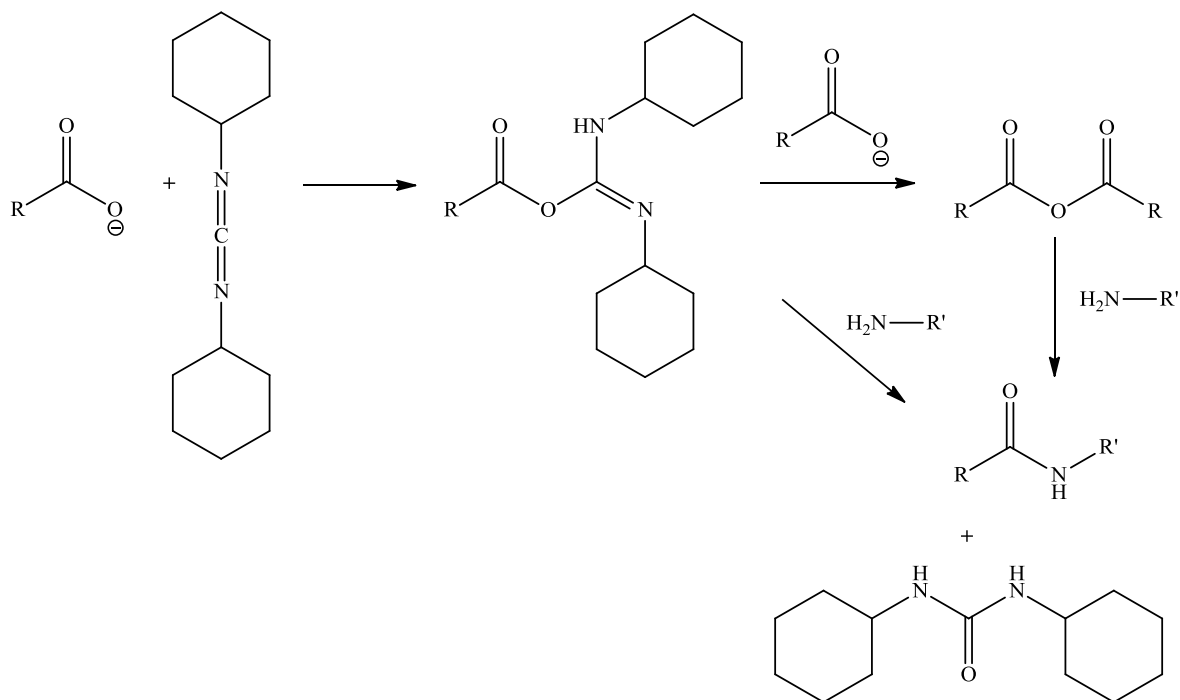


Figure 2.11 Amide bond formation using DCC.

These intermediates are highly reactive and thus, side-reactions can pose a serious problem and can result in extensive racemisation. In particular, the *O*-acylisourea can undergo an intramolecular acyl transfer to form the much less reactive *N*-acylurea (Figure 2.12). This side-reaction can sometimes compete significantly with the desired attack by external nucleophiles and can also occur intermolecularly between the urea and a symmetrical anhydride.¹⁹ Thus, formation of the inert *N*-acylurea can lead to considerably lower yields and may also give rise to problems during purification.

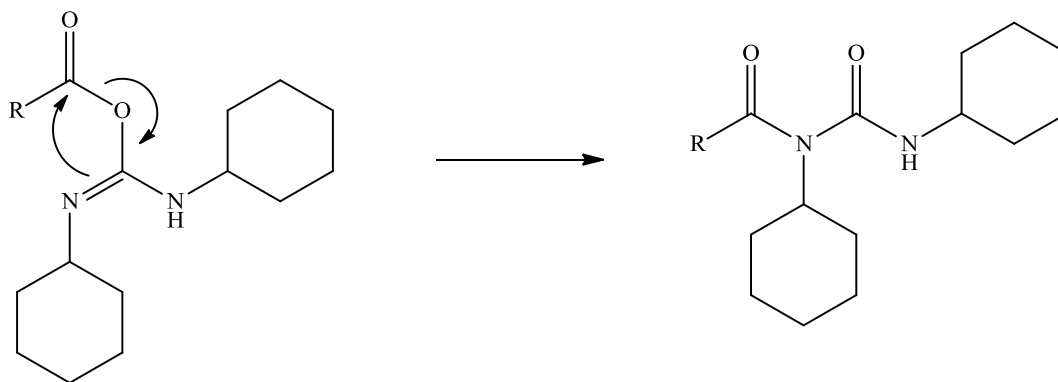


Figure 2.12 Acyl transfer of *O*-acylisourea to *N*-acylurea.

These issues can be eliminated by performing the coupling reaction in the presence of an α -nucleophile, most commonly HOBt. This α -nucleophile reacts very rapidly with the *O*-acylisourea before any side-reactions can occur, resulting in an acylating agent of lower potency, which favours aminolysis and thus eliminates other side-reactions. The participation of HOBt in the formation of the amide bond can be seen in Figure 2.13. EDC was employed in the synthesis of the *N*-(ferrocenyl)naphthoyl amino acid and dipeptide ethyl esters since the 1-{3-(dimethylamino)propyl}-3-ethyl urea by-product is completely water-soluble, which aids purification.¹⁸

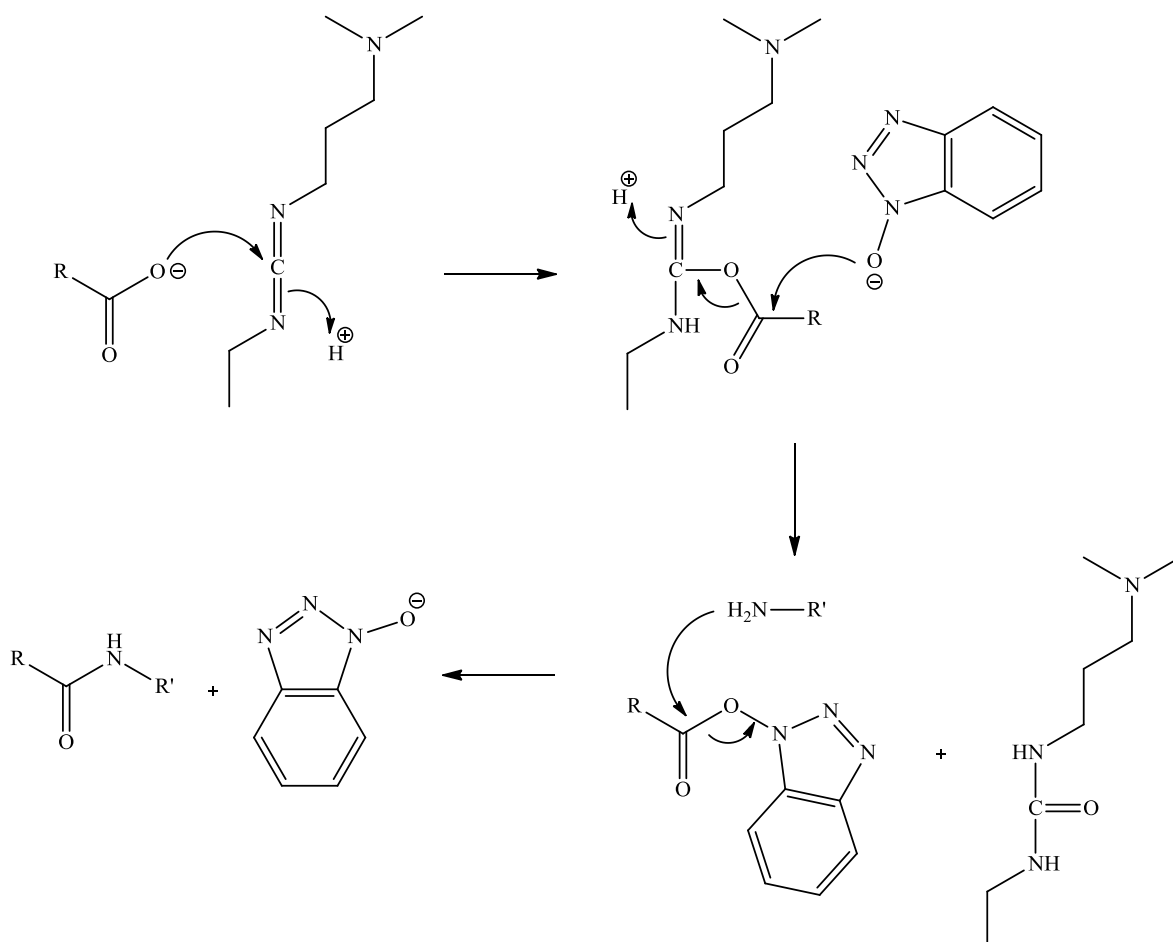


Figure 2.13 Amide bond formation using EDC and HOBt.

2.4. Purification and yields of *N*-(ferrocenyl)naphthoyl amino acid and dipeptide derivatives

The *N*-(ferrocenyl)naphthoyl amino acid derivatives were synthesised by the condensation of 3-ferrocenylnaphthalene-2-carboxylic acid and 6-ferrocenylnaphthalene-2-carboxylic acid, with the α -amino acid ethyl esters of glycine, L-alanine, L-leucine and L-phenylalanine, under the peptide coupling conditions outlined in Section 2.2. The *N*-(ferrocenyl)naphthoyl dipeptide derivatives were similarly prepared by the condensation of the ferrocenylnaphthalene-2-carboxylic acid units with the free *N*-terminal dipeptide ethyl esters. In the case of the dipeptide derivatives, glycine and L-alanine were employed as the *N*-terminal α -amino acid, whilst glycine, L-alanine, L-leucine and L-phenylalanine were employed as the *C*-terminal α -amino acids. Crude *N*-(ferrocenyl)naphthoyl amino acid or dipeptide derivatives were isolated following the coupling procedure and purified by column chromatography, using a mixture of hexane and ethyl acetate as the eluant. The pure *N*-(ferrocenyl)naphthoyl amino acid and dipeptide derivatives were furnished as orange or red solids, with yields in the range of 18% to 95%. All compounds gave spectroscopic and analytical data in accordance with their proposed structures.

The yields for the *N*-(3-ferrocenyl-2-naphthoyl) amino acid and dipeptide derivatives were generally lower than those for the *N*-(6-ferrocenyl-2-naphthoyl) amino acid and dipeptide derivatives. In the case of the *N*-(3-ferrocenyl-2-naphthoyl) series, low yields are a result of steric hindrance around the carboxylic acid functionality, due to the presence of the bulky ferrocenyl group in the *ortho*-position. This assertion is supported by similar observations for the *N*-(ferrocenyl)benzoyl peptide derivatives.¹⁶ The side chain of the reacting α -amino acid can also have an influence on the overall yield. Yields are lower in cases where the side chain of the α -amino acid is large enough to exert a steric effect, *e.g.* the benzyl side chain of L-phenylalanine. In combination, these steric effects account for the difference in yield observed for *N*-(3-ferrocenyl-2-naphthoyl)-L-phenylalanine ethyl ester **83** (40%), compared to that obtained for *N*-(6-ferrocenyl-2-naphthoyl)-L-phenylalanine ethyl ester **95** (78%). Table 2.2 summarises the yields for all of the *N*-(ferrocenyl)naphthoyl amino acid and dipeptide derivatives.

Table 2.2 Percentage yields for *N*-(ferrocenyl)naphthoyl amino acid and dipeptide derivatives.

Compound	No.	% Yield
<i>N</i> -(3-ferrocenyl-2-naphthoyl)-Gly-OEt	80	83
<i>N</i> -(3-ferrocenyl-2-naphthoyl)-L-Ala-OEt	81	95
<i>N</i> -(3-ferrocenyl-2-naphthoyl)-L-Leu-OEt	82	32
<i>N</i> -(3-ferrocenyl-2-naphthoyl)-L-Phe-OEt	83	40
<i>N</i> -(3-ferrocenyl-2-naphthoyl)-Gly-Gly-OEt	84	60
<i>N</i> -(3-ferrocenyl-2-naphthoyl)-Gly-L-Ala-OEt	85	55
<i>N</i> -(3-ferrocenyl-2-naphthoyl)-Gly-L-Leu-OEt	86	42
<i>N</i> -(3-ferrocenyl-2-naphthoyl)-Gly-L-Phe-OEt	87	29
<i>N</i> -(3-ferrocenyl-2-naphthoyl)-L-Ala-Gly-OEt	88	59
<i>N</i> -(3-ferrocenyl-2-naphthoyl)-L-Ala-L-Ala-OEt	89	28
<i>N</i> -(3-ferrocenyl-2-naphthoyl)-L-Ala-L-Leu-OEt	90	18
<i>N</i> -(3-ferrocenyl-2-naphthoyl)-L-Ala-L-Phe-OEt	91	45
<i>N</i> -(6-ferrocenyl-2-naphthoyl)-Gly-OEt	92	62
<i>N</i> -(6-ferrocenyl-2-naphthoyl)-L-Ala-OEt	93	83
<i>N</i> -(6-ferrocenyl-2-naphthoyl)-L-Leu-OEt	94	33
<i>N</i> -(6-ferrocenyl-2-naphthoyl)-L-Phe-OEt	95	78
<i>N</i> -(6-ferrocenyl-2-naphthoyl)-Gly-Gly-OEt	96	83
<i>N</i> -(6-ferrocenyl-2-naphthoyl)-Gly-L-Ala-OEt	51	79
<i>N</i> -(6-ferrocenyl-2-naphthoyl)-Gly-L-Leu-OEt	97	58
<i>N</i> -(6-ferrocenyl-2-naphthoyl)-Gly-L-Phe-OEt	98	56
<i>N</i> -(6-ferrocenyl-2-naphthoyl)-L-Ala-Gly-OEt	99	67
<i>N</i> -(6-ferrocenyl-2-naphthoyl)-L-Ala-L-Ala-OEt	100	29
<i>N</i> -(6-ferrocenyl-2-naphthoyl)-L-Ala-L-Leu-OEt	101	23
<i>N</i> -(6-ferrocenyl-2-naphthoyl)-L-Ala-L-Phe-OEt	102	23

Footnote: Compounds **70-75** are intermediates and hence, are not included in Table 2.2.

2.5. ^1H NMR studies of *N*-(ferrocenyl)naphthoyl amino acid and dipeptide derivatives

All of the ^1H NMR experiments were performed in $\text{DMSO-}d_6$ as the *N*-(ferrocenyl)naphthoyl amino acid and dipeptide derivatives showed limited solubility in other deuterated solvents. In the ^1H NMR spectra of the *N*-(ferrocenyl)naphthoyl amino acid and dipeptide derivatives, the aromatic signal pattern varied depending on the substitution pattern of the naphthalene ring. For the *N*-(3-ferrocenyl-2-naphthoyl) amino acid and dipeptide derivatives, a singlet, doublet, doublet, singlet, triplet, triplet pattern may be observed, with each peak integrating for one proton. More often than not though, several of these signals may overlap due to their close proximity in chemical shift. In the ^1H NMR spectra of the *N*-(6-ferrocenyl-2-naphthoyl) amino acid and dipeptide derivatives, the aromatic region generally shows a singlet, singlet, multiplet, and double doublet splitting pattern, integrating for one, one, three and one proton, respectively.

The chemical shift of the amide proton that forms the amide bond between the naphthoyl group and the peptide appears from δ 8.82-9.08 for the *N*-(ferrocenyl)naphthoyl amino acid derivatives, whilst in the ^1H NMR spectra of the *N*-(ferrocenyl)naphthoyl dipeptide derivatives this signal appears from δ 8.47-8.94. The appearance of these signals in the low field region of the ^1H NMR spectra is due to hydrogen bond interactions between the amide proton and the S=O bond of $\text{DMSO-}d_6$. If CDCl_3 was used to obtain the spectra, the amide protons would most likely appear more upfield since CDCl_3 does not possess the same ability to form hydrogen bonds.

The aromatic peaks of the ferrocene moiety appear upfield of the aromatic region between δ 4.02 and δ 5.01. Since ferrocene is more electron dense than benzene, the ferrocenyl protons experience an increased shielding effect. Characteristic peaks in this region confirm the presence of a mono-substituted ferrocene moiety. However, there is a notable difference in the chemical shift of the ferrocenyl peaks in accordance with the substitution pattern around the central naphthoyl linker.

For the *N*-(6-ferrocenyl-2-naphthoyl) amino acid and dipeptide derivatives, a singlet due to the unsubstituted cyclopentadienyl ring ($\eta^5\text{-C}_5\text{H}_5$) typically appears from δ 4.05-4.10. This signal integrates for five protons. The *ortho* hydrogens on the cyclopentadienyl ($\eta^5\text{-C}_5\text{H}_4$) ring appear in the range δ 4.95-5.01 as a fine triplet or a singlet, each integrating for two

protons. The *meta* hydrogens of the (η^5 -C₅H₄) ring appear from δ 4.45-4.50, also as a fine triplet or a singlet that integrates for two protons.

In the ¹H NMR spectra of the *N*-(3-ferrocenyl-2-naphthoyl) amino acid and dipeptide derivatives, these signals are shifted slightly upfield. The *ortho* (η^5 -C₅H₄) protons appear from δ 4.71-4.83; the *meta* (η^5 -C₅H₄) protons appear from δ 4.21-4.38. The five protons of the unsubstituted (η^5 -C₅H₅) ring are located from δ 4.01-4.09, and are sometimes observed as part of a multiplet with overlapping signals.

In some cases, the ferrocenyl region of the ¹H NMR spectra of *N*-(3-ferrocenyl-2-naphthoyl) amino acid and dipeptide derivatives was found to be more complex than first expected. This complexity is due to magnetic inequivalence and is exemplified in the case of the *N*-(3-ferrocenyl-2-naphthoyl) amino acid derivatives (Figure 2.14). The ¹H NMR spectrum of *N*-(3-ferrocenyl-2-naphthoyl)-glycine ethyl ester **80** shows the typical signal pattern observed for a mono-substituted ferrocene moiety. The *ortho* (η^5 -C₅H₄) protons appear at δ 4.83, the *meta* (η^5 -C₅H₄) protons appear at δ 4.32 and the five protons of the (η^5 -C₅H₅) ring are shown at δ 4.07. For *N*-(3-ferrocenyl-2-naphthoyl)-L-alanine ethyl ester **81** and *N*-(3-ferrocenyl-2-naphthoyl)-L-leucine ethyl ester **82**, there are two signals observed for the *meta* hydrogens, which integrate for one proton each. In the case of *N*-(3-ferrocenyl-2-naphthoyl)-L-phenylalanine ethyl ester **83**, four signals are observed between δ 4.15 and δ 4.75 and correspond to the four protons of the (η^5 -C₅H₄) ring. There is also a discernable upfield shift for these resonances, *e.g.* the *ortho* protons of the glycine derivative **80** come into resonance at δ 4.83, whilst those of the L-phenylalanine derivative **83** appear from δ 4.75-4.76 (Figure 2.14).

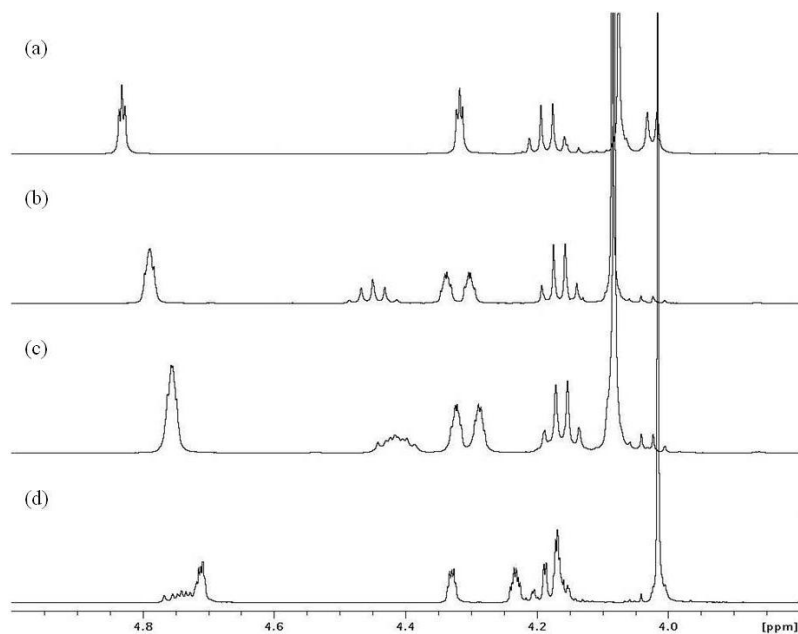


Figure 2.14 Ferrocenyl region (3.8-5.0 ppm) of the ^1H NMR spectra of: (a) *N*-(3-ferrocenyl-2-naphthoyl)-glycine ethyl ester **80**; (b) *N*-(3-ferrocenyl-2-naphthoyl)-L-alanine ethyl ester **81**; (c) *N*-(3-ferrocenyl-2-naphthoyl)-L-leucine ethyl ester **82**; (d) *N*-(3-ferrocenyl-2-naphthoyl)-L-phenylalanine ethyl ester **83**.

Table 2.3 Selected ^1H NMR spectral data (δ , $\text{DMSO-}d_6$) for *N*-(ferrocenyl)naphthoyl amino acid and dipeptide derivatives.

Compound No.	NH's	αH	<i>ortho</i> ($\eta^5\text{-C}_5\text{H}_4$)	<i>meta</i> ($\eta^5\text{-C}_5\text{H}_4$)
81	8.94	4.45	4.78-4.80	4.33-4.35, 4.29-4.31
85	8.72, 8.38	4.31-4.36	4.81	4.31-4.36
87	8.67, 8.43	4.53	4.80	4.30
89	8.54, 8.34	4.49, 4.28-4.33	4.74	4.28-4.33
93	8.96	4.57	5.01	4.50
51	8.84, 8.41	4.30	4.95	4.44
99	8.67, 8.38	4.60	4.96	4.45
102	8.58, 8.36	4.60, 4.43-4.50	4.96	4.43-4.50

2.5.1. ^1H NMR study of *N*-(3-ferrocenyl-2-naphthoyl)-glycine-L-alanine ethyl ester (85)

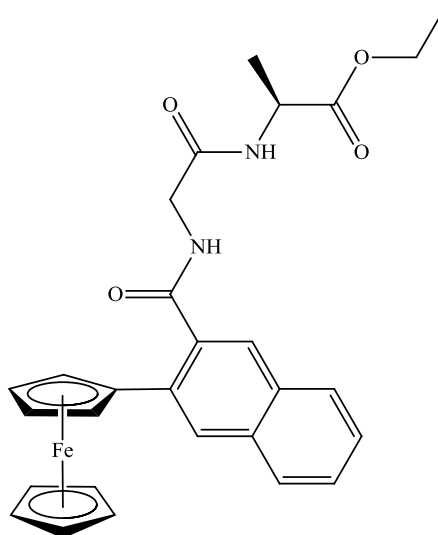


Figure 2.15 *N*-(3-ferrocenyl-2-naphthoyl)-glycine-L-alanine ethyl ester **85**.

In the ^1H NMR spectrum of *N*-(3-ferrocenyl-2-naphthoyl)-glycine-L-alanine ethyl ester **85** the naphthoyl amide proton peak appears downfield at δ 8.72. This signal integrates for one proton and appears as a triplet due to coupling with the adjacent methylene protons of the glycine residue. The remaining amide proton is observed as a doublet at δ 8.38, due to coupling with the α -hydrogen of the L-alanine residue, and integrates for one proton. The 2,3-disubstituted naphthoyl group appears as a singlet at δ 8.32, two doublets at δ 7.99 and δ 7.90, a singlet at δ 7.83 that all integrate for one proton. Between δ 7.49 and δ 7.57 there is a multiplet that integrates for two protons. In the ferrocenyl region, the peak due to the *ortho* protons on the (η^5 -C₅H₄) ring appears as a singlet at δ 4.81 that integrates for two protons. The peak due to the *meta* protons of the (η^5 -C₅H₄) ring is observed in a multiplet with a quintet representing the α -proton of the L-alanine residue. An integration of three is observed for this multiplet which appears from δ 4.31-4.36. The singlet due to the unsubstituted (η^5 -C₅H₅) ring appears in a multiplet with a quartet representing the methylene protons of the ethyl ester. This multiplet occurs from δ 4.02-4.14 and integrates for seven protons. The methylene protons of glycine residue are observed as two doublets of doublets at δ 3.96 and δ 3.87, with both these signals integrating for one proton each.

This splitting pattern is due to the presence of a chiral centre in the molecule. The methylene protons of the glycine residue are diastereotopic, and hence, geminal coupling is observed with a coupling constant of 16.4 Hz, together with coupling to the amide proton, with a coupling constant of 5.6 Hz. The peak due to the L-alanine methyl group appears as a doublet at δ 1.32, and the peak due to the methyl group of the ethyl ester appears as a triplet at δ 1.21.

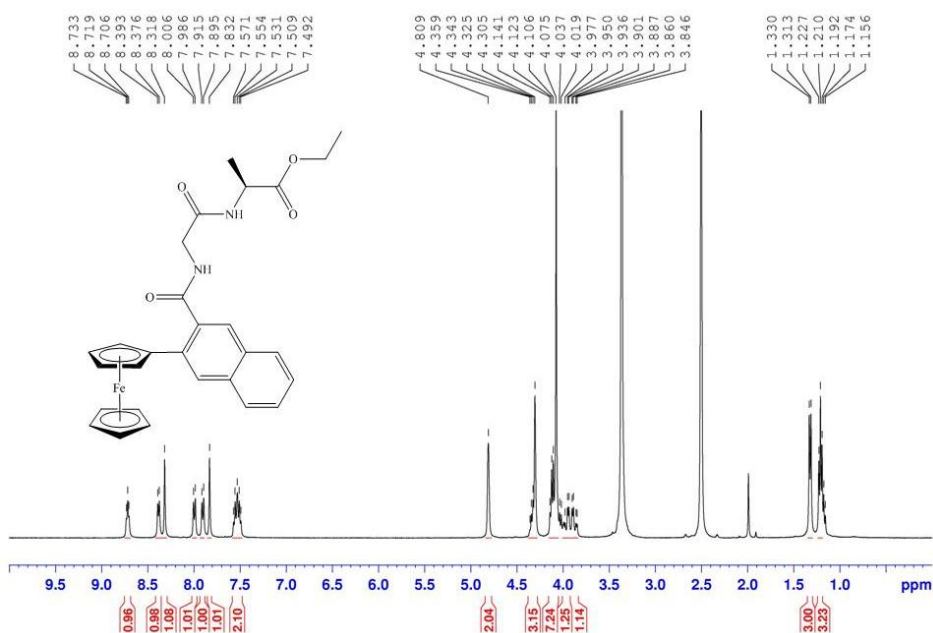


Figure 2.16 ¹H NMR spectrum of *N*-(3-ferrocenyl-2-naphthoyl)-glycine-L-alanine ethyl ester **85**.

2.5.2. ¹H NMR study of *N*-(6-ferrocenyl-2-naphthoyl)-glycine-L-alanine ethyl ester (**51**)

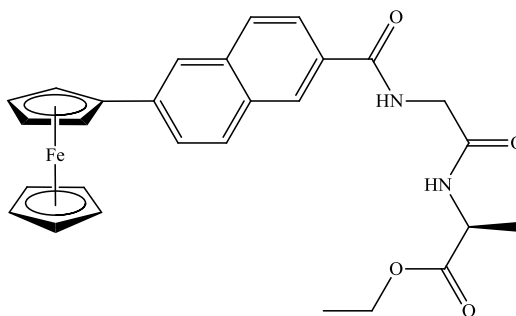


Figure 2.17 *N*-(6-ferrocenyl-2-naphthoyl)-glycine-L-alanine ethyl ester **51**.

The amide protons of *N*-(6-ferrocenyl-2-naphthoyl)-glycine-L-alanine ethyl ester **51** are positioned downfield at δ 8.84 and δ 8.41, and appear as a triplet and doublet, respectively. Both of these signals integrate for one proton. The triplet is due to coupling of the naphthoyl amide proton to the methylene protons of glycine, and the doublet is due to coupling with the α -hydrogen of L-alanine. The aromatic region confirms the presence of six protons, which appear from δ 7.82-8.44. As is typical with a 2,6-disubstituted naphthyl group, the spectrum shows two singlets at δ 8.44 and δ 8.06, a multiplet from δ 7.92-7.97 (three overlapping signals) and a doublet of doublets at δ 7.82. In the ferrocenyl region, the peak due to the *ortho* (η^5 -C₅H₄) protons appears as the furthest downfield signal. This signal appears as a fine triplet at δ 4.95 with a coupling constant of 1.6 Hz. Similarly, the *meta* (η^5 -C₅H₄) protons appear as a fine triplet at δ 4.44. Both these peaks integrate for two protons. The singlet due to the unsubstituted (η^5 -C₅H₅) ring is observed in a multiplet with a doublet of doublets representing one of the methylene protons of glycine. An integration of six protons is shown for this signal, which is observed from δ 4.00-4.05. The other methylene proton can be observed as a doublet of doublets at δ 3.93. The signal due to the L-alanine methyl group appears as a doublet at δ 1.31. The characteristic ethyl ester signals appear as a triplet at δ 1.19 and a multiplet from δ 4.06-4.12, respectively.

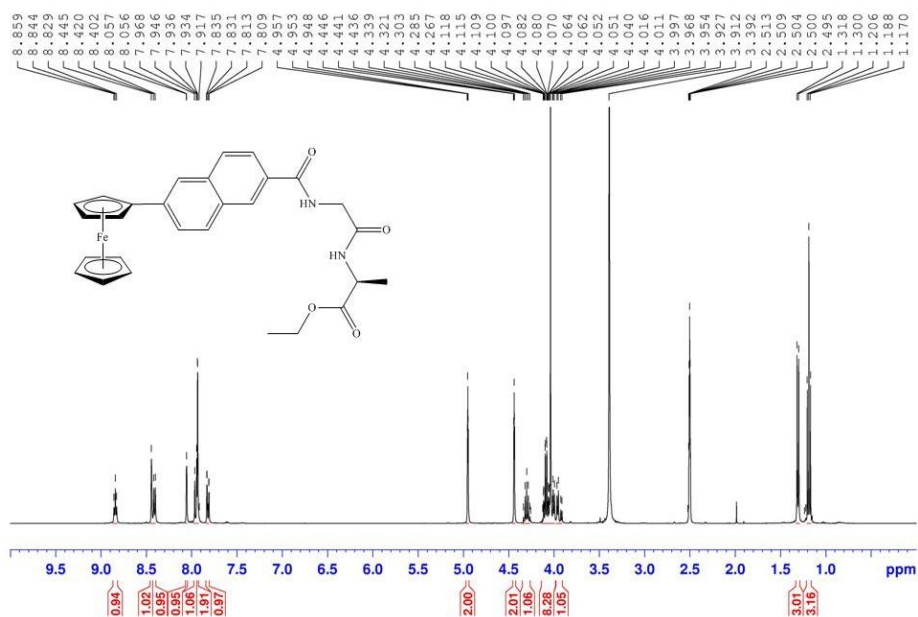


Figure 2.18 ¹H NMR spectrum of *N*-(6-ferrocenyl-2-naphthoyl)-glycine-L-alanine ethyl ester **51**.

2.6. ^{13}C and DEPT 135 NMR studies of *N*-(ferrocenyl)naphthoyl amino acid and dipeptide derivatives

^{13}C and DEPT 135 NMR studies were carried out on all compounds. In a DEPT 135 spectrum, methine and methyl carbons appear as positive peaks, whereas methylene carbons appear as negative peaks *i.e.* below the resonance line. Carbonyl and quaternary carbons are absent in a DEPT 135 spectrum.

In the ^{13}C spectra of the *N*-(ferrocenyl)naphthoyl amino acid and dipeptide derivatives, the amide and ester carbonyl carbons appear downfield in the range of δ 166.0-172.7. In the aromatic region ten carbon signals are observed, since the carbon atoms of the naphthalene ring system are non-equivalent. The four aromatic quaternary carbons can be identified with the aid of DEPT 135 spectra.

Signals due to the ferrocenyl carbons occur from δ 66.6-84.7 in the ^{13}C NMR spectra. As observed for the ^1H NMR spectra of the *N*-(ferrocenyl)naphthoyl amino acid and dipeptide derivatives, there are slight differences in the chemical shift of the ferrocenyl carbons depending on the substitution pattern around the aromatic linker. For the *N*-(6-ferrocenyl-2-naphthoyl) amino acid and dipeptide derivatives, the *ipso* carbon on the substituted cyclopentadienyl ($\eta^5\text{-C}_5\text{H}_4$) ring appears from δ 83.9-84.1, whilst the unsubstituted cyclopentadienyl ring ($\eta^5\text{-C}_5\text{H}_5$) appears as an intense peak at approximately δ 69.5. The signal due to the *meta* ($\eta^5\text{-C}_5\text{H}_4$) carbons generally overlaps with this peak or appears in close proximity at δ 69.4, whilst the *ortho* ($\eta^5\text{-C}_5\text{H}_4$) peak appears slightly upfield at δ 66.6. In the case of the *N*-(3-ferrocenyl-2-naphthoyl) amino acid and dipeptide derivatives, the signal due to the *ortho* ($\eta^5\text{-C}_5\text{H}_4$) carbons is shifted downfield to between δ 68.4 and δ 69.4. This indicates that these carbons have become deshielded with respect to the *ortho* ($\eta^5\text{-C}_5\text{H}_4$) carbons of the *N*-(6-ferrocenyl-2-naphthoyl) amino acid and dipeptide derivatives. The *meta* ($\eta^5\text{-C}_5\text{H}_4$) carbons of the *N*-(3-ferrocenyl-2-naphthoyl) amino acid and dipeptide derivatives come into resonance from δ 68.1-68.6. Two individual peaks corresponding to the *meta* ($\eta^5\text{-C}_5\text{H}_4$) carbons were also observed in close proximity in some ^{13}C NMR spectra, *e.g.* in the spectrum obtained for *N*-(3-ferrocenyl-2-naphthoyl)-L-leucine ethyl ester **82**, indicating the magnetic inequivalence of these species. The *ipso* carbon on the substituted cyclopentadienyl ($\eta^5\text{-C}_5\text{H}_4$) ring and the unsubstituted ($\eta^5\text{-C}_5\text{H}_5$) ring carbons of

the *N*-(3-ferrocenyl-2-naphthoyl) amino acid and dipeptide derivatives remain largely unaffected.

The methylene group of the ethyl ester appears in the very narrow range of δ 60.3-60.6 and is easily identifiable due to the negative resonance in the DEPT 135 spectrum. The methyl carbon comes into resonance at approximately δ 14.

Table 2.4 Selected ^{13}C NMR data (δ , $\text{DMSO-}d_6$) for *N*-(ferrocenyl)naphthoyl amino acid and dipeptide derivatives.

Compound		<i>Ips</i>	<i>ortho</i>	<i>meta</i>	
No.	C=O	($\eta^5\text{-C}_5\text{H}_4$)	($\eta^5\text{-C}_5\text{H}_4$)	($\eta^5\text{-C}_5\text{H}_4$)	($\eta^5\text{-C}_5\text{H}_5$)
81	172.5-169.3	84.3	68.5	68.3, 68.2	69.5
84	169.9-169.3	84.4	68.9	68.3	69.5
87	171.4-168.9	84.3	68.9	68.3	69.5
94	172.7-166.7	84.0	66.6	69.4	69.5
95	171.7-166.5	83.9	66.6	69.4	69.5
98	171.4-166.4	84.1	66.6	69.5	69.5
99	173.0-166.1	84.1	66.6	69.4	69.5
100	172.5-166.0	84.1	66.6	69.4	69.5
101	172.7-166.0	84.1	66.6	69.5	69.5

2.6.1. ^{13}C and DEPT 135 NMR study of *N*-(6-ferrocenyl-2-naphthoyl)-glycine-L-leucine ethyl ester (**97**)

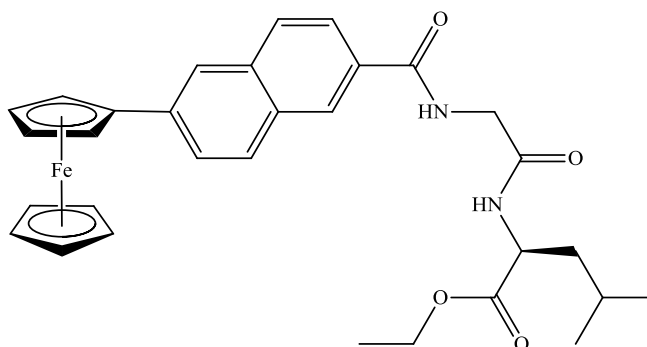


Figure 2.19 *N*-(6-ferrocenyl-2-naphthoyl)-glycine-L-leucine ethyl ester **97**.

The ^{13}C NMR spectrum of *N*-(6-ferrocenyl-2-naphthoyl)-glycine-L-leucine ethyl ester **97** displays three carbonyl carbon atoms at δ 172.5, δ 169.1 and δ 166.5. These are absent from the DEPT 135 spectrum. The aromatic region shows ten individual signals, representing the ten non-equivalent carbon atoms of the 2,6-disubstituted naphthalene group. The absence of the carbon atoms at δ 138.8, δ 134.5, δ 130.7 and δ 130.5 in the DEPT 135 spectrum indicates their quaternary nature. The six remaining carbon atoms appear at δ 128.7, δ 127.5, δ 127.3, δ 125.9, δ 124.5 and δ 122.7, respectively. The signal at δ 84.1 is not present in the DEPT 135 spectrum and therefore it is assigned as the *ipso* ferrocenyl carbon. Upfield from the ferrocenyl *ipso* carbon signal, an intense signal is observed for the unsubstituted ($\eta^5\text{-C}_5\text{H}_5$) ring carbons and the *meta* ($\eta^5\text{-C}_5\text{H}_4$) carbons at δ 69.4. The signal due to the *ortho* ($\eta^5\text{-C}_5\text{H}_4$) carbons appears at δ 66.6. The methylene groups can be assigned from the DEPT 135 spectrum due to the negative peak. The methylene carbons of the ethyl ester, glycine and L-leucine moieties are easily assigned as they show negative resonance peaks in the DEPT 135 spectrum at δ 60.4, δ 42.2 and δ 40.1, respectively. The α -carbon of the L-leucine residue comes into resonance at δ 50.3. The methine carbon of the L-leucine side chain is observed at δ 24.2. The methyl groups of the L-leucine residue are present at δ 22.7 and δ 21.4 and the methyl group of the ethyl ester is present at δ 14.0.

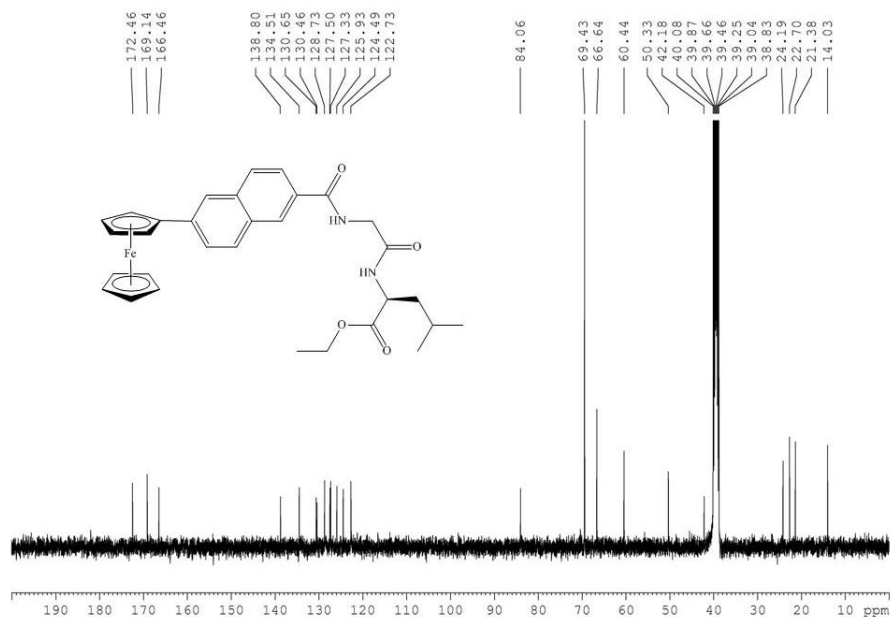


Figure 2.20 ^{13}C NMR spectrum of *N*-(6-ferrocenyl-2-naphthoyl)-glycine-L-leucine ethyl ester **97**.

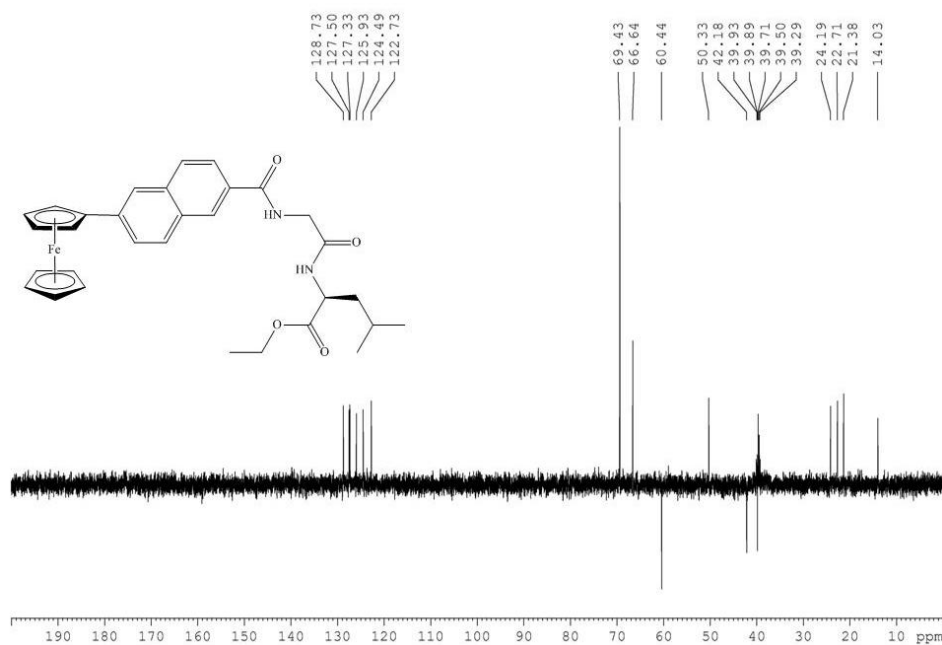


Figure 2.21 DEPT 135 spectrum of *N*-(6-ferrocenyl-2-naphthoyl)-glycine-L-leucine ethyl ester **97**.

2.7. HMQC study of *N*-(6-ferrocenyl-2-naphthoyl)-L-alanine-glycine ethyl ester (**99**)

HMQC (Heteronuclear Multiple Quantum Coherence) is a 2D NMR technique that correlates each ^{13}C atom to the proton to which it is directly attached. Thus, HMQC allows for the complete assignment of proton and carbon spectra, and hence total structure elucidation. In addition, the carbon dimension is frequently utilised to resolve the overlapping proton signals in complex spectra. Since this technique correlates a carbon signal to any directly associated protons, no signals are observed for those carbon atoms lacking protons *i.e.* carbonyl or quaternary carbon atoms. The structure and HMQC spectrum of *N*-(6-ferrocenyl-2-naphthoyl)-L-alanine-glycine ethyl ester **99** is shown in Figures 2.22 and 2.23, respectively.

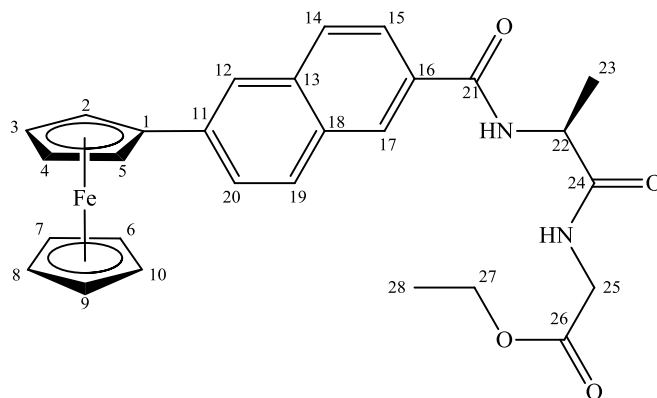


Figure 2.22 *N*-(6-ferrocenyl-2-naphthoyl)-L-alanine-glycine ethyl ester **99**.

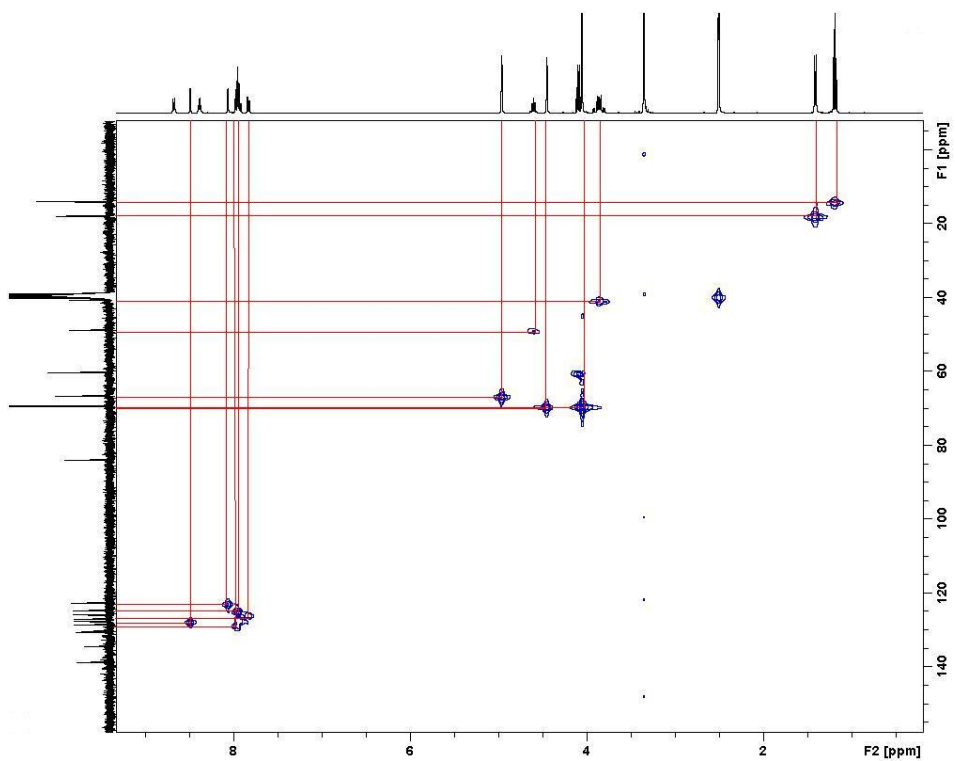


Figure 2.23 HMQC spectrum of *N*-(6-ferrocenyl-2-naphthoyl)-L-alanine-glycine ethyl ester **99**.

Table 2.5 HMQC data for *N*-(6-ferrocenyl-2-naphthoyl)-L-alanine-glycine ethyl ester **99**.

Site	¹ H NMR	¹³ C NMR	HMQC
1		84.1	
2, 5	4.96		66.6
3, 4	4.45		69.4
6 to 10	4.05		69.5
11		138.8	
12	8.06		122.7
13		130.6 ^a	
14	7.94		127.2
15	7.94		127.7
16		134.5	
17	8.48		128.7
18		130.4 ^b	
19	7.94		124.8
20	7.82		125.9
21		166.1	
22	4.60		48.8
23	1.41		17.9
24		169.7	
25	3.89, 3.82		40.7
26		173.0	
27	4.12		60.3
28	1.19		14.0

^{a,b} Signals may be reversed.

2.8. Infra red studies of *N*-(ferrocenyl)naphthoyl amino acid and dipeptide derivatives

Infra red (IR) spectroscopy is a spectroscopic method by which many functional groups can be identified. Compounds can absorb IR radiation and hence various molecular vibrations are induced e.g. stretching, bending, rocking etc. These localised vibrations are very useful for the identification of key functional groups.²²

The region of the spectrum above 1500 cm^{-1} gives the most information on the structure of the molecule, while the fingerprint region (less than 1500 cm^{-1}) contains numerous absorption bands and is of less consequence. The IR spectra of the *N*-(ferrocenyl)naphthoyl amino acid and dipeptide derivatives were obtained either as KBr discs or as pure solids. The spectra of these compounds generally show two bands above 3000 cm^{-1} that correspond to the secondary amide groups. In the carbonyl region it is usual to observe at least two bands for primary and secondary amides. The one at higher frequency is the stretching vibration of the C=O bond; it is called the amide I band and typically appears between 1680 and 1630 cm^{-1} . The amide II band is found between 1570 and 1515 cm^{-1} and is the localised bending vibration of the N-H bond. The ester carbonyl band usually appears at higher frequency, between 1750 and 1735 cm^{-1} . Bands due to aryl rings are present in the 1225 - 950 cm^{-1} region but are not very informative, as are a group of weak overtone and combination bands in the 2000 - 1600 cm^{-1} region.

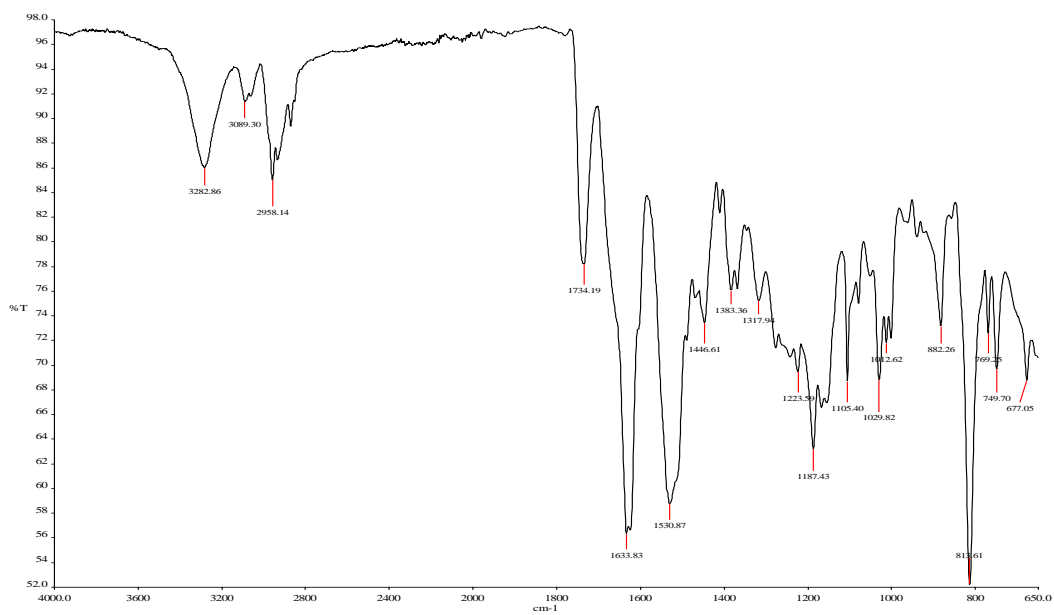


Figure 2.24 IR spectrum of *N*-(6-ferrocenyl-2-naphthoyl)-L-alanine-L-leucine ethyl ester **101**.

Table 2.6 Selected IR data for *N*-(ferrocenyl)naphthoyl amino acid and dipeptide derivatives. The values quoted are in cm^{-1} .

Compound No.	N-H	C=O amide I	C=O amide II	C=O ester
82	3322	1649	1544	1735
83	3342	1645	1544	1734
88	3397	1646	1544	1748
93	3442	1638	1542	1734
96	3407, 3340	1654, 1650	1558	1732
100	3448, 3288	1636	1546	1735

2.9. UV-Vis studies of *N*-(ferrocenyl)naphthoyl amino acid and dipeptide derivatives

The visible and ultraviolet spectra of organic compounds are associated with transitions between electronic energy levels. The transitions are usually between a bonding or a lone pair orbital and an unfilled non-bonding or anti-bonding orbital. The wavelength is then a measure of the separation of the energy levels of the orbitals concerned. The most informative region in the UV-Vis range occurs above 200 nm, as this is where excitation of electrons from *p*- and *d*-orbitals, π -orbitals and particularly, π -conjugated systems, gives rise to readily measured and informative spectra.²²

The UV-Vis spectra of *N*-(ferrocenyl)naphthoyl amino acid and dipeptide derivatives differ significantly. The *N*-(6-ferrocenyl-2-naphthoyl) amino acid and dipeptide derivatives give the strongest absorptions in the visible region, with local maxima at 375 nm and 450 nm, respectively. The strength of these absorbances is an indication of the degree of conjugation between the naphthoyl group and the (η^5 -C₅H₄) group *i.e.* a strong absorbance indicates that these two groups lie roughly in the same plane creating a large chromophore. The absorbance at 375 nm can be assigned to a π to π^* transition of the aromatic spacer group and the absorbance at 450 nm is attributed to a metal to ligand charge transfer band (MLCT). In Figure 2.25, it can be seen that upon substitution of the ferrocene moiety, the MLCT band undergoes a red shift from 420 nm to 450 nm, this is also indicative of conjugation.

The corresponding values in the UV-Vis spectra of the *N*-(ferrocenyl)benzoyl derivatives, show that the absorbances are not as intense as is the case with the *N*-(6-ferrocenyl-2-naphthoyl) amino acid and dipeptide derivatives, and they typically appear at shorter wavelengths.²³ In the case of the *N*-(3-ferrocenyl-2-naphthoyl) amino acid and dipeptide derivatives, the absorbance due to the π to π^* transition of the aromatic spacer group is much weaker, and there is only one absorbance with a local maximum of around 450 nm due to the MLCT band. The weakness of this absorption suggests that the (η^5 -C₅H₄) and naphthoyl groups do not lie in the same plane, hence presenting an increasing barrier to efficient conjugation.

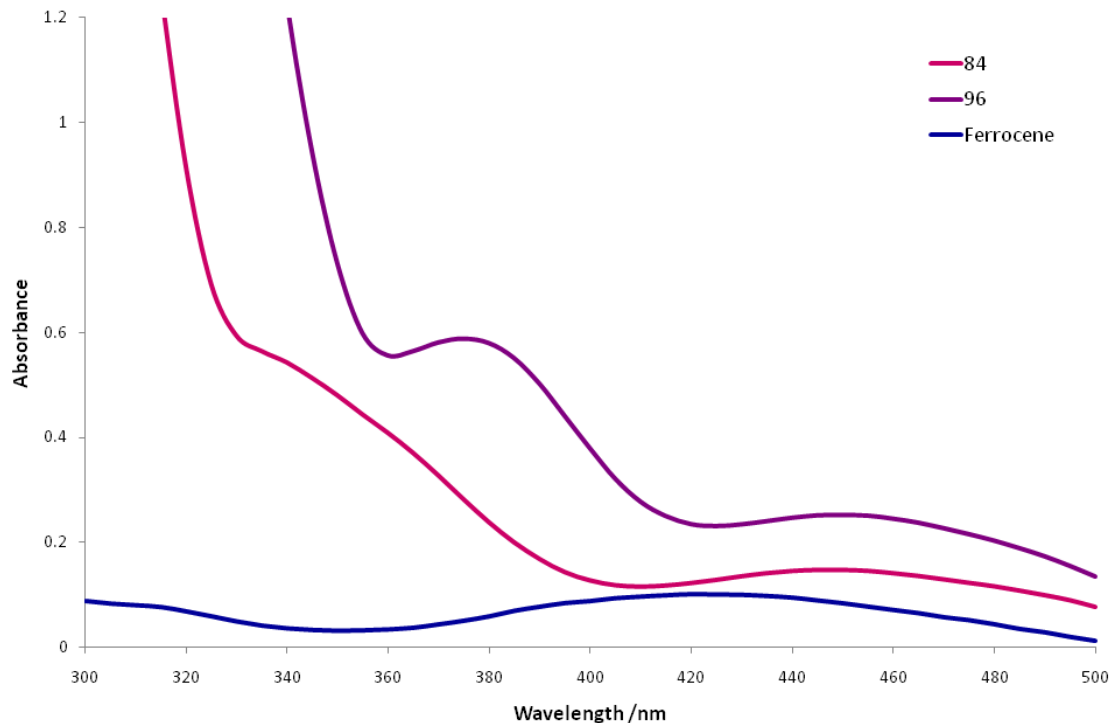


Figure 2.25 UV-Vis spectra of ferrocene, *N*-(3-ferrocenyl-2-naphthoyl)-glycine-glycine ethyl ester **84** and *N*-(6-ferrocenyl-2-naphthoyl)-glycine-glycine ethyl ester **96**.

These absorbances also yield other interesting information. Extinction coefficients are a function of how efficiently a chromophore absorbs UV or visible radiation. Therefore, the extent of conjugation is an important consideration. The UV-Vis spectra show a large disparity in the intensity of the absorbances between the *N*-(6-ferrocenyl-2-naphthoyl) amino acid and dipeptide derivatives, and the corresponding *N*-(3-ferrocenyl-2-naphthoyl) analogues. Since the former compounds are more conjugated than the latter compounds, the bands in the visible region go from being relatively intense for the first group of compounds to much less intense for the second group. This is in accordance with the observations made for the *N*-(ferrocenyl) benzoyl peptide derivatives.²³ Extinction coefficients are given by ϵ and can be calculated from the Beer-Lambert Law *i.e.* $A = \epsilon Cl$, where A is absorbance, C is concentration, l is the path length of the cell. In this UV-Vis study, the spectra of all compounds were obtained at a concentration of 4×10^{-4} M.

Table 2.7 Selected UV-Vis data (nm) for *N*-(ferrocenyl)naphthoyl amino acid and dipeptide derivatives.

Compound No.	λ_{max1} (nm)	ϵ_1	λ_{max2} (nm)	ϵ_2
81	-	-	450	512
94	375	3256	450	1395
84	-	-	445	572
51	375	3451	450	1482
100	375	3233	450	1349
<i>p</i> -Fc-Bz-Ala-Gly-OEt*	352	2400	450	720

* *N*-{*para*-(ferrocenyl)-benzoyl}-L-alanine-glycine ethyl ester as prepared by David Savage.²³

2.10. Cyclic voltammetry studies of *N*-(ferrocenyl)naphthoyl amino acid and dipeptide derivatives

Cyclic Voltammetry (CV) is a versatile electroanalytical technique for studying electroactive molecules.²⁴ It has been employed extensively to evaluate the redox properties of organometallic compounds, including ferrocene.²⁵ In a CV experiment, the voltage applied to the working electrode is scanned from an initial position, A, to a predetermined endpoint, D (Figure 2.26), the scan is then reversed. This forward and reverse scanning can be repeated as many times as is necessary. The potential of the working electrode is controlled *versus* a reference electrode. For the electrochemistry experiments reported Ag|AgCl is used as the reference electrode. This reference is used in preference to other reference electrodes, namely, the normal hydrogen electrode (NHE) and the saturated calomel electrode (SCE). The Ag|AgCl electrode is more robust and is easier to maintain. In addition, it does not have the toxicity and safety problems associated with the SCE and NHE.²⁶

A cyclic voltammogram is obtained by measuring the current at the working electrode during a potential scan. The voltammogram, such as that in Figure 2.26, is a plot of current (vertical axis) *versus* potential (horizontal axis).

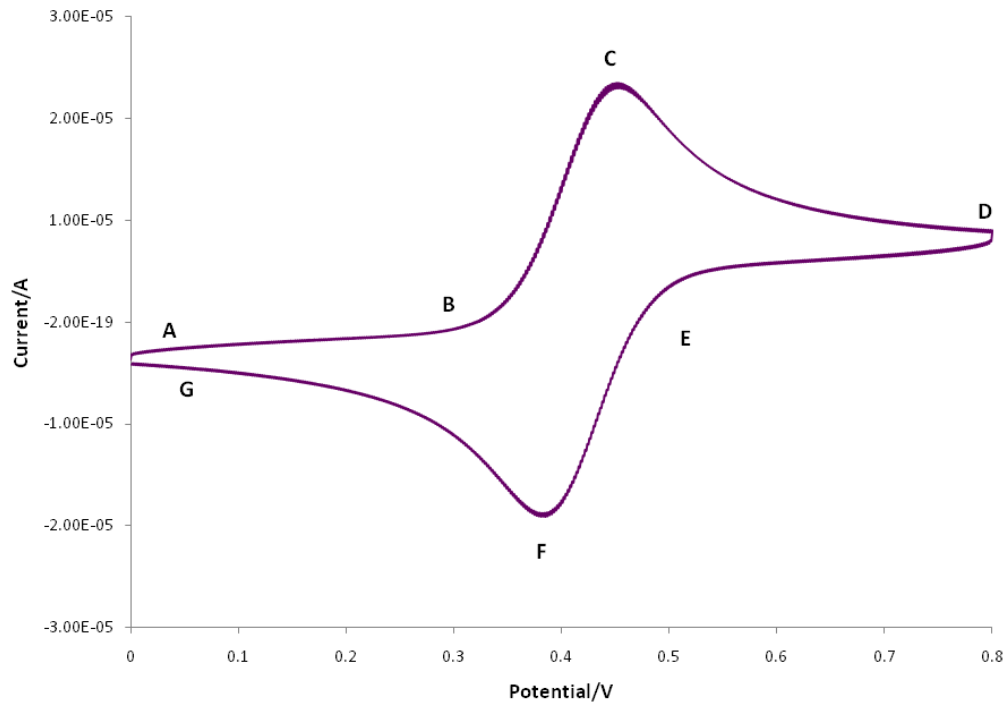


Figure 2.26 Cyclic voltammogram of ferrocene in ACN with glassy carbon working electrode, platinum wire counter electrode and Ag|AgCl reference electrode.

- A.** The initial potential is applied at 0 V. The potential is then scanned in a positive direction.
- B.** When the potential is sufficiently positive, the ferrocenyl compound is oxidised to the ferricenium compound, $\text{Fc} \rightarrow \text{Fc}^+$. The anodic current then begins to increase.
- C.** The anodic current continues to increase until the system surrounding the electrode is depleted of ferrocenyl compound due to its conversion to ferricenium species.
- D-G.** At this stage the ferricenium species begins to get reduced back to the ferrocenyl species, thus the cathodic current begins. As is the case with a redox system that behaves in an ideal fashion, the reverse scan roughly mirrors the forward scan. The reverse scan ends when the current reaches the start point, 0 V.

The *N*-(ferrocenyl)naphthoyl amino acid and dipeptide derivatives exhibit one electron, reversible, redox waves similar to ferrocene, under the same conditions. The $E^{0'}$ (oxidation potential) values for the *N*-(3-ferrocenyl-2-naphthoyl) amino acid and dipeptide derivatives

were in the range of 5-29 mV, whilst the *N*-(6-ferrocenyl-2-naphthoyl) amino acid and dipeptide derivatives showed values in the 42-60 mV range *versus* the ferrocene/ferricenium redox couple (Fc/Fc⁺). Figure 2.27 illustrates the difference in potential of the CVs obtained for *N*-(3-ferrocenyl-2-naphthoyl)-L-alanine-L-phenylalanine ethyl ester **91** and *N*-(6-ferrocenyl-2-naphthoyl)-L-alanine-L-phenylalanine ethyl ester **102**.

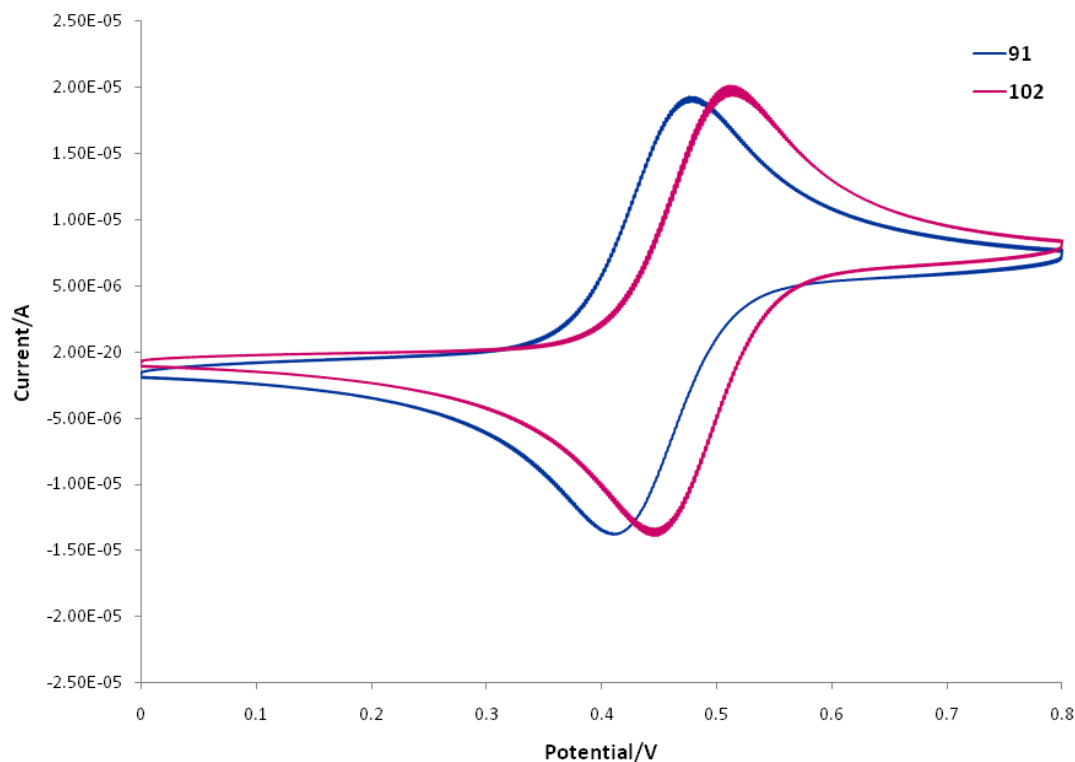


Figure 2.27 Cyclic voltammograms of *N*-(3-ferrocenyl-2-naphthoyl)-L-alanine-L-phenylalanine ethyl ester **91** and *N*-(6-ferrocenyl-2-naphthoyl)-L-alanine-L-phenylalanine ethyl ester **102** (0.1 M TBAP in ACN, Ag|AgCl, 0.1 V s⁻¹).

The $E^{0'}$ values for the *N*-(6-ferrocenyl-2-naphthoyl) amino acid and dipeptide derivatives are comparable with those reported for the *N*-(ferrocenyl)benzoyl peptide derivatives (33 to 78 mV *vs.* Fc/Fc⁺).¹⁶ These $E^{0'}$ values are much lower than those observed for *N*-ferrocenoyl peptide esters, for example *N*-Fc-Ala-Ala-OMe shows a $E^{0'}$ of 190 mV *vs.* Fc/Fc⁺, while *N*-Fc-Ala-Phe-OMe has a $E^{0'}$ of 230 mV *vs.* Fc/Fc⁺.²⁷ The amide carboxyl group is strongly electron withdrawing and consequently *N*-ferrocenoyl peptide esters are difficult to oxidise. The presence of a naphthoyl linker between the ferrocene moiety and

the peptide chain provides extended conjugation to the π -electrons of the Cp rings making initial oxidation of the iron centre easier.

The $E^{0'}$ values determined for the *N*-(3-ferrocenyl-2-naphthoyl) amino acid and dipeptide derivatives are more comparable to that determined for ferrocene itself. The *ortho*-relationship between the two naphthyl substituents imposes a steric restriction on the bulky ferrocene group, forcing it to adopt a position out-of-plane with respect to the naphthoyl ring. Consequently, efficient overlap between the naphthoyl *p*-orbitals and the *p*-orbitals of the Cp ring is prevented in the *N*-(3-ferrocenyl-2-naphthoyl) amino acid and dipeptide derivatives; only minimal conjugation is occurring.

2.11. Mass spectrometric studies of *N*-(ferrocenyl)naphthoyl amino acid and dipeptide derivatives

Mass spectrometry enables the determination of the relative molecular mass of many different types of compounds.²⁸ The mass spectrometer is composed of three distinct parts, namely the ion source, the analyser and the detector. After the sample has been introduced into the ion source ionisation occurs. These ions are then extracted into the analyser, where they are separated according to their mass (*m*) to charge (*z*) ratios (*m/z*). The separated ions are detected and displayed as a mass spectrum.

Since the *N*-(ferrocenyl)naphthoyl amino acid and dipeptide derivatives are non-volatile, a soft ionisation technique such as electrospray ionisation must be employed in their analysis. Thus, the *N*-(ferrocenyl)naphthoyl amino acid and dipeptide derivatives were analysed by electrospray ionisation (ESI) mass spectrometry, which confirmed the correct relative molecular mass for each compound. Examination of the mass spectra revealed the presence of both radical cation species, $[M]^{+\bullet}$ as well as $[M+H]^+$ species at one mass unit higher. Intense adducts due to sodium and potassium were also present 22 and 38 mass units higher than the protonated molecular ion species. Sequence specific fragment ions were not observed or were of low intensity in the mass spectra and therefore tandem mass spectrometry (MS/MS) experiments were performed for several compounds.

2.11.1. Tandem Mass Spectrometry (MS/MS)

Tandem mass spectrometry (MS/MS) is a well-established analytical technique for the determination of the primary sequence of peptides and proteins.²⁹ A tandem mass spectrometer is a mass spectrometer that has more than one analyser, in practice usually two. A collision cell (which functions by fragmenting the ions that were selected by the first analyser) is positioned between the two analysers. The first analyser is used to select user specified sample ions arising from a particular component; usually the $(M+H)^+$ or $(M-H)^-$ ions. These chosen ions pass into the collision cell and are bombarded by the gas molecules, which cause fragment ions to be formed. The resultant fragment ions are analysed according to their mass to charge ratios, by the second analyser. All of the fragment ions arise directly from the precursor ions specified in the experiment. Thus, a fingerprint pattern specific to the compound under investigation is produced.

The identification of fragment ions arising from MS/MS analysis of peptides has been facilitated by a nomenclature system which was devised by Roepstorff.³⁰ This nomenclature system differentiates fragment ions according to the amide bond that fragments and the end of the peptide that retains a charge after fragmentation. The appearance of a, b or c ions suggest that charge retention has occurred at the *N*-terminal, while the appearance of x, y or z ions are consistent with charge retention at the *C*-terminal. A schematic depiction of this system is shown in Figure 2.28.

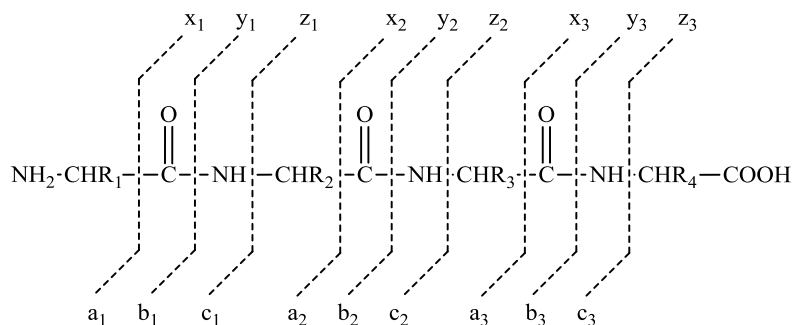


Figure 2.28 The suggested nomenclature for peptide fragment ions produced during MS/MS.³⁰

Positive-ion mode MS/MS data was obtained for *N*-(3-ferrocenyl-2-naphthoyl)-glycine-L-alanine ethyl ester **85** and *N*-(6-ferrocenyl-2-naphthoyl)-glycine-L-alanine ethyl ester **51**

(Figure 2.29). It can be seen that the fragmentation pattern for the two compounds is completely different. The MS/MS spectrum of *N*-(3-ferrocenyl-2-naphthoyl)-glycine-L-alanine ethyl ester **85** shows a major product ion at m/z 447, which corresponds to the loss of the unsubstituted (η^5 -C₅H₅) ring. The formation of this fragment ion is possibly due to steric hindrance between the *ortho* substituted naphthoyl substituents and the (η^5 -C₅H₅) ring. This fragment ion was also observed for the *N-ortho*-(ferrocenyl)-benzoyl amino acid and dipeptide derivatives.^{31,10} The product ion at m/z 373 is due to [M-65-H₂O-Fe]⁺.

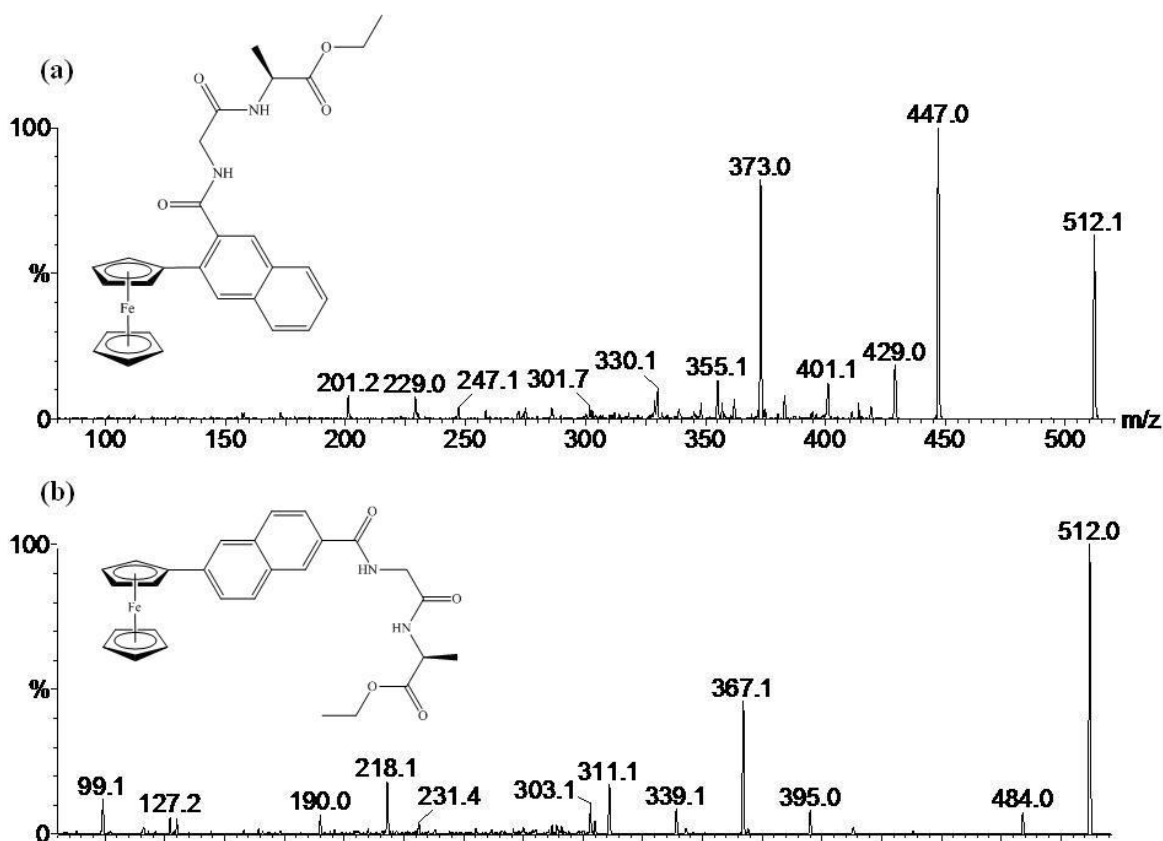


Figure 2.29 MS/MS spectrum of (a) *N*-(3-ferrocenyl-2-naphthoyl)-glycine-L-alanine ethyl ester **85** and (b) *N*-(6-ferrocenyl-2-naphthoyl)-glycine-L-alanine ethyl ester **51**.

In the MS/MS spectrum of *N*-(6-ferrocenyl-2-naphthoyl)-glycine-L-alanine ethyl ester **51** sequence specific ions were observed, which confirm that the glycine residue was linked to the naphthoyl spacer group. A product ion present at m/z 311 confirms the presence of a ferrocenyl naphthyl subunit and the signal at m/z 339 is due to cleavage at the naphthoyl carbonyl group (Figure 2.30). However, the expected a_1 and b_1 product ions at m/z 368 and

m/z 396 were not observed. Instead a_1-1 and b_1-1 product ions were observed at m/z 367 and m/z 395, respectively, thus, a hydrogen atom has also been lost during the fragmentation process. This is unusual as these a_1 and b_1 fragment ions are usually produced without loss of a hydrogen atom.³² Recently, the formation of a_1-1 and b_1-1 ions in the mass spectra of *N*-{*para*-(ferrocenyl)-benzoyl}-glycine-L-alanine ethyl ester has been investigated by tandem mass spectrometry and deuterium labelling studies. The results showed that b_1-1 product ions arise from the loss of a hydrogen atom attached to the nitrogen and not to the α -carbon of the glycine residue.³³

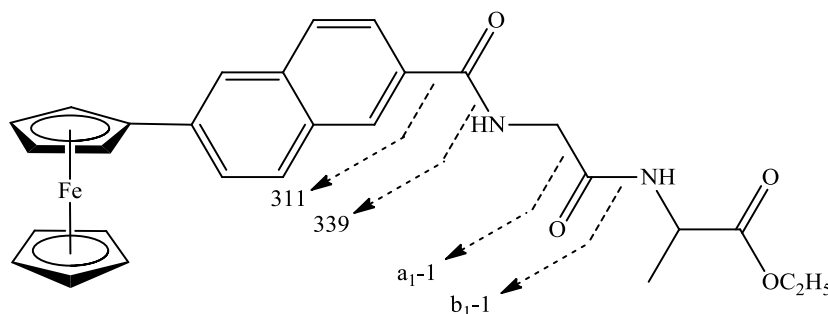


Figure 2.30 Product ions observed in the MS/MS spectrum of *N*-(6-ferrocenyl-2-naphthoyl)-glycine-L-alanine ethyl ester **51**.

2.12. X-ray crystallography study of methyl ferrocenylnaphthalene-2-carboxylate

Crystals suitable for X-ray crystallographic determination of methyl 3-ferrocenylnaphthalene-2-carboxylate **71** and methyl 6-ferrocenylnaphthalene-2-carboxylate **74** were grown from hexane/ethyl acetate yielding red block shaped crystals. Selected bond distances and angles of non hydrogen atoms are given in Table 2.8 and all pertinent crystallographic information is summarised in Table 2.9.

Figure 2.31 shows the molecular structures and asymmetric unit of methyl 3-ferrocenylnaphthalene-2-carboxylate **71**. Compound **71** crystallises in the monoclinic space group $P2_1/c$ with one molecule in the asymmetric unit. The principal dimensions are carboxylate ester C=O 1.199(3) Å, C-O 1.335(2) Å and O-CH₃ 1.449(3) Å and O=C-O 123.6(2) °. The cyclopentadienyl rings of the ferrocene unit (Cp1 and Cp2) are almost eclipsed with C1n...Cg1...Cg2...C2n torsion angles (n = 1-5) in the -0.7(42) to 1.3(3) °

range. Centroids Cg1 and Cg2 are equidistant from the iron core, with Fe...Cg1/Cg2 distances of 1.643(3)/1.646(2), respectively, while the Cg1...Fe...Cg2 angle is almost linear at 178.3(3)°. There are no classical hydrogen bonds present; however, there is a short contact between a (Cp2) ring carbon C3 and a (Cp1) ring hydrogen H20 of another molecule, contact distance being 2.73(1) Å. There is also a short contact of 2.86(4) Å between a (Cp1) ring carbon C5 of one molecule and (Cp2) ring hydrogen H11 of the neighbouring molecule. There are no significant C-H... π (arene) or π ... π stacking interactions.

In compound **71**, the C₁₀H₆ ring and the four-atom O=C-O-CH₃ plane are oriented at 54.45(12)° and the C₁₀H₆/(η^5 -C₅H₄) rings at 28.27(15)°, whereas the angle between the (η^5 -C₅H₄) ring and the O=C-O-CH₃ plane is 68.87(4)°. This data demonstrates the existence of a large distortion in the molecule, which is evident in Figure 2.31. Steric hindrance has forced the atoms of this molecule to adopt this strained conformation in the solid state, resulting in a loss of co-planarity of the conjugating groups. This is supported by the torsion angles for the O25-C14-C19-C15 bonds and C20-C21-C15-C19 bonds which were calculated to be 54.2(3) and 149.5(2)°, respectively.

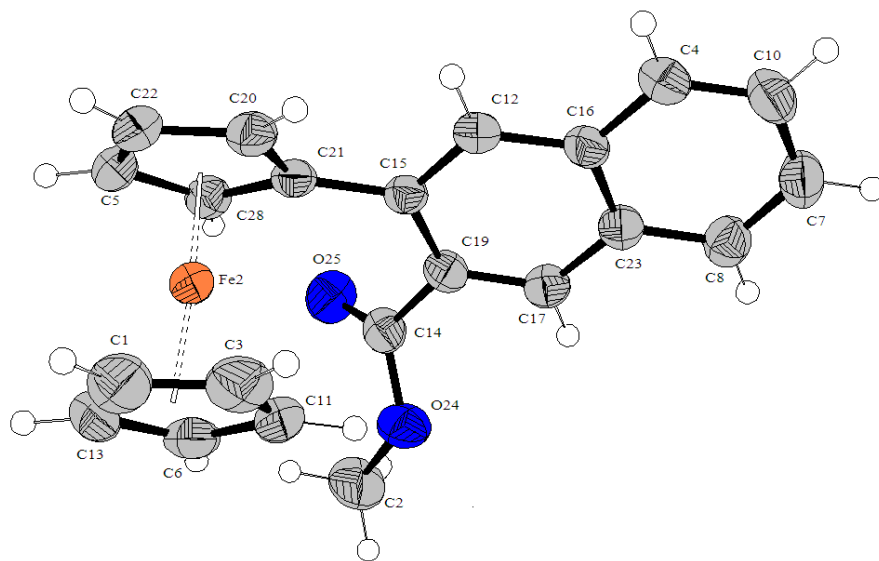


Figure 2.31 Molecular drawing of methyl 3-ferrocenylnaphthalene-2-carboxylate **71** using ORTEP: displacement ellipsoids are drawn at the 50% probability level.

Methyl 6-ferrocenylnaphthalene-2-carboxylate **74** crystallises in the monoclinic space group $P2_1/n$ with one molecule in the asymmetric unit: the molecular structure is depicted in Figure 2.32. The principal dimensions are carboxylate ester C=O 1.198(4) Å, C-O 1.343(4) Å and O-CH₃ 1.438(4) Å and O=C-O 122.5(4)°. In the case of compound **74**, the cyclopentadienyl rings of the ferrocene unit (Cp1 and Cp2) are slightly staggered with C1n...Cg1...Cg2...C2n torsion angles (n = 1-5) in the -12.2(4) to -14.9(2)° range. Centroids Cg1 and Cg2 are equidistant from the iron core, with Fe...Cg1/Cg2 distances of 1.650(3)/1.657(4), respectively, while the Cg1...Fe...Cg2 angle is almost linear at 178.1(3)°. There are no classical hydrogen bonds present; however, there is a significant intermolecular contact between a (Cp2) ring hydrogen H3 and a (Cp2) ring hydrogen H4, contact distance being 2.38(2) Å. There is also a short contact of 2.83(3) Å between a (Cp2) ring carbon C1 and (naphthyl) ring hydrogen H18. There are no significant C-H... π (arene) or π ... π stacking interactions.

The C₁₀H₆ ring and the four-atom O=C-O-CH₃ plane of compound **74** are oriented at 4.45(15)° and the C₁₀H₆/(η^5 -C₅H₄) rings at 3.13(16)°; whereas the angle between (η^5 -C₅H₄) ring and the O=C-O-CH₃ plane is 1.97(5)°. Calculated torsion angles in compound **74** between the O1-C21-C16-C17 bonds and C10-C9-C11-C12 bonds are minimal at 2.9(5) and -4.3(5)°, respectively. Thus, the conjugating groups in this molecule lie almost completely within the same plane in the solid state (Figure 2.32). A similar observation has been reported for the *para*-substituted ferrocenyl methyl benzoate.³⁴

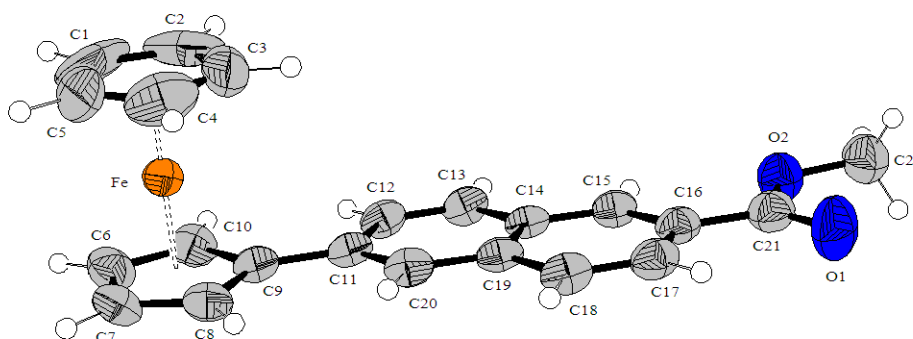


Figure 2.32 Molecular drawing of methyl 6-ferrocenylnaphthalene-2-carboxylate **74** using ORTEP: displacement ellipsoids are drawn at the 50% probability level.

Table 2.8 Representative bond lengths (Å) and angles (°) for methyl 3-ferrocenylnaphthalene-2-carboxylate **71** and methyl 6-ferrocenylnaphthalene-2-carboxylate **74**.

	71		74
Bond Distances/Å		Bond Distances/Å	
Fe2...Cg1	1.643(2)	Fe...Cg1	1.650(3)
Fe2...Cg2	1.646(3)	Fe...Cg2	1.657(4)
Cg1...Fe...Cg2	178.31(3)	Cg1...Fe...Cg2	178.1(3)
C14-O25	1.199(3)	C21-O1	1.198(4)
C14-O24	1.335(2)	C21-O2	1.343(4)
O24-C2	1.449(3)	O2-C22	1.438(4)
Bond Angles/°		Bond Angles/°	
Fe2-C21-C15	125.9(1)	Fe-C9-C11	126.4(6)
C17-C19-C14	115.8(2)	C15-C16-C21	122.5(3)
C15-C19-C14	123.8(2)	C17-C16-C21	118.2(3)
O25-C14-O24	123.6(2)	O1-C21-O2	122.5(4)
O25-C14-C19	125.0(2)	O2-C21-C16	112.4(3)
C14-O24-C2	116.2(2)	C21-O2-C22	116.5(3)
O24-C14-C19	111.3(2)	O1-C21-C16	125.1(4)
C20-C21-C15-C19	149.5(2)	Fe-C9-C11-C20	86.7(3)
C28-C21-C15-C19	156.5(2)	C8-C9-C11-C20	-2.5(3)
Fe2-C21-C15-C19	63.3(2)	C10-C9-C11-C12	-4.3(4)
O24-C14-C19-C15	-129.8(2)	C15-C16-C21-O2	3.7(3)
C14-C19-C15-C21	11.6(3)	C17-C16-C21-O1	2.9(5)

Where Cg1 and Cg2 are the centroids of the (η^5 -C₅H₄) and (η^5 -C₅H₅) rings, respectively.

Table 2.9 Pertinent crystal structure data.

Details	71	74
Empirical formula	C ₂₂ H ₁₈ O ₂ Fe	C ₂₂ H ₁₈ O ₂ Fe
<i>M</i> /g mol ⁻¹	370.21	370.21
Crystal colour, habit	Red block	Red block
Crystal system	Monoclinic	Monoclinic
Space group	P2 ₁ /c	P2 ₁ /n
<i>a</i> /Å	13.9797(15)	14.7851(17)
<i>b</i> /Å	8.7249(9)	6.1301(7)
<i>c</i> /Å	13.9843(15)	18.161(2)
β°	103.111(2)	92.273(3)
<i>V</i> /Å ³	1661.2(3)	1644.8(3)
<i>Z</i>	4	4
Temperature/K	273	298
<i>D</i> _{calc} /g cm ⁻³	1.480	1.495
μ/mm ⁻¹	0.920	0.929
<i>F</i> ₀₀₀	768	768
Crystal dimensions/mm	0.25 x 0.18 x 0.13	0.27 x 0.19 x 0.13
Max. and min. transmission	0.8898 – 0.8027	0.8888 – 0.7876
Refinement method	SHELXL97	SHELXL97
Reflections collected/unique	17252/2927	9115/2883
Final <i>R</i> indices [<i>I</i> > 2σ <i>I</i>]	<i>R</i> ₁ = 0.0285 <i>wR</i> ₂ = 0.0796	<i>R</i> ₁ = 0.0469 <i>wR</i> ₂ = 0.1146
<i>R</i> indices [all data]	<i>R</i> ₁ = 0.0314 <i>wR</i> ₂ = 0.0819	<i>R</i> ₁ = 0.0627 <i>wR</i> ₂ = 0.1220
Goodness of fit	1.018	1.02

2.13. Conclusions

N-(ferrocenyl)benzoyl peptide derivatives have been identified as potential anti-cancer agents following *in vitro* testing in the H1299 NSCLC cell line.¹⁰ This project sought to explore the structure-activity relationship (SAR) of these derivatives, in order to enhance the anti-proliferative effect. The primary focus of this SAR study was centred on altering the conjugating linker, by extending the aromatic framework. Thus, the synthesis of a series of *N*-(ferrocenyl)naphthoyl amino acid and dipeptide derivatives which contain α -amino acids was undertaken. These novel compounds were prepared by condensation of 3-ferrocenylnaphthalene-2-carboxylic acid and 6-ferrocenylnaphthalene-2-carboxylic acid with the appropriate amino acid or dipeptide ethyl ester under solution phase peptide coupling conditions. Purification by column chromatography furnished the required compounds as orange or red solids, in moderate to good yields (18% to 95%).

The *N*-(ferrocenyl)naphthoyl amino acid and dipeptide derivatives were characterised by a range of spectroscopic techniques including ¹H NMR, ¹³C NMR, DEPT 135, HMQC, IR, UV-Vis, MS and CV. The UV-Vis spectra of the *N*-(6-ferrocenyl-2-naphthoyl) amino acid and dipeptide derivatives showed an intense absorbance at 375 nm due to a π to π^* transition of the aromatic spacer group. This absorbance was too weak to be observed in the UV-Vis spectra of the *N*-(3-ferrocenyl-2-naphthoyl) amino acid and dipeptide derivatives. Cyclic voltammetry experiments showed the *N*-(ferrocenyl)naphthoyl amino acid and dipeptide derivatives to exhibit one electron, reversible, redox waves similar to ferrocene, under the same conditions. $E^{0'}$ values for the *N*-(6-ferrocenyl-2-naphthoyl) amino acid and dipeptide derivatives (42-60 mV *vs.* Fc/Fc⁺) were much lower than those observed for *N*-ferrocenoyl peptide esters. However, the $E^{0'}$ values for the *N*-(3-ferrocenyl-2-naphthoyl) amino acid and dipeptide derivatives (5-29 mV *vs.* Fc/Fc⁺) were more comparable to that determined for ferrocene itself. The MS/MS spectrum of *N*-(3-ferrocenyl-2-naphthoyl)-glycine-L-alanine ethyl ester **85**, showed a major product ion at m/z 447, which corresponds to the loss of the unsubstituted (η^5 -C₅H₅) ring. This product ion is absent from the MS/MS spectrum of *N*-(6-ferrocenyl-2-naphthoyl)-glycine-L-alanine ethyl ester **51**.

This data provides evidence that π conjugation is occurring between the ferrocene and naphthalene units in the *N*-(6-ferrocenyl-2-naphthoyl) amino acid and dipeptide derivatives.

In contrast, π conjugation between these two units is minimal in the *N*-(3-ferrocenyl-2-naphthoyl) amino acid and dipeptide derivatives. In the latter case, the *ortho*-relationship of the two naphthyl substituents imposes a steric restriction on the bulky ferrocene group, forcing it to adopt a position out-of-plane with respect to the naphthalene ring. Thus, effective π conjugation is prevented. An X-ray crystallography study illustrates the out-of-plane position adopted by the ferrocene group in methyl 3-ferrocenylnaphthalene-2-carboxylate **71**. In contrast, the molecular structure of methyl 6-ferrocenylnaphthalene-2-carboxylate **74** shows the ferrocene group to lie almost completely within the same plane as the naphthalene unit.

Experimental Procedures

Experimental Note

All chemicals were purchased from Sigma-Aldrich, Lennox Chemicals, Fluorochem Limited or Tokyo Chemical Industry UK Limited; and used as received. Commercial grade reagents were used without further purification. When necessary, all solvents were purified and dried prior to use. Riedel-Haën silica gel was used for thin layer and column chromatography. Melting points were determined using either a Griffin melting point apparatus or a Stuart melting point (SMP3) apparatus and are uncorrected. Optical rotation measurements were made on a Perkin Elmer 343 Polarimeter and are quoted in units of 10^{-1} deg $\text{cm}^2 \text{g}^{-1}$. Infrared spectra were recorded on either a Perkin Elmer Spectrum GX FT-IR or a Perkin Elmer Spectrum 100 FT-IR with ATR. UV-Vis spectra were recorded on a Hewlett Packard 8452 A diode array UV-Vis spectrophotometer. ^1H and ^{13}C NMR spectra were recorded in deuterated solvents on a Bruker Avance 400 NMR. The ^1H and ^{13}C NMR chemical shifts are reported in ppm (parts per million). Tetramethylsilane (TMS) or the residual solvent peaks have been used as an internal reference. All coupling constants (J) are in Hertz. The abbreviations for the peak multiplicities are as follows: s (singlet), d (doublet), dd (doublet of doublets), t (triplet), q (quartet), qt (quintet), m (multiplet) and br (broad). Electrospray ionisation mass spectra were performed on a Micromass LCT mass spectrometer or a Bruker Daltonics Esquire-LC ion trap mass spectrometer. Tandem mass spectra were obtained on a Micromass Quattro *micro*TM LC-MS/MS triple quadrupole mass spectrometer. Elemental analysis was carried out by the microanalytical laboratory at University College Dublin.

Cyclic voltammograms were recorded in anhydrous acetonitrile (Sigma-Aldrich), with 0.1 M tetrabutylammonium perchlorate (TBAP) as a supporting electrolyte, using a CH Instruments 600a electrochemical analyzer (Pico-Amp Booster and Faraday Cage). The experiments were carried out at room temperature. A three-electrode cell consisting of a glassy carbon working-electrode, a platinum wire counter-electrode and an Ag|AgCl reference electrode was used. The glassy carbon electrode was polished with 0.3 μm

alumina followed by 0.05 μm alumina, between each experiment to remove any surface contaminants. The scan rate was 0.1 V s⁻¹. The concentration range of the ferrocene compounds was 1.0 mM in acetonitrile. The $E^{0'}$ values obtained for the test samples were referenced relative to the ferrocene/ferricenium redox couple.

General procedure for the preparation of starting materials for N-(ferrocenyl)naphthoyl peptide derivatives.

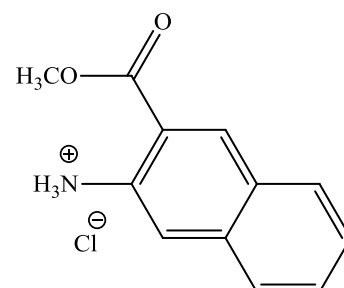
Methyl 3-aminonaphthalene-2-carboxylate hydrochloride 70

3-Amino-2-naphthoic acid (1.51 g, 8.1 mmol) was added slowly to a solution of methanol (50 ml) and thionyl chloride (8 ml) at 0 °C and then refluxed for 24 h. The solution was cooled and the product was isolated by filtration as a pale pink/brown solid (1.45 g, 75%), mp 185-187 °C;

δ_{H} (400 MHz, DMSO-*d*₆): 8.61 (1H, s, ArH), 8.03 (1H, d, *J*

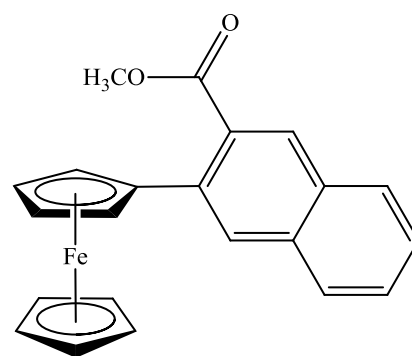
8.0, ArH), 7.84 (1H, d, *J* 8.0, ArH), 7.76 (1H, s, ArH), 7.60 (1H, t, *J* 8.0, ArH), 7.46 (1H, t, *J* 8.0, ArH), 3.92 (3H, s, -OCH₃);

δ_{C} (100 MHz, DMSO-*d*₆): 166.2 (C=O), 135.7 (C_q), 135.3 (C_q), 133.1, 129.5, 129.2, 128.4 (C_q), 126.4, 125.4, 118.4 (C_q), 117.6, 52.4 (-OCH₃).



Methyl 3-ferrocenylnaphthalene-2-carboxylate 71

Concentrated hydrochloric acid (4 ml) was added with intermittent cooling to a solution of methyl 3-aminonaphthalene-2-carboxylate hydrochloride (2.62 g, 11 mmol) in 15 ml of water. A solution of sodium nitrite (0.9 g, 13 mmol) in 15 ml of deionised water was then added slowly to this mixture with stirring, keeping the temperature below 5 °C to furnish a pale brown/yellow



solution. The resulting diazo salt was added to a solution of ferrocene (2.42 g, 13 mmol) in diethyl ether (90 ml) and allowed to react for 18 h. The reaction was then washed with water, the ether layer was dried over MgSO₄ and the solvent was removed *in vacuo* to yield

the crude product. The crude product was purified using column chromatography {eluant 3:2 petroleum ether (40-60°C): diethyl ether} to obtain an orange solid (1.23 g, 30%), mp 119-120 °C;

Anal. Calc. for C₂₂H₁₈O₂Fe: C, 71.4; H, 4.9%. Found: C, 71.35; H, 4.9;

m/z (ESI) 370.4 [M]⁺. C₂₂H₁₈O₂Fe requires 370.2;

λ_{\max} (EtOH)/nm 440 ($\epsilon/\text{dm}^3 \text{ mol}^{-1} \text{ cm}^{-1}$ 574);

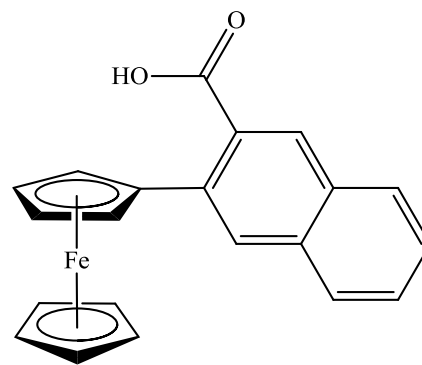
ν_{\max} (KBr)/cm⁻¹ 1720, 1494, 1201;

δ_{H} (400 MHz, DMSO-*d*₆): 8.40 (1H, s, ArH), 8.07 (1H, s, ArH), 8.05 (1H, d, *J* 8.0, ArH), 7.97 (1H, d, *J* 8.0, ArH), 7.61 (1H, t, *J* 8.0, ArH), 7.54 (1H, t, *J* 8.0, ArH), 4.59 {2H, t, *J* 1.6, *ortho* on (η^5 -C₅H₄)}, 4.35 {2H, t, *J* 1.6, *meta* on (η^5 -C₅H₄)}, 4.10 (5H, s, η^5 -C₅H₅), 3.77 (3H, s, -OCH₃);

δ_{C} (100 MHz, DMSO-*d*₆): 169.4 (C=O), 134.2 (C_q), 133.5 (C_q), 130.4 (C_q), 130.3 (C_q), 129.2, 128.1, 128.0, 127.9, 127.5, 126.4, 85.0 (C_{ipso} η^5 -C₅H₄), 69.6 (η^5 -C₅H₅), 68.9 (C_{ortho} η^5 -C₅H₄), 68.3 (C_{meta} η^5 -C₅H₄), 52.2 (-OCH₃).

3-Ferrocenylnaphthalene-2-carboxylic acid 72

Sodium hydroxide (0.1 g, 2.5 mmol) was added to methyl 3-ferrocenylnaphthalene-2-carboxylate (0.92 g, 2.5 mmol) in a 1:1 mixture of water/methanol and was refluxed for 12 h. Concentrated HCl was added until pH 2 was reached. The solution was allowed to cool and filtered to obtain an orange/brown solid (0.81 g, 92%), mp (decomp.) at 145 °C;



m/z (ESI) 356.4 [M]⁺. C₂₁H₁₆O₂Fe requires 356.2;

λ_{\max} (EtOH)/nm 445 ($\epsilon/\text{dm}^3 \text{ mol}^{-1} \text{ cm}^{-1}$ 568);

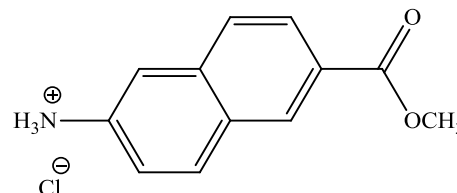
ν_{\max} (KBr)/cm⁻¹ 3430, 1698;

δ_{H} (400 MHz, DMSO-*d*₆): 12.8 (1H, br.s, -COOH), 8.33 (1H, s, ArH), 8.00 (1H, d, *J* 8.0, ArH), 7.99 (1H, s, ArH), 7.95 (1H, d, *J* 8.0, ArH), 7.57 (1H, t, *J* 8.0, ArH), 7.52 (1H, t, *J* 8.0, ArH), 4.70 {2H, t, *J* 1.6, *ortho* on (η^5 -C₅H₄)}, 4.34 {2H, t, *J* 1.6, *meta* on (η^5 -C₅H₄)}, 4.10 (5H, s, η^5 -C₅H₅);

δ_C (100 MHz, DMSO- d_6): 170.8 (C=O), 134.3 (C_q), 133.9 (C_q), 133.1 (C_q), 130.5 (C_q), 128.8, 127.9, 127.4, 127.0, 126.1, 85.2 (C_{ipso} η^5 -C₅H₄), 69.6 (η^5 -C₅H₅), 69.1 (C_{meta} η^5 -C₅H₄), 68.2 (C_{ortho} η^5 -C₅H₄).

Methyl 6-aminonaphthalene-2-carboxylate hydrochloride 73

6-Amino-2-naphthoic acid (1.54 g, 8.2 mmol) was added slowly to a solution of methanol (50 ml) and thionyl chloride (8 ml) at 0 °C and then refluxed for 24 h. The solution was cooled and the product was isolated by filtration as a brown solid (1.43 g, 73%), mp 156-158 °C;

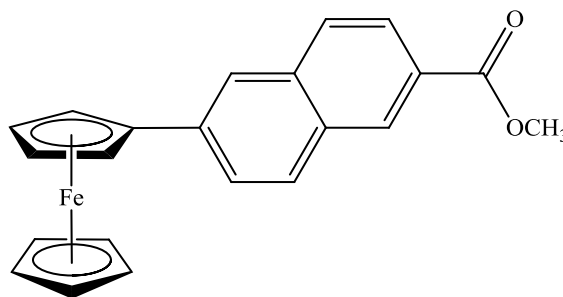


δ_H (400 MHz, DMSO- d_6): 8.56 (1H, s, ArH), 8.09 (1H, d, J 8.8, ArH), 7.93 (1H, dd, J 2.0 and 8.8, ArH), 7.90 (1H, d, J 8.8, ArH), 7.56 (1H, s, ArH), 7.38 (1H, dd, J 2.0 and 8.8, ArH), 3.90 (3H, s, -OCH₃);

δ_C (100 MHz, DMSO- d_6): 166.2 (C=O), 135.9 (C_q), 135.4 (C_q), 131.2, 130.5, 129.6 (C_q), 127.6, 126.1 (C_q), 125.7, 121.8, 117.6, 52.2 (-OCH₃).

Methyl 6-ferrocenylnaphthalene-2-carboxylate 74

Concentrated hydrochloric acid (4 ml) was added with intermittent cooling to a solution of methyl 6-aminonaphthalene-2-carboxylate hydrochloride (2.7 g, 11.5 mmol) in 15 ml of water. A solution of sodium nitrite (1.0 g, 14.5 mmol) in 15 ml of deionised water was



then added slowly to this mixture with stirring, keeping the temperature below 5 °C furnishing a pale brown/yellow solution. The resulting diazo salt was added to a solution of ferrocene (2.8 g, 14.5 mmol) in diethyl ether (90 ml) and allowed to react for 18 h. The reaction mixture was then washed with water, the ether layer was dried over MgSO₄, and the solvent removed *in vacuo* to yield the crude product. The crude product was purified using column chromatography {eluant 3:2 petroleum ether (40-60°C): diethyl ether} to obtain a red solid (0.88 g, 21%), mp 158-159 °C;

Anal. Calc. for C₂₂H₁₈O₂Fe: C, 71.4; H, 4.9%. Found: C, 71.6; H, 5.2;

m/z (ESI) 370.4 [M]⁺⁺. C₂₂H₁₈O₂Fe requires 370.2;

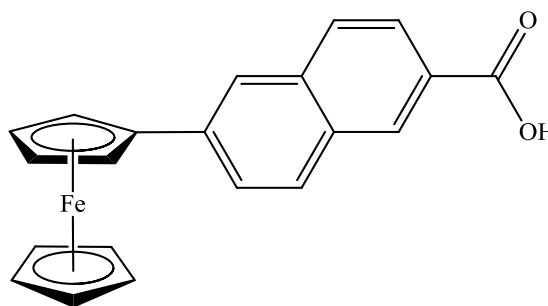
λ_{\max} (EtOH)/nm 380 ($\epsilon/\text{dm}^3 \text{ mol}^{-1} \text{ cm}^{-1}$ 3211), 455 (1523);

ν_{\max} (KBr)/cm⁻¹ 1708, 1494, 1450, 1219;

δ_{H} (400 MHz, DMSO-*d*₆): 8.58 (1H, s, ArH), 8.09 (1H, s, ArH), 8.07 (1H, d, *J* 8.8, ArH), 7.93-7.98 (2H, m, ArH), 7.85 (1H, dd, *J* 1.6 and 8.8, ArH), 4.99 {2H, t, *J* 1.6, *ortho* on (η^5 -C₅H₄)}, 4.47 {2H, t, *J* 1.6, *meta* on (η^5 -C₅H₄)}, 4.05 (5H, s, η^5 -C₅H₅), 3.92 (3H, s, -OCH₃);
 δ_{C} (100 MHz, DMSO-*d*₆): 166.4 (C=O), 140.0 (C_q), 135.4 (C_q), 130.6 (C_q), 130.4, 129.2, 127.8, 126.1, 125.8 (C_q), 125.1, 122.7, 83.7 (C_{ipso} η^5 -C₅H₄), 69.6 (C_{meta} η^5 -C₅H₄), 69.5 (η^5 -C₅H₅), 66.8 (C_{ortho} η^5 -C₅H₄), 52.2 (-OCH₃).

6-Ferrocenylnaphthalene-2-carboxylic acid 75

Sodium hydroxide (0.08 g, 2.0 mmol) was added to methyl 6-ferrocenylnaphthalene-2-carboxylate (0.70 g, 1.9 mmol) in a 1:1 mixture of water/methanol and was refluxed for 12 h. Concentrated HCl was added until pH 2 was reached. The solution was allowed



to cool and filtered to obtain an orange solid (0.63 g, 93%), mp (decomp.) at 205 °C;

m/z (ESI) 356.4 [M]⁺⁺. C₂₁H₁₆O₂Fe requires 356.2;

λ_{\max} (EtOH)/nm 375 ($\epsilon/\text{dm}^3 \text{ mol}^{-1} \text{ cm}^{-1}$ 2635), 450 (1296);

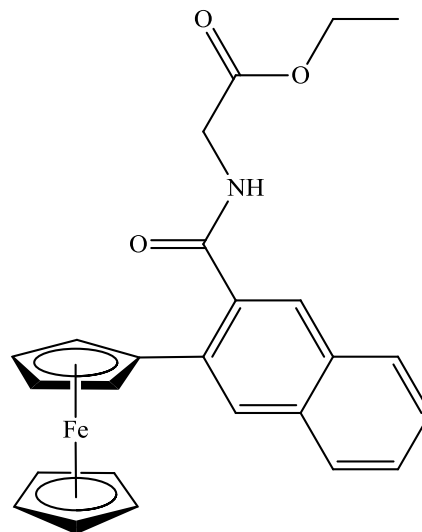
ν_{\max} (KBr)/cm⁻¹ 3435, 1682;

δ_{H} (400 MHz, DMSO-*d*₆): 12.8 (1H, br.s, -COOH), 8.57 (1H, s, ArH), 8.07 (1H, s, ArH), 8.03 (1H, d, *J* 8.4, ArH), 7.94 (2H, s, ArH), 7.83 (1H, dd, *J* 1.6 and 8.4, ArH), 4.97 {2H, t, *J* 1.6, *ortho* on (η^5 -C₅H₄)}, 4.45 {2H, t, *J* 1.6, *meta* on (η^5 -C₅H₄)}, 4.04 (5H, s, η^5 -C₅H₅);
 δ_{C} (100 MHz, DMSO-*d*₆): 167.5 (C=O), 139.7 (C_q), 135.3 (C_q), 130.6 (C_q), 130.4, 129.1, 127.6, 127.0 (C_q), 125.9, 125.5, 122.7, 83.8 (C_{ipso} η^5 -C₅H₄), 69.6 (C_{meta} η^5 -C₅H₄), 69.5 (η^5 -C₅H₅), 66.7 (C_{ortho} η^5 -C₅H₄).

General procedure for the preparation of *N*-(ferrocenyl)naphthoyl amino acid and dipeptide derivatives.

***N*-(3-ferrocenyl-2-naphthoyl)-glycine ethyl ester 80**

Glycine ethyl ester hydrochloride (0.17 g, 1.2 mmol) was added to a solution of 3-ferrocenylnaphthalene-2-carboxylic acid (0.43 g, 1.2 mmol), 1-hydroxybenzotriazole (0.22 g, 1.6 mmol), triethylamine (0.5 ml) and *N*-(3-dimethylaminopropyl)-*N'*-ethylcarbodiimide hydrochloride (0.3 g, 1.6 mmol) in 50 ml of dichloromethane at 0 °C. After 30 minutes the solution was raised to room temperature and the reaction was allowed to proceed for 48 h. The reaction mixture was then washed with water. The



dichloromethane layer was dried over MgSO₄ and the solvent was removed *in vacuo*. The product was purified by column chromatography (eluant 1:1 hexane:ethyl acetate) to give the title compound as an orange solid (0.44 g, 83%), mp 105-106 °C; $E^{0'}/mV$ 13 vs. Fc/Fc⁺; Anal. Calc. for C₂₅H₂₃NO₃Fe: C, 68.0; H, 5.25; N, 3.2%. Found: C, 67.7; H, 5.5; N, 3.25; m/z (ESI) 441.4 [M]⁺. C₂₅H₂₃NO₃Fe requires 441.3;

λ_{max} (EtOH)/nm 450 ($\epsilon/dm^3 mol^{-1} cm^{-1}$ 466);

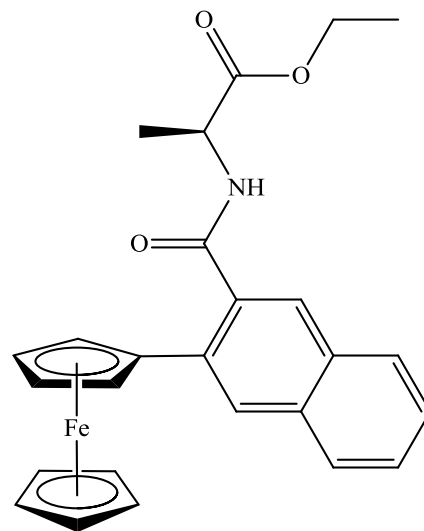
ν_{max} (KBr)/cm⁻¹ 3296, 1736, 1647, 1544, 1191;

δ_H (400 MHz, DMSO-*d*₆): 8.98 (1H, t, *J* 5.6, -CONH-), 8.35 (1H, s, ArH), 8.01 (1H, d, *J* 8.0, ArH), 7.93 (1H, d, *J* 8.0, ArH), 7.82 (1H, s, ArH), 7.56 (1H, t, *J* 8.0, ArH), 7.52 (1H, t, *J* 8.0, ArH), 4.83 {2H, t, *J* 1.6, *ortho* on (η^5 -C₅H₄)}, 4.32 {2H, t, *J* 1.6, *meta* on (η^5 -C₅H₄)}, 4.18 (2H, q, *J* 7.2, -OCH₂CH₃), 4.07 (5H, s, η^5 -C₅H₅), 4.03 (2H, d, *J* 5.6, -NHCH₂-), 1.27 (3H, t, *J* 7.2, -OCH₂CH₃);

δ_C (100 MHz, DMSO-*d*₆): 170.1 (C=O), 169.8 (C=O), 134.6 (C_q), 134.3 (C_q), 133.0 (C_q), 130.4 (C_q), 128.1, 127.7, 127.4, 127.1, 126.8, 126.1, 84.1 (C_{ipso} η^5 -C₅H₄), 69.6 (η^5 -C₅H₅), 68.9 (C_{ortho} η^5 -C₅H₄), 68.3 (C_{meta} η^5 -C₅H₄), 60.6 (-OCH₂-, -ve DEPT), 41.1 (-NHCH₂-, -ve DEPT), 14.1 (-OCH₂CH₃).

N*-(3-ferrocenyl-2-naphthoyl)-L-alanine ethyl ester **81*

The synthesis followed that of **80** using the following reagents: 3-ferrocenylnaphthalene-2-carboxylic acid (0.36 g, 1.0 mmol), 1-hydroxybenzotriazole (0.14 g, 1.0 mmol), triethylamine (0.5 ml), *N*-(3-dimethylaminopropyl)-*N'*-ethylcarbodiimide hydrochloride (0.19 g, 1.0 mmol) and L-alanine ethyl ester hydrochloride (0.19 g, 1.2 mmol). The product was purified by column chromatography (eluant 1:1 hexane:ethyl acetate) to give the title compound as an orange solid (0.24 g, 95%), mp 49 °C;



$E^{0'}/\text{mV}$ 8 vs. Fc/Fc^+ ;

$[\alpha]_D^{20}$ +13 (*c* 0.01 in EtOH);

Anal. calcd. for $\text{C}_{26}\text{H}_{25}\text{NO}_3\text{Fe}$: C, 68.6; H, 5.5; N, 3.1%. Found: C, 68.8; H, 5.8; N, 3.3;

m/z (ESI) 455.5 $[\text{M}]^{+}$. $\text{C}_{26}\text{H}_{25}\text{NO}_3\text{Fe}$ requires 455.3;

λ_{max} (EtOH)/nm 450 ($\epsilon/\text{dm}^3 \text{ mol}^{-1} \text{ cm}^{-1}$ 512);

ν_{max} (KBr)/ cm^{-1} 3288, 1734, 1647, 1544, 1494, 1200;

δ_{H} (400 MHz, $\text{DMSO}-d_6$): 8.94 (1H, d, J 7.2, -CONH-), 8.34 (1H, s, ArH), 8.00 (1H, d, J 8.0, ArH), 7.93 (1H, d, J 8.0, ArH), 7.80 (1H, s, ArH), 7.50-7.58 (2H, m, ArH), 4.78-4.80 {2H, m, *ortho* on (η^5 - C_5H_4)}, 4.45 (1H, qt, J 7.2, -NHCH-), 4.33-4.35 {1H, m, *meta* on (η^5 - C_5H_4)}, 4.29-4.31 {1H, m, *meta* on (η^5 - C_5H_4)}, 4.16 (2H, q, J 7.2, - OCH_2CH_3), 4.09 (5H, s, η^5 - C_5H_5), 1.38 (3H, d, J 7.2, - CH_3), 1.27 (3H, t, J 7.2, - OCH_2CH_3);

δ_{C} (100 MHz, $\text{DMSO}-d_6$): 172.5 (C=O), 169.3 (C=O), 134.7 (C_q), 134.3 (C_q), 132.9 (C_q), 130.4 (C_q), 128.2, 127.7, 127.4, 127.1, 126.8, 126.1, 84.3 (C_{ipso} η^5 - C_5H_4), 69.5 (η^5 - C_5H_5), 68.5 (C_{ortho} η^5 - C_5H_4), 68.3 (C_{meta} η^5 - C_5H_4), 68.2 (C_{meta} η^5 - C_5H_4), 60.6 (- OCH_2 - , -ve DEPT), 48.0 (α -C), 16.7 (- CH_3), 14.1 (- OCH_2CH_3).

N*-(3-ferrocenyl-2-naphthoyl)-L-leucine ethyl ester **82*

The synthesis followed that of **80** using the following reagents: 3-ferrocenyl-naphthalene-2-carboxylic acid (0.36 g, 1.0 mmol), 1-hydroxybenzotriazole (0.22 g, 1.6 mmol), triethylamine (0.5 ml), *N*-(3-dimethylaminopropyl)-*N'*-ethylcarbodiimide hydrochloride (0.29 g, 1.5 mmol) and L-leucine ethyl ester hydrochloride (0.23 g, 1.2 mmol). The product was purified by column chromatography (eluant 1:1 hexane:ethyl acetate) to give the title compound as an orange solid (0.16 g, 32%), mp 75-76 °C;

$E^{0'}/mV$ 16 vs. Fc/Fc^{+} ;

$[\alpha]_D^{20} +6$ (c 0.01 in EtOH);

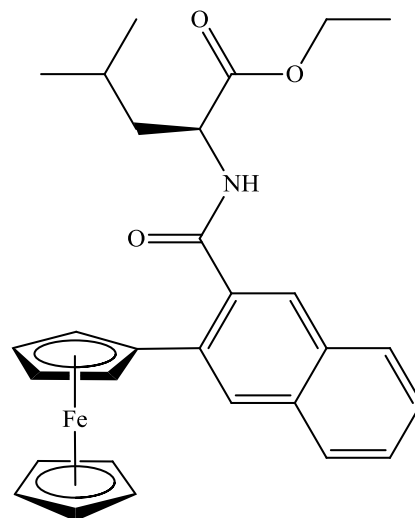
m/z (ESI) 498.1714 $[M+H]^+$. $C_{29}H_{33}NO_3Fe$ requires 498.1732;

λ_{max} (EtOH)/nm 445 ($\epsilon/dm^3 mol^{-1} cm^{-1}$ 627);

ν_{max} (KBr)/ cm^{-1} 3322, 1735, 1649, 1544, 1494, 1209;

δ_H (400 MHz, DMSO- d_6): 8.87 (1H, d, J 7.6, -CONH-), 8.36 (1H, s, ArH), 8.01 (1H, d, J 8.0, ArH), 7.94 (1H, d, J 8.0, ArH), 7.74 (1H, s, ArH), 7.50-7.58 (2H, m, ArH), 4.75-4.76 {2H, m, *ortho* on (η^5 -C₅H₄)}, 4.39-4.44 (1H, m, -NHCH-), 4.32-4.33 {1H, m, *meta* on (η^5 -C₅H₄)}, 4.28-4.29 {1H, m, *meta* on (η^5 -C₅H₄)}, 4.16 (2H, q, J 7.2, -OCH₂CH₃), 4.08 (5H, s, η^5 -C₅H₅), 1.65-1.76 (2H, m, -CH₂CH-) 1.50-1.58 (1H, m, -CH₂CH-), 1.26 (3H, t, J 7.2, -OCH₂CH₃), 0.91-0.94 {6H, m, -CH(CH₃)₂};

δ_C (100 MHz, DMSO- d_6): 172.5 (C=O), 169.7 (C=O), 134.9 (C_q), 134.2 (C_q), 132.9 (C_q), 130.4 (C_q), 128.2, 127.7, 127.4, 127.1, 126.5, 126.1, 84.3 (C_{ipso} η^5 -C₅H₄), 69.5 (η^5 -C₅H₅), 68.4 (C_{ortho} η^5 -C₅H₄), 68.2 (C_{meta} η^5 -C₅H₄), 68.1 (C_{meta} η^5 -C₅H₄), 60.5 (-OCH₂-, -ve DEPT), 50.8 (α -C), 39.4 (-CH₂-, -ve DEPT), 24.3 (-CH-), 22.9 (-CH₃), 21.2 (-CH₃), 14.1(-OCH₂CH₃).



***N*-(3-ferrocenyl-2-naphthoyl)-L-phenylalanine ethyl ester 83**

The synthesis followed that of **80** using the following reagents: 3-ferrocenylnaphthalene-2-carboxylic acid (0.36 g, 1.0 mmol), 1-hydroxybenzotriazole (0.22 g, 1.6 mmol), triethylamine (0.5 ml), *N*-(3-dimethylaminopropyl)-*N'*-ethylcarbodiimide hydrochloride (0.29 g, 1.5 mmol) and L-phenylalanine ethyl ester hydrochloride (0.24 g, 1.0 mmol). The product was purified by column chromatography (eluant 1:1 hexane:ethyl acetate) to give the title compound as an orange solid (0.21 g, 40%), mp 48-49 °C;

$E^{0'}/mV$ 10 vs. Fc/Fc^+ ;

$[\alpha]_D^{20}$ -24 (c 0.01 in EtOH);

Anal. Calc. for $C_{32}H_{29}NO_3Fe$: C, 72.3; H, 5.5; N, 2.6%. Found: C, 72.15; H, 5.7; N, 2.6;

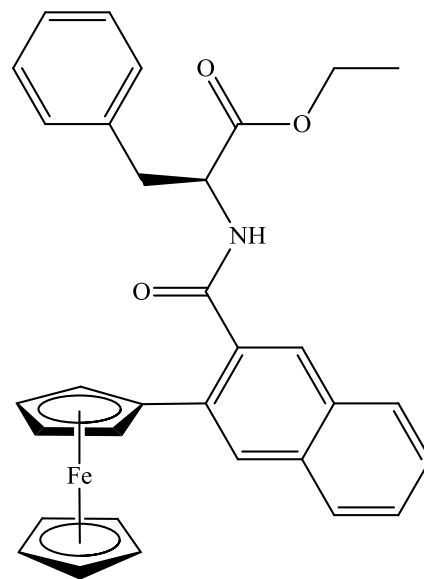
m/z (ESI) 532.1572 $[M+H]^+$. $C_{32}H_{30}NO_3Fe$ requires 532.1575;

λ_{max} (EtOH)/nm 450 ($\epsilon/dm^3 mol^{-1} cm^{-1}$ 582);

ν_{max} (KBr)/ cm^{-1} 3342, 1734, 1645, 1544, 1494, 1193;

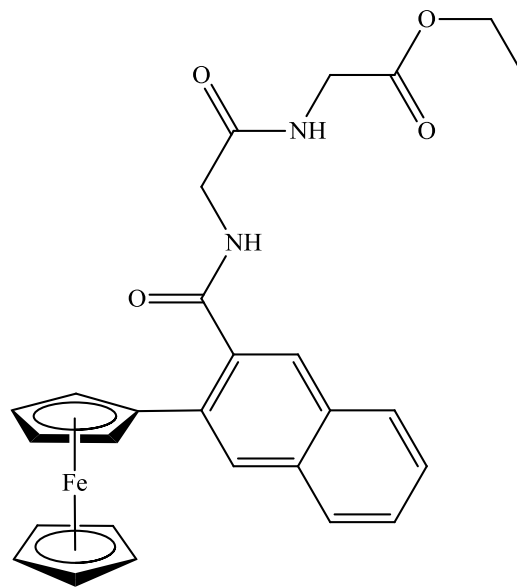
δ_H (400 MHz, DMSO- d_6): 9.01 (1H, d, J 7.6, -CONH-), 8.29 (1H, s, ArH), 7.98 (1H, d, J 8.0, ArH), 7.82 (1H, d, J 8.0, ArH), 7.49-7.57 (2H, m, ArH), 7.47 (1H, s, ArH), 7.34-7.43 (5H, m, -CH₂Ph), 4.71-4.75 (2H, m, -NHCH-), (η^5 -C₅H₄), 4.32-4.34 (1H, m, η^5 -C₅H₄), 4.22-4.24 (1H, m, η^5 -C₅H₄), 4.15-4.21 {3H, m, -OCH₂CH₃, (η^5 -C₅H₄)}, 4.01 (5H, s, η^5 -C₅H₅), 3.22 (1H, dd, J 7.6 and 13.6, -CH₂Ph), 3.01 (1H, dd, J 7.6 and 13.6, -CH₂Ph), 1.25 (3H, t, J 7.2, -OCH₂CH₃);

δ_C (100 MHz, DMSO- d_6): 171.5 (C=O), 169.4 (C=O), 137.5 (C_q), 134.7 (C_q), 134.3 (C_q), 132.9 (C_q), 130.3 (C_q), 129.3, 128.3, 128.1, 127.5, 127.4, 127.1, 126.6, 126.5, 126.1, 83.9 (C_{ipso} η^5 -C₅H₄), 69.5 (η^5 -C₅H₅), 68.9 (η^5 -C₅H₄), 68.8 (η^5 -C₅H₄), 68.3 (η^5 -C₅H₄), 68.1 (η^5 -C₅H₄), 60.7 (-OCH₂-, -ve DEPT), 53.7 (α -C), 36.4 (-CH₂Ph, -ve DEPT), 14.1 (-OCH₂CH₃).



N*-(3-ferrocenyl-2-naphthoyl)-glycine-glycine ethyl ester **84*

The synthesis followed that of **80** using the following reagents: 3-ferrocenylnaphthalene-2-carboxylic acid (0.32 g, 0.9 mmol), 1-hydroxybenzotriazole (0.22 g, 1.6 mmol), triethylamine (0.5 ml), *N*-(3-dimethylaminopropyl)-*N'*-ethylcarbodiimide hydrochloride (0.3 g, 1.6 mmol) and glycine-glycine ethyl ester hydrochloride (0.18 g, 0.9 mmol). The product was purified by column chromatography (eluant 1:1 hexane:ethyl acetate) to give the title compound as an orange solid (0.27 g, 60%), mp 136-137 °C;



$E^{0'}/\text{mV}$ 8 vs. Fc/Fc^+ ;

Anal. calcd. for $\text{C}_{27}\text{H}_{26}\text{N}_2\text{O}_4\text{Fe}$: C, 65.1; H, 5.3; N, 5.6%. Found: C, 64.8; H, 5.3; N, 5.5;

m/z (ESI) 499.1342 $[\text{M}+\text{H}]^+$. $\text{C}_{27}\text{H}_{27}\text{N}_2\text{O}_4\text{Fe}$ requires 499.1320;

λ_{max} (EtOH)/nm 445 ($\epsilon/\text{dm}^3 \text{ mol}^{-1} \text{ cm}^{-1}$ 572);

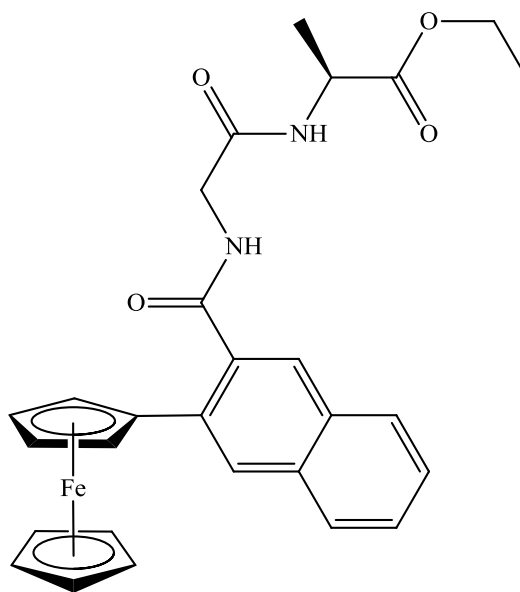
ν_{max} (KBr)/ cm^{-1} 3360, 1730, 1671, 1655, 1541, 1495, 1219;

δ_{H} (400 MHz, $\text{DMSO}-d_6$): 8.74 (1H, t, J 5.6, -CONH-), 8.29-8.32 (2H, m, ArH, -CONH-), 8.00 (1H, d, J 8.0, ArH), 7.90 (1H, d, J 8.0, ArH), 7.87 (1H, s, ArH), 7.50-7.58 (2H, m, ArH), 4.79 {2H, t, J 1.6, *ortho* on ($\eta^5\text{-C}_5\text{H}_4$)}, 4.31 {2H, t, J 1.6, *meta* on ($\eta^5\text{-C}_5\text{H}_4$)}, 4.12 (2H, q, J 7.2, - OCH_2CH_3), 4.08 (5H, s, $\eta^5\text{-C}_5\text{H}_5$), 3.91-3.94 (4H, m, - NHCH_2 -), 1.22 (3H, t, J 7.2, - OCH_2CH_3);

δ_{C} (100 MHz, $\text{DMSO}-d_6$): 169.9 (C=O), 169.8 (C=O), 169.3 (C=O), 134.9 (C_q), 134.2 (C_q), 132.9 (C_q), 130.5 (C_q), 128.1, 127.6, 127.4, 127.0, 126.7, 126.0, 84.4 ($\text{C}_{\text{ipso}} \eta^5\text{-C}_5\text{H}_4$), 69.5 ($\eta^5\text{-C}_5\text{H}_5$), 68.9 ($\text{C}_{\text{ortho}} \eta^5\text{-C}_5\text{H}_4$), 68.3 ($\text{C}_{\text{meta}} \eta^5\text{-C}_5\text{H}_4$), 60.5(- OCH_2 -, -ve DEPT), 41.9(- NHCH_2 -, -ve DEPT), 40.7(- NHCH_2 -, -ve DEPT), 14.1 (- OCH_2CH_3).

***N*-(3-ferrocenyl-2-naphthoyl)-glycine-L-alanine ethyl ester 85**

The synthesis followed that of **80** using the following reagents: 3-ferrocenylnaphthalene-2-carboxylic acid (0.53 g, 1.5 mmol), 1-hydroxybenzotriazole (0.30 g, 2.2 mmol), triethylamine (0.5 ml), *N*-(3-dimethylaminopropyl)-*N'*-ethylcarbodiimide hydrochloride (0.38 g, 2.0 mmol) and glycine-L-alanine ethyl ester hydrochloride (0.32 g, 1.5 mmol). The product was purified by column chromatography (eluant 1:1 hexane:ethyl acetate - 100% ethyl acetate) to give the title compound as an orange solid (0.42 g, 55%), mp 70-71 °C;



$E^{0'}/\text{mV}$ 5 vs. Fc/Fc^+ ;

$[\alpha]_D^{20}$ -35 (*c* 0.01 in EtOH);

m/z (ESI) 513.1487 $[\text{M}+\text{H}]^+$. $\text{C}_{28}\text{H}_{29}\text{N}_2\text{O}_4\text{Fe}$ requires 513.1477;

$\lambda_{\text{max}}(\text{EtOH})/\text{nm}$ 450 ($\epsilon/\text{dm}^3 \text{ mol}^{-1} \text{ cm}^{-1}$ 525);

$\nu_{\text{max}}(\text{KBr})/\text{cm}^{-1}$ 3393, 3291, 1734, 1646, 1544, 1494, 1205;

δ_{H} (400 MHz, $\text{DMSO}-d_6$): 8.72 (1H, t, J 5.6, -CONH-), 8.38 (1H, d, J 6.8, -CONH-), 8.32 (1H, s, ArH), 7.99 (1H, d, J 8.0, ArH), 7.90 (1H, d, J 8.0, ArH), 7.83 (1H, s, ArH), 7.49-7.57 (2H, m, ArH), 4.81 {2H, s, *ortho* on (η^5 - C_5H_4)}, 4.31-4.36 {3H, m, -NHCH-, *meta* on (η^5 - C_5H_4)}, 4.02-4.14 (7H, m, - OCH_2CH_3 , η^5 - C_5H_5), 3.96 (1H, dd, J 5.6 and 16.4, -NHCH₂-), 3.87 (1H, dd, J 5.6 and 16.4, -NHCH₂-), 1.32 (3H, d, J 7.2, -CH₃), 1.21 (3H, t, J 7.2, -OCH₂CH₃);

δ_{C} (100 MHz, $\text{DMSO}-d_6$): 169.8 (C=O), 169.4 (C=O), 168.7 (C=O), 135.0 (C_q), 134.3 (C_q), 132.9 (C_q), 130.5 (C_q), 128.1, 127.6, 127.4, 127.0, 126.7, 126.0, 84.3 (C_{ipso} η^5 - C_5H_4), 69.5 (η^5 - C_5H_5), 69.0 (C_{ortho} η^5 - C_5H_4), 68.3 (C_{meta} η^5 - C_5H_4), 60.5 (-OCH₂-, -ve DEPT), 47.7 (α -C), 41.8 (-NHCH₂-, -ve DEPT), 17.1 (-CH₃), 14.1 (-OCH₂CH₃).

N*-(3-ferrocenyl-2-naphthoyl)-glycine-L-leucine ethyl ester **86*

The synthesis followed that of **80** using the following reagents: 3-ferrocenylnaphthalene-2-carboxylic acid (0.36 g, 1.0 mmol), 1-hydroxybenzotriazole (0.16 g, 1.2 mmol), triethylamine (0.5 ml), *N*-(3-dimethylaminopropyl)-*N'*-ethylcarbodiimide hydrochloride (0.23 g, 1.2 mmol) and glycine-L-leucine ethyl ester hydrochloride (0.25 g, 1.0 mmol). The product was purified by column chromatography (eluant 1:1 hexane: ethyl acetate) to give the title compound as an orange solid (0.23 g, 42%), mp 69-70 °C;

$E^{0'}/\text{mV}$ 26 vs. Fc/Fc⁺;

$[\alpha]_D^{20} +8$ (*c* 0.06 in CH₃CN);

Anal. calcd. for C₃₁H₃₄N₂O₄Fe: C, 67.15; H, 6.2; N, 5.05%. Found: C, 66.7; H, 6.3; N, 4.8;

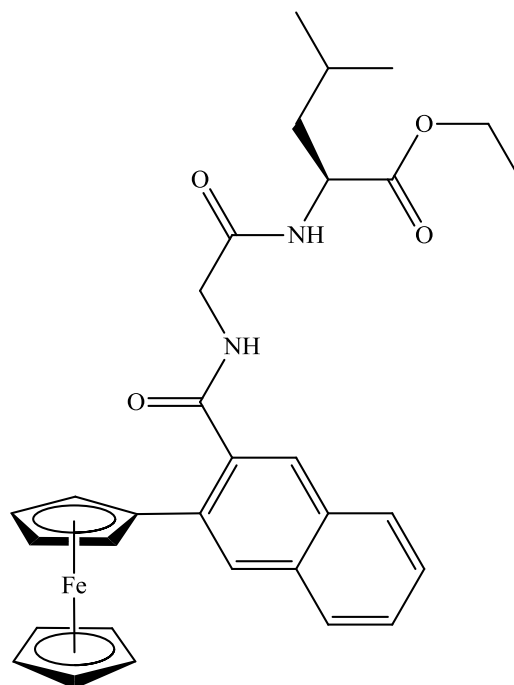
m/z (MALDI-TOF) 554.3 [M]⁺. C₃₁H₃₄N₂O₄Fe requires 554.5;

λ_{max} (CH₃CN)/nm 450 ($\epsilon/\text{dm}^3 \text{ mol}^{-1} \text{ cm}^{-1}$ 526);

ν_{max} (neat)/cm⁻¹ 3285, 2959, 1732, 1645, 1516, 1261, 1193;

δ_{H} (400 MHz, DMSO-*d*₆): 8.69 (1H, t, *J* 5.6, -CONH-), 8.31-8.33 (2H, m, -CONH-, ArH), 7.99 (1H, d, *J* 8.0, ArH), 7.90 (1H, d, *J* 8.0, ArH), 7.83 (1H, s, ArH), 7.49-7.57 (2H, m, ArH), 4.81 {2H, s, *ortho* on (η^5 -C₅H₄)}, 4.33-4.39 (1H, m, -NHCH-), 4.30 {2H, s, *meta* on (η^5 -C₅H₄)}, 4.08-4.14 (7H, m, -OCH₂CH₃, η^5 -C₅H₅), 3.97 (1H, dd, *J* 5.6 and 16.4, -NHCH₂-), 3.89 (1H, dd, *J* 5.6 and 16.4, -NHCH₂-), 1.50-1.73 (3H, m, -CH₂CH-), 1.21 (3H, t, *J* 7.2, -OCH₂CH₃), 0.88-0.93 {6H, m, -CH(CH₃)₂};

δ_{C} (100 MHz, DMSO-*d*₆): 172.5 (C=O), 169.8 (C=O), 168.9 (C=O), 135.0 (C_q), 134.3 (C_q), 133.0 (C_q), 130.5 (C_q), 128.1, 127.6, 127.4, 127.0, 126.7, 126.0, 84.3 (C_{ipso} η^5 -C₅H₄), 69.5 (η^5 -C₅H₅), 68.9 (C_{ortho} η^5 -C₅H₄), 68.3 (C_{meta} η^5 -C₅H₄), 60.5 (-OCH₂-, -ve DEPT), 50.4 (α -C), 41.8 (-NHCH₂-, -ve DEPT), 40.1 (-CH₂-, -ve DEPT), 24.2 (-CH-), 22.7 (-CH₃), 21.4 (-CH₃), 14.0 (-OCH₂CH₃).



N*-(3-ferrocenyl-2-naphthoyl)-glycine-L-phenylalanine ethyl ester **87*

The synthesis followed that of **80** using the following reagents: 3-ferrocenylnaphthalene-2-carboxylic acid (0.36 g, 1.0 mmol), 1-hydroxybenzotriazole (0.18 g, 1.3 mmol), triethylamine (0.9 ml), *N*-(3-dimethylaminopropyl)-*N'*-ethylcarbodiimide hydrochloride (0.25 g, 1.3 mmol) and glycine-L-phenylalanine ethyl ester hydrochloride (0.29 g, 1.0 mmol). The product was purified by column chromatography (eluant 1:1 hexane: ethyl acetate) to give the title compound as an orange solid (0.17 g, 29%), mp 67-68 °C;

$E^{0'}/\text{mV}$ 24 vs. Fc/Fc⁺;

$[\alpha]_D^{20}$ +10 (*c* 0.06 in CH₃CN);

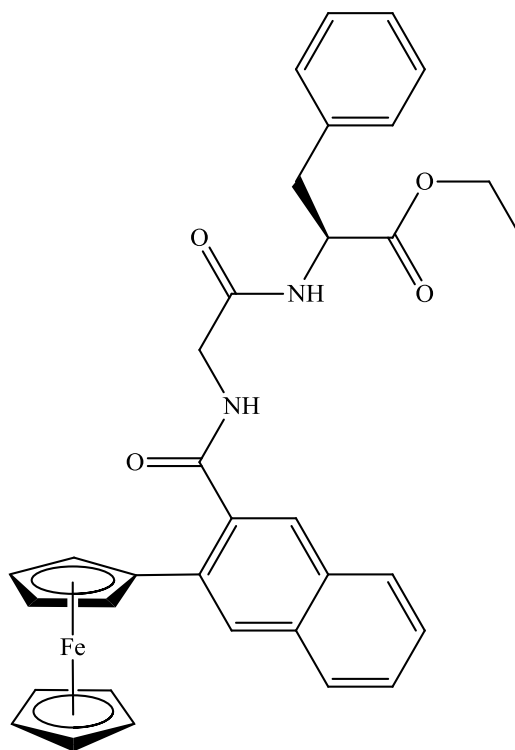
m/z (MALDI-TOF) 588.3 [M]⁺⁺. C₃₄H₃₂N₂O₄Fe requires 588.5;

λ_{max} (CH₃CN)/nm 450 ($\epsilon/\text{dm}^3 \text{ mol}^{-1} \text{ cm}^{-1}$ 518);

ν_{max} (neat)/cm⁻¹ 3280, 3059, 1734, 1645, 1513, 1261, 1197;

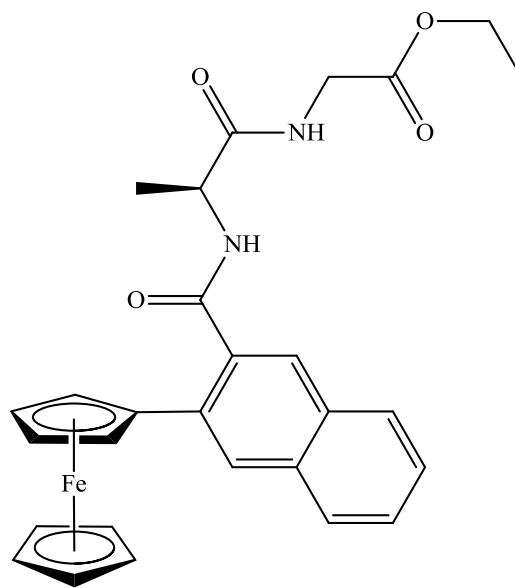
δ_{H} (400 MHz, DMSO-*d*₆): 8.67 (1H, t, *J* 5.6, -CONH-), 8.43 (1H, d, *J* 7.6, -CONH-), 8.31 (1H, s, ArH), 7.99 (1H, d, *J* 8.0, ArH), 7.90 (1H, d, *J* 8.0, ArH), 7.80 (1H, s, ArH), 7.49-7.57 (2H, m, ArH), 7.21-7.32 (5H, m, -CH₂Ph), 4.80 {2H, t, *J* 1.6, *ortho* on (η^5 -C₅H₄)}, 4.51-4.57 (1H, m, -NHCH-), 4.30 {2H, t, *J* 1.6, *meta* on (η^5 -C₅H₄)}, 4.01-4.10 (7H, m, -OCH₂CH₃, η^5 -C₅H₅), 3.85-3.96 (2H, m, -NHCH₂-), 3.05 (1H, dd, *J* 7.6 and 13.6, -CH₂Ph), 2.98 (1H, dd, *J* 7.6 and 13.6, -CH₂Ph), 1.13 (3H, t, *J* 7.2, -OCH₂CH₃);

δ_{C} (100 MHz, DMSO-*d*₆): 171.4 (C=O), 169.8 (C=O), 168.9 (C=O), 136.9 (C_q), 135.0 (C_q), 134.2 (C_q), 133.0 (C_q), 130.5 (C_q), 129.1, 128.3, 128.1, 127.6, 127.4, 127.0, 126.7, 126.6, 126.0, 84.3 (C_{ipso} η^5 -C₅H₄), 69.5 (η^5 -C₅H₅), 68.9 (C_{ortho} η^5 -C₅H₄), 68.3 (C_{meta} η^5 -C₅H₄), 60.6 (-OCH₂-, -ve DEPT), 53.8 (α -C), 41.8 (-NHCH₂-, -ve DEPT), 37.0 (-CH₂Ph, -ve DEPT), 14.1 (-OCH₂CH₃).



N*-(3-ferrocenyl-2-naphthoyl)-L-alanine-glycine ethyl ester **88*

The synthesis followed that of **80** using the following reagents: 3-ferrocenylnaphthalene-2-carboxylic acid (0.36 g, 1.0 mmol), 1-hydroxybenzotriazole (0.16 g, 1.2 mmol), triethylamine (0.5 ml), *N*-(3-dimethylaminopropyl)-*N'*-ethylcarbodiimide hydrochloride (0.23 g, 1.2 mmol) and L-alanine-glycine ethyl ester hydrochloride (0.32 g, 1.5 mmol). The product was purified by column chromatography (eluant 1:1 hexane:ethyl acetate) to give the title compound as an orange solid (0.30 g, 59%), mp 63-64 °C;



$E^{0'}/\text{mV}$ 10 vs. Fc/Fc^+ ;

$[\alpha]_D^{20}$ -75 (*c* 0.01 in EtOH);

m/z (ESI) 513.1453 $[\text{M}+\text{H}]^+$. $\text{C}_{28}\text{H}_{29}\text{N}_2\text{O}_4\text{Fe}$ requires 513.1477;

$\lambda_{\text{max}}(\text{EtOH})/\text{nm}$ 445 ($\epsilon/\text{dm}^3 \text{ mol}^{-1} \text{ cm}^{-1}$ 483) nm;

$\nu_{\text{max}}(\text{KBr})/\text{cm}^{-1}$ 3397, 3291, 1748, 1646, 1544, 1494, 1197;

δ_{H} (400 MHz, $\text{DMSO}-d_6$): 8.64 (1H, d, *J* 7.2, -CONH-), 8.38 (1H, s, ArH), 8.35 (1H, t, *J* 5.6, -CONH-), 8.06 (1H, d, *J* 8.0, ArH), 7.97 (1H, d, *J* 8.0, ArH), 7.92 (1H, s, ArH), 7.49-7.58 (2H, m, ArH), 4.79 {2H, t, *J* 1.6, *ortho* on ($\eta^5\text{-C}_5\text{H}_4$)}, 4.56 (1H, qt, *J* 7.2, -NHCH-), 4.32-4.35 {1H, m, *meta* on ($\eta^5\text{-C}_5\text{H}_4$)}, 4.29-4.32 {1H, m, *meta* on ($\eta^5\text{-C}_5\text{H}_4$)}, 4.01-4.14 (7H, m, -OCH₂CH₃, $\eta^5\text{-C}_5\text{H}_5$), 3.99 (1H, dd, *J* 5.6 and 17.6, -NHCH₂-), 3.89 (1H, dd, *J* 5.6 and 17.6, -NHCH₂-), 1.37 (3H, d, *J* 7.2, -CH₃), 1.27 (3H, t, *J* 7.2, -OCH₂CH₃);

δ_{C} (100 MHz, $\text{DMSO}-d_6$): 169.7 (C=O), 169.5 (C=O), 169.2 (C=O), 135.1 (C_q), 134.2 (C_q), 132.9 (C_q), 130.5 (C_q), 128.2, 127.6, 127.4, 126.9, 126.7, 126.0, 84.7 (C_{ipso} $\eta^5\text{-C}_5\text{H}_4$), 69.5 ($\eta^5\text{-C}_5\text{H}_5$), 68.6 (C_{ortho} $\eta^5\text{-C}_5\text{H}_4$), 68.2 (C_{meta} $\eta^5\text{-C}_5\text{H}_4$), 60.4 (-OCH₂-, -ve DEPT), 48.4 ($\alpha\text{-C}$), 40.7 (-NHCH₂-, -ve DEPT), 17.7 (-CH₃), 14.0 (-OCH₂CH₃).

N*-(3-ferrocenyl-2-naphthoyl)-L-alanine-L-alanine ethyl ester **89*

The synthesis followed that of **80** using the following reagents: 3-ferrocenylnaphthalene-2-carboxylic acid (0.43 g, 1.2 mmol), 1-hydroxybenzotriazole (0.22 g, 1.6 mmol), triethylamine (0.5 ml), *N*-(3-dimethylaminopropyl)-*N'*-ethylcarbodiimide hydrochloride (0.29 g, 1.5 mmol) and L-alanine-L-alanine ethyl ester hydrochloride (0.29 g, 1.3 mmol). The product was purified by column chromatography (eluant 1:1 hexane:ethyl acetate) to give the title compound as an orange solid (0.18 g, 28%), mp 59-60 °C;

$E^{0'}/\text{mV}$ 9 vs. Fc/Fc⁺;

$[\alpha]_D^{20}$ -122 (*c* 0.02 in EtOH);

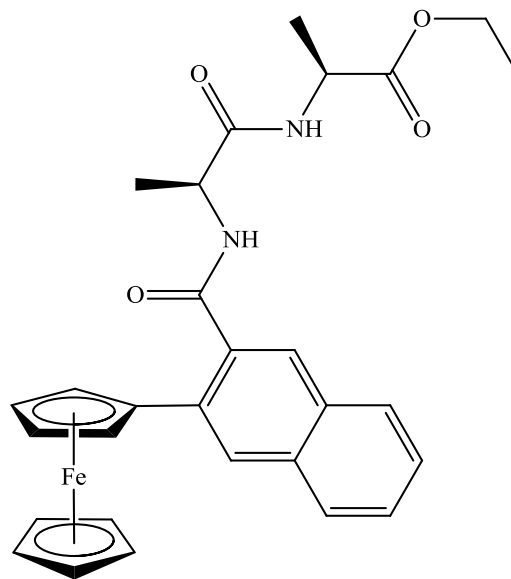
m/z (ESI) 527.1649 [M+H]⁺. C₂₉H₃₁N₂O₄Fe requires 527.1633;

λ_{max} (EtOH)/nm 445 ($\epsilon/\text{dm}^3 \text{ mol}^{-1} \text{ cm}^{-1}$ 498);

ν_{max} (KBr)/cm⁻¹ 3448, 3292, 1733, 1638, 1550, 1495, 1202;

δ_{H} (400 MHz, DMSO-*d*₆): 8.54 (1H, d, *J* 7.2, -CONH-), 8.34 (1H, d, *J* 7.2, -CONH-), 8.32 (1H, s, ArH), 7.99 (1H, d, *J* 8.0, ArH), 7.91 (1H, d, *J* 8.0, ArH), 7.81 (1H, s, ArH), 7.49-7.57 (2H, m, ArH), 4.74-4.75 {2H, m, *ortho* on (η^5 -C₅H₄)}, 4.49 (1H, qt, *J* 7.2, -NHCH-), 4.28-4.33 {3H, m, *meta* on (η^5 -C₅H₄), -NHCH-}, 4.09-4.10 (7H, m, -OCH₂CH₃, η^5 -C₅H₅), 1.30-1.33 (6H, m, -CH₃), 1.19 (3H, t, *J* 7.2, -OCH₂CH₃);

δ_{C} (100 MHz, DMSO-*d*₆): 172.5 (C=O), 172.2 (C=O), 169.1 (C=O), 135.1 (C_q), 134.2 (C_q), 132.9 (C_q), 130.5 (C_q), 128.2, 127.6, 127.4, 126.9, 126.7, 126.0, 84.6 (C_{ipso} η^5 -C₅H₄), 69.5 (η^5 -C₅H₅), 68.6 (C_{ortho} η^5 -C₅H₄), 68.2 (C_{meta} η^5 -C₅H₄), 68.1 (C_{meta} η^5 -C₅H₄), 60.4 (-OCH₂-, -ve DEPT), 48.3 (α -C), 47.7 (α -C), 17.8 (-CH₃), 16.9 (-CH₃), 14.0 (-OCH₂CH₃).



N*-(3-ferrocenyl-2-naphthoyl)-L-alanine-L-leucine ethyl ester **90*

The synthesis followed that of **80** using the following reagents: 3-ferrocenylnaphthalene-2-carboxylic acid (0.43 g, 1.2 mmol), 1-hydroxybenzotriazole (0.22 g, 1.6 mmol), triethylamine (0.5 ml), *N*-(3-dimethylaminopropyl)-*N'*-ethylcarbodiimide hydrochloride (0.29 g, 1.5 mmol) and L-alanine-L-leucine ethyl ester hydrochloride (0.32 g, 1.2 mmol). The product was purified by column chromatography (eluant 1:1 hexane:ethyl acetate) to give the title compound as an orange solid (0.12 g, 18%), mp 64-65 °C;

$E^{0'}/\text{mV}$ 29 vs. Fc/Fc⁺;

$[\alpha]_D^{20}$ -63 (*c* 0.06 in CH₃CN);

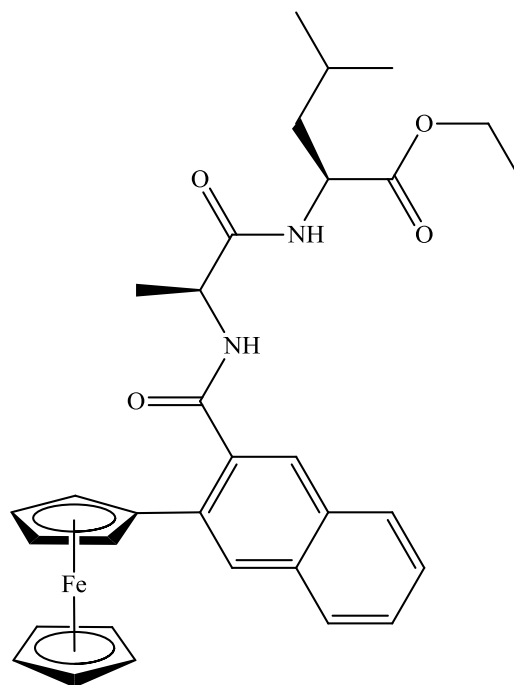
m/z (ESI) 568.0 [M]⁺⁺. C₃₂H₃₆N₂O₄Fe requires 568.5;

λ_{max} (CH₃CN)/nm 450 ($\epsilon/\text{dm}^3 \text{ mol}^{-1} \text{ cm}^{-1}$ 479);

ν_{max} (neat)/cm⁻¹ 3285, 3092, 1734, 1637, 1510, 1259, 1195;

δ_{H} (400 MHz, DMSO-*d*₆): 8.54 (1H, d, *J* 7.2, -CONH-), 8.32 (1H, s, ArH), 8.27 (1H, d, *J* 7.2, -CONH-), 7.99 (1H, d, *J* 7.6, ArH), 7.90 (1H, d, *J* 7.6, ArH), 7.80 (1H, s, ArH), 7.49-7.57 (2H, m, ArH), 4.75 {2H, s, *ortho* on (η^5 -C₅H₄)}, 4.51 (1H, qt, *J* 7.2, -NHCH-), 4.26-4.36 {3H, m, *meta* on (η^5 -C₅H₄)}, -NHCH-, 4.07-4.14 (7H, m, -OCH₂CH₃, η^5 -C₅H₅), 1.47-1.75 (3H, m, -CH₂CH-), 1.31 (3H, d, *J* 7.2, -CH₃), 1.19 (3H, t, *J* 7.2, -OCH₂CH₃), 0.87-0.93 {6H, m, -CH(CH₃)₂};

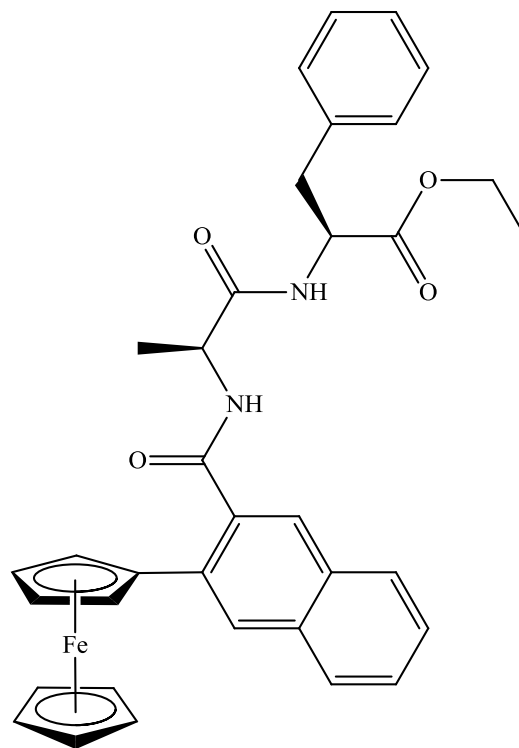
δ_{C} (100 MHz, DMSO-*d*₆): 172.5 (C=O), 172.4 (C=O), 169.1 (C=O), 135.1 (C_q), 134.2 (C_q), 132.9 (C_q), 130.5 (C_q), 128.1, 127.6, 127.4, 127.0, 126.7, 126.0, 84.5 (C_{ipso} η^5 -C₅H₄), 69.5 (η^5 -C₅H₅), 68.5 (C_{ortho} η^5 -C₅H₄), 68.2 (C_{meta} η^5 -C₅H₄), 60.4 (-OCH₂-, -ve DEPT), 50.3 (α -C), 48.3 (α -C), 36.9 (-CH₂-, -ve DEPT), 24.2 (-CH-), 22.8 (-CH₃), 21.4 (-CH₃), 17.8 (-CH₃), 14.0 (-OCH₂CH₃).



***N*-(3-ferrocenyl-2-naphthoyl)-L-alanine-L-phenylalanine ethyl ester 91**

The synthesis followed that of **80** using the following reagents: 3-ferrocenylnaphthalene-2-carboxylic acid (0.36 g, 1.0 mmol), 1-hydroxybenzotriazole (0.23 g, 1.7 mmol), triethylamine (0.5 ml), *N*-(3-dimethylaminopropyl)-*N'*-ethylcarbodiimide hydrochloride (0.29 g, 1.5 mmol) and L-alanine-L-phenylalanine ethyl ester hydrochloride (0.35 g, 1.2 mmol). The product was purified by column chromatography (eluant 1:1 hexane:ethyl acetate) to give the title compound as fine yellow needles (0.27 g, 45%), mp 78-79 °C; E^0/mV 24 vs. Fc/Fc⁺;

$[\alpha]_D^{20}$ -72 (*c* 0.06 in CH₃CN);



Anal. Calc. for C₃₅H₃₄N₂O₄Fe: C, 69.8; H, 5.7; N, 4.65%. Found: C, 69.75; H, 5.7; N, 4.5; *m/z* (ESI) 602.0 [M]⁺. C₃₅H₃₄N₂O₄Fe requires 602.5;

λ_{\max} (CH₃CN)/nm 450 (ϵ /dm³ mol⁻¹ cm⁻¹ 510);

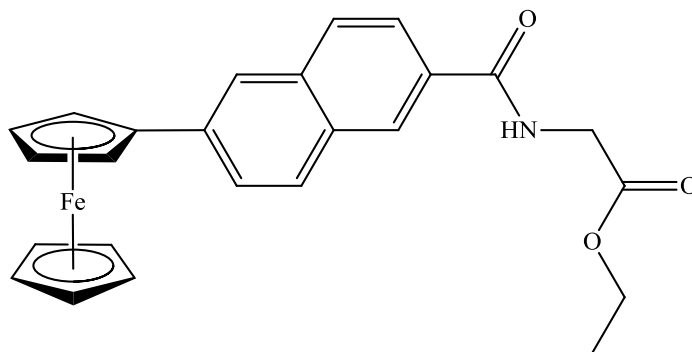
ν_{\max} (neat)/cm⁻¹ 3361, 3058, 1736, 1679, 1637, 1530, 1245, 1197;

δ_H (400 MHz, DMSO-*d*₆): 8.47 (1H, d, *J* 7.2, -CONH-), 8.32-8.35 (2H, m, -CONH-, ArH), 8.00 (1H, d, *J* 8.0, ArH), 7.90 (1H, d, *J* 7.6, ArH), 7.77 (1H, s, ArH), 7.50-7.58 (2H, m, ArH), 7.21-7.31 (5H, m, -CH₂Ph), 4.72-4.73 {2H, m, *ortho* on (η^5 -C₅H₄)}, 4.46-4.53 (2H, m, -NHCH-, -NHCH-), 4.29-4.31 {1H, m, *meta* on (η^5 -C₅H₄)}, 4.26-4.28 {1H, m, *meta* on (η^5 -C₅H₄)}, 4.02-4.09 (7H, m, -OCH₂CH₃, η^5 -C₅H₅), 2.97-3.07 (2H, m, -CH₂Ph), 1.27 (3H, d, *J* 7.2, -CH₃), 1.11 (3H, t, *J* 7.2, -OCH₂CH₃);

δ_C (100 MHz, DMSO-*d*₆): 172.4 (C=O), 171.3 (C=O), 169.1 (C=O), 136.9 (C_q), 135.1 (C_q), 134.2 (C_q), 132.9 (C_q), 130.5 (C_q), 129.1, 128.2, 128.1, 127.6, 127.4, 130.0, 126.7, 126.5, 126.0, 84.6 (*C*_{ipso} η^5 -C₅H₄), 69.5 (η^5 -C₅H₅), 69.4 (*C*_{ortho} η^5 -C₅H₄), 68.6 (*C*_{meta} η^5 -C₅H₄), 68.2 (*C*_{meta} η^5 -C₅H₄), 60.5 (-OCH₂-, -ve DEPT), 53.7 (α -C), 48.4 (α -C), 36.7 (-CH₂Ph, -ve DEPT), 17.8 (-CH₃), 13.9 (-OCH₂CH₃).

***N*-(6-ferrocenyl-2-naphthoyl)-glycine ethyl ester 92**

The synthesis followed that of **80** using the following reagents: 6-ferrocenylnaphthalene-2-carboxylic acid (0.36 g, 1.0 mmol), 1-hydroxybenzotriazole (0.20 g, 1.5 mmol), triethylamine (0.5 ml), *N*-(3-dimethylaminopropyl)-*N'*-



ethylcarbodiimide hydrochloride (0.3 g, 1.6 mmol) and glycine ethyl ester hydrochloride (0.1 g, 0.7 mmol). The product was purified by column chromatography (eluant 1:1 hexane:ethyl acetate) to give the title compound as an orange solid (0.19 g, 62%), mp 114-115 °C;

$E^{0'}/\text{mV}$ 42 vs. Fc/Fc^+ ;

Anal. Calc. for $\text{C}_{25}\text{H}_{23}\text{NO}_3\text{Fe}$: C, 68.0; H, 5.25; N, 3.2%. Found: C, 67.8; H, 5.4; N, 3.1;

m/z (ESI) 441.4 $[\text{M}]^+$. $\text{C}_{25}\text{H}_{23}\text{NO}_3\text{Fe}$ requires 441.3;

λ_{max} (EtOH)/nm 375 ($\epsilon/\text{dm}^3 \text{ mol}^{-1} \text{ cm}^{-1}$ 2683), 450 (1149);

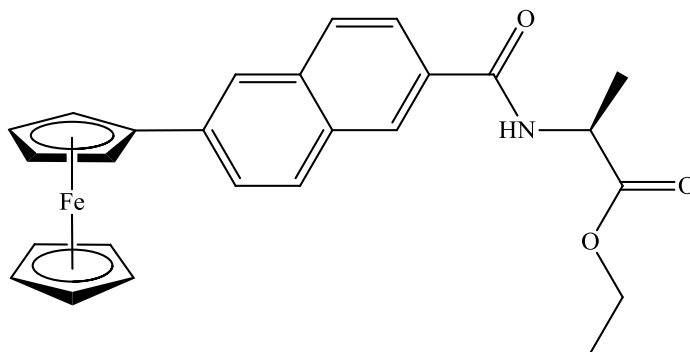
ν_{max} (KBr)/ cm^{-1} 3306, 1745, 1638, 1545, 1494, 1215;

δ_{H} (400 MHz, $\text{DMSO-}d_6$): 9.08 (1H, t, J 5.6, -CONH-), 8.44 (1H, s, ArH), 8.07 (1H, s, ArH), 7.97 (1H, d, J 8.8, ArH), 7.94 (1H, d, J 8.4, ArH), 7.92 (1H, dd, J 1.6 and 8.4, ArH), 7.83 (1H, dd, J 1.6 and 8.8, ArH), 4.96 {2H, t, J 1.6, *ortho* on ($\eta^5\text{-C}_5\text{H}_4$)}, 4.45 {2H, t, J 1.6, *meta* on ($\eta^5\text{-C}_5\text{H}_4$)}, 4.15 (2H, q, J 7.2, -OCH₂CH₃), 4.04-4.07 (7H, m, -NHCH₂-, $\eta^5\text{-C}_5\text{H}_5$), 1.22 (3H, t, J 7.2, -OCH₂CH₃);

δ_{C} (100 MHz, $\text{DMSO-}d_6$): 169.9 (C=O), 166.7 (C=O), 138.9 (C_{q}), 134.6 (C_{q}), 130.6 (C_{q}), 130.1 (C_{q}), 128.8, 127.6, 127.5, 125.9, 124.3, 122.7, 84.0 ($C_{\text{ipso}} \eta^5\text{-C}_5\text{H}_4$), 69.5 ($\eta^5\text{-C}_5\text{H}_5$), 69.4 ($C_{\text{meta}} \eta^5\text{-C}_5\text{H}_4$), 66.6 ($C_{\text{ortho}} \eta^5\text{-C}_5\text{H}_4$), 60.5 (-OCH₂-, -ve DEPT), 41.4 (-NHCH₂-, -ve DEPT), 14.1 (-OCH₂CH₃).

***N*-(6-ferrocenyl-2-naphthoyl)-L-alanine ethyl ester 93**

The synthesis followed that of **80** using the following reagents: 6-ferrocenylnaphthalene-2-carboxylic acid (0.36 g, 1.0 mmol), 1-hydroxybenzotriazole (0.20 g, 1.5 mmol), triethylamine (0.5 ml), *N*-(3-dimethylaminopropyl)-*N'*-



ethylcarbodiimide hydrochloride (0.29 g, 1.5 mmol) and L-alanine ethyl ester hydrochloride (0.14 g, 0.9 mmol). The product was purified by column chromatography (eluant 1:1 hexane:ethyl acetate) to give the title compound as an orange solid (0.34 g, 83.3%), mp 57-58 °C;

E^0/mV 42 vs. Fc/Fc^+ ;

$[\alpha]_D^{20}$ +32 (*c* 0.01 in EtOH);

Anal. Calc. for $C_{26}H_{25}NO_3Fe$: C, 68.6; H, 5.5; N, 3.1%. Found: C, 68.1; H, 5.8; N, 2.95;

m/z (ESI) 456.1265 $[M+H]^+$. $C_{26}H_{26}NO_3Fe$ requires 456.1262;

λ_{max} (EtOH)/nm 375 ($\epsilon/dm^3 mol^{-1} cm^{-1}$ 3636), 450 (1614);

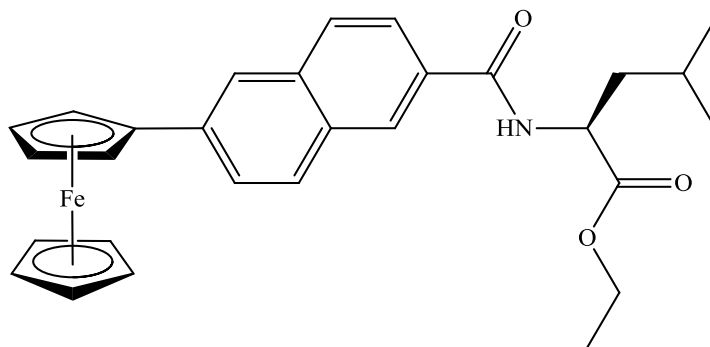
ν_{max} (KBr)/ cm^{-1} 3442, 1734, 1638, 1542, 1494, 1204;

δ_H (400 MHz, DMSO- d_6): 8.96 (1H, d, *J* 7.2, -CONH-), 8.51 (1H, s, ArH), 8.12 (1H, s, ArH), 8.02 (1H, d, *J* 8.8, ArH), 7.99-8.00 (2H, m, ArH), 7.88 (1H, dd, *J* 1.6 and 8.8, ArH), 5.01 {2H, t, *J* 2.0, *ortho* on (η^5 - C_5H_4)}, 4.57 (1H, qt, *J* 7.2, -NHCH-), 4.50 {2H, t, *J* 2.0, *meta* on (η^5 - C_5H_4)}, 4.19 (2H, q, *J* 7.2, -OCH₂CH₃), 4.10 (5H, s, η^5 - C_5H_5), 1.51 (3H, d, *J* 7.2, -CH₃), 1.27 (3H, t, *J* 7.2, -OCH₂CH₃);

δ_C (100 MHz, DMSO- d_6): 172.7 (C=O), 166.4 (C=O), 138.9 (C_q), 134.6 (C_q), 130.6 (C_q), 130.1 (C_q), 128.7, 127.6, 127.4, 126.0, 124.6, 122.7, 84.0 (C_{ipso} η^5 - C_5H_4), 69.5 (η^5 - C_5H_5), 69.4 (C_{meta} η^5 - C_5H_4), 66.6 (C_{ortho} η^5 - C_5H_4), 60.4 (-OCH₂-, -ve DEPT), 48.5 (α -C), 16.7 (-CH₃), 14.1 (-OCH₂CH₃).

***N*-(6-ferrocenyl-2-naphthoyl)-L-leucine ethyl ester 94**

The synthesis followed that of **80** using the following reagents: 6-ferrocenylnaphthalene-2-carboxylic acid (0.32 g, 0.9 mmol), 1-hydroxybenzotriazole (0.14 g, 1.0 mmol), triethylamine (0.5 ml), *N*-(3-



dimethylaminopropyl)-*N'*-ethylcarbodiimide hydrochloride (0.21 g, 1.1 mmol) and L-leucine ethyl ester hydrochloride (0.2 g, 1.0 mmol). The product was purified by column chromatography (eluant 1:1 hexane:ethyl acetate) to give the title compound as an orange solid (0.14 g, 33.3%), mp 109 °C;

E^0/mV 42 vs. Fc/Fc^+ ;

$[\alpha]_D^{20}$ +12 (*c* 0.01 in EtOH);

Anal. Calc. for $C_{29}H_{31}NO_3Fe$: C, 70.0; H, 6.3; N, 2.8%. Found: C, 70.35; H, 6.7; N, 2.6;

m/z (ESI) 498.1712 $[M+H]^+$. $C_{29}H_{32}NO_3Fe$ requires 498.1732;

λ_{max} (EtOH)/nm 375 ($\epsilon/dm^3 mol^{-1} cm^{-1}$ 3256), 450 (1395);

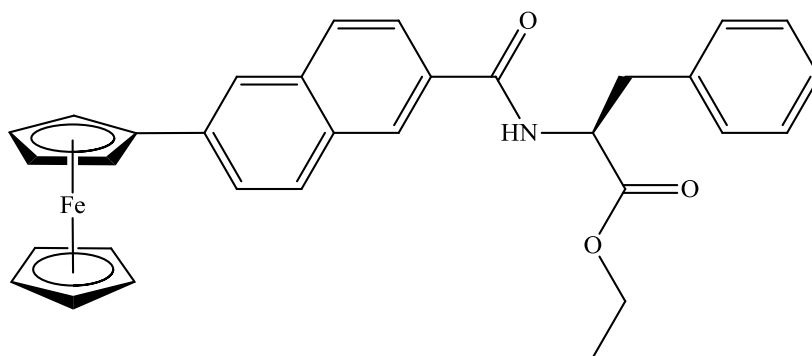
ν_{max} (KBr)/ cm^{-1} 3437, 1733, 1638, 1544, 1493, 1200;

δ_H (400 MHz, DMSO- d_6): 8.82 (1H, d, J 7.2, -CONH-), 8.45 (1H, s, ArH), 8.06 (1H, s, ArH), 7.97 (1H, d, J 8.4, ArH), 7.93 (2H, s, ArH), 7.83 (1H, dd, J 1.6 and 8.4, ArH), 4.96 {2H, t, J 1.6, *ortho* on (η^5 - C_5H_4)}, 4.52-4.57 (1H, m, -NHCH-), 4.45 {2H, t, J 1.6, *meta* on (η^5 - C_5H_4)}, 4.09-4.17 (2H, m, -OCH₂CH₃), 4.05 (5H, s, η^5 - C_5H_5), 1.73-1.88 (2H, m, -CH₂CH-), 1.58-1.65 (1H, m, -CH₂CH-), 1.21 (3H, t, J 7.2, -OCH₂CH₃), 0.96 {3H, d, J 6.4, -CH(CH₃)₂}, 0.91 {3H, d, J 6.4, -CH(CH₃)₂};

δ_C (100 MHz, DMSO- d_6): 172.7 (C=O), 166.7 (C=O), 138.9 (C_q), 134.6 (C_q), 130.6 (C_q), 130.2 (C_q), 128.7, 127.6, 127.3, 125.9, 124.6, 122.7, 84.0 (C_{ipso} η^5 - C_5H_4), 69.5 (η^5 - C_5H_5), 69.4 (C_{meta} η^5 - C_5H_4), 66.6 (C_{ortho} η^5 - C_5H_4), 60.4 (-OCH₂-, -ve DEPT), 51.1 (α -C), 39.3 (-CH₂-, -ve DEPT), 24.5 (-CH-), 22.9 (-CH₃), 21.2 (-CH₃), 14.1 (-OCH₂CH₃).

***N*-(6-ferrocenyl-2-naphthoyl)-L-phenylalanine ethyl ester 95**

The synthesis followed that of **80** using the following reagents: 6-ferrocenylnaphthalene-2-carboxylic acid (0.32 g, 0.9 mmol), 1-hydroxybenzotriazole



(0.14 g, 1.0 mmol), triethylamine (0.5 ml), *N*-(3-dimethylaminopropyl)-*N'*-ethylcarbodiimide hydrochloride (0.21 g, 1.1 mmol) and L-phenylalanine ethyl ester hydrochloride (0.26 g, 1.1 mmol). The product was purified by column chromatography (eluant 1:1 hexane:ethyl acetate) to give the title compound as an orange solid (0.38 g, 77.8%), mp 151-152 °C;

$E^{0'}/\text{mV}$ 46 vs. Fc/Fc⁺;

$[\alpha]_D^{20}$ +52 (*c* 0.01 in EtOH);

Anal. Calc. for C₃₂H₂₉NO₃Fe: C, 72.3; H, 5.5; N, 2.6%. Found: C, 72.3; H, 5.55; N, 2.6;

m/z (ESI) 532.1552 [M+H]⁺. C₃₂H₃₀NO₃Fe requires 532.1575;

λ_{max} (EtOH)/nm 375 ($\epsilon/\text{dm}^3 \text{ mol}^{-1} \text{ cm}^{-1}$ 3696), 450 (1582);

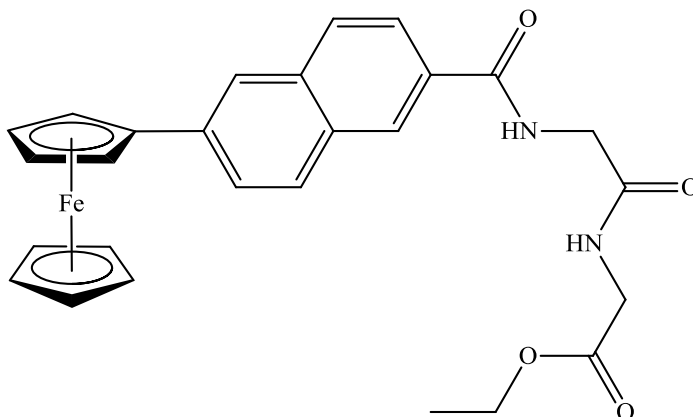
ν_{max} (KBr)/cm⁻¹ 3435, 1741, 1623, 1544, 1494, 1208;

δ_{H} (400 MHz, DMSO-*d*₆): 8.95 (1H, d, *J* 7.6, -CONH-), 8.38 (1H, s, ArH), 8.05 (1H, s, ArH), 7.95 (1H, d, *J* 8.4, ArH), 7.92 (1H, d, *J* 8.4, ArH), 7.86 (1H, dd, *J* 1.6 and 8.4, ArH), 7.82 (1H, dd, *J* 1.6 and 8.4, ArH), 7.21-7.35 (5H, m, -CH₂Ph), 4.96 {2H, t, *J* 1.6, *ortho* on (η^5 -C₅H₄)}, 4.68-4.74 (1H, m, -NHCH-), 4.45 {2H, t, *J* 1.6, *meta* on (η^5 -C₅H₄)}, 4.11 (2H, q, *J* 7.2, -OCH₂CH₃), 4.05 (5H, s, η^5 -C₅H₅), 3.16-3.19 (2H, m, -CH₂Ph), 1.14 (3H, t, *J* 7.2, -OCH₂CH₃);

δ_{C} (100 MHz, DMSO-*d*₆): 171.7 (C=O), 166.5 (C=O), 138.9 (C_q), 137.7 (C_q), 134.6 (C_q), 130.6 (C_q), 130.1 (C_q), 129.1, 128.7, 128.2, 127.6, 127.4, 126.5, 125.9, 124.5, 122.7, 83.9 (C_{ipso} η^5 -C₅H₄), 69.5 (η^5 -C₅H₅), 69.4 (C_{meta} η^5 -C₅H₄), 66.6 (C_{ortho} η^5 -C₅H₄), 60.5 (-OCH₂-, -ve DEPT), 54.5 (α -C), 36.4 (-CH₂Ph, -ve DEPT), 14.0 (-OCH₂CH₃).

***N*-(6-ferrocenyl-2-naphthoyl)-glycine-glycine ethyl ester 96**

The synthesis followed that of **80** using the following reagents: 6-ferrocenylnaphthalene-2-carboxylic acid (0.29 g, 0.8 mmol), 1-hydroxybenzotriazole (0.14 g, 1.0 mmol), triethylamine (0.5 ml), *N*-(3-dimethylaminopropyl)-*N'*-



ethylcarbodiimide hydrochloride (0.19 g, 1.0 mmol) and glycine-glycine ethyl ester hydrochloride (0.15 g, 0.8 mmol). The product was purified by column chromatography (eluant 1:1 hexane:ethyl acetate) to give the title compound as an orange solid (0.33 g, 83%), mp 179-180 °C;

$E^{0'}/\text{mV}$ 47 vs. Fc/Fc^+ ;

Anal. calcd. for $\text{C}_{27}\text{H}_{26}\text{N}_2\text{O}_4\text{Fe}$: C, 65.1; H, 5.3; N, 5.6%. Found: C, 64.7; H, 5.2; N, 5.5;

m/z (ESI) 499.1296 $[\text{M}+\text{H}]^+$. $\text{C}_{27}\text{H}_{27}\text{N}_2\text{O}_4\text{Fe}$ requires 499.1320;

λ_{max} (EtOH)/nm 375 ($\epsilon/\text{dm}^3 \text{ mol}^{-1} \text{ cm}^{-1}$ 3485), 450 (1497);

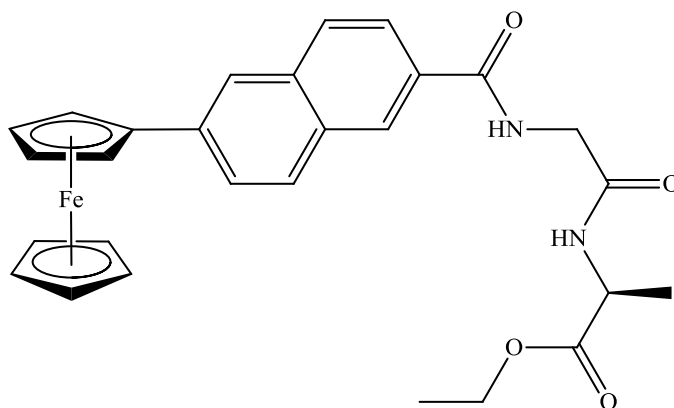
ν_{max} (KBr)/ cm^{-1} 3407, 3340, 1732, 1654, 1650, 1558, 1494, 1213;

δ_{H} (400 MHz, $\text{DMSO}-d_6$): 8.94 (1H, t, J 5.6, -CONH-), 8.46 (1H, s, ArH), 8.38 (1H, t, J 5.6, -CONH-), 8.06 (1H, s, ArH), 7.92-7.97 (3H, m, ArH), 7.82 (1H, dd, J 1.6 and 8.4, ArH), 4.96 {2H, t, J 1.6, *ortho* on ($\eta^5\text{-C}_5\text{H}_4$)}, 4.45 {2H, t, J 1.6, *meta* on ($\eta^5\text{-C}_5\text{H}_4$)}, 4.10 (2H, q, J 7.2, - OCH_2CH_3), 4.05 (5H, s, $\eta^5\text{-C}_5\text{H}_5$), 3.98 (2H, d, J 5.6, - NHCH_2 -), 3.87 (2H, d, J 5.6, - NHCH_2 -), 1.20 (3H, t, J 7.2, - OCH_2CH_3);

δ_{C} (100 MHz, $\text{DMSO}-d_6$): 169.8 (C=O), 169.6 (C=O), 166.5 (C=O), 138.8 (C_q), 134.5 (C_q), 130.6 (C_q), 130.4 (C_q), 128.7, 127.6, 127.3, 125.9, 124.6, 122.7, 84.0 ($\text{C}_{\text{ipso}} \eta^5\text{-C}_5\text{H}_4$), 69.5 ($\eta^5\text{-C}_5\text{H}_5$), 69.4 ($\text{C}_{\text{meta}} \eta^5\text{-C}_5\text{H}_4$), 66.6 ($\text{C}_{\text{ortho}} \eta^5\text{-C}_5\text{H}_4$), 60.4 (- OCH_2 -, -ve DEPT), 42.5 (- NHCH_2 -, -ve DEPT), 40.7 (- NHCH_2 -, -ve DEPT), 14.0 (- OCH_2CH_3).

***N*-(6-ferrocenyl-2-naphthoyl)-glycine-L-alanine ethyl ester 51**

The synthesis followed that of **80** using the following reagents: 6-ferrocenylnaphthalene-2-carboxylic acid (0.26 g, 0.7 mmol), 1-hydroxybenzotriazole (0.14 g, 1.0 mmol), triethylamine (0.5 ml), *N*-(3-dimethylaminopropyl)-*N'*-ethylcarbodiimide hydrochloride



(0.19 g, 1.0 mmol) and glycine-L-alanine ethyl ester hydrochloride (0.15 g, 0.7 mmol). The product was purified by column chromatography (eluant 1:1 hexane:ethyl acetate) to give the title compound as an orange solid (0.28 g, 79%), mp 130 °C;

$E^{\circ'}/\text{mV}$ 56 vs. Fc/Fc^+ ;

$[\alpha]_D^{20}$ -78 (*c* 0.01 in EtOH);

Anal. Calc. for $\text{C}_{28}\text{H}_{28}\text{N}_2\text{O}_4\text{Fe}$: C, 65.6; H, 5.5; N, 5.5%. Found: C, 65.4; H, 5.6; N, 5.4;

m/z (ESI) 513.1486 $[\text{M}+\text{H}]^+$. $\text{C}_{28}\text{H}_{29}\text{N}_2\text{O}_4\text{Fe}$ requires 513.1477;

λ_{max} (EtOH)/nm 375 ($\epsilon/\text{dm}^3 \text{ mol}^{-1} \text{ cm}^{-1}$ 3451), 450 (1482);

ν_{max} (KBr)/ cm^{-1} 3419, 3284, 1748, 1646, 1546, 1494;

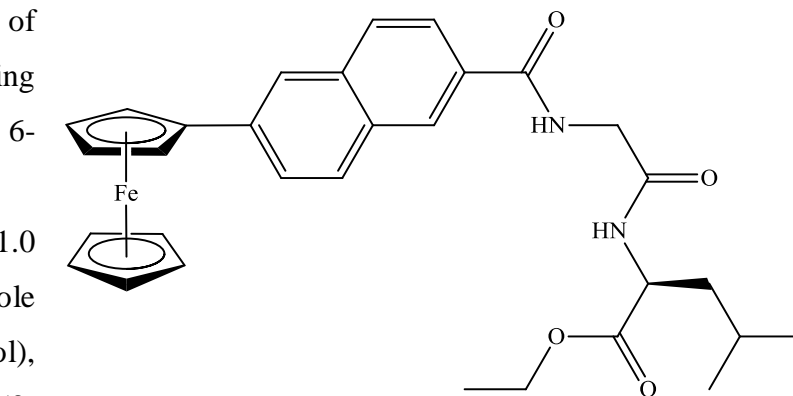
δ_{H} (400 MHz, $\text{DMSO}-d_6$): 8.84 (1H, t, *J* 5.6, -CONH-), 8.44 (1H, s, ArH), 8.41 (1H, d, *J* 7.2, -CONH-), 8.06 (1H, s, ArH), 7.92-7.97 (3H, m, ArH), 7.82 (1H, dd, *J* 1.6 and 8.8, ArH), 4.95 {2H, t, *J* 1.6, *ortho* on (η^5 - C_5H_4)}, 4.44 {2H, t, *J* 1.6, *meta* on (η^5 - C_5H_4)}, 4.30 (1H, qt, *J* 7.2, -NHCH-), 4.06-4.12 (2H, m, - OCH_2CH_3), 4.00-4.05 (6H, m, η^5 - C_5H_5 , -NHCH₂-), 3.93 (1H, dd, *J* 5.6 and 16.4, -NHCH₂-), 1.31 (3H, d, *J* 7.2, -CH₃), 1.19 (3H, t, *J* 7.2, - OCH_2CH_3);

δ_{C} (100 MHz, $\text{DMSO}-d_6$): 172.5 (C=O), 168.9 (C=O), 166.5 (C=O), 138.8 (C_q), 134.5 (C_q), 130.6 (C_q), 130.4 (C_q), 128.7, 127.5, 127.3, 125.9, 124.5, 122.7, 84.0 (C_{ipso} η^5 - C_5H_4), 69.5 (η^5 - C_5H_5), 69.4 (C_{meta} η^5 - C_5H_4), 66.6 (C_{ortho} η^5 - C_5H_4), 60.5 (- OCH_2 -, -ve DEPT), 47.7 (α -C), 42.2 (-NHCH₂-, -ve DEPT), 17.0 (-CH₃), 14.0 (- OCH_2CH_3).

***N*-(6-ferrocenyl-2-naphthoyl)-glycine-L-leucine ethyl ester 97**

The synthesis followed that of **80** using the following reagents:

6-ferrocenylnaphthalene-2-carboxylic acid (0.36 g, 1.0 mmol), 1-hydroxybenzotriazole (0.16 g, 1.2 mmol), triethylamine (0.5 ml), *N*-(3-



dimethylaminopropyl)-*N'*-ethylcarbodiimide hydrochloride (0.23 g, 1.2 mmol) and glycine-L-leucine ethyl ester hydrochloride (0.25 g, 1.0 mmol). The product was purified by column chromatography (eluant 1:1 hexane: ethyl acetate) to give the title compound as an orange solid (0.32 g, 58%), mp 160-161 °C;

$E^{0'}/\text{mV}$ 60 vs. Fc/Fc⁺;

$[\alpha]_D^{20}$ -12 (*c* 0.06 in CH₃CN);

Anal. calcd. for C₃₁H₃₄N₂O₄Fe: C, 67.15; H, 6.2; N, 5.05%. Found: C, 67.2; H, 6.2; N, 5.05; *m/z* (MALDI-TOF) 554.3 [M]⁺. C₃₁H₃₄N₂O₄Fe requires 554.5;

λ_{max} (CH₃CN)/nm 370 ($\epsilon/\text{dm}^3 \text{ mol}^{-1} \text{ cm}^{-1}$ 3336), 445 (1422);

ν_{max} (neat)/cm⁻¹ 3298, 2955, 1744, 1682, 1644, 1624, 1512, 1184;

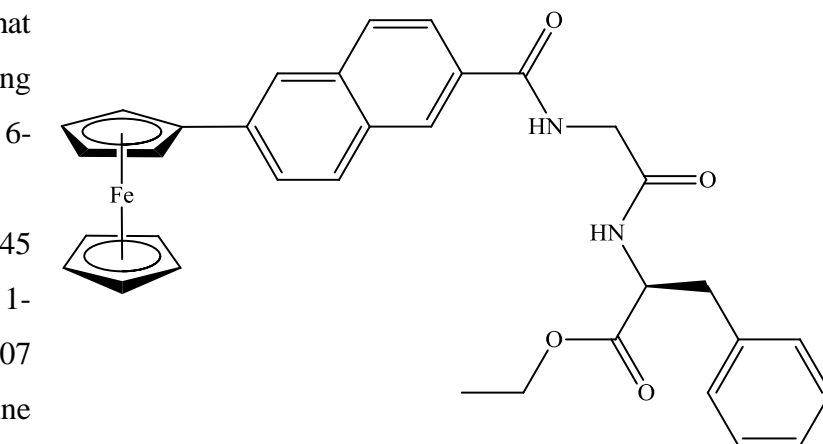
δ_{H} (400 MHz, DMSO-*d*₆): 8.82 (1H, t, *J* 5.6, -CONH-), 8.44 (1H, s, ArH), 8.34 (1H, d, *J* 8.4, -CONH-), 8.06 (1H, s, ArH), 7.93-7.97 (3H, m, ArH), 7.82 (1H, dd, *J* 1.2 and 8.4, ArH), 4.96 {2H, t, *J* 2.0, *ortho* on (η^5 -C₅H₄)}, 4.45 {2H, t, *J* 2.0, *meta* on (η^5 -C₅H₄)}, 4.30-4.35 (1H, m, -NHCH-), 4.07-4.13 (7H, m, -OCH₂CH₃, η^5 -C₅H₅), 3.93-3.99 (2H, m, -NHCH₂-), 1.48-1.72 (3H, m, -CH₂CH-), 1.19 (3H, t, *J* 7.2, -OCH₂CH₃), 0.86-0.92 {6H, m, -CH(CH₃)₂};

δ_{C} (100 MHz, DMSO-*d*₆): 172.5 (C=O), 169.1 (C=O), 166.5 (C=O), 138.8 (C_q), 134.5 (C_q), 130.7 (C_q), 130.5 (C_q), 128.7, 127.5, 127.3, 125.9, 124.5, 122.7, 84.1 (C_{ipso} η^5 -C₅H₄), 69.4 (η^5 -C₅H₅, C_{meta} η^5 -C₅H₄), 66.6 (C_{ortho} η^5 -C₅H₄), 60.4 (-OCH₂-, -ve DEPT), 50.3 (α -C), 42.2 (-NHCH₂-, -ve DEPT), 40.1 (-CH₂-, -ve DEPT), 24.2 (-CH-), 22.7 (-CH₃), 21.4 (-CH₃), 14.0 (-OCH₂CH₃).

N*-(6-ferrocenyl-2-naphthoyl)-glycine-L-phenylalanine ethyl ester **98*

The synthesis followed that of **80** using the following reagents:

6-ferrocenylnaphthalene-2-carboxylic acid (0.16 g, 0.45 mmol),
1-hydroxybenzotriazole (0.07 g, 0.5 mmol), triethylamine (0.1 ml), *N*-(3-



dimethylaminopropyl)-*N'*-ethylcarbodiimide hydrochloride (0.10 g, 0.5 mmol) and glycine-L-phenylalanine ethyl ester hydrochloride (0.13 g, 0.45 mmol). The product was purified by column chromatography (eluant 1:1 hexane: ethyl acetate) to give the title compound as an orange solid (0.15 g, 56%), mp 53-54 °C;

E^0/mV 59 vs. Fc/Fc^+ ;

$[\alpha]_D^{20}$ +18 (*c* 0.06 in CH_3CN);

m/z (MALDI-TOF) 588.3 $[M]^+$. $C_{34}H_{32}N_2O_4Fe$ requires 588.5;

$\lambda_{max}(CH_3CN)/nm$ 370 ($\epsilon/dm^3 mol^{-1} cm^{-1}$ 2894), 445 (1242);

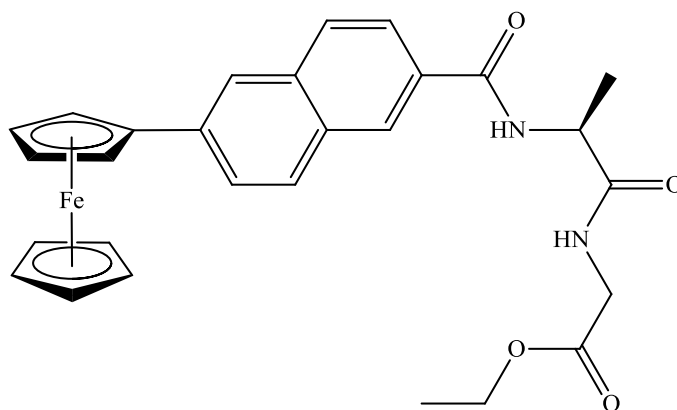
$\nu_{max}(neat)/cm^{-1}$ 3290, 3062, 1735, 1640, 1521, 1298, 1209;

δ_H (400 MHz, $DMSO-d_6$): 8.86 (1H, t, *J* 5.6, -CONH-), 8.43-8.47 (2H, m, -CONH-, ArH), 8.10 (1H, s, ArH), 7.97-8.00 (3H, m, ArH), 7.86 (1H, dd, *J* 1.2 and 8.4, ArH), 7.23-7.33 (5H, m, -CH₂Ph), 5.00 {2H, t, *J* 1.6, *ortho* on ($\eta^5-C_5H_4$)}, 4.49-4.56 {3H, m, -NHCH-, *meta* on ($\eta^5-C_5H_4$)}, 3.93-4.10 (9H, m, -OCH₂CH₃, $\eta^5-C_5H_5$, -NHCH₂-), 2.98-3.13 (2H, m, -CH₂Ph), 1.15 (3H, t, *J* 7.2, -OCH₂CH₃);

δ_C (100 MHz, $DMSO-d_6$): 171.4 (C=O), 169.1 (C=O), 166.4 (C=O), 138.8 (C_q), 136.9 (C_q), 134.5 (C_q), 130.7 (C_q), 130.4 (C_q), 129.1, 128.7, 128.2, 127.5, 127.3, 126.6, 125.9, 124.5, 122.7, 84.1 (*C*_{ipso} $\eta^5-C_5H_4$), 69.4 ($\eta^5-C_5H_5$, *C*_{meta} $\eta^5-C_5H_4$), 66.6 (*C*_{ortho} $\eta^5-C_5H_4$), 60.5 (-OCH₂-, -ve DEPT), 53.7 (α -C), 42.3 (-NHCH₂-, -ve DEPT), 36.9 (-CH₂Ph, -ve DEPT), 14.1 (-OCH₂CH₃).

***N*-(6-ferrocenyl-2-naphthoyl)-L-alanine-glycine ethyl ester 99**

The synthesis followed that of **80** using the following reagents: 6-ferrocenylnaphthalene-2-carboxylic acid (0.24 g, 0.6 mmol), 1-hydroxybenzotriazole (0.16 g, 1.2 mmol), triethylamine (0.5 ml), *N*-(3-dimethylaminopropyl)-*N'*-ethylcarbodiimide hydrochloride



(0.19 g, 1.0 mmol) and L-alanine-glycine ethyl ester hydrochloride (0.24 g, 1.1 mmol). The product was purified by column chromatography (eluant 1:1 hexane:ethyl acetate) to give the title compound as an orange solid (0.24 g, 67%), mp 138-139 °C;

$E^{\circ'}/\text{mV}$ 42 vs. Fc/Fc^+ ;

$[\alpha]_D^{20}$ -44 (*c* 0.01 in EtOH);

m/z (ESI) 513.1486 $[\text{M}+\text{H}]^+$. $\text{C}_{28}\text{H}_{29}\text{N}_2\text{O}_4\text{Fe}$ requires 513.1477;

$\lambda_{\text{max}}(\text{EtOH})/\text{nm}$ 375 ($\epsilon/\text{dm}^3 \text{ mol}^{-1} \text{ cm}^{-1}$ 2990), 450 (1266);

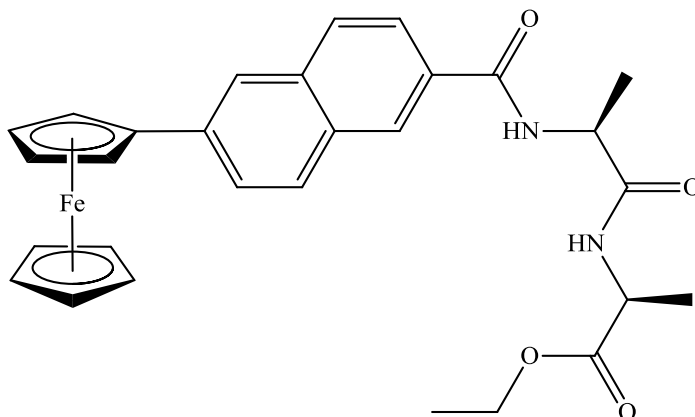
$\nu_{\text{max}}(\text{KBr})/\text{cm}^{-1}$ 3415, 3284, 1751, 1637, 1546, 1494, 1262;

δ_{H} (400 MHz, $\text{DMSO}-d_6$): 8.67 (1H, d, J 7.2, -CONH-), 8.48 (1H, s, ArH), 8.38 (1H, t, J 5.6, -CONH-), 8.06 (1H, s, ArH), 7.94 (3H, m, ArH), 7.82 (1H, dd, J 1.6 and 8.4, ArH), 4.96 {2H, t, J 1.6, *ortho* on (η^5 - C_5H_4)}, 4.60 (1H, qt, J 7.2, -NHCH-), 4.45 {2H, t, J 1.6, *meta* on (η^5 - C_5H_4)}, 4.12 (2H, q, J 7.2, - OCH_2CH_3), 4.05 (5H, s, η^5 - C_5H_5), 3.89 (1H, dd, J 5.6 and 17.6, -NHCH₂-), 3.82 (1H, dd, J 5.6 and 17.6, -NHCH₂-), 1.41 (3H, d, J 7.2, -CH₃), 1.19 (3H, t, J 7.2, - OCH_2CH_3);

δ_{C} (100 MHz, $\text{DMSO}-d_6$): 173.0 (C=O), 169.7 (C=O), 166.1 (C=O), 138.8 (C_q), 134.5 (C_q), 130.6 (C_q), 130.4 (C_q), 128.7, 127.7, 127.2, 125.9, 124.8, 122.7, 84.1 (C_{ipso} η^5 - C_5H_4), 69.5 (η^5 - C_5H_5), 69.4 (C_{meta} η^5 - C_5H_4), 66.6 (C_{ortho} η^5 - C_5H_4), 60.3 (- OCH_2 -, -ve DEPT), 48.8 (α -C), 40.7 (-NHCH₂-, -ve DEPT), 17.9 (-CH₃), 14.0 (- OCH_2CH_3).

***N*-(6-ferrocenyl-2-naphthoyl)-L-alanine-L-alanine ethyl ester 100**

The synthesis followed that of **80** using the following reagents: 6-ferrocenylnaphthalene-2-carboxylic acid (0.29 g, 0.8 mmol), 1-hydroxybenzotriazole (0.14 g, 1.0 mmol), triethylamine (0.9 ml), *N*-(3-dimethylaminopropyl)-*N'*-



ethylcarbodiimide hydrochloride (0.19 g, 1.0 mmol) and L-alanine-L-alanine ethyl ester hydrochloride (0.15 g, 0.8 mmol). The product was purified by column chromatography (eluant 1:1 hexane:ethyl acetate) to give the title compound as an orange solid (0.12 g, 29%), mp 80-81 °C;

$E^{0'}/\text{mV}$ 42 vs. Fc/Fc^+ ;

$[\alpha]_D^{20}$ +58 (c 0.01 in EtOH);

m/z (ESI) 527.1616 $[\text{M}+\text{H}]^+$. $\text{C}_{29}\text{H}_{31}\text{N}_2\text{O}_4\text{Fe}$ requires 527.1633;

λ_{max} (EtOH)/nm 375 ($\epsilon/\text{dm}^3 \text{ mol}^{-1} \text{ cm}^{-1}$ 3233), 450 (1349);

ν_{max} (KBr)/ cm^{-1} 3448, 3288, 1735, 1636, 1546, 1495, 1204;

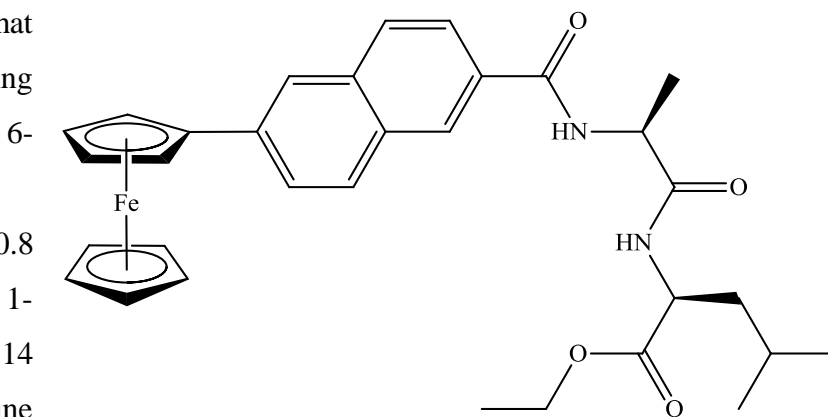
δ_{H} (400 MHz, $\text{DMSO}-d_6$): 8.59 (1H, d, J 7.2, -CONH-), 8.46 (1H, s, ArH), 8.40 (1H, d, J 7.2, -CONH-), 8.05 (1H, s, ArH), 7.92-7.97 (3H, m, ArH), 7.82 (1H, dd, J 1.6 and 8.8, ArH), 4.96 {2H, t, J 1.6, *ortho* on (η^5 - C_5H_4)}, 4.59 (1H, qt, J 7.2, -NHCH-), 4.45 {2H, t, J 1.6, *meta* on (η^5 - C_5H_4)}, 4.27 (1H, qt, J 7.2, -NHCH-), 4.04-4.11 (7H, m, - OCH_2CH_3 , η^5 - C_5H_5), 1.40 (3H, d, J 7.2, - CH_3), 1.32 (3H, d, J 7.2, - CH_3), 1.18 (3H, t, J 7.2, - OCH_2CH_3);

δ_{C} (100 MHz, $\text{DMSO}-d_6$): 172.5 (C=O), 169.4 (C=O), 166.0 (C=O), 138.7 (C_q), 134.5 (C_q), 130.6 (C_q), 130.5 (C_q), 128.7, 127.6, 127.2, 125.9, 124.7, 122.8, 84.1 ($\text{C}_{\text{ipso}} \eta^5$ - C_5H_4), 69.5 (η^5 - C_5H_5), 69.4 ($\text{C}_{\text{meta}} \eta^5$ - C_5H_4), 66.6 ($\text{C}_{\text{ortho}} \eta^5$ - C_5H_4), 60.4 (- OCH_2 -, -ve DEPT), 48.5 (α -C), 47.7 (α -C), 17.9 (- CH_3), 16.8 (- CH_3), 14.0 (- OCH_2CH_3).

***N*-(6-ferrocenyl-2-naphthoyl)-L-alanine-L-leucine ethyl ester 101**

The synthesis followed that of **80** using the following reagents:

6-ferrocenylnaphthalene-2-carboxylic acid (0.29 g, 0.8 mmol),
1-hydroxybenzotriazole (0.14 g, 1.0 mmol), triethylamine



(0.9 ml), *N*-(3-dimethylaminopropyl)-*N'*-ethylcarbodiimide hydrochloride (0.19 g, 1.0 mmol) and L-alanine-L-leucine ethyl ester hydrochloride (0.18 g, 0.8 mmol). The product was purified by column chromatography (eluant 1:1 hexane: ethyl acetate) to give the title compound as an orange solid (0.10 g, 23 %), mp 73-74 °C;

$E^{0'}/\text{mV}$ 60 vs. Fc/Fc⁺;

$[\alpha]_D^{20}$ +29 (*c* 0.06 in CH₃CN);

Anal. calcd. for C₃₂H₃₆N₂O₄Fe: C, 67.6; H, 6.4; N, 4.9%. Found: C, 67.55; H, 6.4; N, 4.7;

m/z (ESI) 568.0 [M]⁺. C₃₂H₃₆N₂O₄Fe requires 568.5;

λ_{max} (CH₃CN)/nm 370 ($\epsilon/\text{dm}^3 \text{ mol}^{-1} \text{ cm}^{-1}$ 3064), 445 (1298);

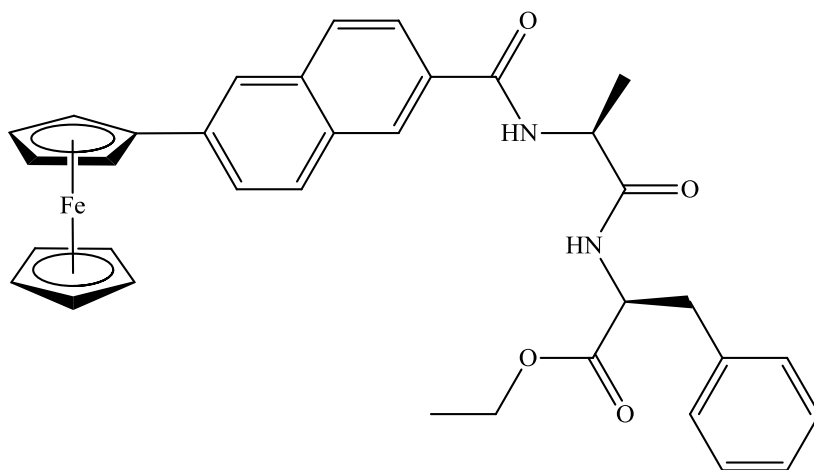
ν_{max} (neat)/cm⁻¹ 3282, 3089, 1734, 1633, 1530, 1187;

δ_{H} (400 MHz, DMSO-*d*₆): 8.58 (1H, d, *J* 7.2, -CONH-), 8.46 (1H, s, ArH), 8.29 (1H, d, *J* 7.2, -CONH-), 8.05 (1H, s, ArH), 7.90-7.97 (3H, m, ArH), 7.79-7.86 (1H, m, ArH), 4.95 {2H, t, *J* 1.6, *ortho* on (η^5 -C₅H₄)}, 4.60 (1H, qt, *J* 7.2, -NHCH-), 4.44 {2H, t, *J* 1.6, *meta* on (η^5 -C₅H₄)}, 4.26-4.32 (1H, m, -NHCH-), 4.00-4.14 (7H, m, -OCH₂CH₃, η^5 -C₅H₅), 1.48-1.73 (3H, m, -CH₂CH-), 1.39 (3H, d, *J* 7.2, -CH₃), 1.17 (3H, t, *J* 7.2, -OCH₂CH₃), 0.86-0.93 {6H, m, -CH(CH₃)₂};

δ_{C} (100 MHz, DMSO-*d*₆): 172.7 (C=O), 172.4 (C=O), 166.0 (C=O), 138.7 (C_q), 134.5 (C_q), 130.6 (C_q), 130.5 (C_q), 128.7, 127.6, 127.2, 125.9, 124.7, 122.7, 84.1 (C_{ipso} η^5 -C₅H₄), 69.4 (η^5 -C₅H₅, C_{meta} η^5 -C₅H₄), 66.6 (C_{ortho} η^5 -C₅H₄), 60.4 (-OCH₂-, -ve DEPT), 50.4 (α -C), 48.6 (α -C), 39.7 (-CH₂-, -ve DEPT), 24.2 (-CH-), 22.7 (-CH₃), 21.4 (-CH₃), 17.9 (-CH₃), 14.0 (-OCH₂CH₃).

***N*-(6-ferrocenyl-2-naphthoyl)-L-alanine-L-phenylalanine ethyl ester 102**

The synthesis followed that of **80** using the following reagents: 6-ferrocenylnaphthalene-2-carboxylic acid (0.36 g, 1.0 mmol), 1-hydroxybenzotriazole (0.18 g, 1.3 mmol), triethylamine (0.5 ml), *N*-



(3-dimethylaminopropyl)-*N'*-ethylcarbodiimide hydrochloride (0.25 g, 1.3 mmol) and L-alanine-L-phenylalanine ethyl ester (0.26 g, 1.0 mmol). The product was purified by column chromatography (eluant 1:1 hexane: ethyl acetate) to give the title compound as an orange solid (0.12 g, 23%), mp 75 °C;

E^0/mV 59 vs. Fc/Fc⁺;

$[\alpha]_D^{20}$ +36 (*c* 0.06 in CH₃CN);

m/z (MALDI-TOF) 602.3 [M]⁺. C₃₅H₃₄N₂O₄Fe requires 602.5;

λ_{max} (CH₃CN)/nm 370 ($\epsilon/dm^3 mol^{-1} cm^{-1}$ 2774), 445 (1188);

ν_{max} (neat)/cm⁻¹ 3282, 2963, 1736, 1634, 1526, 1260, 1187;

δ_H (400 MHz, DMSO-*d*₆): 8.58 (1H, d, *J* 7.2, -CONH-), 8.45 (1H, s, ArH), 8.36 (1H, d, *J* 7.2, -CONH-), 8.06 (1H, s, ArH), 7.93-7.97 (3H, m, ArH), 7.82 (1H, dd, *J* 1.6 and 8.4, ArH), 7.17-7.25 (5H, m, -CH₂Ph), 4.96 {2H, t, *J* 2.0, *ortho* on (η^5 -C₅H₄)}, 4.60 (1H, qt, *J* 7.2, -NHCH-), 4.43-4.50 {3H, m, -NHCH-, *meta* on (η^5 -C₅H₄)}, 4.00-4.08 (7H, m, -OCH₂CH₃, η^5 -C₅H₅), 2.96-3.07 (2H, m, -CH₂Ph), 1.36 (3H, d, *J* 7.2, -CH₃), 1.10 (3H, t, *J* 7.2, -OCH₂CH₃);

δ_C (100 MHz, DMSO-*d*₆): 172.6 (C=O), 171.3 (C=O), 166.0 (C=O), 138.8 (C_q), 137.0 (C_q), 134.5 (C_q), 130.6 (C_q), 130.4 (C_q), 129.1, 128.7, 128.2, 127.6, 127.2, 126.5, 125.9, 124.7, 122.7, 84.1 (*C*_{ipso} η^5 -C₅H₄), 69.4 (η^5 -C₅H₅, *C*_{meta} η^5 -C₅H₄), 66.6 (*C*_{ortho} η^5 -C₅H₄), 60.4 (-OCH₂-, -ve DEPT), 53.7 (α -C), 48.6 (α -C), 36.6 (-CH₂Ph, -ve DEPT), 17.8 (-CH₃), 14.1 (-OCH₂CH₃).

References

1. J. M. Berg, J. L. Tymoczko, L. Stryer, *Biochemistry*, 5th ed., W. H. Freeman, **2002**.
2. G. Jaouen, *Bioorganometallics : Biomolecules, Labeling, Medicine*, Wiley-VCH, **2006**.
3. J. T. Chantson, M. V. V. Falzacappa, S. Crovella and N. Metzler-Nolte, *Journal of Organometallic Chemistry*, 2005, **690**, 4564-4572.
4. J. T. Chantson, M. V. V. Falzacappa, S. Crovella and N. Metzler-Nolte, *Chemmedchem*, 2006, **1**, 1268-1274.
5. J. Deruiter, B. E. Swearingen, V. Wandrekar and C. A. Mayfield, *Journal of Medicinal Chemistry*, 1989, **32**, 1033-1038.
6. D. J. Burdick, K. Paris, K. Weese, M. Stanley, M. Beresini, K. Clark, R. S. McDowell, J. C. Marsters and T. R. Gadek, *Bioorganic & Medicinal Chemistry Letters*, 2003, **13**, 1015-1018.
7. D. J. Burdick, J. C. Marsters, I. Aliagas-Martin, M. Stanley, M. Beresini, K. Clark, R. S. McDowell and T. R. Gadek, *Bioorganic & Medicinal Chemistry Letters*, 2004, **14**, 2055-2059.
8. G. Tabbi, C. Cassino, G. Cavigliolo, D. Colangelo, A. Ghiglia, I. Viano and D. Osella, *Journal of Medicinal Chemistry*, 2002, **45**, 5786-5796.
9. A. Goel, D. Savage, S. R. Alley, P. N. Kelly, D. O'Sullivan, H. Mueller-Bunz and P. T. M. Kenny, *Journal of Organometallic Chemistry*, 2007, **692**, 1292-1299.
10. A. J. Corry, A. Goel, S. R. Alley, P. N. Kelly, D. O'Sullivan, D. Savage and P. T. M. Kenny, *Journal of Organometallic Chemistry*, 2007, **692**, 1405-1410.
11. A. J. Corry, N. O'Donovan, Á. Mooney, D. O'Sullivan, D. K. Rai and P. T. M. Kenny, *Journal of Organometallic Chemistry*, 2009, **694**, 880-885.
12. A. J. Corry, A. Mooney, D. O'Sullivan and P. T. M. Kenny, *Inorganica Chimica Acta*, 2009, **362**, 2957-2961.
13. P. Pigeon, S. Top, A. Vessieres, M. Huche, E. A. Hillard, E. Salomon and G. Jaouen, *Journal of Medicinal Chemistry*, 2005, **48**, 2814-2821.
14. P. Beagley, M. A. L. Blackie, K. Chibale, C. Clarkson, J. R. Moss and P. J. Smith, *Dalton Transactions*, 2002, 4426-4433.
15. N. J. Long, *Metalloenes : An Introduction to Sandwich Complexes*, Blackwell Science, **1998**.
16. A. J. Corry, Ph.D. Thesis, Dublin City University, **2009**.
17. M. Rosenblum, J. O. Santer and W. G. Howells, *Journal of the American Chemical Society*, 1963, **85**, 1450-&.
18. M. Bodanszky and A. Bodanszky, *The Practice of Peptide Synthesis* Springer-Verlag, **1993**.
19. J. Jones, *Amino Acid and Peptide Synthesis*, Oxford University Press, **2002**.
20. E. Valeur and M. Bradley, *Chemical Society Reviews*, 2009, **38**, 606-631.
21. C. Montalbetti and V. Falque, *Tetrahedron*, 2005, **61**, 10827-10852.
22. D. H. Williams and I. Fleming, *Spectroscopic Methods in Organic Chemistry*, McGraw-Hill, **1995**.
23. D. M. Savage, Ph.D. Thesis, Dublin City University, **2003**.

24. Z. Chen, A. R. Graydon and P. D. Beer, *Journal of the Chemical Society-Faraday Transactions*, 1996, **92**, 97-102.
25. G. A. Mabbott, *Journal of Chemical Education*, 1983, **60**, 697-702.
26. V. S. Bagotsky, *Fundamentals of Electrochemistry*, John Wiley & Sons, Inc., **2006**.
27. D. R. van Staveren, T. Weyhermuller and N. Metzler-Nolte, *Dalton Transactions*, 2003, 210-220.
28. R. M. Silverstein, F. X. Webster and D. Kiemle, *Spectrometric Identification of Organic Compounds*, 7th ed., Wiley, **2005**.
29. P. T. M. Kenny, K. Nomoto and R. Orlando, *Rapid Communications in Mass Spectrometry*, 1992, **6**, 95-97.
30. P. Roepstorff and J. Fohlman, *Biomedical Mass Spectrometry*, 1984, **11**, 601-601.
31. D. Savage, G. Malone, S. R. Alley, J. F. Gallagher, A. Goel, P. N. Kelly, H. Mueller-Bunz and P. T. M. Kenny, *Journal of Organometallic Chemistry*, 2006, **691**, 463-469.
32. K. Biemann, *Biomedical and Environmental Mass Spectrometry*, 1988, **16**, 99-111.
33. A. Goel and P. T. M. Kenny, *Rapid Communications in Mass Spectrometry*, 2008, **22**, 2398-2401.
34. D. Savage, J. F. Gallagher, Y. Ida and P. T. M. Kenny, *Inorganic Chemistry Communications*, 2002, **5**, 1034-1040.

Chapter 3

Biological Evaluation of *N*-(ferrocenyl)naphthoyl amino acid and dipeptide derivatives which contain α -amino acids

3.1. Introduction

The introduction and development of animal cell culture during in the 1940s and 1950s revolutionised the field of cancer drug discovery. Prior to this period of time, the toxicity of synthetic and natural compounds could only be evaluated in whole animal studies. Aside from the obvious ethical problems associated with animal studies, high costs and lack of reproducibility were among the disadvantages associated with this method of evaluation. *In vitro* toxicity testing has been proven to be less costly and time-consuming than *in vivo* methods, as well as being easier to carry out, thereby permitting a larger number of assays to be performed. Also, there is a good reproducibility of results associated with *in vitro* toxicity tests and the quantities of test compounds required for the assays are much lower.¹ Nowadays, the first step in the biological evaluation of synthetic and natural compounds is to perform an *in vitro* study. Where large libraries of compounds are concerned, *in vitro* studies enable the identification of the most active compounds in an efficient manner.

3.1.1. Miniaturised *in vitro* methods

In vitro miniaturised colorimetric end-point assays are used extensively to ascertain whether a substance has the ability to either enhance cell growth or promote cell death. These *in vitro* assays involve the determination of cell number (the most common measure of cell growth) after the cells have been treated with the test substance for a specific period of time.¹ The test substance is considered to have an anti-proliferative effect on treated cells, if a reduction in cell number is evident when compared to untreated controls.

Unfortunately, there is one considerable limitation to the use of *in vitro* colorimetric end-point assays; it is not possible to establish whether the test substance is cytotoxic or cytostatic.² Cytostatic agents only affect the growth rate of cells temporarily, in a reversible manner. The anti-proliferative effect of such drugs is lost once the cytostatic agent is

removed. Cytotoxic agents, on the other hand, cause irreversible cell damage, which leads to cell death by either an apoptotic or necrotic pathway. In either case, cell growth is impaired. Thus, it is not possible to distinguish between these two agents.

There are several different colorimetric assays which can be employed for the end-point determination of cell number. When selecting the appropriate colorimetric end-point, a number of factors must be considered. These include the sensitivity and linear range of the colorimetric assay, which can vary depending on both the cell line being analysed and the end-point being employed.² The range of linearity of optical density (OD) to cell number is offset by the sensitivity of the end-point assay. In general, end-points with high sensitivity give a low range of linearity of OD with cell number.

3.1.1.1. MTT assay

In the MTT assay, a solution of the soluble yellow dye known as 3-(4,5-dimethylthiazol-2-yl)-2,5-diphenyltetrazolium bromide (MTT), is added to the cells at the end-point of the assay. MTT is reduced by the succinate dehydrogenase enzyme in the mitochondria of metabolically active cells to form a dark blue, insoluble formazan product (Figure 3.1). The formazan crystals produced are then solubilised in DMSO to give a coloured solution, the absorbance of which is then quantified at 570 nm.

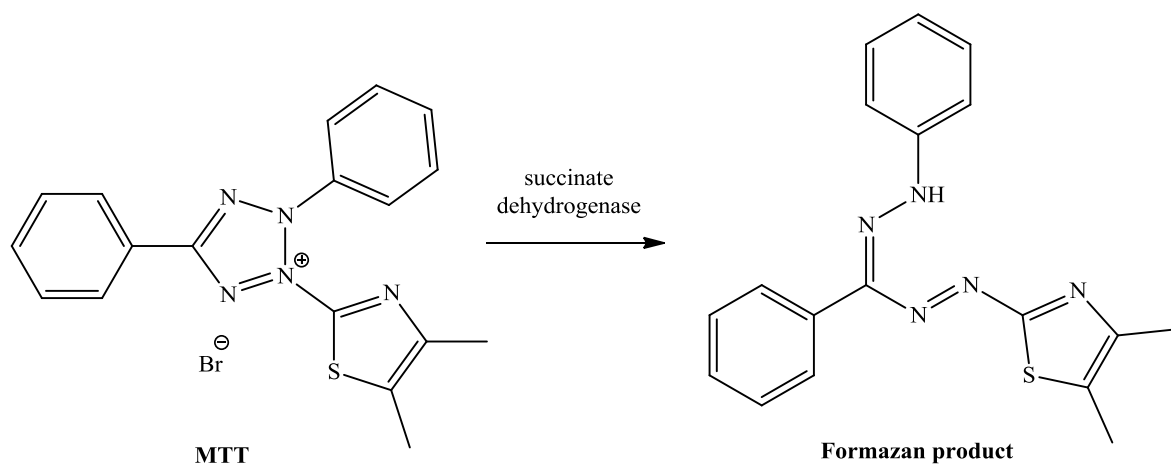


Figure 3.1 The succinate dehydrogenase catalysed conversion of the MTT dye to the insoluble formazan product.

The MTT end-point determination of cell number exhibits a good linear relationship of OD to cell number, however, the sensitivity of the assay is quite poor. It has also been shown that cells which are actively growing reduce MTT to a greater extent than cells which are not, which may lead to differences in assay sensitivity in various cell lines.² In addition, MTT is a mutagenic agent, and therefore requires care in its handling and disposal.

3.1.1.2. Neutral red assay

The neutral red assay is based on the accumulation of the neutral red dye (Figure 3.2) in the lysosomes of viable cells. At the end-point, a neutral red solution is added to the cells and incubated to allow accumulation. Following washing, an acetic acid/ethanol mixture is added to elute the bound dye and the absorbance of the coloured solution is measured at 570 nm.² This assay is generally more sensitive than the MTT assay.

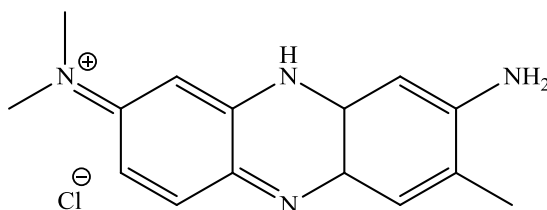


Figure 3.2 Neutral red dye used to determine cell number at the end-point of the assay.

3.1.1.3. Protein staining assays

The crystal violet dye elution assay is a protein staining assay in which the cells are fixed with formalin and stained with crystal violet. The sulforhodamine B assay is also a protein binding assay in which cells are fixed with trichloroacetic acid before staining with the dye. Both these methods are very sensitive but they exhibit a loss of linearity of OD vs. cell number at higher densities.¹

The sulforhodamine B assay was developed by Skehan *et al* in the National Cancer Institute (NCI) for use in their NCI60 cell line drug screen. This assay was shown to overcome some of the problems associated with the MTT assay and proved to be robust and feasible for large-scale screening.³

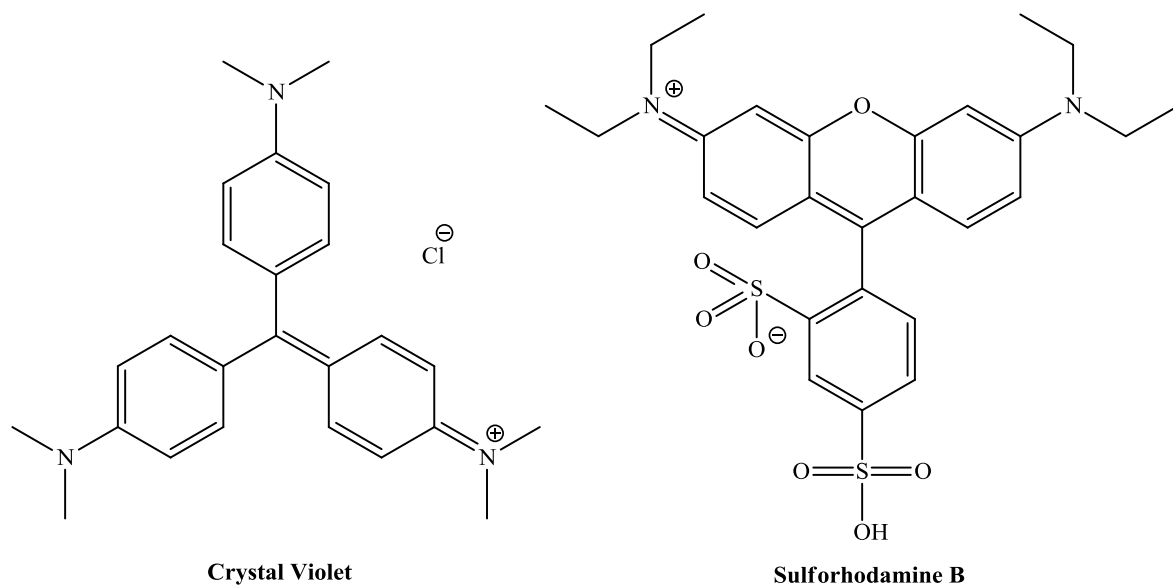


Figure 3.3 Structures of the dyes employed in the protein binding dye assays.

3.1.1.4. Acid phosphatase assay

In the acid phosphatase assay, a solution of the *p*-nitrophenyl phosphate substrate is added at the end-point of the assay. This substrate is dephosphorylated by the acid phosphatase enzyme, which is located in the lysosomes of cells, to yield *p*-nitrophenol. In the presence of strong alkali, the *p*-nitrophenol chromophore can be quantified by measuring the absorbance at 405 nm (Figure 3.4).

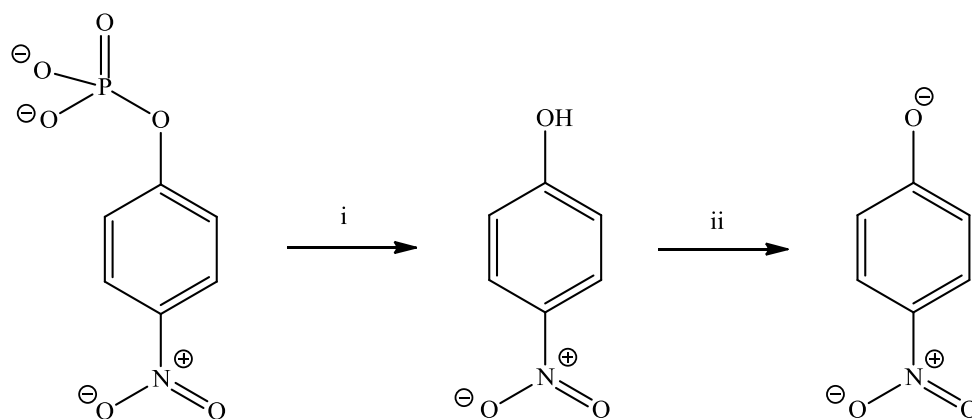


Figure 3.4 Acid phosphatase end-point assay: (i) Phosphatase catalysed reaction (in water); (ii) Colour reaction in strong base (NaOH).

The acid phosphatase assay is highly sensitive but, as a consequence, it also has a low range of linearity between OD and cell number. This assay is easier to perform than the neutral red assay, as it involves fewer steps and use of fewer reagents. It is also more convenient than the MTT assay because of the inherent problem of removal of the medium from the insoluble crystals. The reproducibility between replicate wells is excellent in the acid phosphatase assay and in many cases it has been shown to be better than the neutral red assay and the MTT assay.⁴ For these reasons, the acid phosphatase assay was the chosen colorimetric end-point assay for the *in vitro* biological evaluation of *N*-(ferrocenyl)naphthoyl amino acid and dipeptide derivatives.

3.2. Preliminary *in vitro* study of selected *N*-(ferrocenyl)naphthoyl dipeptide derivatives

Previous studies carried out to evaluate the *in vitro* anti-cancer activity of the *N*-(ferrocenyl)benzoyl peptide derivatives were performed in the H1299 cell line, which is a non-small cell lung cancer (NSCLC) derived cell line. The effect of these compounds on H1299 cell growth was expressed as an IC₅₀ value, which corresponds to the concentration of the drug required for 50% inhibition of cell growth. The *N*-(ferrocenyl)benzoyl dipeptide derivatives were shown to exert a strong inhibitory effect on cancer cell proliferation. *N*-(ferrocenyl)benzoyl dipeptide derivatives, such as *N*-{*meta*-(ferrocenyl)-benzoyl}-glycine-L-alanine ethyl ester **103** (IC₅₀ = 4.0 μM), demonstrated the strongest anti-proliferative effect.⁵ Thus, a preliminary investigation into the *in vitro* anti-cancer activity of the *N*-(ferrocenyl)naphthoyl amino acid and dipeptide derivatives was conducted with six dipeptide derivatives in the H1299 cell line.

To determine the IC₅₀ values of these six compounds, individual 96-well plates containing H1299 cells were treated with the test compound at concentrations ranging from 0.1 μM to 100 μM. The cells were then incubated for 5-6 days, until cell confluency was reached. Cell survival was determined by performing the acid phosphatase assay. The data obtained for each compound is shown in Figure 3.5. The IC₅₀ value for each compound was calculated using data obtained from three independent experiments (Table 3.1). The IC₅₀ values of the platinum anti-cancer drugs cisplatin and carboplatin in this cell line⁶ are also included

since, both drugs are frequently used in combination with a second agent (such as gemcitabine, paclitaxel, vinorelbine, and docetaxel) as the standard therapy for NSCLC.⁷ This is despite the fact that NSCLC is known to be inherently resistant to platinum therapy.⁸

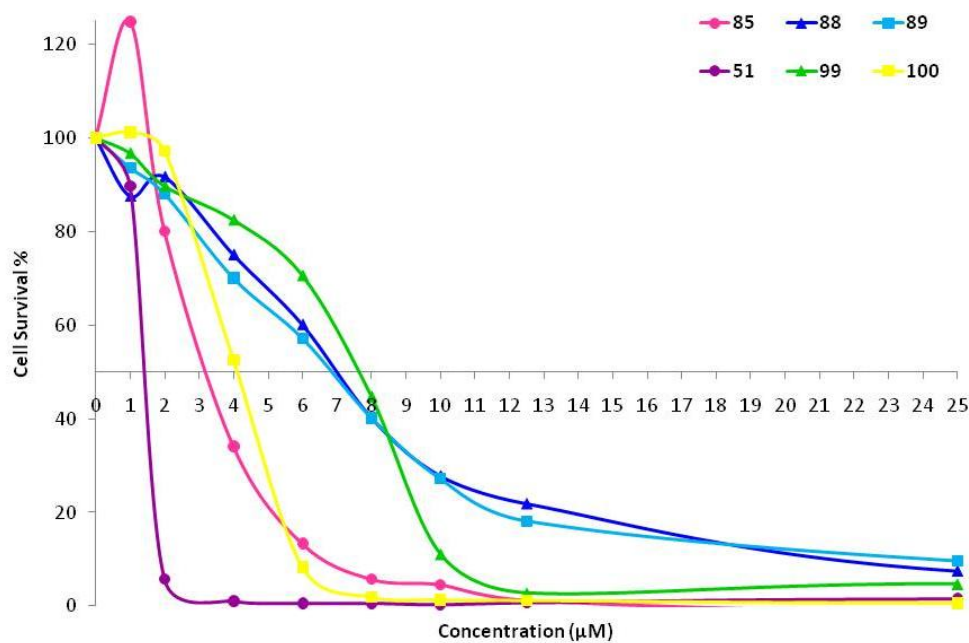


Figure 3.5 IC₅₀ plot for compounds **51**, **85**, **88**, **89**, **99** and **100** in the H1299 cell line.

Table 3.1 IC₅₀ values in the H1299 cell line.

Compound	Number	IC ₅₀ value (µM)
Cisplatin	1	1.4 ± 0.1
Carboplatin	2	9.9 ± 1.6
<i>N</i> -(3-ferrocenyl-2-naphthoyl)-Gly-L-Ala-OEt	85	3.7 ± 0.7
<i>N</i> -(3-ferrocenyl-2-naphthoyl)-L-Ala-Gly-OEt	88	6.9 ± 1.5
<i>N</i> -(3-ferrocenyl-2-naphthoyl)-L-Ala-L-Ala-OEt	89	7.8 ± 0.2
<i>N</i> -(6-ferrocenyl-2-naphthoyl)-Gly-L-Ala-OEt	51	1.3 ± 0.1
<i>N</i> -(6-ferrocenyl-2-naphthoyl)-L-Ala-Gly-OEt	99	7.8 ± 0.2
<i>N</i> -(6-ferrocenyl-2-naphthoyl)-L-Ala-L-Ala-OEt	100	3.7 ± 0.6

The six *N*-(ferrocenyl)naphthoyl dipeptide derivatives were shown to exert a strong anti-proliferative effect in the H1299 cell line; the IC₅₀ value of each compound is below 10 μM. Thus, the *N*-(ferrocenyl)naphthoyl dipeptide derivatives are significantly more active than carboplatin in this cell line (Table 3.1). Furthermore, the *N*-(ferrocenyl)naphthoyl dipeptide derivatives are more potent than the corresponding *N*-(ferrocenyl)benzoyl analogues *e.g.* the IC₅₀ value of *N*-(3-ferrocenyl-2-naphthoyl)-L-alanine-glycine ethyl ester **88** is three times lower than that of *N*-{*ortho*-(ferrocenyl)-benzoyl}-L-alanine-glycine ethyl ester **104** (IC₅₀ = 21 μM). Finally, the *in vitro* anti-proliferative effect of the most active compound, *N*-(6-ferrocenyl-2-naphthoyl)-glycine-L-alanine ethyl ester **51**, exceeds that of the well-known platinum-based anti-cancer drug cisplatin. The results obtained from this preliminary study demonstrate the effectiveness of the *N*-(ferrocenyl)naphthoyl dipeptide derivatives as anti-cancer agents. In addition, these findings emphasise the need to assess the *in vitro* anti-cancer activity of all the *N*-(ferrocenyl)naphthoyl amino acid and dipeptide derivative that have been prepared to date.

3.3. *In vitro* evaluation in the H1299 cell line and the Sk-Mel-28 cell line

The panel of *N*-(ferrocenyl)naphthoyl amino acid and dipeptide derivatives were evaluated *in vitro* by performing a comprehensive screen of every compound at a single dose (10 μM) in the H1299 cell line. This approach follows that adopted by the NCI for the NCI60 cell line drug screen. Screening of the compounds was also performed in the metastatic melanoma cell line, Sk-Mel-28, in collaboration with Dr. Norma O'Donovan and Dr. Thamir Maghoub of the National Institute for Cellular Biotechnology (NICB), DCU. Only the compounds that are shown to inhibit both H1299 and Sk-Mel-28 cell growth by 50% or more (in comparison to the controls) will progress to further studies, whereby an IC₅₀ value can be determined. The six *N*-(ferrocenyl)naphthoyl dipeptide derivatives selected for the preliminary study were included in these comprehensive screens, since they have not been tested previously in the Sk-Mel-28 cell line.

The comprehensive screen was performed by treating individual wells of a 96-well plate containing either H1299 or Sk-Mel-28 cells with a 10 μM solution of each test compound. This was achieved by preparing 1 mM stock solutions of the test compounds in DMSO and

the required dilute solutions of each test sample were then prepared by spiking the cell culture medium with a calculated amount of the stock solution. Since DMSO can have an adverse effect on cells, a DMSO control was included in the assay, along with controls for normal (untreated) cell growth. In this case, the DMSO control wells contained a 2% DMSO solution. The cells were incubated for 5 days, until cell confluency was reached. At this point, cell survival was determined by the acid phosphatase assay. The H1299 cells treated with the 2% DMSO solution showed a significant decrease in cell growth compared to the untreated controls, with only 36% cell growth, on average. Clearly, the effect of DMSO on H1299 cell proliferation is too strong, making any results obtained from this assay inaccurate. As a consequence, the compound screen was repeated, this time using 10 mM stock solutions, to reduce the DMSO level to 0.2%. At this level, the cells treated with the DMSO solution exhibited normal cell growth. The Sk-Mel-28 cells appear to be more robust, since cell growth was unaffected when treated with the 2% DMSO solution.

In the H1299 cell line, almost every *N*-(ferrocenyl)naphthoyl amino acid and dipeptide derivative was shown to inhibit cell growth by 50% or more. This is not that surprising, since in the preliminary study, an IC_{50} value below 10 μ M was found for each *N*-(ferrocenyl)naphthoyl dipeptide derivative. Hence, it was necessary to repeat the comprehensive screen in this cell line, this time testing each derivative at a concentration of 1 μ M (using 1 mM stock solution to give a 0.2% DMSO solution). The Sk-Mel-28 cells showed a greater resistance than the H1299 cells to the test compounds. Thus, it was not necessary to perform the compound screen at 1 μ M in this cell line. The results of the comprehensive screens are expressed as the percentage cell growth \pm standard deviation (relative to the DMSO controls). Standard deviations have been calculated using data obtained from three independent experiments.

3.3.1. Methyl ferrocenylnaphthalene-2-carboxylate

The intermediate compounds, methyl 3-ferrocenylnaphthalene-2-carboxylate **71** and methyl 6-ferrocenylnaphthalene-2-carboxylate **74** were shown to have a weak anti-proliferative effect in the H1299 cell line at the higher concentration of 10 μM . However, cell growth inhibition did not reach above 20% and therefore, this effect was not deemed to be significant. At the lower concentration of 1 μM , these two intermediates did not inhibit cell growth. Likewise, growth in the Sk-Mel-28 cell line was unaffected by these two intermediates.

Table 3.2 Percentage cell growth in the presence of methyl ferrocenylnaphthalene-2-carboxylate.

Compound	No.	10 μM	1 μM	10 μM
		H1299	H1299	Sk-Mel-28
Methyl 3-ferrocenylnaphthalene-2-carboxylate	71	72.9 \pm 8.7	102.1 \pm 13.3	103.4 \pm 0.6
Methyl 6-ferrocenylnaphthalene-2-carboxylate	74	82.6 \pm 3.2	117.5 \pm 12.2	89.8 \pm 10.4

3.3.2. *N*-(ferrocenyl)naphthoyl amino acid derivatives

The *N*-(3-ferrocenyl-2-naphthoyl) amino acid derivatives were shown to inhibit cell growth in the H1299 cell line by 50% or more, when tested at the higher concentration of 10 μM (Table 3.3). The effect of these compounds on cell proliferation follows a distinct pattern that correlates with the structure of these derivatives. As the side chain of the α -amino acid side chain is enlarged, adding steric bulk, the anti-proliferative effect increases. Thus, *N*-(3-ferrocenyl-2-naphthoyl)-L-phenylalanine ethyl ester **83** shows the greatest anti-proliferative effect, with approximately 96% cell growth inhibition.

In contrast, the anti-proliferative effect of the *N*-(6-ferrocenyl-2-naphthoyl) amino acid derivatives in the H1299 cell line declines as the side chain of the α -amino acid is extended. *N*-(6-ferrocenyl-2-naphthoyl)-glycine ethyl ester **92** displayed a stronger anti-proliferative

effect than the other *N*-(6-ferrocenyl-2-naphthoyl) amino acid derivatives. This compound inhibited cell growth by approximately 94%. A very high percentage of cell survival was seen when the H1299 cell line was treated with 1 μ M solutions of the *N*-(ferrocenyl)naphthoyl amino acid derivatives, indicating that cell growth is unaffected by these compounds at lower concentrations.

Table 3.3 Percentage cell growth of H1299 cells in the presence of *N*-(ferrocenyl)naphthoyl amino acid derivatives.

Compound	No.	10 μM	1 μM
<i>N</i> -(3-ferrocenyl-2-naphthoyl)-Gly-OEt	80	43.7 \pm 8.1	112.9 \pm 14.6
<i>N</i> -(3-ferrocenyl-2-naphthoyl)-L-Ala-OEt	81	27.8 \pm 3.4	98.8 \pm 1.5
<i>N</i> -(3-ferrocenyl-2-naphthoyl)-L-Leu-OEt	82	22.4 \pm 6.4	103.4 \pm 4.5
<i>N</i> -(3-ferrocenyl-2-naphthoyl)-L-Phe-OEt	83	3.5 \pm 0.6	85.8 \pm 11.8
<i>N</i> -(6-ferrocenyl-2-naphthoyl)-Gly-OEt	92	6.0 \pm 3.0	101.1 \pm 8.9
<i>N</i> -(6-ferrocenyl-2-naphthoyl)-L-Ala-OEt	93	44.4 \pm 6.9	91.4 \pm 14.4
<i>N</i> -(6-ferrocenyl-2-naphthoyl)-L-Leu-OEt	94	57.3 \pm 2.3	101.4 \pm 2.2
<i>N</i> -(6-ferrocenyl-2-naphthoyl)-L-Phe-OEt	95	40.9 \pm 4.2	102.3 \pm 5.3

The Sk-Mel-28 cell line was found to be more resistant to the *N*-(ferrocenyl)naphthoyl amino acid derivatives (Table 3.4). The *N*-(3-ferrocenyl-2-naphthoyl) amino acid derivatives did not have any noticeable effect on cell proliferation. Similarly, the majority of the *N*-(6-ferrocenyl-2-naphthoyl) amino acid derivatives were ineffective at inhibiting cell growth. *N*-(6-ferrocenyl-2-naphthoyl)-glycine ethyl ester **92** was the only compound capable of producing a significant anti-proliferative effect (~70% inhibition).

Table 3.4 Percentage cell growth of Sk-Mel-28 cells in the presence of *N*-(ferrocenyl)naphthoyl amino acid derivatives.

Compound	No.	10 μM
<i>N</i> -(3-ferrocenyl-2-naphthoyl)-Gly-OEt	80	97.1 \pm 8.1
<i>N</i> -(3-ferrocenyl-2-naphthoyl)-L-Ala-OEt	81	99.5 \pm 3.2
<i>N</i> -(3-ferrocenyl-2-naphthoyl)-L-Leu-OEt	82	103.1 \pm 1.7
<i>N</i> -(3-ferrocenyl-2-naphthoyl)-L-Phe-OEt	83	82.9 \pm 16.7
<i>N</i> -(6-ferrocenyl-2-naphthoyl)-Gly-OEt	92	31.4 \pm 10.1
<i>N</i> -(6-ferrocenyl-2-naphthoyl)-L-Ala-OEt	93	89.6 \pm 21.4
<i>N</i> -(6-ferrocenyl-2-naphthoyl)-L-Leu-OEt	94	95.7 \pm 9.5
<i>N</i> -(6-ferrocenyl-2-naphthoyl)-L-Phe-OEt	95	95.6 \pm 7.6

3.3.3. *N*-(ferrocenyl)naphthoyl dipeptide derivatives

At the higher concentration of 10 μ M, the *N*-(ferrocenyl)naphthoyl dipeptide derivatives were found to strongly inhibit cell proliferation in the H1299 cell line (Table 3.5). The weakest anti-proliferative effect was observed for the *N*-(6-ferrocenyl-2-naphthoyl)-L-alanine-L-phenylalanine ethyl ester **102**, however, this compound still achieved an appreciable level of cell inhibition (>50%). Six compounds in particular were shown to inhibit cell growth by almost 99%. Interestingly, none of these compounds contained either L-leucine or L-phenylalanine in the peptide chain. This indicates that although incorporation of bulkier amino acids is not completely detrimental to the anti-proliferative effect, the presence of the small, neutral α -amino acids glycine and L-alanine within the peptide chain is more favourable for biological activity.

The screen performed at the lower concentration of 1 μ M in the H1299 cell line identified two compounds that inhibited cell growth by more than 50%. *N*-(6-ferrocenyl-2-naphthoyl)-glycine-L-alanine ethyl ester **51** showed a strong anti-proliferative effect (~70% growth inhibition), whilst *N*-(6-ferrocenyl-2-naphthoyl)-glycine-glycine ethyl ester **96** demonstrated a remarkable anti-proliferative effect (~95% growth inhibition). In the preliminary *in vitro* study, *N*-(6-ferrocenyl-2-naphthoyl)-glycine-L-alanine ethyl ester **51**

was identified as the most active compound out of the six derivatives that were tested in the H1299 cell line. Thus, the results of this screen correlate well with the data obtained in the preliminary *in vitro* study.

Table 3.5 Percentage cell growth of H1299 cells in the presence of *N*-(ferrocenyl)naphthoyl dipeptide derivatives.

Compound	No.	10 μM	1 μM
<i>N</i> -(3-ferrocenyl-2-naphthoyl)-Gly-Gly-OEt	84	16.8 \pm 4.0	115.2 \pm 13.3
<i>N</i> -(3-ferrocenyl-2-naphthoyl)-Gly-L-Ala-OEt	85	0.4 \pm 0.8	74.6 \pm 15.2
<i>N</i> -(3-ferrocenyl-2-naphthoyl)-Gly-L-Leu-OEt	86	13.8 \pm 5.1	103.7 \pm 5.2
<i>N</i> -(3-ferrocenyl-2-naphthoyl)-Gly-L-Phe-OEt	87	4.7 \pm 2.8	101.3 \pm 11.3
<i>N</i> -(3-ferrocenyl-2-naphthoyl)-L-Ala-Gly-OEt	88	10.5 \pm 3.3	102.6 \pm 4.9
<i>N</i> -(3-ferrocenyl-2-naphthoyl)-L-Ala-L-Ala-OEt	89	0.9 \pm 0.8	86.5 \pm 14.3
<i>N</i> -(3-ferrocenyl-2-naphthoyl)-L-Ala-L-Leu-OEt	90	25.2 \pm 9.8	109 \pm 14.0
<i>N</i> -(3-ferrocenyl-2-naphthoyl)-L-Ala-L-Phe-OEt	91	11.3 \pm 2.8	97.6 \pm 12.2
<i>N</i> -(6-ferrocenyl-2-naphthoyl)-Gly-Gly-OEt	96	0.5 \pm 0.8	4.4 \pm 0.9
<i>N</i> -(6-ferrocenyl-2-naphthoyl)-Gly-L-Ala-OEt	51	0.4 \pm 0.7	31.3 \pm 12.1
<i>N</i> -(6-ferrocenyl-2-naphthoyl)-Gly-L-Leu-OEt	97	4.9 \pm 0.9	103.2 \pm 11.0
<i>N</i> -(6-ferrocenyl-2-naphthoyl)-Gly-L-Phe-OEt	98	16.2 \pm 5.3	102.9 \pm 22.2
<i>N</i> -(6-ferrocenyl-2-naphthoyl)-L-Ala-Gly-OEt	99	0.4 \pm 0.7	118.0 \pm 9.1
<i>N</i> -(6-ferrocenyl-2-naphthoyl)-L-Ala-L-Ala-OEt	100	0.1 \pm 0.6	85.8 \pm 5.7
<i>N</i> -(6-ferrocenyl-2-naphthoyl)-L-Ala-L-Leu-OEt	101	13.0 \pm 3.5	107.4 \pm 16.1
<i>N</i> -(6-ferrocenyl-2-naphthoyl)-L-Ala-L-Phe-OEt	102	40.7 \pm 8.0	98.8 \pm 10.9

As noted for the *N*-(ferrocenyl)naphthoyl amino acid derivatives, the Sk-Mel-28 cell line was more resistant than the H1299 cell line to treatment with the *N*-(ferrocenyl)naphthoyl dipeptide derivatives (Table 3.6). Only two *N*-(ferrocenyl)naphthoyl dipeptide derivatives were found to inhibit cell growth by more than 50% in the Sk-Mel-28 cell line. *N*-(6-ferrocenyl-2-naphthoyl)-glycine-L-alanine ethyl ester **51** showed the strongest anti-proliferative effect, with approximately 99% growth inhibition, whilst *N*-(6-ferrocenyl-2-

naphthoyl)-glycine-glycine ethyl ester **96** inhibited cell growth by approximately 80%. Thus, these two compounds display a remarkable anti-proliferative effect in both cell lines, and are clearly the most active compounds belonging to this series of *N*-(ferrocenyl)naphthoyl amino acid and dipeptide derivatives.

Table 3.6 Percentage cell growth of Sk-Mel-28 cells in the presence of *N*-(ferrocenyl)naphthoyl dipeptide derivatives.

Compound	No.	10 μM
<i>N</i> -(3-ferrocenyl-2-naphthoyl)-Gly-Gly-OEt	84	94.8 \pm 6.4
<i>N</i> -(3-ferrocenyl-2-naphthoyl)-Gly-L-Ala-OEt	85	42.0 \pm 21.8
<i>N</i> -(3-ferrocenyl-2-naphthoyl)-Gly-L-Leu-OEt	86	89.8 \pm 14.6
<i>N</i> -(3-ferrocenyl-2-naphthoyl)-Gly-L-Phe-OEt	87	87.3 \pm 18.3
<i>N</i> -(3-ferrocenyl-2-naphthoyl)-L-Ala-Gly-OEt	88	58.0 \pm 23.8
<i>N</i> -(3-ferrocenyl-2-naphthoyl)-L-Ala-L-Ala-OEt	89	62.3 \pm 29.4
<i>N</i> -(3-ferrocenyl-2-naphthoyl)-L-Ala-L-Leu-OEt	90	93.1 \pm 9.2
<i>N</i> -(3-ferrocenyl-2-naphthoyl)-L-Ala-L-Phe-OEt	91	97.4 \pm 8.8
<i>N</i> -(6-ferrocenyl-2-naphthoyl)-Gly-Gly-OEt	96	19.0 \pm 5.6
<i>N</i> -(6-ferrocenyl-2-naphthoyl)-Gly-L-Ala-OEt	51	0.7 \pm 0.8
<i>N</i> -(6-ferrocenyl-2-naphthoyl)-Gly-L-Leu-OEt	97	79.0 \pm 18.2
<i>N</i> -(6-ferrocenyl-2-naphthoyl)-Gly-L-Phe-OEt	98	95.4 \pm 10.7
<i>N</i> -(6-ferrocenyl-2-naphthoyl)-L-Ala-Gly-OEt	99	74.7 \pm 23.8
<i>N</i> -(6-ferrocenyl-2-naphthoyl)-L-Ala-L-Ala-OEt	100	55.9 \pm 34
<i>N</i> -(6-ferrocenyl-2-naphthoyl)-L-Ala-L-Leu-OEt	101	86.3 \pm 15.8
<i>N</i> -(6-ferrocenyl-2-naphthoyl)-L-Ala-L-Phe-OEt	102	102.6 \pm 3.9

3.3.4. IC₅₀ value determination

In the case of *N*-(6-ferrocenyl-2-naphthoyl)-glycine-L-alanine ethyl ester **51**, an IC₅₀ value of 1.3 \pm 0.1 μ M had been determined during the preliminary study in the H1299 cell line. Hence, further studies were conducted to determine the IC₅₀ value for *N*-(6-ferrocenyl-2-

naphthoyl)-glycine-glycine ethyl ester **96** in the H1299 cell line, and the IC₅₀ values for both compounds in the Sk-Mel-28 cell line. Thus, individual 96-well plates containing the appropriate cell line were treated with the test compound at appropriate concentration ranges. The cells were then incubated for 5-6 days, until cell confluency was reached. Cell survival was determined by performing the acid phosphatase assay. The IC₅₀ value for each compound was calculated using CalcuSyn software, and standard deviations have been calculated using data obtained from three independent experiments (Table 3.7).

An exceptional IC₅₀ value of 0.13 ± 0.02 μM was calculated for *N*-(6-ferrocenyl-2-naphthoyl)-glycine-glycine ethyl ester **96** in the H1299 cell line. Thus, the anti-proliferative effect of this compound is an order of magnitude greater than that of both *N*-(6-ferrocenyl-2-naphthoyl)-glycine-L-alanine ethyl ester **51** (1.3 ± 0.1 μM) and the platinum-based anti-cancer drug cisplatin **1** (1.4 ± 0.1 μM). Previous studies carried out in our laboratories determined an IC₅₀ value of 20 μM for *N*-{*ortho*-(ferrocenyl)-benzoyl}-glycine-glycine ethyl ester **105** in this cell line.⁹ Thus, in this instance, over a 150-fold improvement in biological activity has been achieved by replacing the benzoyl linker with the naphthoyl linker. This is an extremely encouraging finding; there is only one other ferrocenyl compound that has been reported recently in the literature to have a comparable IC₅₀ value (0.09 ± 0.01 μM) and this value was determined in the MDA-MB-231 breast cancer cell line.¹⁰

In the Sk-Mel-28 cell line, IC₅₀ values of 3.74 ± 0.37 μM and 1.10 ± 0.13 μM were calculated for *N*-(6-ferrocenyl-2-naphthoyl)-glycine-L-alanine ethyl ester **51** and *N*-(6-ferrocenyl-2-naphthoyl)-glycine-glycine ethyl ester **96**, respectively. Although the anti-proliferative effect of these compounds is not as strong in the Sk-Mel-28 cell line as in the H1299 cell line, these results are promising nonetheless, since metastatic melanoma is notoriously resistant to chemotherapeutic drugs.¹¹

Table 3.7 IC₅₀ values in the H1299 and Sk-Mel-28 cell lines.

Compound	No.	H1299 (μM)	Sk-Mel-28 (μM)
<i>N</i> -(6-ferrocenyl-2-naphthoyl)-Gly-Gly-OEt	96	0.13 ± 0.02	1.10 ± 0.13
<i>N</i> -(6-ferrocenyl-2-naphthoyl)-Gly-L-Ala-OEt	51	1.3 ± 0.1	3.74 ± 0.37

3.4. Structure-activity relationship of *N*-(ferrocenyl)naphthoyl amino acid and dipeptide derivatives

The *in vitro* biological data obtained for the *N*-(ferrocenyl)naphthoyl amino acid and dipeptide derivatives is fundamental in aiding the establishment of a SAR for these ferrocenyl-peptide bioconjugates. These *in vitro* studies have shown that the *N*-(ferrocenyl)naphthoyl amino acid and dipeptide derivatives exert a moderate to strong anti-proliferative effect in the H1299 and Sk-Mel-28 cell lines. In the H1299 cell line, these derivatives are more effective at inhibiting cell proliferation than the corresponding *N*-(ferrocenyl)benzoyl analogues. Thus, employing a naphthalene ring as the conjugated linker between the redox active ferrocene unit and the peptide chain enhances the anti-proliferative effect of the ferrocenyl-peptide bioconjugates. This improvement in biological activity may be due to an improvement in conjugation with the redox active ferrocene unit or the increase in lipophilicity associated with the introduction of the naphthalene ring.

The intermediate compounds methyl 3-ferrocenylnaphthalene-2-carboxylate **71** and methyl 6-ferrocenylnaphthalene-2-carboxylate **74**, showed almost no anti-proliferative effect in either cell line. The same observations have been made for the *N*-(ferrocenyl)benzoyl dipeptide esters in the H1299 cell line.⁵ Thus, the peptide chain of these novel ferrocenyl-peptide bioconjugates is essential for biological activity.

N-(6-ferrocenyl-2-naphthoyl)-glycine-L-alanine ethyl ester **51** and *N*-(6-ferrocenyl-2-naphthoyl)-glycine-glycine ethyl ester **96** have been identified as the most potent ferrocenyl-peptide bioconjugates, in both the H1299 and Sk-Mel-28 cell lines. Evidently, these two *N*-(6-ferrocenyl-2-naphthoyl) dipeptide derivatives are more effective than the corresponding *N*-(3-ferrocenyl-2-naphthoyl) dipeptide analogues at inhibiting cell proliferation. The superior biological effect of the *N*-(6-ferrocenyl-2-naphthoyl) dipeptide derivatives may be a consequence, at least in part, of the presence of more effective conjugation between the ferrocene and naphthalene units, compared to the *N*-(3-ferrocenyl-2-naphthoyl) dipeptide derivatives. In relation to the dipeptide chain, the incorporation of the α -amino acids L-leucine and L-phenylalanine was not detrimental to the anti-proliferative effect. However, as illustrated by the two most potent members of this series, compounds that contained only the small neutral α -amino acids glycine and L-alanine

within the dipeptide chain produced a stronger anti-proliferative effect. This anti-proliferative effect is strongest when glycine is the *N*-terminal α -amino acid.

In the case of the *N*-(ferrocenyl)naphthoyl amino acid derivatives, the situation is not so clear cut. Substitution at the α -carbon of the amino acid is not beneficial to the activity of the *N*-(6-ferrocenyl-2-naphthoyl) amino acid derivatives. For the *N*-(3-ferrocenyl-2-naphthoyl) amino acid derivatives, the anti-proliferative effect is greatest when chiral α -amino acids with bulky side chains are employed. Also, *N*-(3-ferrocenyl-2-naphthoyl)-L-phenylalanine ethyl ester **83** inhibits cell growth in the H1299 cell line to a greater extent than some of the *N*-(3-ferrocenyl-2-naphthoyl) dipeptide derivatives. This is not the case for the *N*-(6-ferrocenyl-2-naphthoyl) amino acid derivatives; *N*-(6-ferrocenyl-2-naphthoyl)-glycine-L-alanine ethyl ester **51** and *N*-(6-ferrocenyl-2-naphthoyl)-glycine-glycine ethyl ester **96** clearly exert a stronger anti-proliferative effect than the *N*-(6-ferrocenyl-2-naphthoyl)-glycine ethyl ester **92**. This improvement in biological activity for *N*-(3-ferrocenyl-2-naphthoyl)-L-leucine ethyl ester **82** and *N*-(3-ferrocenyl-2-naphthoyl)-L-phenylalanine ethyl ester **83** is not yet fully understood however, it is possible that conformation adopted by these compounds as a result of steric hindrance, alters the molecular properties in a way that is beneficial to the activity.

In summary, for these ferrocenyl-peptide bioconjugates, the greatest anti-proliferative effect is achieved when:

- (i) A naphthalene unit is employed as the conjugated linker.
- (ii) The ferrocene unit is substituted in the 6-position of the naphthalene linker.
- (iii) A dipeptide chain is present.
- (iv) Glycine is the *N*-terminal amino acid in the dipeptide chain.
- (v) Either glycine or L-alanine is the *C*-terminal amino acid in the dipeptide chain.

Figure 3.6 illustrates the main features of the SAR for the *N*-(ferrocenyl)naphthoyl amino acid and dipeptide derivatives.

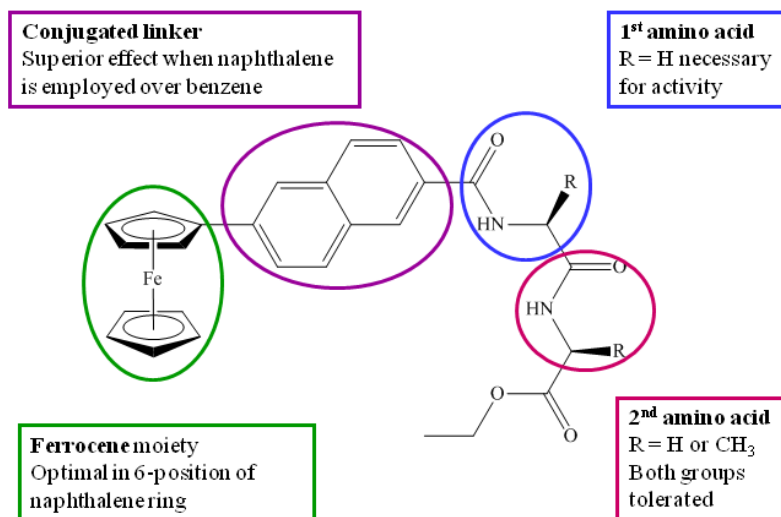


Figure 3.6 Structure-activity relationship (SAR) for the *N*-(ferrocenyl)naphthoyl amino acid and dipeptide derivatives.

3.5. Conclusions

As part of a primary SAR study of ferrocenyl-peptide bioconjugates, a series of *N*-(ferrocenyl)naphthoyl amino acid and dipeptide derivatives were evaluated for *in vitro* anti-proliferative effect in lung cancer (H1299) and melanoma (Sk-Mel-28) cell lines. These novel ferrocenyl-peptide bioconjugates exhibited a strong anti-proliferative effect in the H1299 cell line, whilst the Sk-Mel-28 cells were slightly more resistant to these compounds. *N*-(6-ferrocenyl-2-naphthoyl)-glycine-L-alanine ethyl ester **51** and *N*-(6-ferrocenyl-2-naphthoyl)-glycine-glycine ethyl ester **96** have been identified as the most potent ferrocenyl-peptide bioconjugates. In particular, a remarkable inhibitory effect on cell proliferation was observed for *N*-(6-ferrocenyl-2-naphthoyl)-glycine-glycine ethyl ester **96** in the H1299 cell line; the IC₅₀ value of this compound lies in the nanomolar range. Thus, these two compounds show great promise as potential lead compounds in the development of novel bioorganometallic anti-cancer agents.

It has been clearly demonstrated in this primary SAR study that employing a naphthalene ring as the conjugated linker between the redox active ferrocene unit and the peptide chain enhances the anti-proliferative effect of the ferrocenyl-peptide bioconjugates relative to the

N-(ferrocenyl)benzoyl peptide derivatives. In addition, the incorporation of the α -amino acids L-leucine and L-phenylalanine, into the peptide chain was shown in some cases to be beneficial to the *in vitro* biological activity. However, as illustrated by the two most potent ferrocenyl-peptide bioconjugates, the presence of only the small, neutral α -amino acids glycine and L-alanine within the peptide chain produces the strongest anti-proliferative effect.

Materials and Methods

Cells and cell culture

Cell culture media, supplements and related solutions were purchased from Sigma-Aldrich (Dublin, Ireland) unless otherwise stated. The H1299 cell line was obtained from the American Type Culture Collection (ATCC) and the Sk-Mel-28 cell line was obtained from the Department of Developmental Therapeutics, National Cancer Institute (NCI). Cell lines were grown as a monolayer culture at 37°C, under a humidified atmosphere of 95% O₂ and 5% CO₂ in 75 cm² flasks. Both cell lines were grown in RPMI-1640 medium supplemented with 10% foetal calf serum (FCS). Stock solutions of the ferrocenyl compounds (10 mM) were prepared in dimethyl sulfoxide (Sigma-Aldrich).

All cell culture work was carried out in a class II laminar airflow cabinet (Holten LaminAir). All experiments involving cytotoxic compounds were conducted in a cytoguard laminar airflow cabinet (Holten LaminAir Maxisafe). Before and after use the laminar airflow cabinet was cleaned with 70% industrial methylated spirits (IMS). Any items brought into the cabinet were also swabbed with IMS. Only one cell line was used in the laminar airflow cabinet at a time and upon completion of work with any given cell line the laminar airflow cabinet was allowed to clear for at least 15 minutes before use. This was to eliminate any possibility of cross-contamination between cell lines. The cabinets were cleaned weekly with industrial disinfectants (Virkon or TEGO). These disinfectants were alternated fortnightly. Cells were fed with fresh media or subcultured every 2-3 days in order to maintain active cell growth.

Sub-culturing of cell lines

Media and trypsin/EDTA solution (0.25% trypsin (Gibco), 0.01% EDTA (Sigma-Aldrich) solution in PBS) were incubated at 37 °C for 20 min in a water bath. The cell culture medium was removed from the tissue culture flask and discarded into a sterile bottle. The flask was then rinsed out with trypsin/EDTA solution (2 ml) to ensure the removal of any residual media. Fresh trypsin/EDTA solution (3 ml) was then added to the flask and the flask was incubated at 37 °C for the required period of time (dependant of each cell line)

until all cells were detached from the inside surface of the tissue culture flask. The trypsin was deactivated by adding an equal volume of complete media to the flask. The cell suspension was removed from the flask and placed in a sterile universal container (Sterilin, 128a) and centrifuged at 1000 rpm for 5 minutes. The supernatant was then discarded from the universal container and the pellet was suspended in complete medium. A cell count was performed. An aliquot of cells was then used to re-seed a flask at the required density, topping the flask up with fresh medium.

Assessment of cell number

Cells were trypsinised, pelleted and resuspended in media. A 10 μ l aliquot of the cell suspension was then applied to the chamber of a glass coverslip enclosed haemocytometer. Cells in the 16 squares of the four grids of the chamber were counted. The average cell number, per 16 squares, was multiplied by a factor of 10⁴ and the relevant dilution factor to determine the number of cells per ml in the original cell suspension.

Cryopreservation of cells

Cells for cryopreservation were harvested in the log phase of growth and counted as described above. Cell pellets were resuspended in a suitable volume of warm FCS. An equal volume of a 10% DMSO solution in FCS was added dropwise to the cell suspension. A total volume of 1 ml of this suspension was then placed in a cryovial (Greiner). These vials were then placed in the -20 °C freezer for 20 minutes and then in the -80 °C freezer overnight. Following this period the vials were removed from the -80 °C freezer and transferred to the liquid nitrogen tanks for storage (-196 °C).

Thawing of cryopreserved cells

A volume of 10 ml of fresh warmed growth media and 1 ml of warm FCS were added to a sterile T75 cm² tissue culture flask. The cryopreserved cells were removed from the liquid nitrogen tank and thawed rapidly at 37 °C. The cells were removed from the vials and transferred to the aliquoted media. Following incubation at 37 °C for several hours, the thawed cells were fed with a suitable volume of fresh growth media.

***In vitro* proliferation assays**

Adherent cells in the exponential phase of growth were harvested by trypsinisation and a cell suspension of 1×10^4 cells/ml was prepared in fresh culture medium. The cell suspension (100 μ l) was added to a flat bottom 96-well plate (Costar, 3599), the plate was agitated gently in order to ensure even dispersion of cells over the surface of the wells, and then cells were incubated for an initial 24 hours in a 37 °C, 5% CO₂ incubator, to allow cell attachment to the wells. A 10 μ M stock solution of the test sample was prepared in dimethyl sulfoxide; dilute solutions of the test sample were prepared at 2X final concentration by spiking the cell culture medium with a calculated amount of the stock solution. 100 μ l aliquot of each dilute solution was added to each well of the plate, the plate was gently agitated, and then incubated at 37 °C, 5% CO₂ for 5-6 days, until cell confluency reached 80-90%. Assessment of cell survival in the presence of the test sample was determined by the acid phosphatase assay. For the comprehensive screen, cell growth % in the presence of each test sample was calculated relative to the DMSO control cells. For the preliminary study, the concentration of drug that causes 50% growth inhibition (the IC₅₀ value) was determined by plotting % survival of cells (relative to the control cells) against concentration of the test sample. In subsequent studies, the IC₅₀ value was determined using CalcuSyn (Biosoft, UK).

Acid phosphatase assay

Following an incubation period of 5-6 days, drug media was removed from the 96-well plate and each well was washed with PBS (100 μ l). This was then removed and 100 μ l of freshly prepared phosphatase substrate (10 mM *p*-nitrophenol phosphate in 0.1 M sodium acetate, 0.1% triton X-100, pH 5.5) was added to each well. The plate was wrapped in tinfoil and incubated in the dark at 37 °C for 2 h. The enzymatic reaction was stopped by the addition of 1 M NaOH (50 μ l) to each well. The absorbance of each well was read in a dual beam plate reader (Synergy HT, Bio-Tek, USA) at 405 nm with a reference wavelength of 620 nm.

References

1. *Essential cell biology : a practical approach* J. Davey and M. Lord, Eds.; Oxford University Press, **2003**.
2. *Animal Cell Culture Techniques*; M. Clynes, Ed.; Springer-Verlag, **1998**.
3. R. H. Shoemaker, *Nature Reviews Cancer*, 2006, **6**, 813-823.
4. A. Martin and M. Clynes, *In Vitro Cellular & Developmental Biology*, 1991, **27A**, 183-184.
5. A. J. Corry, N. O'Donovan, Á. Mooney, D. O'Sullivan, D. K. Rai and P. T. M. Kenny, *Journal of Organometallic Chemistry*, 2009, **694**, 880-885.
6. L. Breen, L. Murphy, J. Keenan and M. Clynes, *Toxicology in Vitro*, 2008, **22**, 1234-1241.
7. T. E. Stinchcombe and M. A. Socinski, *Proc Am Thorac Soc*, 2009, **6**, 233-241.
8. G. Giaccone, *Drugs*, 2000, **59**, 9-17.
9. A. J. Corry, A. Mooney, D. O'Sullivan and P. T. M. Kenny, *Inorganica Chimica Acta*, 2009, **362**, 2957-2961.
10. D. Plazuk, A. Vessieres, E. A. Hillard, O. Buriez, E. Labbe, P. Pigeon, M. A. Plamont, C. Amatore, J. Zakrzewski and G. Jaouen, *Journal of Medicinal Chemistry*, 2009, **52**, 4964-4967.
11. A. J. Eustace, J. Crown, M. Clynes and N. O'Donovan, *Journal of Translational Medicine*, 2008, **6**, 53-64.

Chapter 4

Synthesis and structural characterisation of *N*-naphthoyl dipeptide derivatives and *N*-(ferrocenyl)naphthoyl amino acid and dipeptide derivatives which contain unusual amino acids

4.1. Introduction

A preliminary structure-activity relationship (SAR) study of novel ferrocenyl-peptide bioconjugates has demonstrated that *N*-(ferrocenyl)naphthoyl amino acid and dipeptide derivatives are effective at inhibiting the *in vitro* proliferation of lung cancer (H1299) and melanoma (Sk-Mel-28) cell lines. In particular, two ferrocenyl-peptide bioconjugates were identified as having an exceptional inhibitory effect in both cell lines: *N*-(6-ferrocenyl-2-naphthoyl)-glycine-L-alanine ethyl ester **51** and *N*-(6-ferrocenyl-2-naphthoyl)-glycine-glycine ethyl ester **96**. Since the introduction of a naphthoyl linker between the redox active ferrocene unit and the peptide chain has been shown to dramatically enhance the anti-proliferative effect of the ferrocenyl-peptide bioconjugates it was decided to retain this unit for further studies. Thus, a secondary SAR study was undertaken, this time focussing on varying the peptide chain in the hope that the biological activity of the two potential lead compounds could be optimised. Since *N*-benzoyl peptides have been shown to have biological activity,¹ the synthesis of *N*-naphthoyl analogues of the two most active derivatives was also undertaken to determine whether the redox active ferrocenyl unit of these derivatives contributes toward the observed biological effect.

Isosterism is a strategy commonly employed in lead optimisation, whereby specific functional groups within a molecule are replaced by another group that presents a comparable electronic and steric arrangement. Figure 4.1 illustrates the known isosteric replacements for the amide bond.² Perhaps the most well-established modification is *N*-methylation. This is a strategy widely used by scientists to alter pharmacological properties of peptides, such as metabolic stability, selectivity, potency and bioavailability.³ There are also prominent examples of naturally occurring *N*-methylated cyclic peptides that are biologically active, of which the immunosuppressant drug cyclosporin A is perhaps the most well known.⁴ The *N*-methylated derivatives can be readily prepared by incorporating

sarcosine (*N*-methyl-glycine) and *N*-methyl-L-alanine into the peptide chain of the *N*-(ferrocenyl)naphthoyl dipeptide derivatives. The inclusion of *N*-methyl amino acids within the dipeptide chain may also yield information concerning the importance of hydrogen bond formation for biological activity, since the presence of an *N*-methyl group blocks the ability of the nitrogen atom to act as a hydrogen bond donor.

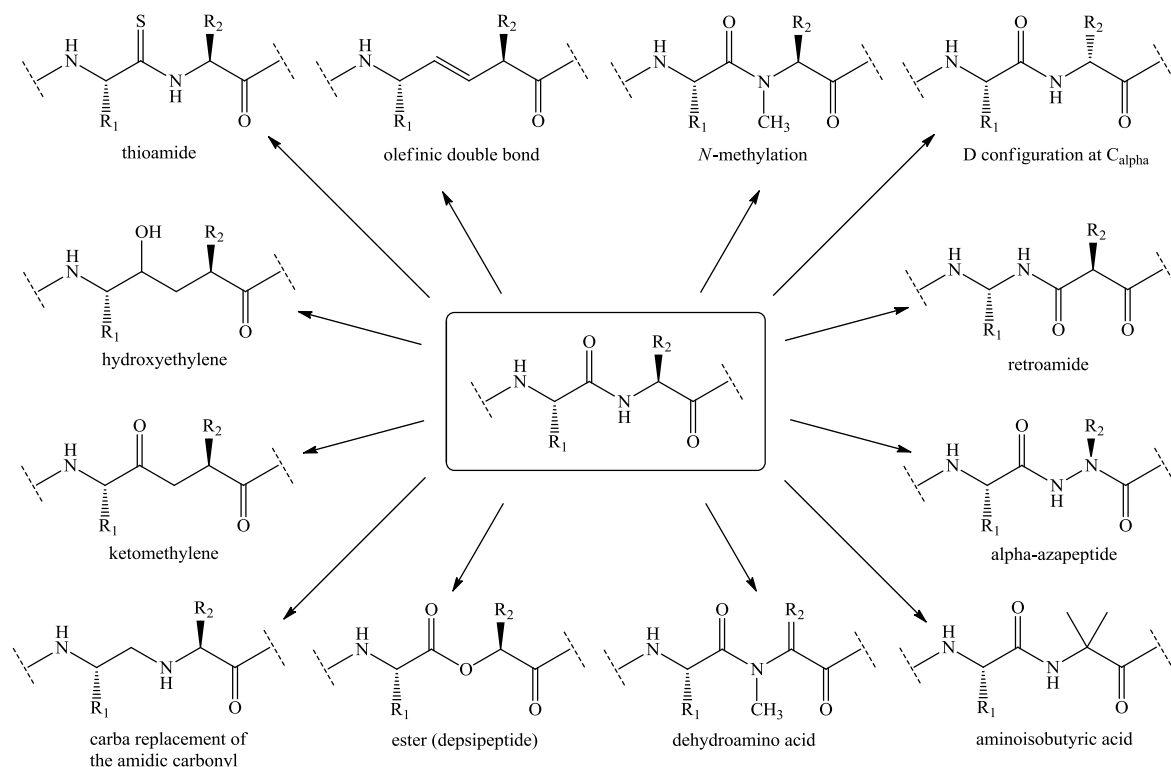


Figure 4.1 Established isosteric replacements for amide bonds.²

Another frequently used modification is to invert the stereochemistry of the α -carbon of the chiral α -amino acids. This is easily achieved by incorporating D- α -amino acids into the peptide chain, in place of the naturally occurring L- α -amino acids. Previous studies of the *N*-(ferrocenyl)benzoyl peptide derivatives have indicated that the amino acids β -alanine and γ -aminobutyric acid could be of use as a potential isosteric replacement for glycine in the peptide chain.⁵ Thus, the synthesis of a series of analogues of *N*-(6-ferrocenyl-2-naphthoyl)-glycine-glycine ethyl ester **96**, which incorporate these two amino acids in the peptide chain, was undertaken to investigate this option further.

In relation to the *N*-(ferrocenyl)naphthoyl amino acid derivatives, it was noted that *N*-(6-ferrocenyl)-glycine ethyl ester **92** exhibited a significant anti-proliferative effect in the Sk-Mel-28 cell line but did not inhibit cell proliferation in the H1299 cell line, at the lower concentration of 1 μ M. The inclusion of an additional glycine moiety to give *N*-(6-ferrocenyl-2-naphthoyl)-glycine-glycine ethyl ester **96** resulted in a dramatic increase in anti-proliferative effect. This striking difference in biological activity indicates that the length of the “peptide” chain has some influence on the anti-proliferative effect of these compounds. In order to investigate this effect further, the preparation of a homologous series of *N*-(ferrocenyl)naphthoyl amino acid derivatives was undertaken using the achiral amino acids β -alanine, γ -aminobutyric acid and δ -amino-n-valeric acid. These non-essential amino acids contain a varying number of methylene units between the *N*-terminal amine and the *C*-terminal carboxyl functional groups. The glycine ethyl ester chain represents the shortest chain in this homologous series, whilst the δ -amino-n-valeric acid ethyl ester chain is the longest. The β -alanine ethyl ester and γ -aminobutyric acid ethyl ester derivatives have an intermediate chain length.

4.2. Protection of the amino terminus of an amino acid

The synthesis of dipeptide molecules requires the protection of the *N*-terminus of one amino acid and protection of the *C*-terminus of another prior to a coupling reaction between the two. Therefore, when both the amino and carboxyl amino acids are coupled, only the required dipeptide is isolated.

Since the amino group is both basic and nucleophilic, it is important to suppress these characteristics. This can be achieved by draining the electron density away and/or by concealing it by using bulky groups as a barrier of steric hindrance. It must also be possible to remove the protecting group easily under mild conditions so as not to damage other potentially vulnerable parts of the molecule.⁶

A variety of protecting groups have been employed for the protection of the *N*-terminal and are usually selected so as they are orthogonal to the rest of the molecule (*i.e.* can be added or removed without affecting the other susceptible functional groups).

4.2.1. *t*-Butoxycarbonyl (Boc) protecting group

The *tert*-butoxycarbonyl group is probably the most universally used amino protecting group. This can be explained by the fact that it is easy to use, gives good yields and does not cause racemisation. The standard method by which the Boc group is introduced onto the peptide is via its anhydride (Figure 4.2).

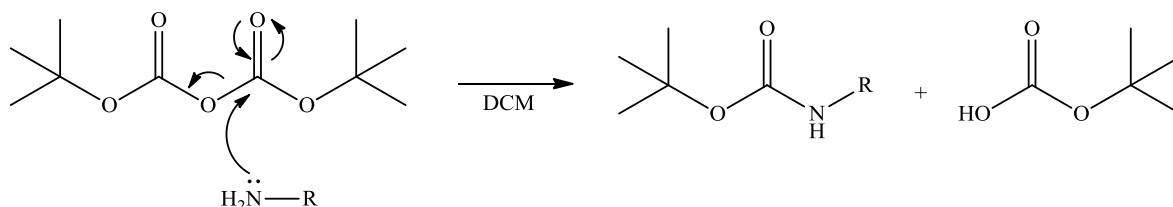


Figure 4.2 The introduction of the Boc protecting group *via* the di-*t*-butyl dicarbonate derivative.

The Boc group is stable towards catalytic hydrogenolysis, basic and nucleophilic reagents but is acid labile. Boc removal is conveniently carried out by dissolution in TFA at ambient temperature and proceeds by unimolecular fission, facilitated by the stability of the carbonium ion produced (Figure 4.3).⁶

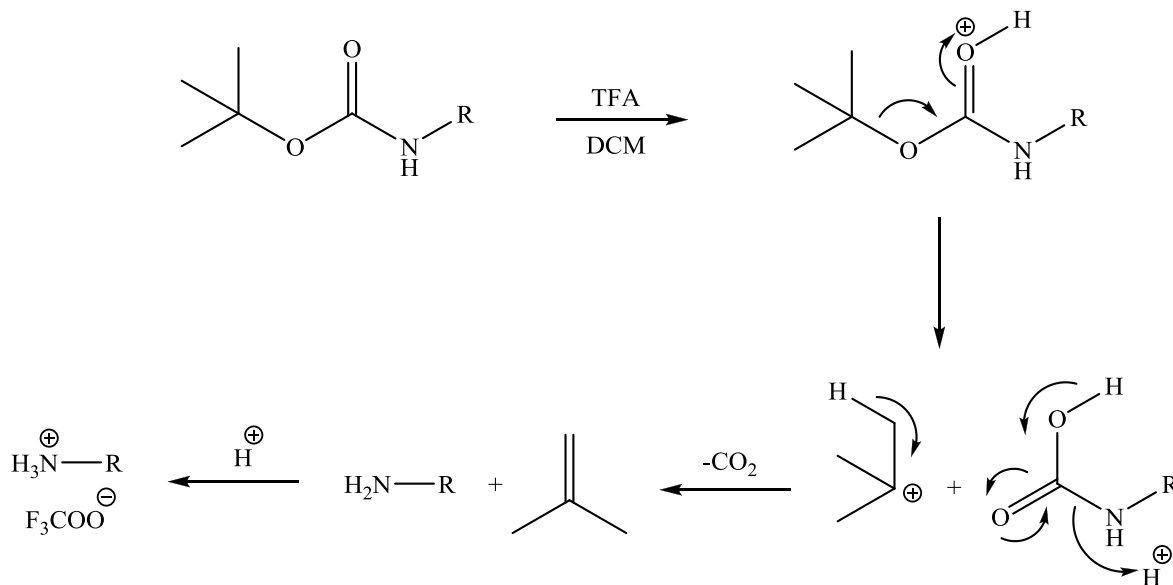
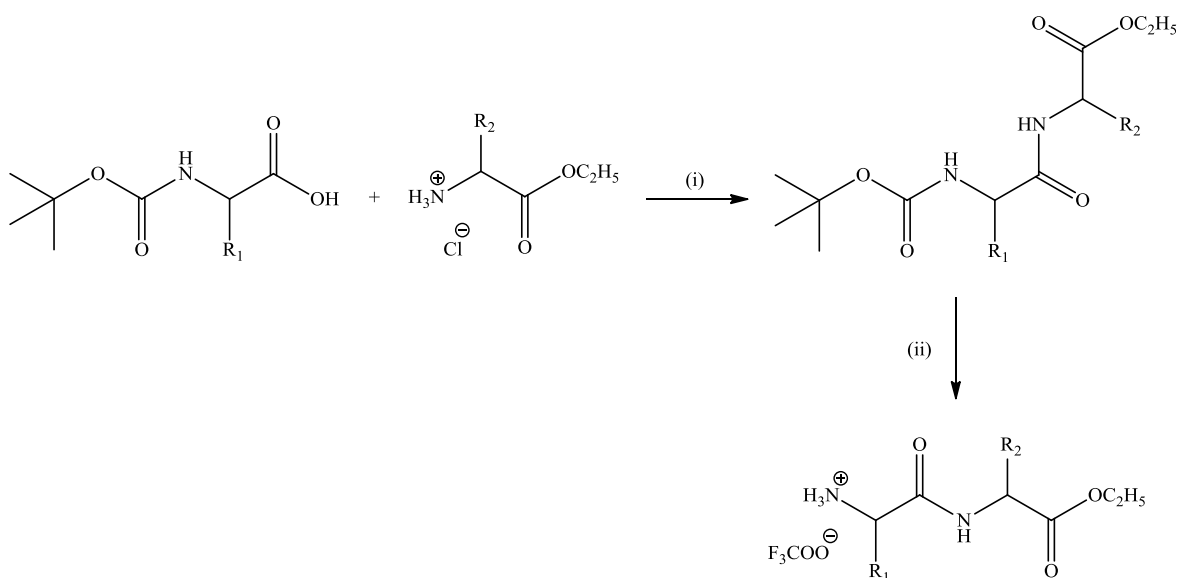


Figure 4.3 The removal of the Boc protecting group using TFA.

4.3. The synthesis of *N*-naphthoyl dipeptide derivatives and *N*-(ferrocenyl)naphthoyl amino acid and dipeptide derivatives which contain unusual amino acids

4.3.1. *N*-(ferrocenyl)naphthoyl dipeptide derivatives

The dipeptide moieties required for this study are not commercially available and thus they were prepared by conventional peptide chemistry. Equimolar amounts of the Boc protected amino acids were reacted with amino acid ethyl ester hydrochloride salts, *via* the EDC/HOBt peptide coupling protocol (Scheme 4.1). Upon completion of this reaction, the dipeptide was washed with water and purified by column chromatography. In each case the eluant was a 1:1 hexane:ethyl acetate mixture. Yields following purification were moderate to good and ranged from 38-73% (Table 4.1). Subsequent removal of the Boc protecting group using trifluoroacetic acid (TFA, Scheme 4.1) allowed for reaction at the *N*-terminus with 3-ferrocenylnaphthalene-2-carboxylic acid and 6-ferrocenylnaphthalene-2-carboxylic acid to yield the required *N*-(ferrocenyl)naphthoyl dipeptide derivatives.



Scheme 4.1 The synthesis and deprotection of Boc protected dipeptide ethyl esters: (i) EDC, HOBt, Et₃N; (ii) TFA, DCM.

Table 4.1 Percentage yields for Boc protected dipeptide ethyl esters.

Compound	Number	% Yield
Boc-glycine-sarcosine-OEt	106	70
Boc-sarcosine-glycine-OEt	107	56
Boc-sarcosine-sarcosine-OEt	108	54
Boc-glycine- <i>N</i> -Methyl-L-alanine-OEt	109	38
Boc-glycine-D-alanine-OEt	110	73
Boc-glycine- β -alanine-OEt	111	71
Boc- β -alanine-glycine-OEt	112	70
Boc-glycine- γ -aminobutyric acid-OEt	113	46
Boc- γ -aminobutyric acid-glycine-OEt	114	68

The crude *N*-(ferrocenyl)naphthoyl dipeptide derivatives were purified in the usual manner by column chromatography employing a mixture of hexane and ethyl acetate as eluant. All compounds gave spectroscopic and analytical data in accordance with their proposed structures. Yields were found to vary according to the nature of the *N*-terminal of the reacting amino acid. In particular, yields for reactions that involved the coupling of secondary amino acids to ferrocenyl naphthalene-2-carboxylic acid were much lower compared to those that involved the coupling of primary amino acids *e.g.* the yield of *N*-(6-ferrocenyl-2-naphthoyl)-sarcosine-sarcosine ethyl ester **121** was 12%, compared to 43% for *N*-(6-ferrocenyl-2-naphthoyl)-glycine-sarcosine ethyl ester **119**. Such low yields may be due to the spontaneous formation of diketopiperazine upon removal of the Boc protecting group from the *N*-terminal amino acid (Figure 4.4).⁷ Table 4.2 summarises the yields of the *N*-(ferrocenyl)naphthoyl dipeptide derivatives that have been prepared.

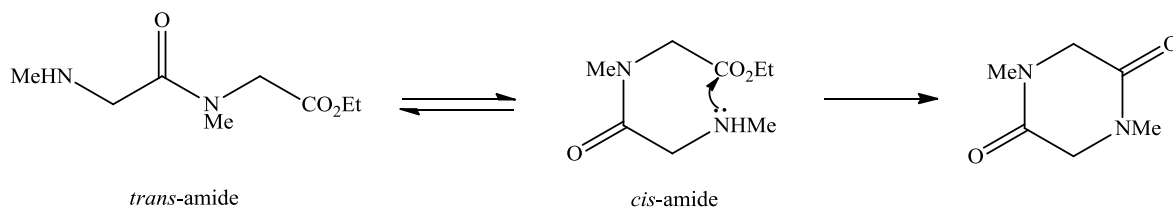
**Figure 4.4** Spontaneous diketopiperazine cyclisation of sarcosine-sarcosine ethyl ester.

Table 4.2 Percentage yields for *N*-(ferrocenyl)naphthoyl dipeptide derivatives.

Compound	Number	% Yield
<i>N</i> -(3-ferrocenyl-2-naphthoyl)-Gly-Sar-OEt	115	33
<i>N</i> -(3-ferrocenyl-2-naphthoyl)-Sar-Gly-OEt	116	20
<i>N</i> -(3-ferrocenyl-2-naphthoyl)-Sar-Sar-OEt	117	31
<i>N</i> -(3-ferrocenyl-2-naphthoyl)-Gly- <i>N</i> -Me-L-Ala-OEt	118	38
<i>N</i> -(6-ferrocenyl-2-naphthoyl)-Gly-Sar-OEt	119	43
<i>N</i> -(6-ferrocenyl-2-naphthoyl)-Sar-Gly-OEt	120	35
<i>N</i> -(6-ferrocenyl-2-naphthoyl)-Sar-Sar-OEt	121	12
<i>N</i> -(6-ferrocenyl-2-naphthoyl)-Gly- <i>N</i> -Me-L-Ala-OEt	122	9
<i>N</i> -(3-ferrocenyl-2-naphthoyl)-Gly-D-Ala-OEt	123	41
<i>N</i> -(6-ferrocenyl-2-naphthoyl)-Gly-D-Ala-OEt	124	41
<i>N</i> -(3-ferrocenyl-2-naphthoyl)-Gly- β -Ala-OEt	125	30
<i>N</i> -(3-ferrocenyl-2-naphthoyl)- β -Ala-Gly-OEt	126	59
<i>N</i> -(3-ferrocenyl-2-naphthoyl)-Gly-GABA-OEt	127	40
<i>N</i> -(3-ferrocenyl-2-naphthoyl)-GABA-Gly-OEt	128	53
<i>N</i> -(6-ferrocenyl-2-naphthoyl)-Gly- β -Ala-OEt	129	43
<i>N</i> -(6-ferrocenyl-2-naphthoyl)- β -Ala-Gly-OEt	130	34
<i>N</i> -(6-ferrocenyl-2-naphthoyl)-Gly-GABA-OEt	131	38
<i>N</i> -(6-ferrocenyl-2-naphthoyl)-GABA-Gly-OEt	132	27

4.3.2. *N*-naphthoyl dipeptide derivatives and *N*-(ferrocenyl)naphthoyl amino acid derivatives

The *N*-naphthoyl dipeptide derivatives were synthesised by the condensation of 2-naphthoic acid with glycine-glycine ethyl ester and glycine-L-alanine ethyl ester using the EDC/HOBt peptide coupling protocol. The *N*-(ferrocenyl)naphthoyl amino acid derivatives were similarly prepared by the condensation of 3-ferrocenylnaphthalene-2-carboxylic acid and 6-ferrocenylnaphthalene-2-carboxylic acid with the amino acid ethyl esters of β -alanine, γ -aminobutyric acid and δ -amino-n-valeric acid. Crude *N*-naphthoyl dipeptide derivatives and

N-(ferrocenyl)naphthoyl amino acid derivatives were purified by column chromatography, using a mixture of hexane and ethyl acetate as the eluant. All compounds gave spectroscopic and analytical data in accordance with their proposed structures. Yields were found to vary according to the substitution pattern around the naphthoyl linker, *e.g.* the yields were higher for the *N*-(6-ferrocenyl-2-naphthoyl) amino acid derivatives (46-81%) compared to the *N*-(3-ferrocenyl-2-naphthoyl) amino acid derivatives (35-40%). This disparity is due to steric hindrance around the carboxylic acid functionality in the *N*-(3-ferrocenyl-2-naphthoyl) series, due to the presence of the bulky ferrocenyl group in the *ortho*-position. Table 4.3 summarises the yields of the *N*-naphthoyl dipeptide derivatives and *N*-(ferrocenyl)naphthoyl amino acid derivatives.

Table 4.3 Percentage yields for *N*-naphthoyl dipeptide derivatives and *N*-(ferrocenyl)naphthoyl amino acid derivatives.

Compound	Number	% Yield
<i>N</i> -(2-naphthoyl)-Gly-Gly-OEt	133	89
<i>N</i> -(2-naphthoyl)-Gly-L-Ala-OEt	134	52
<i>N</i> -(3-ferrocenyl-2-naphthoyl)- β -Ala-OEt	135	40
<i>N</i> -(3-ferrocenyl-2-naphthoyl)-GABA-OEt	136	36
<i>N</i> -(3-ferrocenyl-2-naphthoyl)- δ -Ava-OEt	137	35
<i>N</i> -(6-ferrocenyl-2-naphthoyl)- β -Ala-OEt	138	64
<i>N</i> -(6-ferrocenyl-2-naphthoyl)-GABA-OEt	139	81
<i>N</i> -(6-ferrocenyl-2-naphthoyl)- δ -Ava-OEt	140	46

4.4. ^1H and ^{13}C NMR studies of *N*-(ferrocenyl)naphthoyl dipeptide derivatives which contain *N*-methyl amino acids

^1H and ^{13}C NMR spectra were obtained for the *N*-(ferrocenyl)naphthoyl dipeptide derivatives which contain *N*-methyl amino acids in $\text{DMSO-}d_6$. The presence of either one or two *N*-methyl amino acids within the peptide chain of these compounds was found to have a strong influence on the appearance of these spectra. Signal multiplicities and/or broad signals were observed in the ^1H and ^{13}C NMR spectra for either some or all resonating nuclei, depending on the particular compound in question. These observations have been attributed to the presence of rotamers in solution, which arise from *cis/trans* isomerisation about the tertiary amide bond.

The amide bond is characterised by short C-N bond lengths, co-planarity and restricted rotation about the C-N bond (Figure 4.5).⁸ The partial double-bond character of the C-N bond causes restrictions in the number of energy minima in amide bond torsion (dihedral angle ω). The amide bond possesses just two minimum-energy structures: the geometric isomers at the angle $\omega \approx 0^\circ$ (*cis*) and $\omega \approx 180^\circ$ (*trans*).⁹

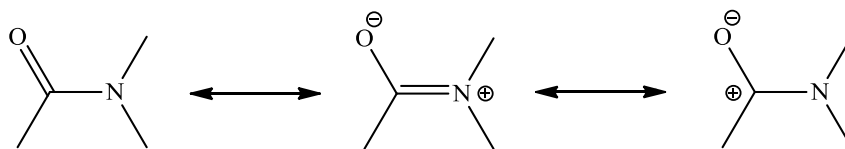


Figure 4.5 Canonical structures of the amide bond.

In terms of thermodynamics, the *trans*-isomer of a secondary amide bond is more stable than the *cis*-isomer, due to the absence of steric hindrance of the groups flanking the C-N bond when the *trans* configuration is adopted. For this reason, the *cis*-isomer of secondary amides is present in solution only at very low concentrations (~1%).⁸ In contrast, tertiary amides isomerise far more readily between *cis* and *trans* conformations, since both conformers have similar steric strain.

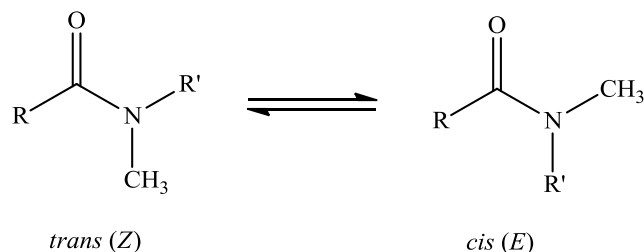


Figure 4.6 Inter-conversion between the *trans* ($\omega \approx 180^\circ$) and *cis* ($\omega \approx 0^\circ$) configurations of a tertiary amide bond.

The effect of the presence of *cis* and *trans* isomers on NMR spectra depends on the lifetime of each rotameric state. Using the uncertainty principle, the lower limit for the lifetime (t) is $t\delta\nu \approx 1/2\pi$, where $\delta\nu$ is the difference in frequency between the two signals in Hz. If t shows a slow interconversion rate between the two states, two sets of distinguishable signals will be observed. A rapid exchange between the two states gives a low t value and only a single peak appears. At an intermediate value for t , the two peaks are indistinguishable leading to the observation of broad peaks.

4.4.1. ^1H NMR studies of *N*-(ferrocenyl)naphthoyl dipeptide derivatives which contain *N*-methyl amino acids

The interpretation of the ^1H NMR spectra obtained for the *N*-(ferrocenyl)naphthoyl dipeptide derivatives which contain *N*-methyl amino acids was significantly hampered by the presence of different rotamers in solution. In cases where both amino acids in the dipeptide chain are *N*-methylated, *cis/trans* isomerisation can result in the presence of up to four different rotameric species. Signal multiplicity in the ^1H NMR spectra of these *N*-(ferrocenyl)naphthoyl dipeptide derivatives varies according to the naphthoyl linker employed and the location of the *N*-methyl amino acid in the dipeptide chain. In the case of *N*-(6-ferrocenyl-2-naphthoyl)-sarcosine-glycine ethyl ester **120**, the only indications of isomerisation are the distortion of peaks appearing between δ 3.96 and δ 4.26 and the appearance of two broad singlets at δ 8.53 and δ 8.61, which together integrate for one proton and correspond to the amide N-H of the glycine residue. These observations suggest

that any alteration in chemical shift due to isomerisation is restricted to the dipeptide chain; the remainder of the molecule is unaffected. In contrast, signal multiplicities are observed for every signal within the ^1H NMR spectrum of *N*-(3-ferrocenyl-2-naphthoyl)-sarcosine-glycine ethyl ester **116**.

The most informative region of the ^1H NMR spectra of these *N*-(ferrocenyl)naphthoyl dipeptide derivatives is from δ 2.60-3.15, where the *N*-methyl protons are the only nuclei to come into resonance. Thus, the number and type of signals appearing in this region are indicative of the number of rotamers present in solution. For example, the ^1H NMR spectrum of *N*-(3-ferrocenyl-2-naphthoyl)-glycine-sarcosine ethyl ester **115** shows two sharp signals at δ 2.90 and δ 3.11, which together integrate for 3 protons and indicate the presence of two rotamers. In the case of *N*-(6-ferrocenyl-2-naphthoyl)-glycine-sarcosine ethyl ester **119**, two sharp signals appear at δ 2.88 and δ 3.12, together with a broad signal at δ 3.01. This extra broad signal indicates that there are more than two rotamers present in solution. It is evident that *cis/trans* isomerisation is also occurring about the glycine amide bond, except in this case inter-conversion between the two states occurs at an intermediate rate.

Table 4.4 Selected ^1H NMR spectral data (δ , DMSO- d_6) for *N*-(ferrocenyl)naphthoyl dipeptide derivatives which contain *N*-methyl amino acids.

Compound No.	-NH-	-N(CH ₃)-	<i>ortho</i> ($\eta^5\text{-C}_5\text{H}_4$)	<i>meta</i> ($\eta^5\text{-C}_5\text{H}_4$)
115	8.63 & 8.59	3.11 & 2.90	4.84	4.31
116	8.49 & 8.41	3.05 & 2.76	4.91 & 4.81 & 4.78 & 4.74	4.44 & 4.42 & 4.41 & 4.40
118	8.57-8.63	2.99 & 2.77	4.83-4.85	4.30-4.32
119	8.72 & 7.45- 7.51	3.12 & 3.01 & 2.88	4.95-4.97	4.44-4.46
120	8.61 & 8.53	3.08	5.01	4.49-4.52
122	8.75-8.78	3.06 & 2.80	5.02	4.51

4.4.2. ^{13}C NMR and DEPT 135 studies of *N*-(ferrocenyl)naphthoyl dipeptide derivatives which contain *N*-methyl amino acids

The resolved and decoupled nature of ^{13}C NMR and DEPT 135 spectra, make it relatively easier to interpret and assign the ^{13}C NMR and DEPT 135 spectra of the *N*-(ferrocenyl)naphthoyl dipeptide derivatives which contain *N*-methyl amino acids. In most cases, signal multiplicities in these spectra only occur for the carbon atoms of the dipeptide chain, suggesting that the chemical shift of the other carbon atoms of the molecule are unaltered upon isomerisation. *N*-(3-ferrocenyl-2-naphthoyl)-sarcosine-glycine ethyl ester **116** is the exception; the number of resonance signals observed in both the ^{13}C NMR and DEPT 135 spectra of this compound was double the number anticipated.

Aside from signal multiplicities, the ^{13}C NMR and DEPT 135 spectra of these *N*-(ferrocenyl)naphthoyl dipeptide derivatives resemble those of the other *N*-(ferrocenyl)naphthoyl amino acid and peptide derivatives. The amide and ester carbonyl carbons of these *N*-(ferrocenyl)naphthoyl dipeptide derivatives appear at downfield positions in the range of δ 166.4-171.3. The ten non-equivalent carbon atoms of the naphthalene ring system appear from δ 122.7-138.8. DEPT 135 spectra were utilised to identify the four aromatic quaternary carbons occurring in this range. Signals due to the ferrocenyl carbons occur in the range of δ 66.6-84.3 in the ^{13}C NMR spectra.

The methylene group of the ethyl ester more often than not appears as two signals, in the narrow range of δ 58.9-61.1, which are easily identifiable due to the negative resonance in the DEPT 135 spectrum. The methyl carbon comes into resonance at approximately δ 14 and can in some cases be observed as two signals. The carbon of the *N*-methyl group comes into resonance from δ 30.0-40.0 and the signal multiplicity varies according to the number of rotamers present in solution.

Table 4.5 Selected ^{13}C NMR spectral data (δ , $\text{DMSO-}d_6$) for *N*-(ferrocenyl)naphthoyl dipeptide derivatives which contain *N*-methyl amino acids.

Compound No.	-N(CH ₃)-	<i>ipso</i> ($\eta^5\text{-C}_5\text{H}_4$)	($\eta^5\text{-C}_5\text{H}_5$)	-OCH ₂ CH ₃
115	33.5 & 32.9	82.6	67.9	59.3 & 58.9, 14.1
116	37.32 & 33.25	83.3	69.65 & 69.64	60.48 & 60.43, 14.06 & 13.98
117	37.4 & 35.2 & 34.5 & 33.4	83.2	69.6	60.9 & 60.5, 14.1 & 13.9
119	35.2 & 34.5 & 30.7	84.1	69.4	60.9 & 60.5, 14.0
120	39.3 & 34.1	84.1	69.41	60.5 & 59.7, 14.1
122	30.9	84.1	69.5	60.6, 14.1 & 14.0

4.4.3. ^1H and ^{13}C NMR study of *N*-(3-ferrocenyl-2-naphthoyl)-sarcosine-glycine ethyl ester (116)

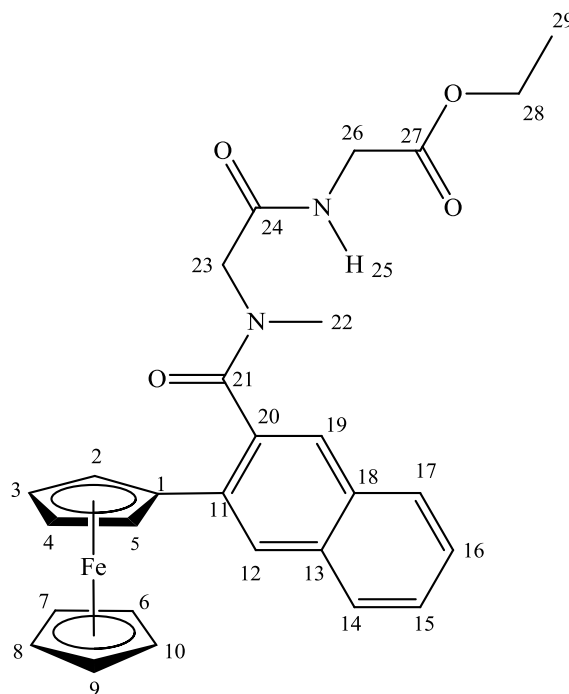


Figure 4.7 *N*-(3-ferrocenyl-2-naphthoyl)-sarcosine-glycine ethyl ester **116**.

N-(3-ferrocenyl-2-naphthoyl)-sarcosine-glycine ethyl ester **116** is the only compound belonging to this series for which every resonance (except one) was doubled in both the ^1H and ^{13}C NMR spectra. This doubling effect indicates that there are two different rotameric species present in solution and more importantly, that each particular atom in one of the rotamers has a different chemical shift to the corresponding atom in the other rotamer. Hence, *N*-(3-ferrocenyl-2-naphthoyl)-sarcosine-glycine ethyl ester **116** was selected for further NMR experiments to allow for the full assignment of the ^1H and ^{13}C NMR spectra. These experiments were undertaken in collaboration with Dr. John O'Brien of the School of Chemistry, TCD. The NMR experiments performed included a number of selective ROE and TOCSY experiments, as well as a number of 2D-NMR experiments including HH-COSY, NH-COSY, HSQC, HMBC, and ROESY.

Figure 4.7 illustrates the structure of *N*-(3-ferrocenyl-2-naphthoyl)-sarcosine-glycine ethyl ester **116** and the numbering system employed in the NMR assignment. The ^1H and ^{13}C NMR spectra of *N*-(3-ferrocenyl-2-naphthoyl)-sarcosine-glycine ethyl ester **116** are shown in Figure 4.8 and 4.9, respectively. Table 4.6 summarises the ^1H and ^{13}C resonances of both rotamers. Unfortunately, it was not possible to assign the geometry of the tertiary amide bond in either rotamer.

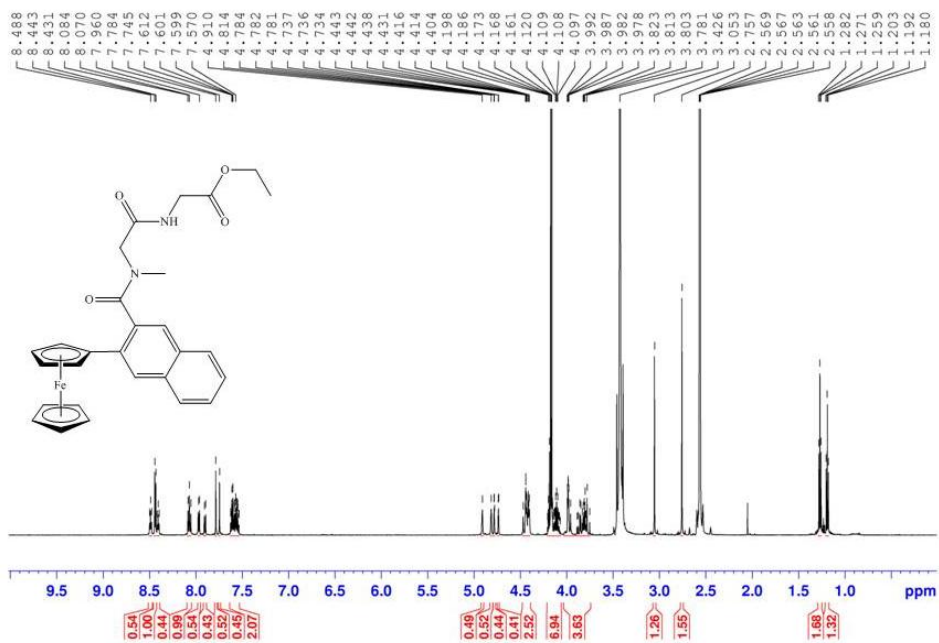


Figure 4.8 ^1H NMR spectrum of *N*-(3-ferrocenyl-2-naphthoyl)-sarcosine-glycine ethyl ester **116**.

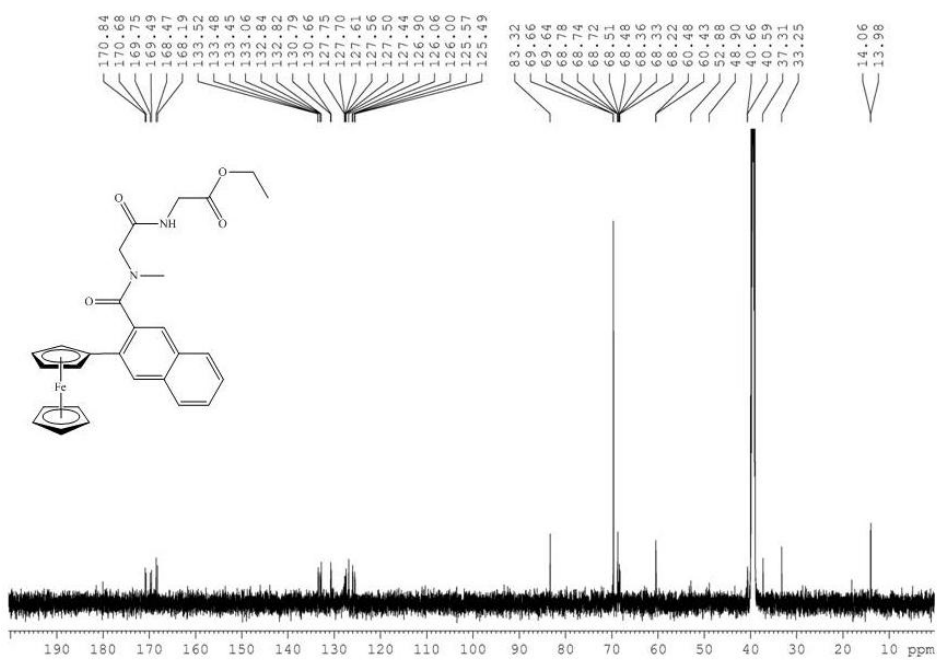


Figure 4.9 ^{13}C NMR spectrum of *N*-(3-ferrocenyl-2-naphthoyl)-sarcosine-glycine ethyl ester **116**.

Table 4.6 ^1H and ^{13}C NMR data (δ , DMSO- d_6) obtained for *N*-(3-ferrocenyl-2-naphthoyl)-sarcosine-glycine ethyl ester **116**.

Site	^1H NMR	^{13}C NMR	^1H NMR	^{13}C NMR
	rotamer A	rotamer A	rotamer B	rotamer B
1	-	83.3	-	83.3
2	4.81	68.75	4.74	68.51
3	4.42	68.33	4.44	68.36
4	4.40	68.18	4.41	68.22
5	4.91	68.77	4.78	68.71
6 to 10	4.21	69.65	4.22	69.64
11	-	133.48	-	133.45
12	8.44	127.61	8.43	127.75
13	-	132.84	-	132.82
14	8.08	127.50	8.06	127.44
15	7.61	126.89	7.60	126.89
16	7.57	126.06	7.55	126.00
17	7.90	127.56	7.96	127.70
18	-	130.79	-	130.66
19	7.78	125.57	7.75	125.49
20	-	133.52	-	133.06
21	-	170.84	-	170.68
22	2.76	37.32	3.05	33.25
23	3.97, 4.46	48.90	3.81, 3.76	52.87
24	-	168.47	-	168.19
25	8.49		8.41	
26	3.96, 4.00	40.66	3.79, 3.86	40.59
27	-	169.75	-	169.49
28	4.18	60.48	4.11	60.43
29	1.27	13.98	1.19	14.06

4.4.4. Variable temperature ^1H NMR study of *N*-(3-ferrocenyl-2-naphthoyl)-sarcosine-sarcosine ethyl ester (**117**)

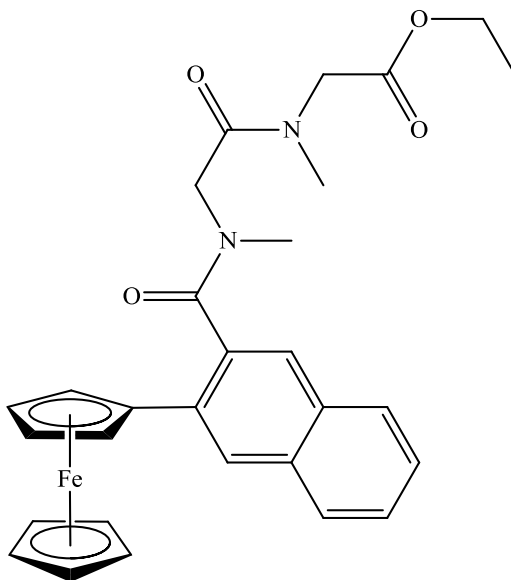


Figure 4.10 *N*-(3-ferrocenyl-2-naphthoyl)-sarcosine-sarcosine ethyl ester **117**.

The ^1H NMR spectrum of *N*-(3-ferrocenyl-2-naphthoyl)-sarcosine-sarcosine ethyl ester **117** obtained at room temperature is highly complex due to the presence of four rotamers in solution for which the rate of interconversion is slow on the NMR time scale. One possible way to overcome this problem is to perform the ^1H NMR experiment at a higher temperature so that the rate of interconversion increases. Once a particular temperature, known as the coalescence temperature (T_c), is reached, the rate of interconversion will be such that separate signals due to rotamers will coalesce to form one broad signal. At temperatures above the T_c , this broad signal will sharpen to give a single line. This is due to the fact that the rate of interconversion has increased to the point where a rapid exchange between rotamers has been established. Thus, a variable temperature study of the ^1H NMR spectrum of *N*-(3-ferrocenyl-2-naphthoyl)-sarcosine-sarcosine ethyl ester **117** was performed at 25, 40, 60, 80 and 100 $^\circ\text{C}$ in $\text{DMSO-}d_6$ (Figure 4.11 to Figure 4.14).

The aromatic region of the ^1H NMR spectrum (Figure 4.11) of *N*-(3-ferrocenyl-2-naphthoyl)-sarcosine-sarcosine ethyl ester **117** does not alter significantly upon heating. In contrast, the signals present in the ferrocenyl region of the spectrum appear less defined as

the sample is heated indicating that at the upper limit of the temperature range, the point of the coalescence is being approached. This is clearly illustrated in Figure 4.12.

The *N*-methyl region (δ 2.2-3.5) of the ^1H NMR spectrum is more informative (Figure 4.13). At room temperature (25 °C), the signals due to the two *N*-methyl groups appear as complex multiplets from δ 2.91-3.10 and δ 2.64-2.78. As the sample is heated, these signals start to appear slightly broadened at 60 °C. In the ^1H NMR spectrum obtained at 80 °C, this broadening effect is more apparent. At 100 °C, these signals appear even sharper; the *N*-methyl group that appeared as a multiplet at δ 2.64-2.78 at 25 °C is now present as a sharp singlet at approximately δ 2.75. The other signal due to the second *N*-methyl group is masked by the large signal due to H_2O contained in the $\text{DMSO-}d_6$ solvent. This signal is shifted gradually upfield upon heating due to weakening of hydrogen bonds present in solution. The complex signal due to the methyl group of the ethyl ester is also shown to coalesce upon heating (Figure 4.14). Thus, this variable temperature NMR study indicates that the coalescence temperature (T_c) of *N*-(3-ferrocenyl-2-naphthoyl)-sarcosine-sarcosine ethyl ester lies close to the upper limit of the temperature range.

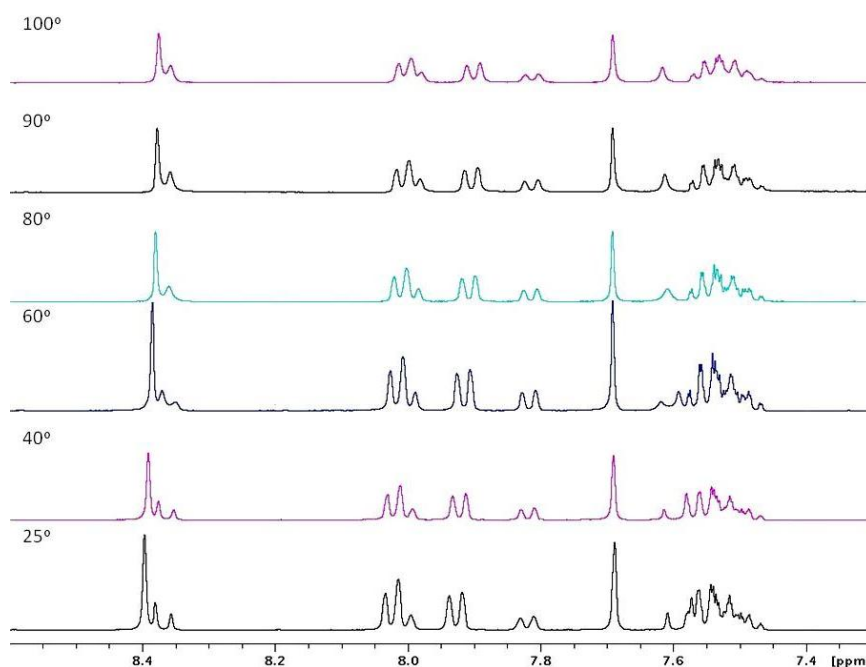


Figure 4.11 Variable temperature NMR study of *N*-(3-ferrocenyl-2-naphthoyl)-sarcosine-sarcosine ethyl ester **117**: the aromatic region (7.3-8.6 ppm) of the ^1H NMR spectrum.

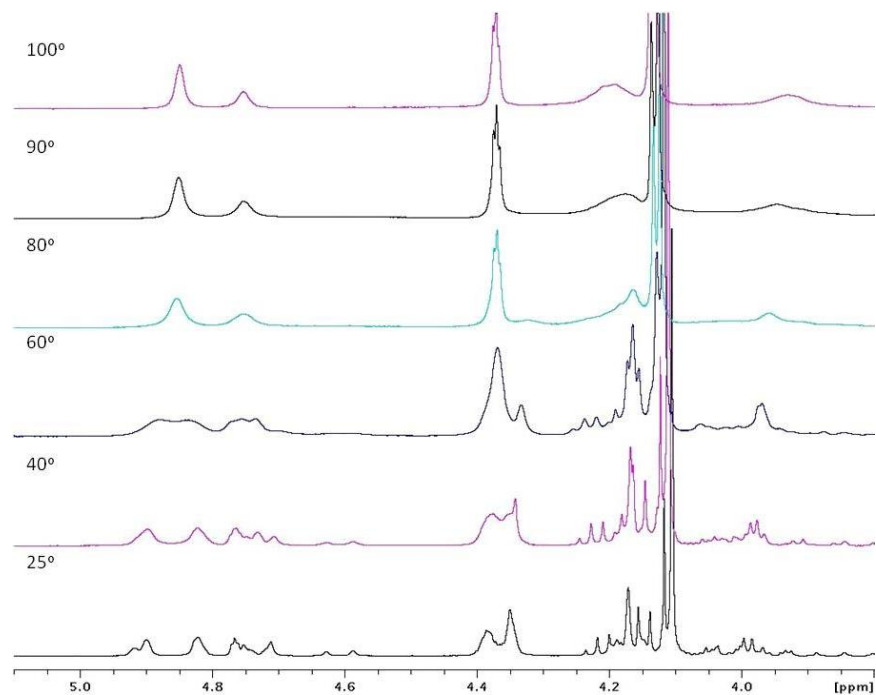


Figure 4.12 Variable temperature NMR study of *N*-(3-ferrocenyl-2-naphthoyl)-sarcosine-sarcosine ethyl ester **117**: the ferrocenyl region (3.8-5.1 ppm) of the ^1H NMR spectrum.

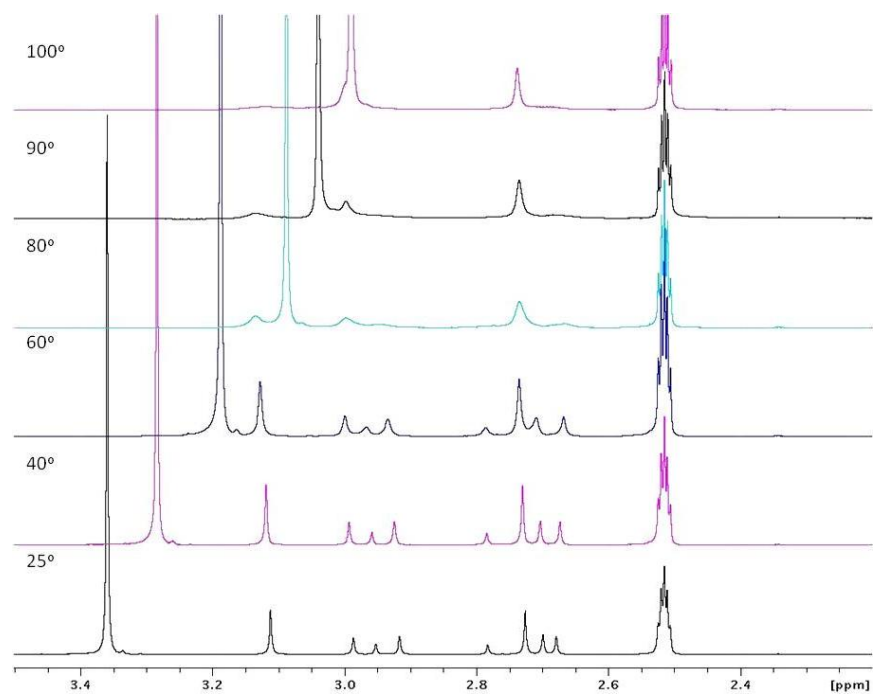


Figure 4.13 Variable temperature NMR study of *N*-(3-ferrocenyl-2-naphthoyl)-sarcosine-sarcosine ethyl ester **117**: the *N*-methyl region (2.2-3.5 ppm) of the ^1H NMR spectrum.

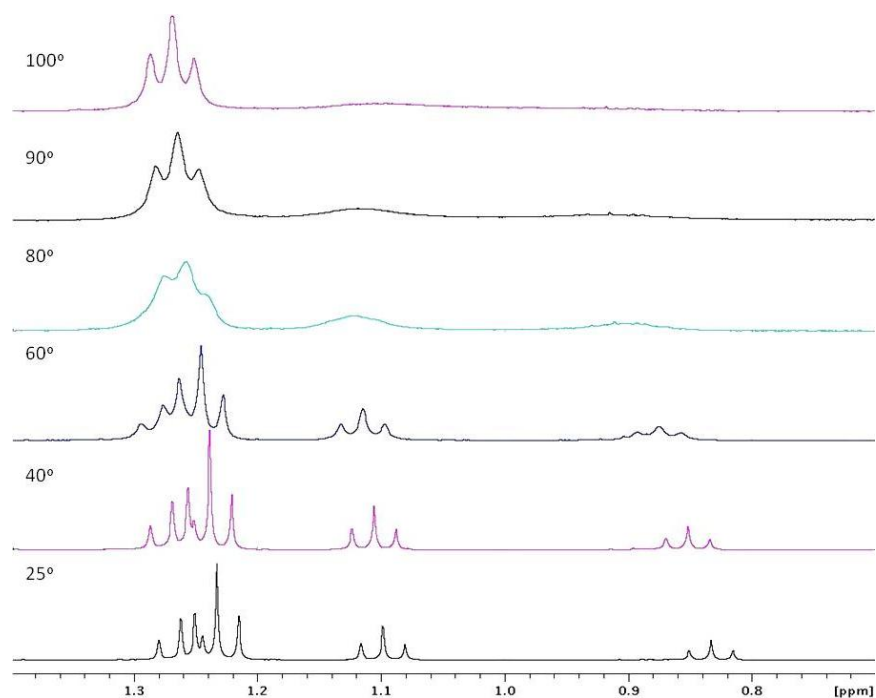


Figure 4.14 Variable temperature NMR study of *N*-(3-ferrocenyl-2-naphthoyl)-sarcosine-sarcosine ethyl ester **117**: the alkyl region (0.7-1.4 ppm) of the ^1H NMR spectrum.

4.5. ^1H NMR studies of *N*-naphthoyl dipeptide derivatives and *N*-(ferrocenyl)naphthoyl amino acid and dipeptide derivatives

The ^1H NMR studies of *N*-naphthoyl dipeptide derivatives and *N*-(ferrocenyl)naphthoyl amino acid and dipeptide derivatives were performed in $\text{DMSO-}d_6$, except in cases where signals were masked by the solvent peaks in the region δ 2.0 to δ 3.5, in which case, acetone- d_6 was employed. In the ^1H NMR spectra of the *N*-naphthoyl dipeptide derivatives, the aromatic region shows a singlet, multiplet, and multiplet splitting pattern, integrating for one, four and two protons, respectively. The aromatic peak patterns for the *N*-(ferrocenyl)naphthoyl amino acid and dipeptide derivatives are similar to those described in Chapter 2, Section 2.5.

The chemical shifts at which the amide protons of the *N*-(ferrocenyl)naphthoyl amino acid and dipeptide derivatives appear depends on the solvent that is employed. The amide proton peaks appear slightly further downfield from δ 8.36-8.83 in the cases where $\text{DMSO-}d_6$ was

employed, compared to the range of δ 6.95-8.01 in acetone- d_6 . For the samples obtained in acetone- d_6 , a slight downfield shift is discernable for the amide protons of the *N*-(6-ferrocenyl-2-naphthoyl) amino acid and dipeptide derivatives (δ 7.33-8.01) relative to the amide protons of the *N*-(3-ferrocenyl-2-naphthoyl) amino acid and dipeptide derivatives (δ 6.95-7.46). In the case of the *N*-naphthoyl dipeptide derivatives, the amide protons appear in the range of δ 8.40-9.05.

The ^1H NMR spectra of the *N*-(ferrocenyl)naphthoyl amino acid and dipeptide derivatives showed peaks in the range of δ 3.91-5.02 that are representative of a monosubstituted ferrocene derivative. A singlet due to the unsubstituted cyclopentadienyl ring ($\eta^5\text{-C}_5\text{H}_5$) typically appears from δ 3.91-4.17, with an integration of five protons. The *ortho* hydrogens on the cyclopentadienyl ($\eta^5\text{-C}_5\text{H}_4$) ring appear in the range δ 4.64-5.02 as a fine triplet or a singlet, each integrating for two protons. The *meta* hydrogens of the ($\eta^5\text{-C}_5\text{H}_4$) ring appear from δ 4.18-4.50, also as a fine triplet or a singlet that integrates for two protons. These signals are absent from the ^1H NMR spectra of the *N*-naphthoyl dipeptide derivatives.

Table 4.7 Selected ^1H NMR spectral data (δ) for *N*-naphthoyl dipeptide derivatives and *N*-(ferrocenyl)naphthoyl amino acid and dipeptide derivatives.

Compound No.	NH's	($\eta^5\text{-C}_5\text{H}_5$)	<i>ortho</i> ($\eta^5\text{-C}_5\text{H}_4$)	<i>meta</i> ($\eta^5\text{-C}_5\text{H}_4$)
124	8.83, 8.39	3.91-4.14	4.97	4.46
125*	7.36-7.44, 7.09	3.96-4.01	4.66	4.20
129*	7.34, 8.01	3.91-3.97	4.79	4.30
132	8.67, 8.38	4.08-4.17	5.02	4.50
134	8.88, 8.40	-	-	-
135	8.50	4.09-4.13	4.72	4.33

* ^1H NMR spectra obtained in acetone- d_6 .

4.5.1. ^1H NMR study of *N*-(3-ferrocenyl-2-naphthoyl)- γ -aminobutyric acid ethyl ester (136)

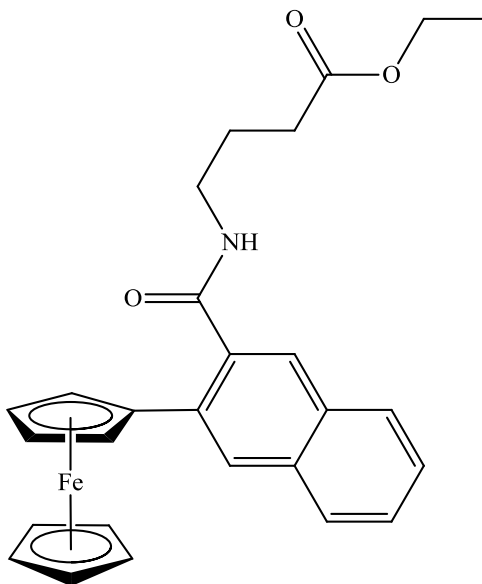


Figure 4.15 *N*-(3-ferrocenyl-2-naphthoyl)- γ -aminobutyric acid ethyl ester **136**.

The ^1H NMR spectrum of *N*-(3-ferrocenyl-2-naphthoyl)- γ -aminobutyric acid ethyl ester **136** was obtained in $\text{DMSO-}d_6$ and hence, the amide proton peak is positioned downfield at δ 8.40. This signal integrates for one proton and appears as a triplet due to the adjacent methylene group. The signals in the aromatic region confirm the presence of six protons, which appear from δ 7.48- 8.33.

The characteristic monosubstituted ferrocenyl splitting pattern is observed from δ 4.06-4.73. The peak due to the *ortho* protons of the substituted ($\eta^5\text{-C}_5\text{H}_4$) ring appears as the furthest downfield ferrocenyl signal at δ 4.73, and is observed as a fine triplet with a coupling constant of 2 Hz. Similarly, the signal due to the *meta* ($\eta^5\text{-C}_5\text{H}_4$) protons also appears as a fine triplet at δ 4.32. Both the *ortho* and *meta* peaks integrate for two protons each. The singlet due to the unsubstituted ($\eta^5\text{-C}_5\text{H}_5$) ring appears in a multiplet with a quartet representing the methylene protons of the ethyl ester. This multiplet occurs from δ 4.06-4.11 and integrates for seven protons.

From δ 1.76-3.23, there are three signals that integrate for two protons each, representing the three methylene groups of the γ -aminobutyric acid chain. The furthest downfield of

these signals appears as a quartet at δ 3.23 and represents the methylene group adjacent to the amide group. The coupling constant observed is 5.6 Hz. The central methylene group of the γ -aminobutyric acid chain appears as a quintet at δ 1.76, with a coupling constant of 7.2 Hz. The remaining signal at δ 2.35 appears as a triplet, and is due to the methylene group adjacent to the ester carboxyl group. The methyl group of the ethyl ester appears as a triplet at δ 1.20, with a coupling constant of 7.2 Hz.

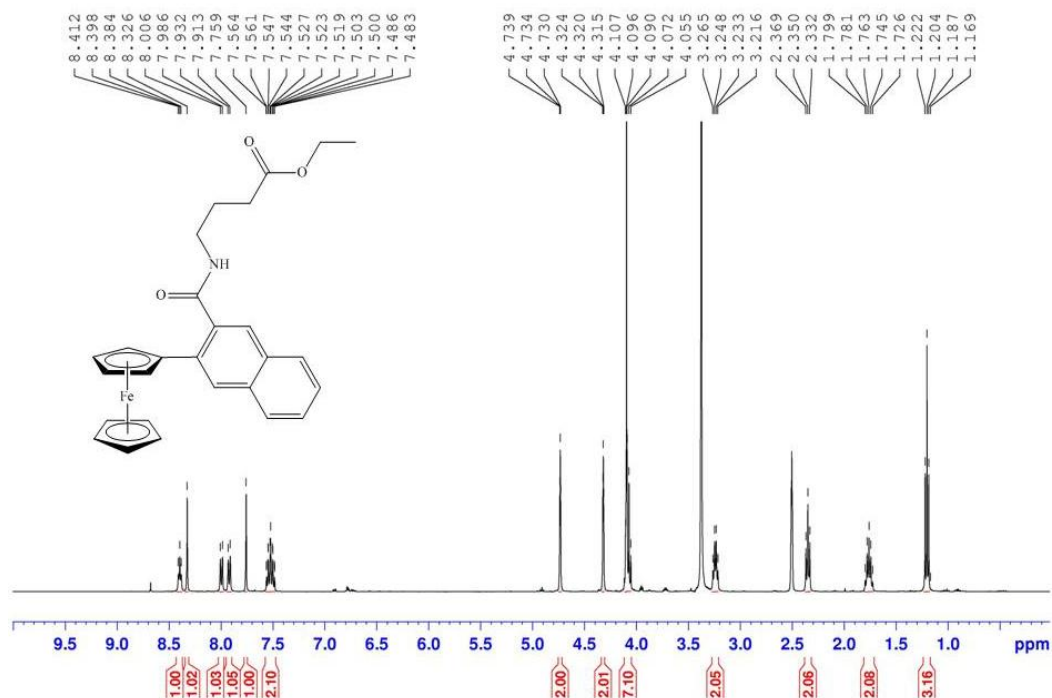


Figure 4.16 ¹H NMR spectrum of *N*-(3-ferrocenyl-2-naphthoyl)- γ -aminobutyric acid ethyl ester **136**.

4.6. ¹³C NMR and DEPT 135 studies of *N*-naphthoyl dipeptide derivatives and *N*-(ferrocenyl)naphthoyl amino acid and dipeptide derivatives

¹³C NMR and DEPT 135 spectra were obtained for all of the *N*-naphthoyl dipeptide derivatives and *N*-(ferrocenyl)naphthoyl amino acid and dipeptide derivatives. In the ¹³C spectra of the *N*-(ferrocenyl)naphthoyl amino acid and dipeptide derivatives and *N*-naphthoyl dipeptide derivatives, the amide and ester carbonyl carbons appear at downfield positions usually in the range of δ 166.2-173.5. In the aromatic region, ten carbon peaks are

observed, which correspond to the ten non-equivalent carbon atoms of the naphthalene ring system. The four aromatic quaternary carbons of the *N*-(ferrocenyl)naphthoyl amino acid and dipeptide derivatives, and the three aromatic quaternary carbons of the *N*-naphthoyl dipeptide derivatives were easily identified with the aid of DEPT 135 spectra.

The ferrocenyl carbon atoms of the *N*-(ferrocenyl)naphthoyl amino acid and dipeptide derivatives are present from δ 86.2-66.6. In cases where the ^{13}C and DEPT 135 spectra were obtained in acetone- d_6 , a slight downfield shift is discernable for the ferrocenyl carbon atoms. The *ipso* carbon on the substituted cyclopentadienyl ($\eta^5\text{-C}_5\text{H}_4$) ring appears in the range of δ 84.0-84.5 in DMSO- d_6 and from δ 85.4-86.2 in acetone- d_6 . Similarly, the unsubstituted cyclopentadienyl ring ($\eta^5\text{-C}_5\text{H}_5$) appears as an intense peak at approximately δ 70.5 in acetone- d_6 and δ 69.5 in DMSO- d_6 . For the *N*-(6-ferrocenyl-2-naphthoyl) amino acid and dipeptide derivatives, the signal due to the *meta* ($\eta^5\text{-C}_5\text{H}_4$) carbon atoms generally overlaps with this peak or appears in close proximity, whilst the *ortho* ($\eta^5\text{-C}_5\text{H}_4$) carbon peak appears slightly upfield at δ 67.6 in acetone- d_6 and δ 66.6 in DMSO- d_6 . In the case of the *N*-(3-ferrocenyl-2-naphthoyl) amino acid and dipeptide derivatives, the signal due to the *ortho* ($\eta^5\text{-C}_5\text{H}_4$) carbon atoms is shifted downfield to δ 70.3 in acetone- d_6 and δ 68.8 in DMSO- d_6 . The *meta* ($\eta^5\text{-C}_5\text{H}_4$) carbon atoms come into resonance at approximately δ 69 in acetone- d_6 and δ 68 in DMSO- d_6 . These signals are absent from the ^{13}C NMR spectra of the *N*-naphthoyl dipeptide derivatives.

The methylene group of the ethyl ester appears in the narrow range of δ 59.7-61.4. This peak and the methylene peaks of the peptide chain are easily identified by their negative resonances in DEPT 135 spectra. The methylene carbons of the amino acids and dipeptide chains appear from δ 22.0-44.1. The methyl group of the ethyl ester is at approximately δ 14.1 in all spectra obtained in DMSO- d_6 and at δ 14.5 in all spectra obtained in acetone- d_6 .

Table 4.8 Selected ^{13}C NMR data (δ) for *N*-naphthoyl dipeptide derivatives and *N*-(ferrocenyl)naphthoyl amino acid and dipeptide derivatives.

Compound No.	C=O	<i>Ips</i> o (η^5 - C ₅ H ₄)	(η^5 -C ₅ H ₅)	-OCH ₂ CH ₃	Peptide CH ₂
123	168.6-172.5	84.3	69.5	60.5, 14.0	41.8
126*	169.5-172.0	86.1	70.5	61.4, 14.5	35.9-41.7
130*	167.3-172.4	85.5	70.4	61.4, 14.5	36.3-41.7
133	166.5-169.8	-	-	60.4, 14.0	40.7-42.5
136	169.7-172.6	84.5	69.5	59.7, 14.1	24.2-38.3
138	166.4-171.3	84.0	69.4	59.9, 14.1	33.8-35.6

* ^{13}C and DEPT 135 NMR spectra obtained in acetone-*d*₆.

4.6.1. ^{13}C and DEPT 135 NMR study of *N*-(6-ferrocenyl-2-naphthoyl)- δ -amino-n-valeric acid ethyl ester (**140**)

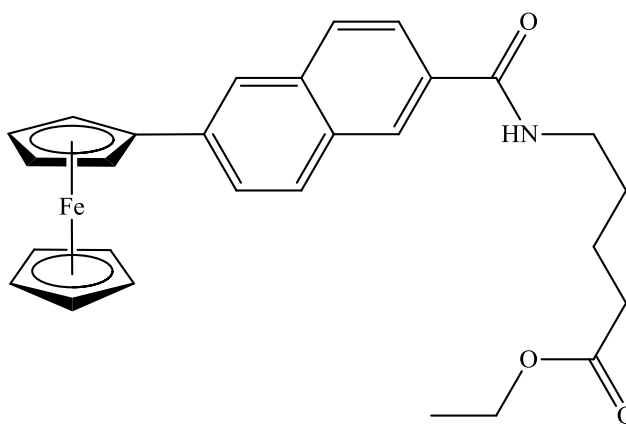


Figure 4.17 *N*-(6-ferrocenyl-2-naphthoyl)- δ -amino-n-valeric acid ethyl ester **140**.

The ^{13}C NMR spectrum of *N*-(6-ferrocenyl-2-naphthoyl)- δ -amino-n-valeric acid ethyl ester **140** displays two carbonyl carbon atoms at δ 172.8 and δ 166.2. Both signals are absent from the DEPT 135 spectrum. The aromatic region shows ten individual signals, representing the ten non-equivalent carbons of the 2,6-disubstituted naphthalene group. The absence of the carbons at δ 138.6, δ 134.4, δ 131.1 and δ 130.7 in the DEPT 135 spectrum

indicates their quaternary nature. The six remaining carbons appear at δ 128.7, δ 127.3, δ 127.1, δ 125.9, δ 124.5 and δ 122.7, respectively.

The signal at δ 84.1 in the ferrocenyl region represents the *ipso* carbon of the (η^5 -C₅H₄) as this does not appear in the DEPT 135 spectrum. The unsubstituted ring appears as an intense signal at δ 69.4 together with the *meta* (η^5 -C₅H₄) carbon atoms. The *ortho* (η^5 -C₅H₄) carbon atoms appear at δ 66.6. The methylene groups of the ethyl ester and δ -amino-n-valeric acid moiety are easily assigned as they show negative resonance peaks in the DEPT 135 spectrum at δ 59.7, δ 38.8, δ 33.2, δ 28.6 and δ 22.0. The methyl carbon of the ester group is observed in the most upfield position at δ 14.1.

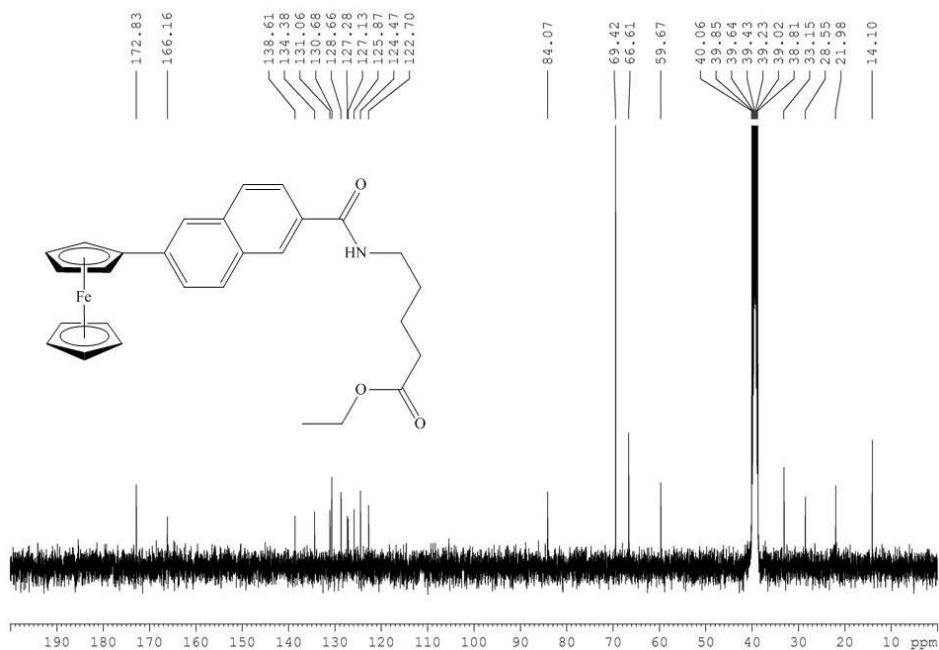


Figure 4.18 ¹³C NMR spectrum of *N*-(6-ferrocenyl-2-naphthoyl)- δ -amino-n-valeric acid ethyl ester **140**.

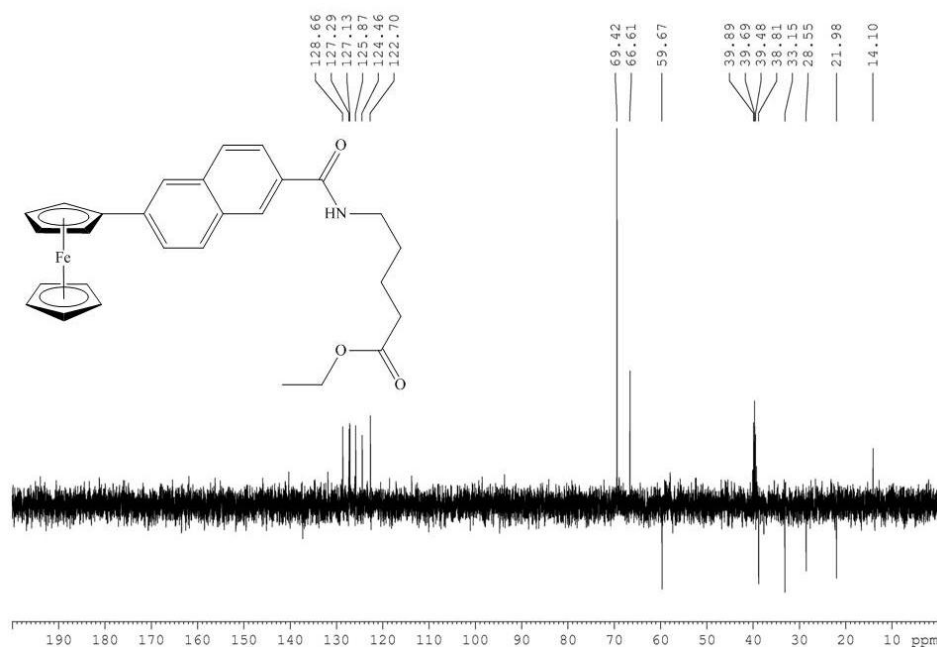


Figure 4.19 DEPT 135 spectrum of *N*-(6-ferrocenyl-2-naphthoyl)- δ -amino-n-valeric acid ethyl ester **140**.

4.7. COSY study of *N*-(6-ferrocenyl-2-naphthoyl)-glycine- γ -aminobutyric acid ethyl ester (**131**)

COSY (Correlation Spectroscopy) is a 2D-NMR technique that indicates all of the spin-spin coupled protons in one spectrum. In a COSY spectrum, two identical chemical shift axes are plotted orthogonally and the one-dimensional spectrum appears on the diagonal from the bottom left to the top right of the resulting square. All peaks that are mutually spin-spin coupled are shown by cross-peaks in the third dimension, which are placed symmetrically about the diagonal.¹⁰ In the COSY spectrum of *N*-(6-ferrocenyl-2-naphthoyl)-glycine- γ -aminobutyric acid ethyl ester **131** the proton spectrum is plotted along each axis. It is clear that the amide proton of the glycine **a** (δ 8.01) correlates with the methylene group **b** of the glycine residue (δ 3.90-3.96), while the amide proton of the γ -aminobutyric acid **c** (δ 7.33) couples with the methylene group **d** (δ 3.15) of the γ -aminobutyric acid chain. The central methylene group of the γ -aminobutyric acid chain **e** (δ 1.66) is easily identified due to its coupling with the methylene protons **d** and **f** (δ 2.22)

positioned on either side. Correlation is also present between the *ortho* and *meta* protons of the substituted (η^5 -C₅H₄) ring, **i** and **j**. The methylene **g** (δ 3.90-3.96) and methyl protons **h** (δ 1.06) of the ethyl ester only show coupling with each other, as do the aromatic protons of the naphthoyl group **k-p**.

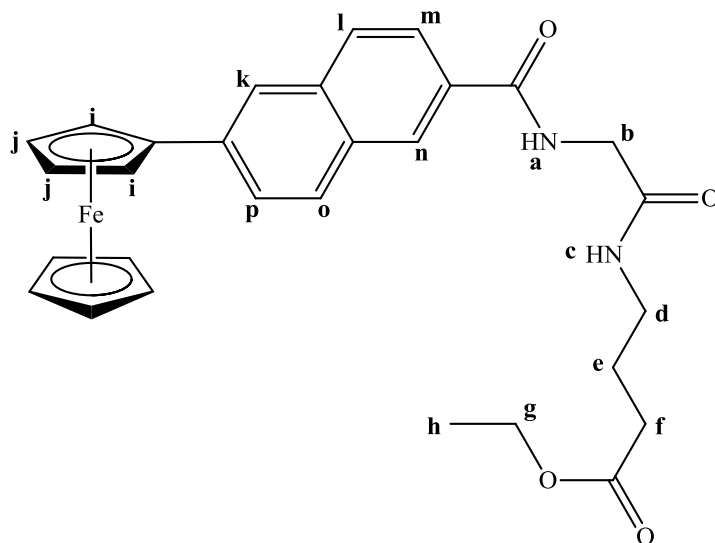


Figure 4.20 *N*-(6-ferrocenyl-2-naphthoyl)-glycine- γ -aminobutyric acid ethyl ester **131**.

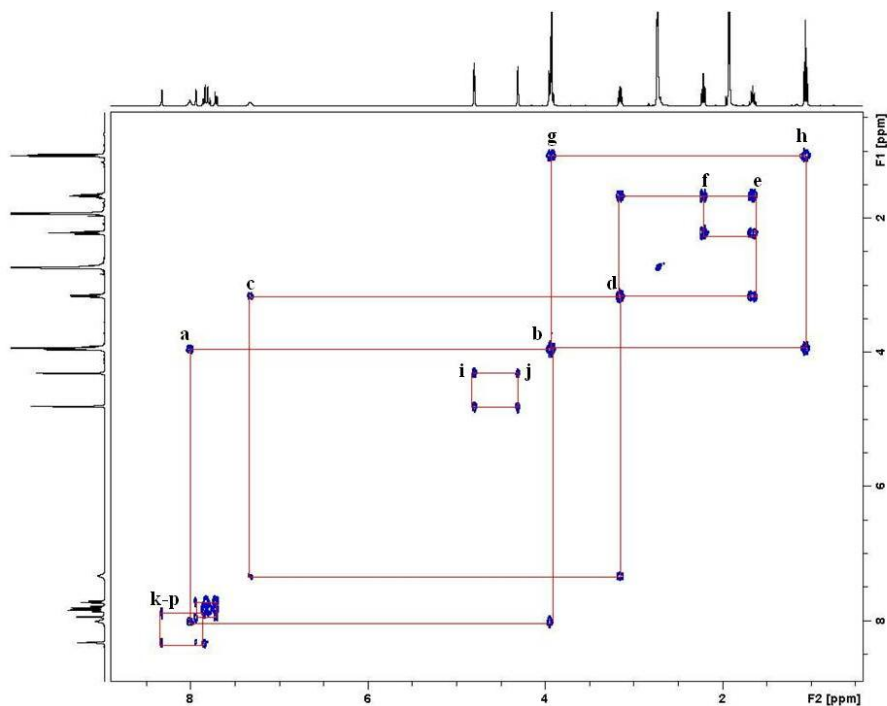


Figure 4.21 COSY spectrum of *N*-(6-ferrocenyl-2-naphthoyl)-glycine- γ -aminobutyric acid ethyl ester **131**.

4.8. Infra red studies of *N*-naphthoyl dipeptide derivatives and *N*-(ferrocenyl)naphthoyl amino acid and dipeptide derivatives

The IR spectra of the *N*-(naphthoyl) dipeptide derivatives and the *N*-(ferrocenyl)naphthoyl amino acid and dipeptide derivatives were obtained from the pure solid and all show characteristic peaks, as described in Chapter 2 (Section 2.8). Table 4.9 summarises the main absorptions for a representative selection of compounds. In the case of the *N*-(ferrocenyl)naphthoyl dipeptide derivatives which contain tertiary amide bonds, the amide II band which is normally found between 1570 and 1515 cm^{-1} is absent from the IR spectrum (Figure 4.22). However, the stretching vibration of the C=O bond is still observed between 1680 and 1630 cm^{-1} . The ester carbonyl band appears at higher frequency, between 1750 and 1735 cm^{-1} . Bands due to aryl rings are present in the 1225-950 cm^{-1} region but are of little diagnostic value, as are a group of weak overtone and combination bands in the 2000-1600 cm^{-1} region.

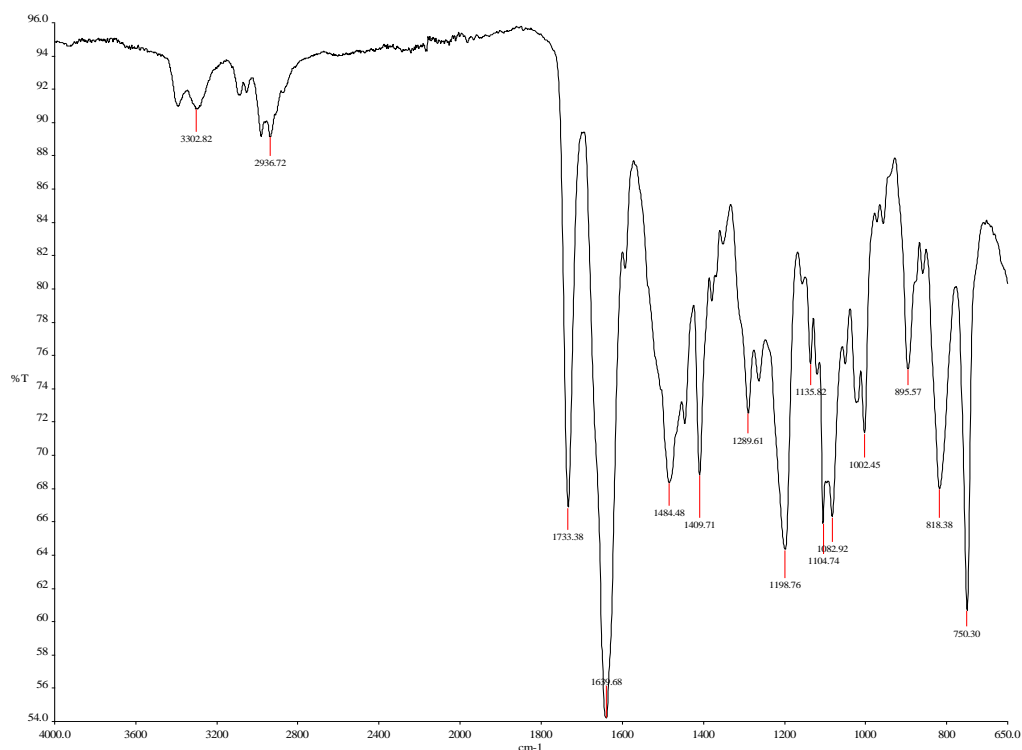


Figure 4.22 IR spectrum of *N*-(3-ferrocenyl-2-naphthoyl)-glycine-*N*-methyl-L-alanine ethyl ester **118**.

Table 4.9 Selected IR data for *N*-naphthoyl dipeptide derivatives and *N*-(ferrocenyl)naphthoyl amino acid and dipeptide derivatives. The values quoted are in cm⁻¹.

Compound No.	N-H	C=O amide I	C=O amide II	C=O ester
117	-	1635	-	1741
119	3300	1626	1507	1739
123	3285	1643	1516	1733
127	3281	1640	1521	1727
130	3357, 3282	1678, 1633	1540	1735
134	3364, 3319	1672, 1644	1532	1750

4.9. UV-Vis studies of *N*-(ferrocenyl)naphthoyl amino acid and dipeptide derivatives

The UV-Vis spectra obtained for *N*-(ferrocenyl)naphthoyl amino acid and dipeptide derivatives are comparable to those obtained for the compounds prepared in Chapter 2 (Section 2.9). The *N*-(3-ferrocenyl-2-naphthoyl) amino acid and dipeptide derivatives have much weaker absorbances at around 450 nm than the *N*-(6-ferrocenyl-2-naphthoyl) amino acid and dipeptide derivatives, so for this reason the UV-Vis spectra of the first set of compounds were obtained at a concentration of 1×10^{-3} M, whilst the latter set were analysed at a concentration of 5×10^{-4} M. The difference in the intensity of these absorbances is indicative of the degree of conjugation that exists between the substituted (η^5 -C₅H₄) ring and the naphthoyl ring. Extinction coefficients (ϵ) were calculated for each local maxima from the Beer-Lambert Law *i.e.* $A = \epsilon Cl$, where A is absorbance, C is concentration, l is the path length of the cell. Table 4.10 summarises the main features of the UV-Vis spectra obtained for a representative selection of compounds.

Table 4.10 Selected UV-Vis data (nm) for *N*-(ferrocenyl)naphthoyl amino acid and dipeptide derivatives.

Compound No.	λ_{max1} (nm)	ϵ_1	λ_{max2} (nm)	ϵ_2
115	-	-	450	537
122	370	2450	450	1016
124	370	3048	445	1288
129	370	3006	450	1288
137	-	-	450	508

4.10. Cyclic voltammetry studies of *N*-(ferrocenyl)naphthoyl amino acid and dipeptide derivatives

The cyclic voltammograms obtained for the *N*-(ferrocenyl)naphthoyl amino acid and dipeptide derivatives are comparable to those obtained for the compounds prepared in Chapter 2 (Section 2.10). Thus, the *N*-(ferrocenyl)naphthoyl amino acid and dipeptide derivatives exhibit one electron, reversible, redox waves similar to ferrocene, under the same conditions. The $E^{0'}$ (oxidation potential) values for the *N*-(3-ferrocenyl-2-naphthoyl) amino acid and dipeptide derivatives were in the range of 24-38 mV, whilst the *N*-(6-ferrocenyl-2-naphthoyl) amino acid and dipeptide derivatives showed values in the 55-65 mV range *versus* the ferrocene/ferricenium redox couple (Fc/Fc⁺). Figure 4.23 illustrates the difference in potential of the CVs obtained for *N*-(3-ferrocenyl-2-naphthoyl)- β -alanine-glycine ethyl ester **126** and *N*-(6-ferrocenyl-2-naphthoyl)- β -alanine-glycine ethyl ester **130**.

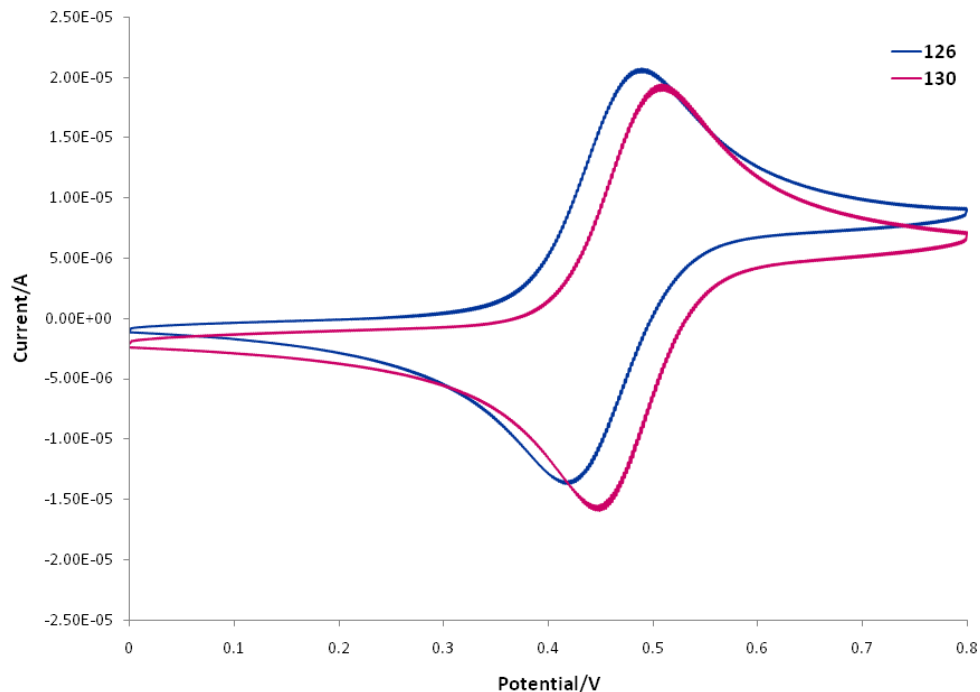


Figure 4.23 Cyclic voltammograms of *N*-(3-ferrocenyl-2-naphthoyl)- β -alanine-glycine ethyl ester **126** and *N*-(6-ferrocenyl-2-naphthoyl)- β -alanine-glycine ethyl ester **130** (0.1 M TBAP in ACN, Ag|AgCl, 0.1 V s⁻¹).

4.11. Conclusions

N-(6-ferrocenyl-2-naphthoyl)-glycine-L-alanine ethyl ester **51** and *N*-(6-ferrocenyl-2-naphthoyl)-glycine-glycine ethyl ester **96** have been identified as potential lead compounds in the development of bioorganometallic anti-cancer agents, following a primary SAR study. This project sought to optimise the biological activity of these novel ferrocenyl-peptide bioconjugates by conducting a secondary SAR study. The focus of this study was directed to the peptide chain, whereby isosteric replacements for the amide bond were employed to generate an additional series of novel *N*-(ferrocenyl)naphthoyl dipeptide derivatives. In addition, *N*-naphthoyl analogues of the two potential lead compounds were prepared to determine whether the redox active ferrocenyl unit of these derivatives contributes toward the observed biological effect. A homologous series of novel *N*-(ferrocenyl)naphthoyl amino acid derivatives were also prepared to investigate the

significance of peptide chain length in relation to the anti-proliferative effect. These novel compounds were isolated in moderately good yields and have been characterised by a range of spectroscopic techniques including ^1H NMR, ^{13}C NMR, DEPT 135, COSY, IR, UV-Vis and CV. Each compound gave spectroscopic data in accordance with their proposed structures.

Experimental Procedures

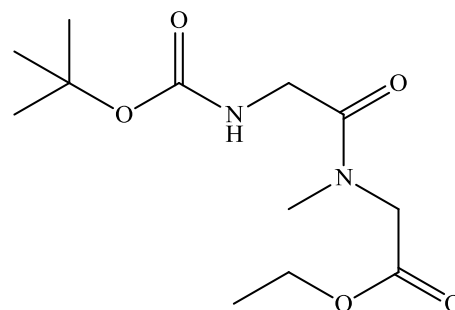
Experimental Note

All chemicals were purchased from Sigma-Aldrich, Lennox Chemicals, Fluorochem Limited or Tokyo Chemical Industry UK Limited; and used as received. Commercial grade reagents were used without further purification. When necessary, all solvents were purified and dried prior to use. Riedel-Haën silica gel was used for thin layer and column chromatography. Melting points were determined using either a Stuart melting point (SMP3) apparatus and are uncorrected. Optical rotation measurements were made on a Perkin Elmer 343 Polarimeter and are quoted in units of 10^{-1} deg $\text{cm}^2 \text{g}^{-1}$. Infrared spectra were recorded on either a Perkin Elmer Spectrum 100 FT-IR with ATR. UV-Vis spectra were recorded on a Hewlett Packard 8452 A diode array UV-Vis spectrophotometer. ^1H and ^{13}C NMR spectra were recorded in deuterated solvents on either a Bruker Avance 400 NMR or a Bruker Avance Ultrashield 600 NMR. The ^1H and ^{13}C NMR chemical shifts are reported in ppm (parts per million). Tetramethylsilane (TMS) or the residual solvent peaks have been used as an internal reference. All coupling constants (J) are in Hertz. The abbreviations for the peak multiplicities are as follows: s (singlet), d (doublet), dd (doublet of doublets), t (triplet), q (quartet), qt (quintet), m (multiplet) and br (broad). Elemental analysis was carried out by the microanalytical laboratory at University College Dublin. Cyclic voltammograms were recorded in anhydrous acetonitrile (Sigma-Aldrich), with 0.1 M tetrabutylammonium perchlorate (TBAP) as a supporting electrolyte, using a CH Instruments 600a electrochemical analyzer (Pico-Amp Booster and Faraday Cage). The experiments were carried out at room temperature. A three-electrode cell consisting of a glassy carbon working-electrode, a platinum wire counter-electrode and an Ag|AgCl reference electrode was used. The glassy carbon electrode was polished with 0.3 μm alumina followed by 0.05 μm alumina, between each experiment to remove any surface contaminants. The scan rate was 0.1 V s^{-1} . The concentration range of the ferrocene compounds was 1.0 mM in acetonitrile. The $E^{0'}$ values obtained for the test samples were referenced relative to the ferrocene/ferricenium redox couple.

General procedure for the preparation of Boc protected dipeptide ethyl esters.

Boc-glycine-sarcosine ethyl ester 106

Sarcosine ethyl ester hydrochloride (0.80 g, 5 mmol) was added to a solution of *N*-Boc-glycine (0.88 g, 5 mmol), 1-hydroxybenzotriazole (0.70 g, 5.2 mmol), triethylamine (0.9 ml) and *N*-(3-dimethylaminopropyl)-*N'*-ethylcarbodiimide



hydrochloride (0.99 g, 5.2 mmol) in 50 ml of

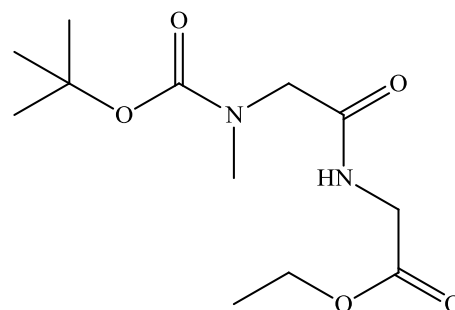
dichloromethane at 0 °C. After 30 min the solution was raised to room temperature and the reaction was allowed to proceed for 48 h. The reaction mixture was then washed with water. The dichloromethane layer was dried over MgSO₄ and the solvent was removed *in vacuo*. The product was purified by column chromatography (eluant 1:1 hexane:ethyl acetate) to give the title compound as a white solid (0.95 g, 70%), mp 54-56 °C;

δ_{H} (400 MHz, CDCl₃): 5.46 (1H, br. s, -CONH-), 3.89-4.24 {6H, m, -OCH₂CH₃, -NHCH₂-, -N(CH₃)CH₂-}, 3.04 & 3.01 {3H, s, s, -N(CH₃-)}, 1.45 {9H, s, (CH₃)₃CO₂CNH-}, 1.28 (3H, t, *J* 7.2, -OCH₂CH₃).

δ_{C} (100 MHz, CDCl₃): 169.3 (C=O), 168.9 (C=O), 155.8 (C=O), 79.7 (C_q), 61.9 & 61.4 (-OCH₂-, -ve DEPT), 50.4 & 49.6 {-N(CH₃)CH₂-, -ve DEPT}, 42.3 (-NHCH₂-, -ve DEPT), 35.2 & 35.1 {-N(CH₃-)}, 28.4 & 28.3 {(CH₃)₃}, 14.2 (-OCH₂CH₃).

Boc-sarcosine-glycine ethyl ester 107

The synthesis followed that of **106** using the following reagents: Boc-sarcosine (0.95 g, 5.0 mmol), 1-hydroxybenzotriazole (0.70 g, 5.2 mmol), triethylamine (0.9 ml), *N*-(3-dimethylaminopropyl)-*N'*-ethylcarbodiimide hydrochloride (0.99 g, 5.2 mmol) and glycine ethyl ester hydrochloride (0.7 g, 5.0 mmol). The product was purified by column chromatography (eluant 1:1 hexane:ethyl acetate) to give the title compound as a white solid (0.78 g, 56%), mp 56-57 °C;

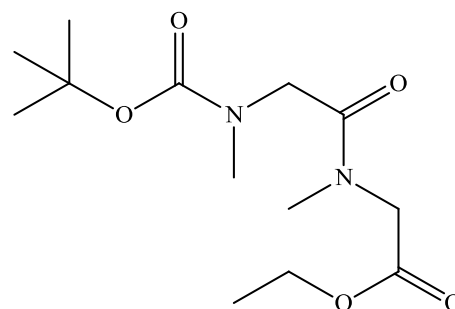


δ_{H} (400 MHz, CDCl_3): 6.39-6.56 (1H, m, -CONH-), 4.14 (2H, q, J 7.2, -OCH₂CH₃), 3.98 (2H, d, J 5.6, -NHCH₂-), 3.85 {2H, s, -N(CH₃)CH₂-}, 2.89 {3H, s, -N(CH₃)-}, 1.41 {9H, s, (CH₃)₃CO₂CN-}, 1.20 (3H, t, J 7.2, -OCH₂CH₃);

δ_{C} (100 MHz, CDCl_3): 169.6 (C=O), 168.9 (C=O), 155.9 (C=O), 80.8 (C_q), 61.6 (-OCH₂-, -ve DEPT), 52.9 {-N(CH₃)CH₂-, -ve DEPT}, 41.1 (-NHCH₂-, -ve DEPT), 35.7 {-N(CH₃)-}, 28.3 {(CH₃)₃}, 14.1 (-OCH₂CH₃).

Boc-sarcosine-sarcosine ethyl ester **108**

The synthesis followed that of **106** using the following reagents: Boc-sarcosine (0.80 g, 5.0 mmol), 1-hydroxybenzotriazole (0.70 g, 5.2 mmol), triethylamine (0.9 ml), *N*-(3-dimethylaminopropyl)-*N'*-ethylcarbodiimide hydrochloride (0.99 g, 5.2 mmol) and sarcosine ethyl ester hydrochloride (0.80



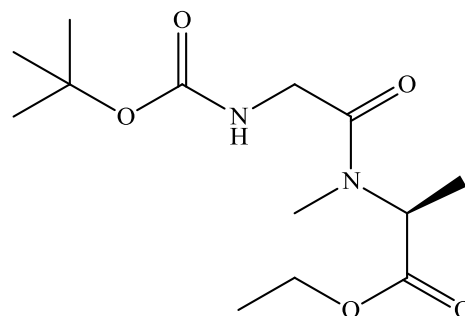
g, 5.0 mmol). The product was purified by column chromatography (eluant 1:1 hexane:ethyl acetate) to give the title compound as a transparent oil (0.77 g, 54%).

δ_{H} (400 MHz, CDCl_3): 4.01-4.25 {6H, m, -OCH₂CH₃, -N(CH₃)CH₂-, -N(CH₃)CH₂-}, 2.91-3.05 {6H, m, -N(CH₃)-, -N(CH₃)-}, 1.47 & 1.44 {9H, s, s, (CH₃)₃CO₂CN-}, 1.25-1.30 (3H, m, -OCH₂CH₃);

δ_{C} (100 MHz, CDCl_3): 169.3 (C=O), 168.9 (C=O), 156.3 (C=O), 80.0 (C_q), 61.2 (-OCH₂-, -ve DEPT), 50.0 {-N(CH₃)CH₂-, -ve DEPT}, 49.6 {-N(CH₃)CH₂-, -ve DEPT}, 35.6 {-N(CH₃)-}, 35.4 {-N(CH₃)-}, 28.4 {(CH₃)₃}, 14.2 (-OCH₂CH₃).

Boc-glycine-*N*-methyl-L-alanine ethyl ester **109**

The synthesis followed that of **106** using the following reagents: Boc-glycine (0.88 g, 5.0 mmol), 1-hydroxybenzotriazole (0.70 g, 5.2 mmol), triethylamine (0.9 ml), *N*-(3-dimethylaminopropyl)-*N'*-ethylcarbodiimide hydrochloride (0.99 g, 5.2 mmol) and *N*-methyl-L-alanine ethyl ester



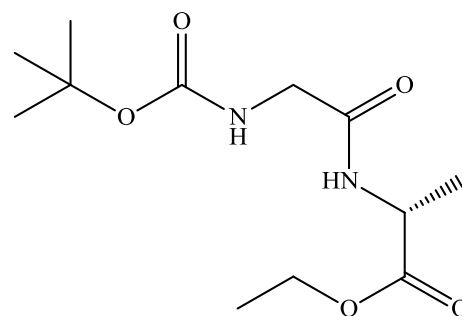
hydrochloride (0.74 g, 5.0 mmol). The product was purified by column chromatography (eluant 1:1 hexane:ethyl acetate) to give the title compound as a transparent oil (0.52 g, 38%).

δ_{H} (400 MHz, CDCl_3): 5.43 {1H, br. s, $(\text{CH}_3)_3\text{CO}_2\text{CNH-}$ }, 5.14 {1H, q, J 7.2, $-\text{N}(\text{CH}_3)\text{CH-}$ }, 4.06-4.16 (2H, m, $-\text{OCH}_2\text{CH}_3$), 3.93 (2H, br. s, $-\text{NHCH}_2-$), 2.84 & 2.80 {3H, s, s, $-\text{N}(\text{CH}_3)-$ }, 1.38 {9H, s, $(\text{CH}_3)_3\text{CO}_2\text{CNH-}$ }, 1.34 (3H, d, J 7.2, $-\text{CH}_3$), 1.19 (3H, t, J 7.2, $-\text{OCH}_2\text{CH}_3$);

δ_{C} (100 MHz, CDCl_3): 171.4 ($\text{C}=\text{O}$), 168.9 ($\text{C}=\text{O}$), 155.8 ($\text{C}=\text{O}$), 79.6 (C_q), 61.4 ($-\text{OCH}_2-$, -ve DEPT), 52.5 (α -C), 42.6 ($-\text{NHCH}_2-$, -ve DEPT), 30.2 $\{-\text{N}(\text{CH}_3)-\}$, 28.4 $\{(\text{CH}_3)_3\}$, 14.4 ($-\text{CH}_3$), 14.2 ($-\text{OCH}_2\text{CH}_3$).

Boc-Glycine-D-Alanine ethyl ester 110

The synthesis followed that of **106** using the following reagents: Boc-glycine (0.88 g, 5.0 mmol), 1-hydroxybenzotriazole (0.70 g, 5.2 mmol), triethylamine (0.9 ml), *N*-(3-dimethylaminopropyl)-*N'*-ethylcarbodiimide hydrochloride (0.99 g, 5.2 mmol) and D-alanine ethyl ester hydrochloride (0.77 g, 5.0 mmol). The product was purified by column chromatography (eluant 1:1 hexane:ethyl acetate) to give the title compound as a transparent oil (1.0g, 73%).



δ_{H} (400 MHz, CDCl_3): 6.54 (1H, br. s, $-\text{CONH-}$), 5.05 (1H, br. s, $-\text{CONH-}$), 4.51 (1H, qt, J 7.2, $-\text{NHCH-}$), 4.14 (2H, q, J 7.2, $-\text{OCH}_2\text{CH}_3$), 3.69-3.80 (2H, m, $-\text{NHCH}_2-$), 1.39 {9H, s, $(\text{CH}_3)_3\text{CO}_2\text{CNH-}$ }, 1.34 (H, d, J 7.2, $-\text{CH}_3$), 1.22 (3H, t, J 7.2, $-\text{OCH}_2\text{CH}_3$);

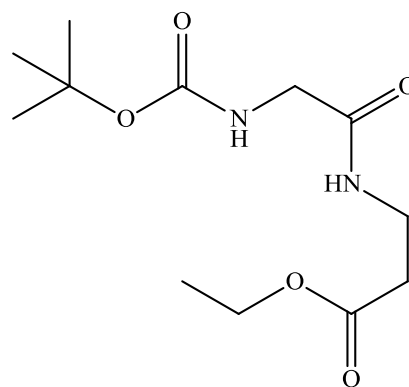
δ_{C} (100 MHz, CDCl_3): 172.3 ($\text{C}=\text{O}$), 168.9 ($\text{C}=\text{O}$), 155.9 ($\text{C}=\text{O}$), 80.4 (C_q), 61.6 ($-\text{OCH}_2-$, -ve DEPT), 48.1 (α -C), 44.3 ($-\text{NHCH}_2-$, -ve DEPT), 28.3 $\{(\text{CH}_3)_3\}$, 18.5 ($-\text{CH}_3$), 14.1 ($-\text{OCH}_2\text{CH}_3$).

Boc-glycine- β -alanine ethyl ester 111

The synthesis followed that of **106** using the following reagents: Boc-glycine (0.72 g, 4.1 mmol), 1-hydroxybenzotriazole (0.70 g, 5.2 mmol), triethylamine (0.9 ml), *N*-(3-dimethylaminopropyl)-*N'*-ethylcarbodiimide hydrochloride (0.99 g, 5.2 mmol) and β -Alanine ethyl ester hydrochloride (0.63 g, 4.1 mmol). The product was purified by column chromatography (eluant 1:1 hexane:ethyl acetate) to give the title compound as a transparent oil (0.80 g, 71%);

δ_{H} (400 MHz, CDCl_3): 6.78 (1H, br. s, -CONH-), 5.28 {1H, br. s, $(\text{CH}_3)_3\text{CO}_2\text{CNH-}$ }, 4.14 (2H, q, J 7.2, -OCH₂CH₃), 3.77 (2H, d, J 5.6, -NHCH₂-), 3.54 (2H, q, J 6.0, -CH₂CH₂-), 2.54 (2H, t, J 6.0, -CH₂CH₂-), 1.46 {9H, s, $(\text{CH}_3)_3\text{CO}_2\text{CNH-}$ }, 1.28 (3H, t, J 7.2, -OCH₂CH₃);

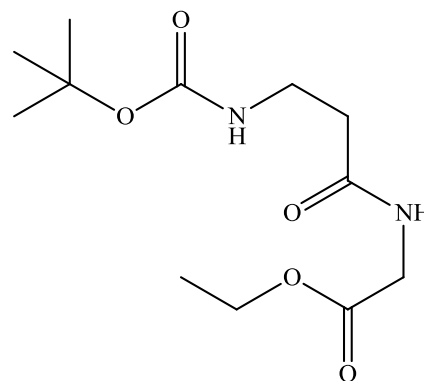
δ_{C} (100 MHz, CDCl_3): 172.5 (C=O), 169.5 (C=O), 156.0 (C=O), 80.2 (C_q), 60.8 (-OCH₂-, -ve DEPT), 44.3 (-NHCH₂-, -ve DEPT), 34.8 (-CH₂CH₂-, -ve DEPT), 33.9 (-CH₂CH₂-, -ve DEPT), 28.3 { $(\text{CH}_3)_3$ }, 14.2 (-OCH₂CH₃).



Boc- β -alanine-glycine ethyl ester 112

The synthesis followed that of **106** using the following reagents: Boc- β -alanine (0.95 g, 5.0 mmol), 1-hydroxybenzotriazole (0.70 g, 5.2 mmol), triethylamine (0.9 ml), *N*-(3-dimethylaminopropyl)-*N'*-ethylcarbodiimide hydrochloride (0.99 g, 5.2 mmol) and glycine ethyl ester hydrochloride (0.70 g, 5.0 mmol). The product was purified by column chromatography (eluant 1:1 hexane:ethyl acetate) to give the title compound as a white solid (0.95 g, 70%), mp 62-63 °C;

δ_{H} (400 MHz, CDCl_3): 6.31 (1H, br. s, -CONH-), 5.24 {1H, br. s, $(\text{CH}_3)_3\text{CO}_2\text{CNH-}$ }, 4.20-4.26 (2H, m, -OCH₂CH₃), 4.03 (2H, d, J 5.6, -NHCH₂-), 3.43 (2H, q, J 6.0, -CH₂CH₂-),

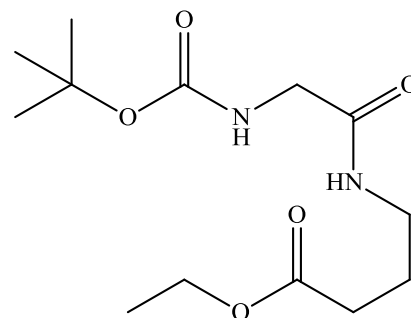


2.48 (2H, t, J 6.0, $-\text{CH}_2\text{CH}_2-$), 1.43 {9H, s, $(\text{CH}_3)_3\text{CO}_2\text{CNH}-$ }, 1.31 (3H, t, J 7.2, $-\text{OCH}_2\text{CH}_3$);

δ_{C} (100 MHz, CDCl_3): 171.8 ($\text{C}=\text{O}$), 169.9 ($\text{C}=\text{O}$), 156.1 ($\text{C}=\text{O}$), 79.4 (C_q), 61.6 ($-\text{OCH}_2-$, -ve DEPT), 41.4 ($-\text{NHCH}_2-$, -ve DEPT), 36.6 ($-\text{CH}_2\text{CH}_2-$, -ve DEPT), 36.0 ($-\text{CH}_2\text{CH}_2-$, -ve DEPT), 28.4 $\{(\text{CH}_3)_3\}$, 14.2 ($-\text{OCH}_2\text{CH}_3$).

Boc-glycine- γ -aminobutyric acid ethyl ester 113

The synthesis followed that of **106** using the following reagents: Boc-glycine (0.88 g, 5.0 mmol), 1-hydroxybenzotriazole (0.70 g, 5.2 mmol), triethylamine (0.9 ml), N -(3-dimethylaminopropyl)- N' -ethylcarbodiimide hydrochloride (0.99 g, 5.2 mmol) and γ -aminobutyric acid ethyl ester hydrochloride (0.84 g, 5.0 mmol). The product was purified by column chromatography (eluant 1:1 hexane:ethyl acetate) to give the title compound as a transparent oil (0.65 g, 46%).

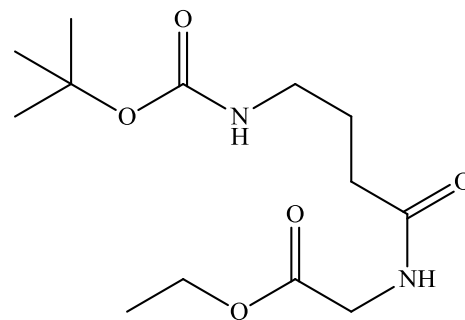


δ_{H} (400 MHz, CDCl_3): 6.33 (1H, br. s, $-\text{CONH}-$), 5.09 (1H, br. s, $-\text{CONH}-$), 4.06 (2H, q, J 7.2, $-\text{OCH}_2\text{CH}_3$), 3.70 (2H, d, J 5.6, $-\text{NHCH}_2-$), 3.25 (2H, q, J 6.0, $-\text{CH}_2\text{CH}_2\text{CH}_2-$), 2.29 (2H, t, J 7.2, $-\text{CH}_2\text{CH}_2\text{CH}_2-$), 1.78 (2H, qt, J 7.2, $-\text{CH}_2\text{CH}_2\text{CH}_2-$), 1.39 {9H, s, $(\text{CH}_3)_3\text{CO}_2\text{CN}-$ }, 1.19 (3H, t, J 7.2, $-\text{OCH}_2\text{CH}_3$);

δ_{C} (100 MHz, CDCl_3): 173.4 ($\text{C}=\text{O}$), 169.5 ($\text{C}=\text{O}$), 156.2 ($\text{C}=\text{O}$), 80.4 (C_q), 60.6 ($-\text{OCH}_2-$, -ve DEPT), 44.4 ($-\text{NHCH}_2-$, -ve DEPT), 38.9 ($-\text{CH}_2\text{CH}_2\text{CH}_2-$, -ve DEPT), 31.7 ($-\text{CH}_2\text{CH}_2\text{CH}_2-$, -ve DEPT), 28.3 $\{(\text{CH}_3)_3\}$, 24.6 ($-\text{CH}_2\text{CH}_2\text{CH}_2-$, -ve DEPT), 14.2 ($-\text{OCH}_2\text{CH}_3$).

Boc- γ -aminobutyric acid-glycine ethyl ester 114

The synthesis followed that of **106** using the following reagents: Boc- γ -aminobutyric acid (1.02 g, 5.0 mmol), 1-hydroxybenzotriazole (0.70 g, 5.2 mmol), triethylamine (0.9 ml), *N*-(3-dimethylaminopropyl)-*N'*-ethylcarbodiimide hydrochloride (0.99 g, 5.2 mmol) and glycine ethyl



ester hydrochloride (0.70 g, 5.0 mmol). The product was purified by column chromatography (eluant 1:1 hexane:ethyl acetate) to give the title compound as a white solid (1.11g, 68%), mp 67-68 °C;

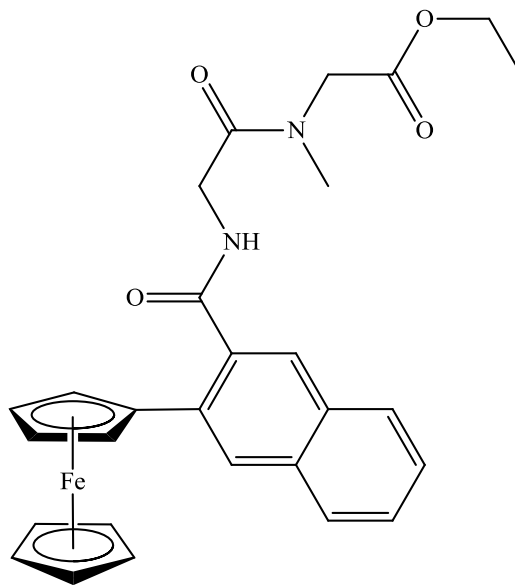
δ_{H} (400 MHz, CDCl_3): 6.58 (1H, br. s, -CONH-), 4.78 {1H, br. s, $(\text{CH}_3)_3\text{CO}_2\text{CNH-}$ }, 4.14 (2H, q, J 7.2, - OCH_2CH_3), 3.96 (2H, d, J 5.6, - NHCH_2 -), 3.14 (2H, br. s, - $\text{CH}_2\text{CH}_2\text{CH}_2$ -), 2.22 (2H, t, J 7.2, - $\text{CH}_2\text{CH}_2\text{CH}_2$ -), 1.76 (2H, qt, J 7.2, - $\text{CH}_2\text{CH}_2\text{CH}_2$ -), 1.37 {9H, s, $(\text{CH}_3)_3\text{CO}_2\text{CNH-}$ }, 1.22 (3H, t, J 7.2, - OCH_2CH_3);

δ_{C} (100 MHz, CDCl_3): 172.9 (C=O), 170.1 (C=O), 156.5 (C=O), 79.4 (C_q), 61.5 (- OCH_2 -, -ve DEPT), 41.4 (- NHCH_2 -, -ve DEPT), 39.6 (- $\text{CH}_2\text{CH}_2\text{CH}_2$ -, -ve DEPT), 33.3 (- $\text{CH}_2\text{CH}_2\text{CH}_2$ -, -ve DEPT), 28.4 $\{(\text{CH}_3)_3\}$, 26.4 (- $\text{CH}_2\text{CH}_2\text{CH}_2$ -, -ve DEPT), 14.1 (- OCH_2CH_3).

General procedure for the preparation of *N*-(ferrocenyl)naphthoyl dipeptide derivatives.

***N*-(3-ferrocenyl-2-naphthoyl)-glycine-sarcosine ethyl ester 115**

Glycine-sarcosine ethyl ester trifluoroacetate salt (0.29 g, 1.0 mmol) was added to a solution of 3-ferrocenylnaphthalene-2-carboxylic acid (0.36 g, 1.0 mmol), 1-hydroxybenzotriazole (0.18 g, 1.3 mmol), triethylamine (5.0 ml) and *N*-(3-dimethylaminopropyl)-*N'*-ethylcarbodiimide hydrochloride (0.25 g, 1 mmol) in 50 ml of dichloromethane at 0 °C. After 30 min the solution was raised to room temperature and the reaction was allowed to proceed for 48 h. The reaction mixture was then washed with water.



The dichloromethane layer was dried over MgSO₄ and the solvent was removed *in vacuo*. The product was purified by column chromatography (eluant 1:1 hexane: ethyl acetate) to give the title compound as an orange solid (0.12 g, 33%), mp 65-66 °C;

E^0/mV 24 vs. Fc/Fc⁺;

m/z (ESI) 512.1385 [M]⁺. C₂₈H₂₈N₂O₄Fe requires 512.1398;

λ_{max} (CH₃CN)/nm 450 ($\epsilon/dm^3 mol^{-1} cm^{-1}$ 537);

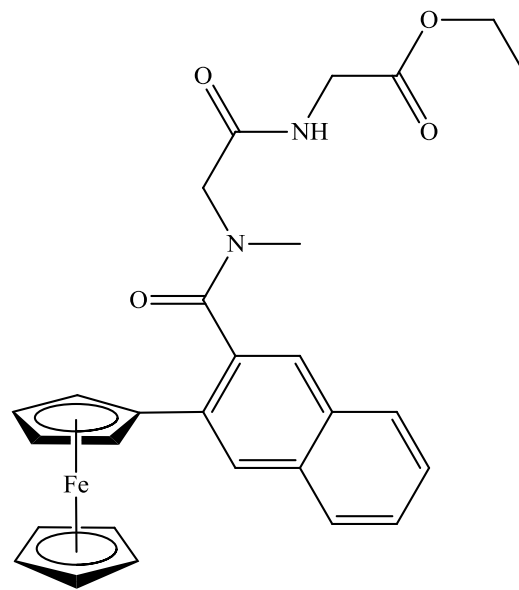
ν_{max} (neat)/cm⁻¹ 3298, 1743, 1645, 1486, 1194;

δ_H (400 MHz, DMSO-*d*₆): 8.63 & 8.59 (1H, t, *J* 5.6, t, *J* 5.6, -CONH-), 8.32 (1H, s, ArH), 7.99 (1H, d, *J* 8.0, ArH), 7.91 (1H, d, *J* 8.0, ArH), 7.85 (1H, s, ArH), 7.50-7.58 (2H, m, ArH), 4.84 {2H, t, *J* 1.6, *ortho* on (η^5 -C₅H₄)}, 4.31 {2H, t, *J* 1.6, *meta* on (η^5 -C₅H₄)}, 4.35 & 4.07-4.22 {11H, m, -OCH₂CH₃, η^5 -C₅H₅, -NHCH₂-, -N(CH₃)CH₂-}, 3.11 & 2.90 {3H, s, s, -N(CH₃-)}, 1.19-1.30 (3H, m -OCH₂CH₃);

δ_C (100 MHz, DMSO-*d*₆): 168.2 (C=O), 167.6 (C=O), 167.5 (C=O), 133.5 (C_q), 132.6 (C_q), 131.3 (C_q), 128.8 (C_q), 126.3, 125.9, 125.7, 125.3, 125.1, 124.4, 82.6 (C_{ipso} η^5 -C₅H₄), 67.9 (η^5 -C₅H₅), 67.3 (C_{ortho} η^5 -C₅H₄), 66.6 (C_{meta} η^5 -C₅H₄), 59.3 & 58.9 (-OCH₂-, -ve DEPT), 47.6 {-N(CH₃)CH₂-, -ve DEPT}, 38.9 (-NHCH₂-, -ve DEPT), 33.5 & 32.9 {-N(CH₃-)}, 14.1 (-OCH₂CH₃).

***N*-(3-ferrocenyl-2-naphthoyl)-sarcosine-glycine ethyl ester 116**

The synthesis followed that of **115** using the following reagents: 3-ferrocenylnaphthalene-2-carboxylic acid (0.36 g, 1.0 mmol), 1-hydroxybenzotriazole (0.18 g, 1.3 mmol), triethylamine (5 ml), *N*-(3-dimethylaminopropyl)-*N'*-ethylcarbodiimide hydrochloride (0.25 g, 1.3 mmol) and sarcosine-glycine ethyl ester trifluoroacetate salt (0.29 g, 1.0 mmol). The product was purified by column chromatography (eluant 1:1 hexane: ethyl acetate) to give the title compound as an orange solid (0.1 g, 20%), mp 67-68 °C; E^0/mV 26 vs. Fc/Fc⁺;



m/z (ESI) 512.1389 [M]⁺. C₂₈H₂₈N₂O₄Fe requires 512.1398;

λ_{\max} (CH₃CN)/nm 450 ($\epsilon/dm^3 mol^{-1} cm^{-1}$ 470);

ν_{\max} (neat)/cm⁻¹ 3291, 3082, 1748, 1684, 1622, 1485, 1192;

δ_H (600 MHz, DMSO-*d*₆): 8.49 & 8.41 (1H, t, *J* 5.8, t, *J* 5.8, -CONH-), 8.44 & 8.43 (1H, s, s, ArH), 8.07 (1H, m, ArH), 7.97 & 7.89 (1H, d, *J* 8.0, d, *J* 8.0, ArH), 7.75 & 7.78 (1H, s, s, ArH), 7.55-7.63 (2H, m, ArH), 4.91, 4.81, 4.78-4.79 & 4.73-4.74 {2H, s, s, m, m, *ortho* on (η^5 -C₅H₄)}, 3.76-4.46 {13H, m, *meta* on (η^5 -C₅H₄), η^5 -C₅H₅, -OCH₂CH₃, -N(CH₃)CH₂-, -NHCH₂-}, 3.05 & 2.76 {3H, s, s, -N(CH₃)-}, 1.19 & 1.27 (3H, t, *J* 7.2, t, *J* 7.2, -OCH₂CH₃);

δ_C (150 MHz, DMSO-*d*₆): 170.84 & 170.68 (C=O), 169.75 & 169.49 (C=O), 168.47 & 168.19 (C=O), 133.52 & 133.06 (C_q), 133.48 & 133.45 (C_q), 132.84 & 132.82 (C_q), 130.79 & 130.66 (C_q), 127.75 & 127.61, 127.70 & 127.56, 127.50 & 127.44, 126.89, 126.06 & 126.00, 125.57 & 125.49, 83.3 (C_{ipso} η^5 -C₅H₄), 69.65 & 69.64 (η^5 -C₅H₅), 68.77 & 68.71 (C_{ortho} η^5 -C₅H₄), 68.75 & 68.51 (C_{ortho} η^5 -C₅H₄), 68.36 & 68.33 (C_{meta} η^5 -C₅H₄), 68.22 & 68.18 (C_{meta} η^5 -C₅H₄), 60.48 & 60.43 (-OCH₂-, -ve DEPT), 52.87 & 48.90 {-N(CH₃)CH₂-, -ve DEPT}, 40.66 & 40.59 (-NHCH₂-, -ve DEPT), 37.32 & 33.25 {-N(CH₃)-}, 14.06 & 13.98 (-OCH₂CH₃).

***N*-(3-ferrocenyl-2-naphthoyl)-sarcosine-sarcosine ethyl ester 117**

The synthesis followed that of **115** using the following reagents: 3-ferrocenyl-naphthalene-2-carboxylic acid (0.32 g, 0.9 mmol), 1-hydroxybenzotriazole (0.12 g, 0.9 mmol), triethylamine (5 ml), *N*-(3-dimethylaminopropyl)-*N'*-ethylcarbodiimide hydrochloride (0.17 g, 0.9 mmol) and sarcosine-sarcosine ethyl ester trifluoroacetate salt (0.27 g, 0.9 mmol). The product was purified by column chromatography (eluant 1:1 hexane: ethyl acetate) to give the title compound as an orange solid (0.15 g, 31.1%), mp 74-75 °C;

$E^{0'}/\text{mV}$ 32 vs. Fc/Fc⁺;

m/z (ESI) 526.2 [M]⁺. C₂₉H₃₀N₂O₄Fe requires 526.4;

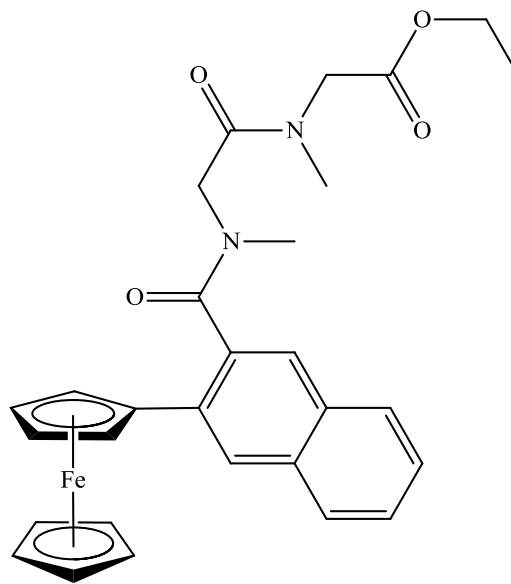
m/z (ESI) 526.1547 [M]⁺. C₂₉H₃₀N₂O₄Fe requires 526.1555;

λ_{max} (CH₃CN)/nm 450 ($\epsilon/\text{dm}^3 \text{ mol}^{-1} \text{ cm}^{-1}$ 568);

ν_{max} (neat)/cm⁻¹ 2928, 1741, 1635, 1483, 1394, 1196;

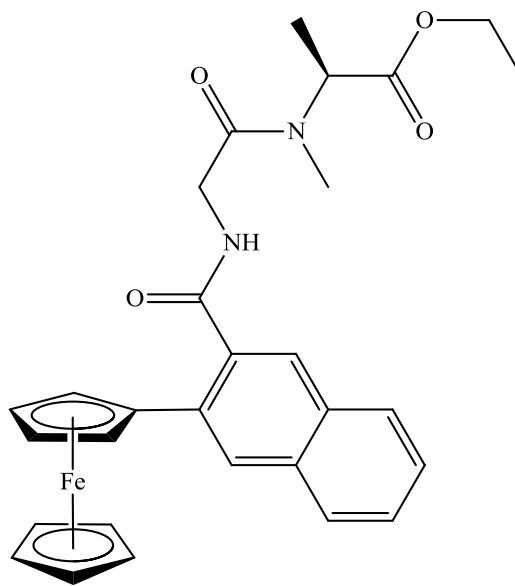
δ_{H} (400 MHz, DMSO-*d*₆): 8.35-8.39 (1H, m, ArH), 7.99-8.03 (1H, m, ArH), 7.93 & 7.81 (1H, d, *J* 8.8, d *J* 8.8, ArH), 7.46-7.68 (3H, m, ArH), 3.79-4.91 {15H, η^5 -C₅H₄, η^5 -C₅H₅, -OCH₂CH₃, -N(CH₃)CH₂-, -N(CH₃)CH₂-}, 2.91-3.10 {3H, m, -N(CH₃)-}, 2.64-2.78 {3H, m, -N(CH₃)-}, 0.81-1.27 (3H, m, -OCH₂CH₃);

δ_{C} (100 MHz, DMSO-*d*₆): 170.8 (C=O), 169.2 (C=O), 168.2 (C=O), 133.7 (C_q), 133.4 (C_q), 132.8 (C_q), 130.8 (C_q), 127.6, 127.5, 126.9, 126.0, 125.9, 125.5, 83.2 (*C*_{ipso} η^5 -C₅H₄), 69.6 (η^5 -C₅H₅), 68.8 (C η^5 -C₅H₄), 68.7 (C η^5 -C₅H₄), 68.4 (C η^5 -C₅H₄), 68.3 (C η^5 -C₅H₄), 60.9 & 60.5 (-OCH₂-, -ve DEPT), 49.2 (-CH₂-, -ve DEPT), 47.7 (-CH₂-, -ve DEPT), 37.4 & 35.2 & 34.5 & 33.4 {-N(CH₃)-}, 14.1 & 13.9 (-OCH₂CH₃).



N*-(3-ferrocenyl-2-naphthoyl)-glycine-*N*-methyl-L-alanine ethyl ester **118*

The synthesis followed that of **115** using the following reagents: 3-ferrocenylnaphthalene-2-carboxylic acid (0.32 g, 0.9 mmol), 1-hydroxybenzotriazole (0.12 g, 0.9 mmol), triethylamine (5 ml), *N*-(3-dimethylaminopropyl)-*N'*-ethylcarbodiimide hydrochloride (0.17 g, 0.9 mmol) and glycine-*N*-methyl-L-alanine ethyl ester trifluoroacetate salt (0.27 g, 0.9 mmol). The product was purified by column chromatography (eluant 1:1 hexane: ethyl acetate) to give the title compound as an orange solid (0.18 g, 38%), mp 62-63 °C;



$E^{0'}/\text{mV}$ 25 vs. Fc/Fc⁺;

$[\alpha]_D^{20}$ -25 (*c* 0.05 in CH₃CN);

m/z (ESI) 526.4 [M]⁺. C₂₉H₃₀N₂O₄Fe requires 526.4;

m/z (ESI) 526.1534 [M]⁺. C₂₉H₃₀N₂O₄Fe requires 526.1555;

λ_{max} (CH₃CN)/nm 445 ($\epsilon/\text{dm}^3 \text{ mol}^{-1} \text{ cm}^{-1}$ 574);

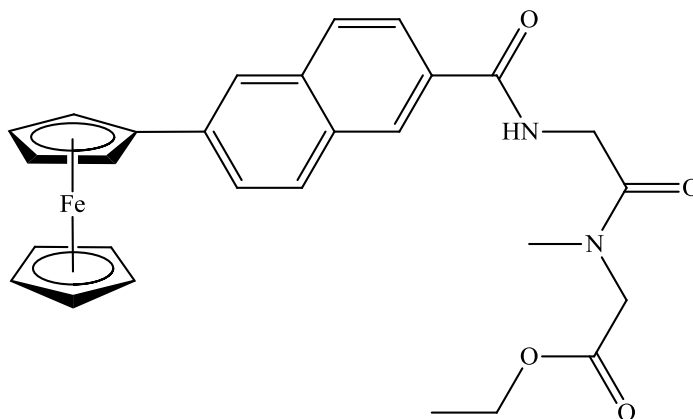
ν_{max} (neat)/cm⁻¹ 3303, 2937, 1734, 1640, 1484, 1199;

δ_{H} (400 MHz, DMSO-*d*₆): 8.57-8.63 (1H, m, -CONH-), 8.32 (1H, s, ArH), 7.99 (1H, d, *J* 8.0, ArH), 7.91 (1H, d, *J* 8.0, ArH), 7.86-7.87 (1H, m, ArH), 7.47-7.58 (2H, m, ArH), 4.88-4.99 {1H, m, -N(CH₃)CH-}, 4.83-4.85 {2H, m, *ortho* on (η^5 -C₅H₄)}, 4.30-4.32 {2H, m, *meta* on (η^5 -C₅H₄)}, 4.03-4.24 (9H, m, -OCH₂CH₃, η^5 -C₅H₅, -NHCH₂-), 2.99 & 2.77 {3H, s, s, -N(CH₃)-}, 1.43 & 1.35 (3H, d, *J* 7.2, d, *J* 7.2, -CH₃), 1.18-1.26 (3H, m, -OCH₂CH₃);

δ_{C} (100 MHz, DMSO-*d*₆): 171.3 (C=O), 169.8 (C=O), 168.7 (C=O), 135.2 (C_q), 134.3 (C_q), 132.9 (C_q), 130.5 (C_q), 128.0, 127.6, 127.4, 126.9, 126.8, 126.0, 84.3 (C_{ipso} η^5 -C₅H₄), 69.5 (η^5 -C₅H₅), 69.0 (C_{ortho} η^5 -C₅H₄), 68.9 (C_{ortho} η^5 -C₅H₄), 68.3 (C_{meta} η^5 -C₅H₄), 61.1 & 60.6 (-OCH₂-, -ve DEPT), 53.6 & 52.7 (α -C), 40.8 (-NHCH₂-, -ve DEPT), 30.9 & 28.7 {-N(CH₃)-}, 15.4 & 15.2 (-CH₃), 14.2 & 14.1 (-OCH₂CH₃).

***N*-(6-ferrocenyl-2-naphthoyl)-glycine-sarcosine ethyl ester 119**

The synthesis followed that of **115** using the following reagents: 6-ferrocenylnaphthalene-2-carboxylic acid (0.32 g, 0.9 mmol), 1-hydroxybenzotriazole (0.16 g, 1.2 mmol), triethylamine (5 ml), *N*-(3-



dimethylaminopropyl)-*N'*-ethylcarbodiimide hydrochloride (0.23 g, 1.2 mmol) and glycine-sarcosine ethyl ester trifluoroacetate salt (0.26 g, 0.9 mmol). The product was purified by column chromatography (eluant 1:1 hexane: ethyl acetate) to give the title compound as an orange solid (0.20 g, 43%), mp 64-65 °C;

$E^{0'}/\text{mV}$ 63 vs. Fc/Fc⁺;

Anal. Calc. for C₂₈H₂₈N₂O₄Fe: C, 65.6; H, 5.5; N, 5.5%. Found: C, 65.3; H, 5.7; N, 5.3;

m/z (ESI) 512.1398 [M]⁺. C₂₈H₂₈N₂O₄Fe requires 512.1398;

λ_{max} (CH₃CN)/nm 370 ($\epsilon/\text{dm}^3 \text{ mol}^{-1} \text{ cm}^{-1}$ 2670), 450 (1098);

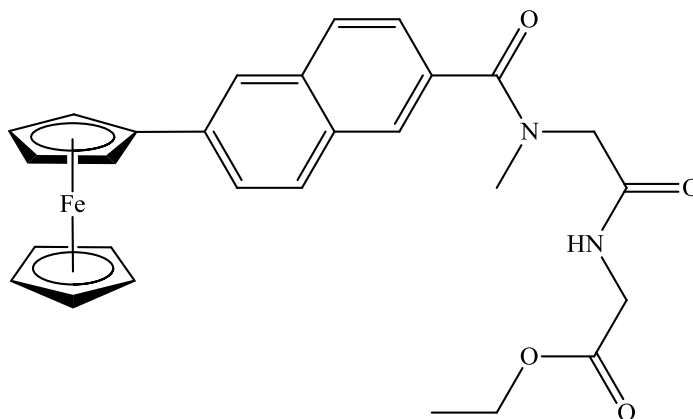
ν_{max} (neat)/cm⁻¹ 3300, 2928, 1739, 1626, 1507, 1480, 1200;

δ_{H} (400 MHz, DMSO-*d*₆): 8.72 & 7.45-7.51 (1H, t, *J* 5.6, m, -CONH-), 8.44-8.48 (1H, m, ArH), 8.05-8.07 (1H, m, ArH), 7.81-7.98 (4H, m, ArH), 4.95-4.97 {2H, m, *ortho* on (η^5 -C₅H₄)}, 4.44-4.46 {2H, m, *meta* on (η^5 -C₅H₄)}, 3.96-4.36 {11H, m, -OCH₂CH₃, η^5 -C₅H₅, -NHCH₂-, -N(CH₃)CH₂-}, 3.12 & 3.01 & 2.88 {3H, s, br. s, s, -N(CH₃)-}, 1.18-1.26 (3H, m, -OCH₂CH₃);

δ_{C} (100 MHz, DMSO-*d*₆): 171.2 (C=O), 169.2 (C=O), 166.4 (C=O), 138.8 (C_q), 134.5 (C_q), 133.4 (C_q), 130.7 (C_q), 128.7, 128.2, 127.4, 125.9, 124.4, 122.7, 84.1 (C_{*ipso*} η^5 -C₅H₄), 69.4 (η^5 -C₅H₅, C_{*meta*} η^5 -C₅H₄), 66.6 (C_{*ortho*} η^5 -C₅H₄), 60.9 & 60.5 (-OCH₂-, -ve DEPT), 49.3 {-N(CH₃)CH₂-, -ve DEPT}, 40.8 (-NHCH₂-, -ve DEPT), 35.2 & 34.5 & 30.7 {-N(CH₃)-}, 14.0 (-OCH₂CH₃).

***N*-(6-ferrocenyl-2-naphthoyl)-sarcosine-glycine ethyl ester 120**

The synthesis followed that of **115** using the following reagents: 6-ferrocenylnaphthalene-2-carboxylic acid (0.36 g, 1.0 mmol), 1-hydroxybenzotriazole (0.18 g, 1.3 mmol), triethylamine (5 ml), *N*-(3-dimethylaminopropyl)-*N'*-



ethylcarbodiimide hydrochloride (0.25 g, 1.3 mmol) and sarcosine-glycine ethyl ester trifluoroacetate salt (0.38 g, 1.3 mmol). The product was purified by column chromatography (eluant 1:1 hexane: ethyl acetate) to give the title compound as a red solid (0.18 g, 35%), mp 66-67 °C;

$E^{0'}/\text{mV}$ 55 vs. Fc/Fc⁺;

m/z (ESI) 512.2 [M]⁺. C₂₈H₂₈N₂O₄Fe requires 512.4;

m/z (ESI) 512.1399 [M]⁺. C₂₈H₂₈N₂O₄Fe requires 512.1398;

λ_{max} (CH₃CN)/nm 370 ($\epsilon/\text{dm}^3 \text{ mol}^{-1} \text{ cm}^{-1}$ 2492), 450 (988);

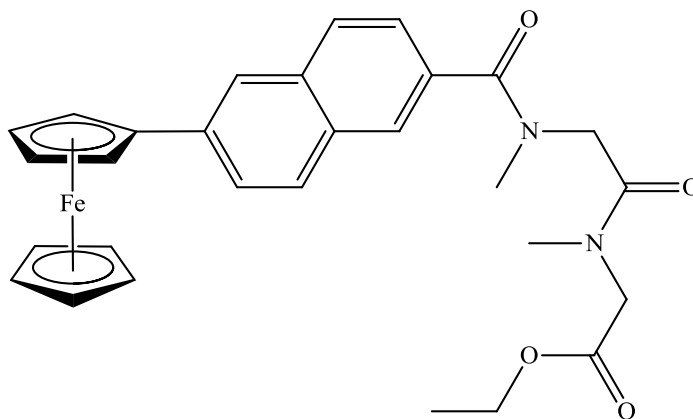
ν_{max} (neat)/cm⁻¹ 3291, 2930, 1745, 1677, 1623, 1507, 1396, 1196;

δ_{H} (600 MHz, DMSO-*d*₆): 8.61 & 8.53 (1H, br. s, br. s, -CONH-), 8.11 (1H, s, ArH), 7.95-8.03 (3H, m, ArH), 7.87 (1H, d, *J* 8.4, ArH), 7.54-7.58 (1H, m, ArH), 5.01 {2H, t, *J* 1.8, *ortho* on (η^5 -C₅H₄)}, 4.49-4.52 {2H, m, *meta* on (η^5 -C₅H₄)}, 3.96-4.26 {11H, m, -OCH₂CH₃, η^5 -C₅H₅, -NHCH₂-, -N(CH₃)CH₂-}, 3.08 {3H, s, -N(CH₃)-}, 1.27 (3H, t, *J* 7.2, -OCH₂CH₃);

δ_{C} (150 MHz, DMSO-*d*₆): 171.1 (C=O), 169.7 (C=O), 168.6 (C=O), 138.2 (C_q), 133.4 (C_q), 132.4 (C_q), 130.7 (C_q), 128.3, 126.5, 125.9, 125.0, 124.8, 122.8, 84.1 (C_{ipso} η^5 -C₅H₄), 69.41 (η^5 -C₅H₅), 69.38 (C_{meta} η^5 -C₅H₄), 66.6 (C_{ortho} η^5 -C₅H₄), 60.5 & 59.7 (-OCH₂-, -ve DEPT), 53.9 & 49.7 {-N(CH₃)CH₂-, -ve DEPT}, 40.7 (-NHCH₂-, -ve DEPT), 39.3 & 34.1 {-N(CH₃)-}, 14.1 (-OCH₂CH₃).

***N*-(6-ferrocenyl-2-naphthoyl)-sarcosine-sarcosine ethyl ester 121**

The synthesis followed that of **115** using the following reagents: 6-ferrocenylnaphthalene-2-carboxylic acid (0.27 g, 0.8 mmol), 1-hydroxybenzotriazole (0.14 g, 1.0 mmol), triethylamine (5 ml), *N*-(3-dimethylaminopropyl)-*N'*-



ethylcarbodiimide hydrochloride (0.20 g, 1.0 mmol) and sarcosine-sarcosine ethyl ester trifluoroacetate salt (0.23 g, 0.8 mmol). The product was purified by column chromatography (eluant 1:1 hexane: ethyl acetate) to give the title compound as an orange solid (0.05 g, 12%), mp 68-69 °C;

$E^{0'}/\text{mV}$ 58 vs. Fc/Fc⁺;

m/z (ESI) 526.2 [M]⁺. C₂₉H₃₀N₂O₄Fe requires 526.4;

m/z (ESI) 526.1536 [M]⁺. C₂₉H₃₀N₂O₄Fe requires 526.1555;

λ_{max} (CH₃CN)/nm 370 ($\epsilon/\text{dm}^3 \text{ mol}^{-1} \text{ cm}^{-1}$ 2106), 450 (836);

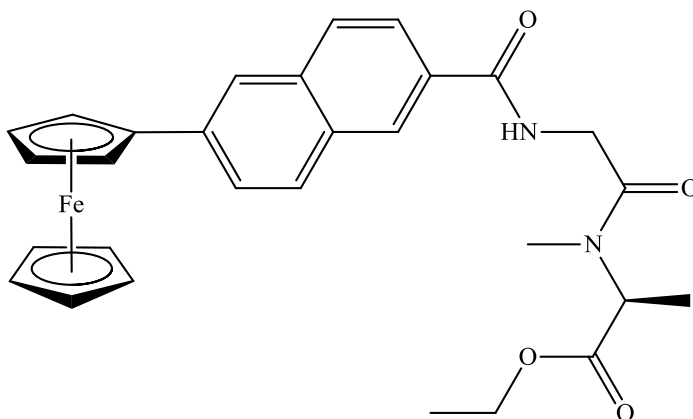
ν_{max} (neat)/cm⁻¹ 2926, 1739, 1663, 1626, 1479, 1394, 1198;

δ_{H} (600 MHz, DMSO-*d*₆): 8.08-8.11 (1H, m, ArH), 7.86-8.02 (4H, m, ArH), 7.54 & 7.42-7.46 (1H, d, *J* 8.4, m, ArH), 5.01 {2H, s, *ortho* on (η^5 -C₅H₄)}, 3.87-4.51 {13H, *meta* on (η^5 -C₅H₄)}, -OCH₂CH₃, η^5 -C₅H₅, -N(CH₃)CH₂-, -N(CH₃)CH₂-, 3.03-3.16 {3H, m, -N(CH₃)-}, 2.88-3.01 {3H, m, -N(CH₃)-}, 1.24-1.32 & 1.00 (3H, m, s, *J* 7.2, -OCH₂CH₃);

δ_{C} (150 MHz, DMSO-*d*₆): 171.0 (C=O), 169.1 (C=O), 168.1 (C=O), 138.1 (C_q), 133.4 (C_q), 132.5 (C_q), 130.7 (C_q), 128.2, 127.5, 126.3, 125.9, 124.7, 122.8, 84.2 (C_{ipso} η^5 -C₅H₄), 69.40 (η^5 -C₅H₅), 69.38 (C_{meta} η^5 -C₅H₄), 66.6 (C_{ortho} η^5 -C₅H₄), 60.58 & 60.54 (-OCH₂-, -ve DEPT), 52.48 & 49.60 & 49.23 & 48.36 {-N(CH₃)CH₂-, -ve DEPT}, 38.34 & 35.19 & 34.47 & 34.35 {-N(CH₃)-}, 14.1 (-OCH₂CH₃).

***N*-(6-ferrocenyl-2-naphthoyl)-glycine-*N*-methyl-L-alanine ethyl ester 122**

The synthesis followed that of **115** using the following reagents: 6-ferrocenylnaphthalene-2-carboxylic acid (0.32 g, 0.9 mmol), 1-hydroxybenzotriazole (0.12 g, 0.9 mmol), triethylamine (5 ml), *N*-(3-



ethylcarbodiimide hydrochloride (0.17 g, 0.9 mmol) and glycine-*N*-methyl-L-alanine ethyl ester trifluoroacetate salt (0.27 g, 0.9 mmol). The product was purified by column chromatography (eluant 1:1 hexane: ethyl acetate) to give the title compound as an orange solid (0.04 g, 9%), mp 63-64 °C;

$E^{0'}/\text{mV}$ 63 vs. Fc/Fc⁺;

$[\alpha]_D^{20}$ -9 (*c* 0.05 in CH₃CN);

m/z (ESI) 526.2 [M]⁺. C₂₉H₃₀N₂O₄Fe requires 526.4;

m/z (ESI) 526.1561 [M]⁺. C₂₉H₃₀N₂O₄Fe requires 526.1555;

λ_{max} (CH₃CN)/nm 370 ($\epsilon/\text{dm}^3 \text{ mol}^{-1} \text{ cm}^{-1}$ 2450), 450 (1016);

ν_{max} (neat)/cm⁻¹ 3332, 2928, 1733, 1639, 1512, 1480, 1203;

δ_{H} (600 MHz, DMSO-*d*₆): 8.75-8.78 (1H, m, -CONH-), 8.46-8.55 (1H, m, ArH), 8.12 (1H, s, ArH), 7.96-8.03 (3H, m, ArH), 7.89 (1H, dd, *J* 1.8 and 8.4, ArH), 5.02 {2H, t, *J* 1.8, *ortho* on (η^5 -C₅H₄)}, 4.95-4.99 {1H, m, -N(CH₃)CH-}, 4.51 {2H, t, *J* 1.8, *meta* on (η^5 -C₅H₄)}, 4.13-4.39 (9H, m, -OCH₂CH₃, η^5 -C₅H₅, -NHCH₂-), 3.06 & 2.80 {3H, s, s, -N(CH₃)-}, 1.49 & 1.39 (3H, d, *J* 7.2, d, *J* 7.2, -CH₃), 1.24-1.29 (3H, m, -OCH₂CH₃);

δ_{C} (150 MHz, DMSO-*d*₆): 171.2 (C=O), 168.8 (C=O), 166.4 (C=O), 138.8 (C_q), 134.5 (C_q), 130.7 (C_q), 130.5 (C_q), 128.8, 127.4, 127.3, 126.0, 124.4, 122.8, 84.1 (C_{ipso} η^5 -C₅H₄), 69.5 (η^5 -C₅H₅), 69.4 (C_{meta} η^5 -C₅H₄), 66.7 (C_{ortho} η^5 -C₅H₄), 60.6 (-OCH₂-, -ve DEPT), 52.8 (α -C), 41.2 (-NHCH₂-, -ve DEPT), 30.9 {-N(CH₃)-}, 15.2 (-CH₃), 14.1 & 14.0 (-OCH₂CH₃).

***N*-(3-ferrocenyl-2-naphthoyl)-glycine-D-alanine ethyl ester 123**

The synthesis followed that of **115** using the following reagents: 3-ferrocenylnaphthalene-2-carboxylic acid (0.32 g, 0.9 mmol), 1-hydroxybenzotriazole (0.16 g, 1.2 mmol), triethylamine (5 ml), *N*-(3-dimethylaminopropyl)-*N'*-ethylcarbodiimide hydrochloride (0.23 g, 1.2 mmol) and glycine-D-alanine ethyl ester trifluoroacetate salt (0.26 g, 0.9 mmol). The product was purified by column chromatography (eluant 1:1 hexane: ethyl acetate) to give the title compound as an orange solid (0.19 g, 41%), mp 63-64 °C;

$E^{0'}/\text{mV}$ 24 vs. Fc/Fc⁺;

$[\alpha]_D^{20} +2$ (*c* 0.05 in CH₃CN);

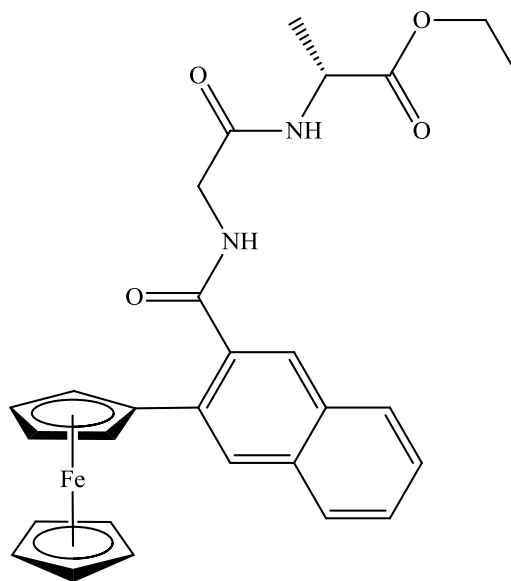
Anal. calcd. for C₂₈H₂₈N₂O₄Fe requires: C, 65.6; H, 5.5; N, 5.5%. Found: C, 64.85; H, 5.4 N, 5.2;

$\lambda_{\text{max}}(\text{CH}_3\text{CN})/\text{nm}$ 435 ($\epsilon/\text{dm}^3 \text{ mol}^{-1} \text{ cm}^{-1}$ 395);

$\nu_{\text{max}}(\text{neat})/\text{cm}^{-1}$ 3285, 3081, 1733, 1643, 1516, 1450, 1203;

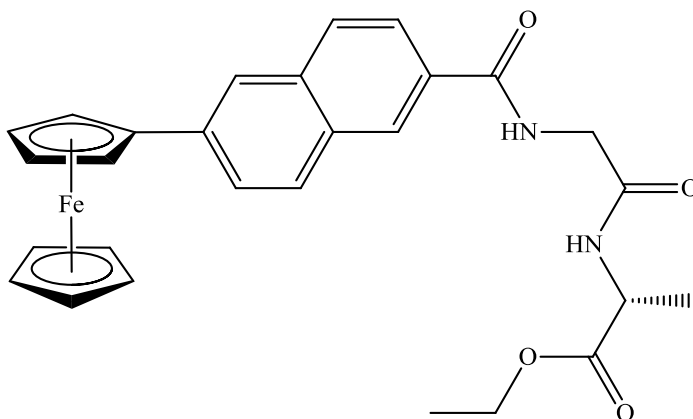
δ_{H} (400 MHz, DMSO-*d*₆): 8.69 (1H, t, *J* 5.6, -CONH-), 8.36 (1H, d, *J* 7.2, -CONH-), 8.32 (1H, s, ArH), 7.99 (1H, d, *J* 8.0, ArH), 7.90 (1H, d, *J* 8.0, ArH), 7.84 (1H, s, ArH), 7.49-7.58 (2H, m, ArH), 4.81-4.82 {2H, m, *ortho* on (η^5 -C₅H₄)}, 4.31-4.37 {3H, m, -NHCH-, *meta* on (η^5 -C₅H₄)}, 4.08-4.16 (7H, m, -OCH₂CH₃, η^5 -C₅H₅), 3.97 (1H, dd, *J* 5.6 and 16.4, -NHCH₂-), 3.88 (1H, dd, *J* 5.6 and 16.4, -NHCH₂-), 1.33 (H, d, *J* 7.2, -CH₃), 1.22 (3H, t, *J* 7.2, -OCH₂CH₃);

δ_{C} (100 MHz, DMSO-*d*₆): 172.5 (C=O), 169.8 (C=O), 168.6 (C=O), 135.0 (C_q), 134.3 (C_q), 132.9 (C_q), 130.5 (C_q), 128.1, 127.6, 127.4, 127.0, 126.7, 126.0, 84.3 (C_{ipso} η^5 -C₅H₄), 69.5 (η^5 -C₅H₅), 69.0 (C_{ortho} η^5 -C₅H₄), 68.3 (C_{meta} η^5 -C₅H₄), 60.5 (-OCH₂-, -ve DEPT), 47.7 (α -C), 41.8 (-NHCH₂-, -ve DEPT), 17.1 (-CH₃), 14.0 (-OCH₂CH₃).



***N*-(6-ferrocenyl-2-naphthoyl)-glycine-D-alanine ethyl ester 124**

The synthesis followed that of **115** using the following reagents: 6-ferrocenylnaphthalene-2-carboxylic acid (0.32 g, 0.9 mmol), 1-hydroxybenzotriazole (0.16 g, 1.2 mmol), triethylamine (5 ml), *N*-(3-



dimethylaminopropyl)-*N'*-ethylcarbodiimide hydrochloride (0.23 g, 1.2 mmol) and glycine-D-alanine ethyl ester trifluoroacetate salt (0.26 g, 0.9 mmol). The product was purified by column chromatography (eluant 1:1 hexane: ethyl acetate) to give the title compound as an orange solid (0.19 g, 41%), mp 73-74 °C;

$E^{0'}/\text{mV}$ 63 vs. Fc/Fc^+ ;

$[\alpha]_D^{20}$ +5 (*c* 0.05 in CH_3CN);

m/z (ESI) 512.2 $[\text{M}]^+$. $\text{C}_{28}\text{H}_{28}\text{N}_2\text{O}_4\text{Fe}$ requires 512.4;

m/z (ESI) 512.1397 $[\text{M}]^+$. $\text{C}_{28}\text{H}_{28}\text{N}_2\text{O}_4\text{Fe}$ requires 512.1398;

$\lambda_{\text{max}}(\text{CH}_3\text{CN})/\text{nm}$ 370 ($\epsilon/\text{dm}^3 \text{ mol}^{-1} \text{ cm}^{-1}$ 3048), 445 (1288);

$\nu_{\text{max}}(\text{neat})/\text{cm}^{-1}$ 3290, 3084, 1733, 1640, 1529, 1450, 1206;

δ_{H} (400 MHz, $\text{DMSO}-d_6$): 8.83 (1H, t, J 5.6, -CONH-), 8.44 (1H, s, ArH), 8.39 (1H, d, J 7.2, -CONH-), 8.06 (1H, s, ArH), 7.94-7.97 (3H, m, ArH), 7.83 (1H, dd, J 1.6 and 8.4, ArH), 4.97 {2H, t, J 2.0, *ortho* on (η^5 - C_5H_4)}, 4.46 {2H, m, J 2.0, *meta* on (η^5 - C_5H_4)}, 4.31 (1H, qt, J 7.2, -NHCH-), 3.91-4.14 (9H, m, - OCH_2CH_3 , η^5 - C_5H_5 , -NHCH₂-), 1.31 (3H, d, J 7.2, -CH₃), 1.20 (3H, t, J 7.2, - OCH_2CH_3);

δ_{C} (100 MHz, $\text{DMSO}-d_6$): 172.5 (C=O), 168.9 (C=O), 166.4 (C=O), 138.8 (C_q), 134.5 (C_q), 130.7 (C_q), 130.5 (C_q), 128.7, 127.5, 127.3, 125.9, 124.5, 122.7, 84.1 (C_{ipso} η^5 - C_5H_4), 69.4 (η^5 - C_5H_5 , C_{meta} η^5 - C_5H_4), 66.6 (C_{ortho} η^5 - C_5H_4), 60.4 (- OCH_2 -, -ve DEPT), 47.7 (α -C), 42.2 (-NHCH₂-, -ve DEPT), 17.1 (-CH₃), 14.0 (- OCH_2CH_3).

***N*-(3-ferrocenyl-2-naphthoyl)-glycine- β -alanine ethyl ester 125**

The synthesis followed that of **115** using the following reagents: 3-ferrocenylnaphthalene-2-carboxylic acid (0.32 g, 0.9 mmol), 1-hydroxybenzotriazole (0.16 g, 1.2 mmol), triethylamine (5 ml), *N*-(3-dimethylaminopropyl)-*N'*-ethylcarbodiimide hydrochloride (0.23 g, 1.2 mmol) and glycine- β -alanine ethyl ester trifluoroacetate salt (0.26 g, 0.9 mmol). The product was purified by column chromatography (eluant 1:1 hexane: ethyl acetate) to give the title compound as an orange solid (0.14 g, 30%), mp 49-50 °C;

E^0/mV 27 vs. Fc/Fc⁺;

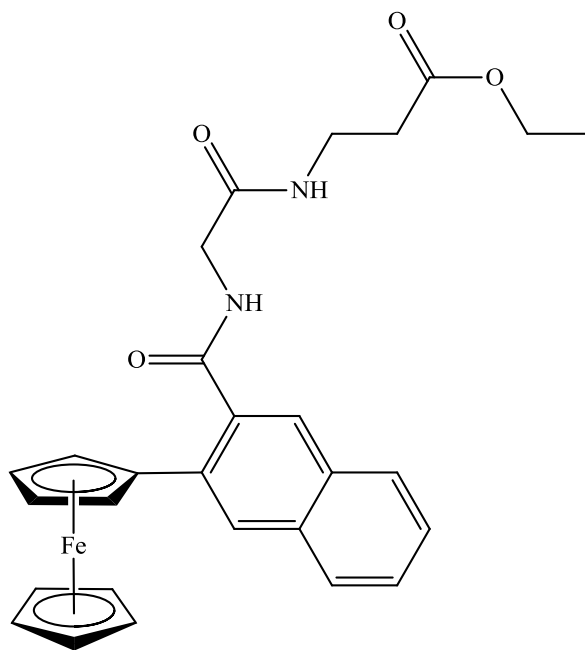
Anal. Calc. for C₂₈H₂₈N₂O₄Fe: C, 65.6; H, 5.5; N, 5.5%. Found: C, 65.6; H, 5.65; N, 5.25;

$\lambda_{max}(CH_3CN)/nm$ 450 ($\epsilon/dm^3 mol^{-1} cm^{-1}$ 533);

$\nu_{max}(neat)/cm^{-1}$ 3285, 3085, 1728, 1644, 1519, 1183;

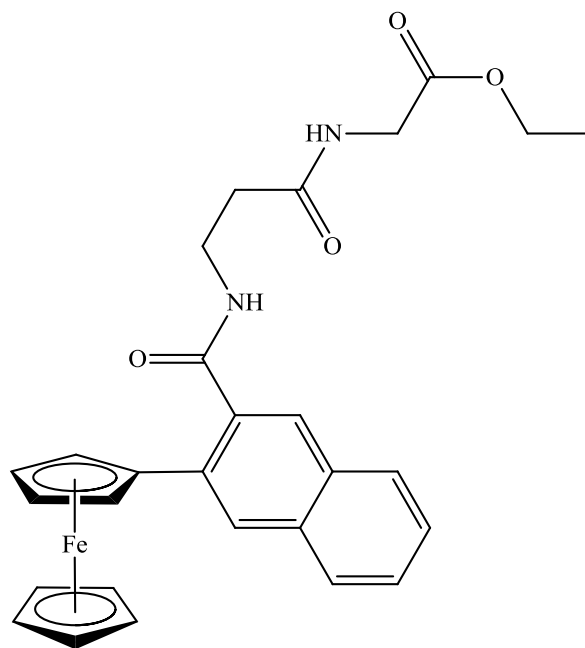
δ_H (400 MHz, acetone-*d*₆): 8.26 (1H, s, ArH), 7.85 (1H, d, *J* 8.0, ArH), 7.77-7.78 (2H, m, ArH), 7.36-7.44 (3H, m, -CONH-, ArH), 7.09 (1H, br. s, -CONH-), 4.66 {2H, t, *J* 2.0, *ortho* on (η^5 -C₅H₄)}, 4.20 {2H, t, *J* 2.0, *meta* on (η^5 -C₅H₄)}, 3.96-4.01 (7H, m, -OCH₂CH₃, η^5 -C₅H₅), 3.84 (2H, d, *J* 5.6, -NHCH₂-), 3.34 (2H, q, *J* 5.6, -CH₂CH₂-), 2.40 (2H, t, *J* 6.8, -CH₂CH₂-), 1.09 (3H, t, *J* 7.2, -OCH₂CH₃);

δ_C (100 MHz, acetone-*d*₆): 172.3 (C=O), 171.1 (C=O), 169.5 (C=O), 136.3 (C_q), 135.3 (C_q), 134.5 (C_q), 132.1 (C_q), 129.6, 128.7, 128.4, 127.9, 127.8, 126.9, 86.1 (C_{ipso} η^5 -C₅H₄), 70.5 (η^5 -C₅H₅), 70.2 (C_{ortho} η^5 -C₅H₄), 69.3 (C_{meta} η^5 -C₅H₄), 60.9 (-OCH₂-, -ve DEPT), 43.9 (-NHCH₂-, -ve DEPT), 35.8 (-CH₂CH₂-, -ve DEPT), 34.8 (-CH₂CH₂-, -ve DEPT), 14.5 (-OCH₂CH₃).



***N*-(3-ferrocenyl-2-naphthoyl)- β -alanine-glycine ethyl ester 126**

The synthesis followed that of **115** using the following reagents: 3-ferrocenylnaphthalene-2-carboxylic acid (0.32 g, 0.9 mmol), 1-hydroxybenzotriazole (0.18 g, 1.3 mmol), triethylamine (5 ml), *N*-(3-dimethylaminopropyl)-*N'*-ethylcarbodiimide hydrochloride (0.25 g, 1.3 mmol) and β -alanine-glycine ethyl ester trifluoroacetate salt (0.29 g, 1.0 mmol). The product was purified by column chromatography (eluant 1:1 hexane: ethyl acetate) to give the title compound as an orange solid (0.30 g, 59%), mp 56-57 °C;



E^0/mV 34 vs. Fc/Fc^+ ;

$\lambda_{max}(CH_3CN)/nm$ 450 ($\epsilon/dm^3 mol^{-1} cm^{-1}$ 521);

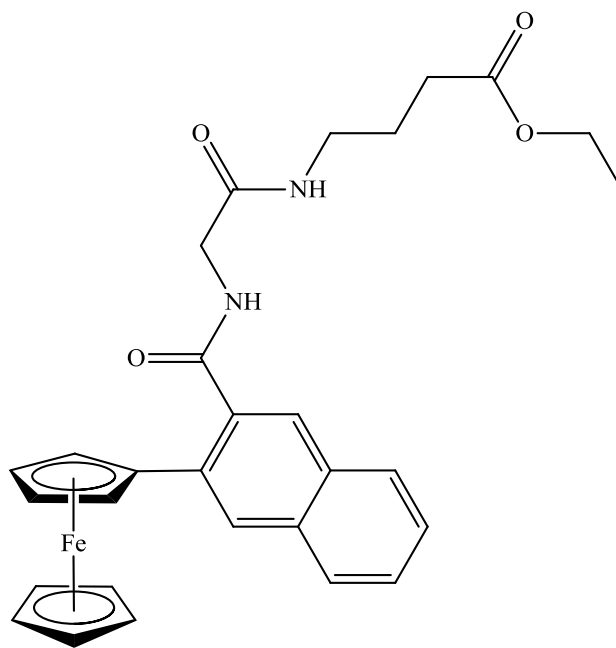
$\nu_{max}(neat)/cm^{-1}$ 3286, 3082, 1745, 1698, 1644, 1521, 1192;

δ_H (400 MHz, acetone- d_6): 8.23 (1H, s, ArH), 7.82 (1H, d, J 8.0, ArH), 7.76 (1H, d, J 8.0, ArH), 7.71 (1H, s, ArH), 7.33-7.45 (3H, m, -CONH-, ArH), 7.17 (1H, br. s, -CONH-), 4.64 (2H, t, J 2.0, *ortho* on (η^5 - C_5H_4)), 4.18 {2H, t, J 2.0, *meta* on (η^5 - C_5H_4)}, 3.96-4.02 (7H, m, - OCH_2CH_3 , η^5 - C_5H_5), 3.80 (2H, d, J 5.6, - $NHCH_2$ -), 3.48 (2H, q, J 5.6, - CH_2CH_2 -), 2.42 (2H, t, J 6.8, - CH_2CH_2 -), 1.07 (3H, t, J 7.2, - OCH_2CH_3);

δ_C (100 MHz, acetone- d_6): 172.0 (C=O), 170.7 (C=O), 169.5 (C=O), 136.9 (C_q), 135.3 (C_q), 134.4 (C_q), 132.2 (C_q), 129.5, 128.7, 128.4, 127.8, 127.6, 126.8, 86.1 (C_{ipso} η^5 - C_5H_4), 70.5 (η^5 - C_5H_5), 70.2 (C_{ortho} η^5 - C_5H_4), 69.2 (C_{meta} η^5 - C_5H_4), 61.4 (- OCH_2 -, -ve DEPT), 41.7 (- $NHCH_2$ -, -ve DEPT), 36.9 (- CH_2CH_2 -, -ve DEPT), 35.9 (- CH_2CH_2 -, -ve DEPT), 14.5 (- OCH_2CH_3).

***N*-(3-ferrocenyl-2-naphthoyl)-glycine- γ -aminobutyric acid ethyl ester 127**

The synthesis followed that of **115** using the following reagents: 3-ferrocenylnaphthalene-2-carboxylic acid (0.32 g, 0.9 mmol), 1-hydroxybenzotriazole (0.16 g, 1.2 mmol), triethylamine (5 ml), *N*-(3-dimethylaminopropyl)-*N'*-ethylcarbodiimide hydrochloride (0.23 g, 1.2 mmol) and glycine- γ -aminobutyric acid ethyl ester trifluoroacetate salt (0.27 g, 0.9 mmol). The product was purified by column chromatography (eluant 1:1



hexane: ethyl acetate) to give the title compound as an orange solid (0.19 g, 40%), mp 47-48 °C;

$E^{0'}/\text{mV}$ 28 vs. Fc/Fc^+ ;

Anal. Calc. for $\text{C}_{29}\text{H}_{30}\text{N}_2\text{O}_4\text{Fe}$: C, 66.2; H, 5.7; N, 5.3%. Found: C, 65.9; H, 5.8; N, 5.1;

$\lambda_{\text{max}}(\text{CH}_3\text{CN})/\text{nm}$ 450 ($\epsilon/\text{dm}^3 \text{ mol}^{-1} \text{ cm}^{-1}$ 451);

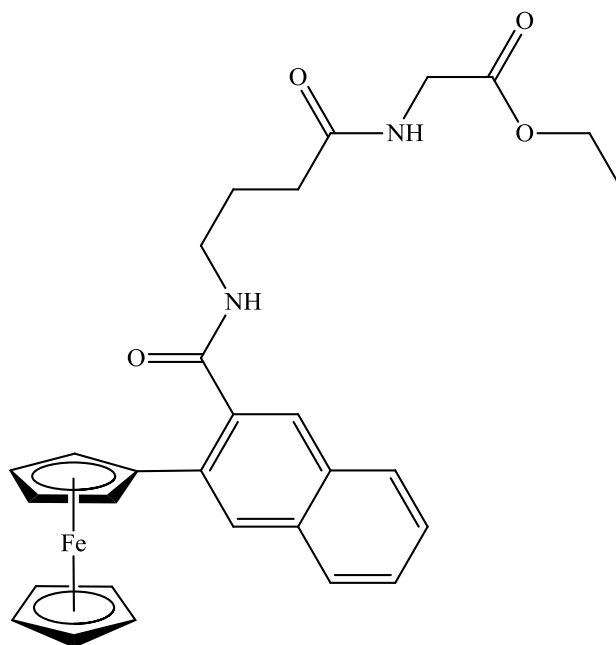
$\nu_{\text{max}}(\text{neat})/\text{cm}^{-1}$ 3281, 3086, 1727, 1640, 1521, 1176;

δ_{H} (400 MHz, acetone- d_6): 8.27 (1H, s, ArH), 7.85 (1H, d, J 8.0, ArH), 7.76-7.78 (2H, m, ArH), 7.36-7.44 (3H, m, -CONH-, ArH), 6.95 (1H, br. s, -CONH-), 4.66 {2H, t, J 2.0, *ortho* on ($\eta^5\text{-C}_5\text{H}_4$)}, 4.20 {2H, t, J 2.0, *meta* on ($\eta^5\text{-C}_5\text{H}_4$)}, 3.93-4.00 (7H, m, $\eta^5\text{-C}_5\text{H}_5$, -OCH₂CH₃), 3.85 (2H, d, J 5.6, -NHCH₂-), 3.13 (2H, q, J 6.8, -CH₂CH₂CH₂-), 2.21 (2H, t, J 7.2, -CH₂CH₂CH₂-), 1.65 (2H, qt, J 7.2, -CH₂CH₂CH₂-), 1.08 (3H, t, J 7.2, -OCH₂CH₃);

δ_{C} (100 MHz, acetone- d_6): 173.4 (C=O), 171.0 (C=O), 169.5 (C=O), 136.4 (C_q), 135.3 (C_q), 134.5 (C_q), 132.1 (C_q), 129.7, 128.7, 128.4, 127.9, 127.7, 126.9, 86.2 (C_{ipso} $\eta^5\text{-C}_5\text{H}_4$), 70.6 ($\eta^5\text{-C}_5\text{H}_5$), 70.3 (C_{ortho} $\eta^5\text{-C}_5\text{H}_4$), 69.3 (C_{meta} $\eta^5\text{-C}_5\text{H}_4$), 60.6 (-OCH₂-, -ve DEPT), 43.9 (-NHCH₂-, -ve DEPT), 39.1 (-CH₂CH₂CH₂-, -ve DEPT), 31.9 (-CH₂CH₂CH₂-, -ve DEPT), 25.8 (-CH₂CH₂CH₂-, -ve DEPT), 14.6 (-OCH₂CH₃).

***N*-(3-ferrocenyl-2-naphthoyl)- γ -aminobutyric acid-glycine ethyl ester 128**

The synthesis followed that of **115** using the following reagents: 3-ferrocenylnaphthalene-2-carboxylic acid (0.36 g, 1.0 mmol), 1-hydroxybenzotriazole (0.18 g, 1.3 mmol), triethylamine (5 ml), *N*-(3-dimethylaminopropyl)-*N'*-ethylcarbodiimide hydrochloride (0.25 g, 1.3 mmol) and γ -aminobutyric acid-glycine ethyl ester trifluoroacetate salt (0.39 g, 1.3 mmol). The product was purified by column chromatography



(eluant 1:1 hexane: ethyl acetate) to give the title compound as an orange solid (0.28 g, 53%), mp 64 °C;

$E^{0'}/\text{mV}$ 38 vs. Fc/Fc^+ ;

$\lambda_{\text{max}}(\text{CH}_3\text{CN})/\text{nm}$ 450 ($\epsilon/\text{dm}^3 \text{ mol}^{-1} \text{ cm}^{-1}$ 509);

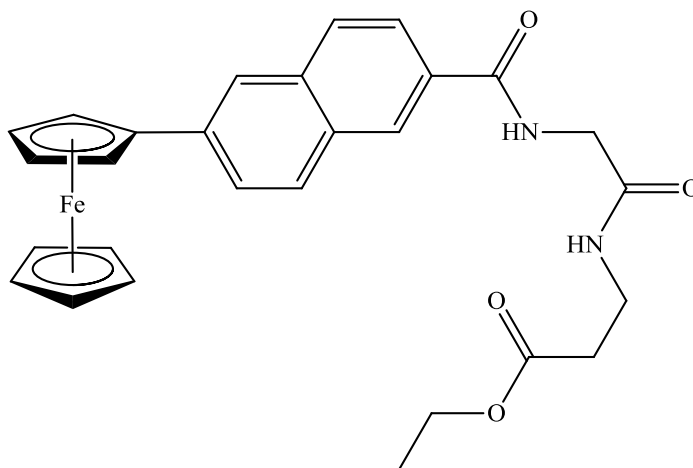
$\nu_{\text{max}}(\text{neat})/\text{cm}^{-1}$ 3280, 3083, 1746, 1698, 1641, 1522, 1194;

δ_{H} (400 MHz, acetone- d_6): 8.24 (1H, s, ArH), 7.83 (1H, d, J 8.0, ArH), 7.75 (1H, d, J 7.6, ArH), 7.66 (1H, s, ArH), 7.34-7.46 (3H, m, -CONH-, ArH), 7.25 (1H, br. s, -CONH-), 4.64 {2H, t, J 2.0, *ortho* on (η^5 - C_5H_4)}, 4.19 {2H, t, J 2.0, *meta* on (η^5 - C_5H_4)}, 3.93-4.00 (7H, m, - OCH_2CH_3 , η^5 - C_5H_5), 3.79 (2H, d, J 6.0, - NHCH_2 -), 3.28 (2H, q, J 5.6, - $\text{CH}_2\text{CH}_2\text{CH}_2$ -), 2.17 (2H, t, J 7.2, - $\text{CH}_2\text{CH}_2\text{CH}_2$ -), 1.74 (2H, qt, J 7.2, - $\text{CH}_2\text{CH}_2\text{CH}_2$ -), 1.07 (3H, t, J 7.2, - OCH_2CH_3);

δ_{C} (100 MHz, acetone- d_6): 173.3 (C=O), 170.9 (C=O), 170.8 (C=O), 137.2 (C_q), 135.3 (C_q), 134.4 (C_q), 132.2 (C_q), 129.4, 128.7, 128.3, 127.7, 127.5, 126.8, 86.1 ($\text{C}_{\text{ipso}} \eta^5$ - C_5H_4), 70.5 (η^5 - C_5H_5), 70.2 ($\text{C}_{\text{ortho}} \eta^5$ - C_5H_4), 69.3 ($\text{C}_{\text{meta}} \eta^5$ - C_5H_4), 61.3 (- OCH_2 -, -ve DEPT), 41.7 (- NHCH_2 -, -ve DEPT), 39.9 (- $\text{CH}_2\text{CH}_2\text{CH}_2$ -, -ve DEPT), 34.0 (- $\text{CH}_2\text{CH}_2\text{CH}_2$ -, -ve DEPT), 26.3 (- $\text{CH}_2\text{CH}_2\text{CH}_2$ -, -ve DEPT), 14.5 (- OCH_2CH_3).

***N*-(6-ferrocenyl-2-naphthoyl)-glycine- β -alanine ethyl ester 129**

The synthesis followed that of **115** using the following reagents: 6-ferrocenylnaphthalene-2-carboxylic acid (0.32 g, 0.9 mmol), 1-hydroxybenzotriazole (0.16 g, 1.2 mmol), triethylamine (5 ml), *N*-(3-dimethylaminopropyl)-*N'*-ethylcarbodiimide hydrochloride



(0.23 g, 1.2 mmol) and glycine- β -alanine ethyl ester trifluoroacetate salt (0.26 g, 0.9 mmol). The product was purified by column chromatography (eluant 1:1 hexane: ethyl acetate) to give the title compound as an orange solid (0.20 g, 43%), mp 148-149 °C; $E^{0'}/\text{mV}$ 61 vs. Fc/Fc⁺;

m/z (ESI) 512.2 [M]⁺. C₂₈H₂₈N₂O₄Fe requires 512.4;

m/z (ESI) 512.1410 [M]⁺. C₂₈H₂₈N₂O₄Fe requires 512.1398;

λ_{max} (CH₃CN)/nm 370 ($\epsilon/\text{dm}^3 \text{ mol}^{-1} \text{ cm}^{-1}$ 3006), 450 (1288);

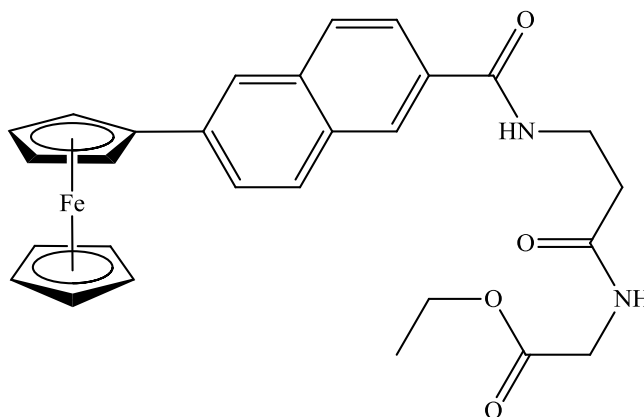
ν_{max} (neat)/cm⁻¹ 3312, 3084, 1728, 1677, 1639, 1625, 1538, 1185;

δ_{H} (400 MHz, acetone-*d*₆): 8.32 (1H, s, ArH), 8.01 (1H, t, *J* 5.6, -CONH-), 7.93 (1H, s, ArH), 7.78-7.86 (3H, m, ArH), 7.71 (1H, dd, *J* 1.6 and 8.4, ArH), 7.34 (1H, br. s, -CONH-), 4.79 {2H, t, *J* 2.0, *ortho* on (η^5 -C₅H₄)}, 4.30 {2H, t, *J* 2.0, *meta* on (η^5 -C₅H₄)}, 3.91-3.97 (9H, m, -OCH₂CH₃, η^5 -C₅H₅, -NHCH₂-), 3.35 (2H, q, *J* 6.8, -CH₂CH₂-), 2.40 (2H, t, *J* 6.8, -CH₂CH₂-), 1.06 (3H, t, *J* 7.2, -OCH₂CH₃);

δ_{C} (100 MHz, acetone-*d*₆): 172.2 (C=O), 169.9 (C=O), 167.7 (C=O), 140.3 (C_q), 136.1 (C_q), 132.2 (C_q), 131.7 (C_q), 129.7, 128.5, 128.4, 126.9, 125.3, 123.9, 85.4 (C_{ipso} η^5 -C₅H₄), 70.4 (η^5 -C₅H₅), 70.3 (C_{meta} η^5 -C₅H₄), 67.6 (C_{ortho} η^5 -C₅H₄), 60.8 (-OCH₂-, -ve DEPT), 44.1 (-NHCH₂-, -ve DEPT), 35.9 (-CH₂CH₂-, -ve DEPT), 34.9 (-CH₂CH₂-, -ve DEPT), 14.5 (-OCH₂CH₃).

***N*-(6-ferrocenyl-2-naphthoyl)- β -alanine-glycine ethyl ester 130**

The synthesis followed that of **115** using the following reagents: 6-ferrocenylnaphthalene-2-carboxylic acid (0.32 g, 0.9 mmol), 1-hydroxybenzotriazole (0.18 g, 1.3 mmol), triethylamine (5 ml), *N*-(3-dimethylaminopropyl)-*N'*-ethylcarbodiimide hydrochloride (0.25



g, 1.3 mmol) and β -alanine-glycine ethyl ester trifluoroacetate salt (0.29 g, 1.0 mmol). The product was purified by column chromatography (eluant 1:1 hexane: ethyl acetate) to give the title compound as an orange solid (0.16 g, 34%), mp 171-172 °C; $E^{0'}/mV$ 60 vs. Fc/Fc⁺; $\lambda_{max}(CH_3CN)/nm$ 370 ($\epsilon/dm^3 mol^{-1} cm^{-1}$ 2758), 450 (1154);

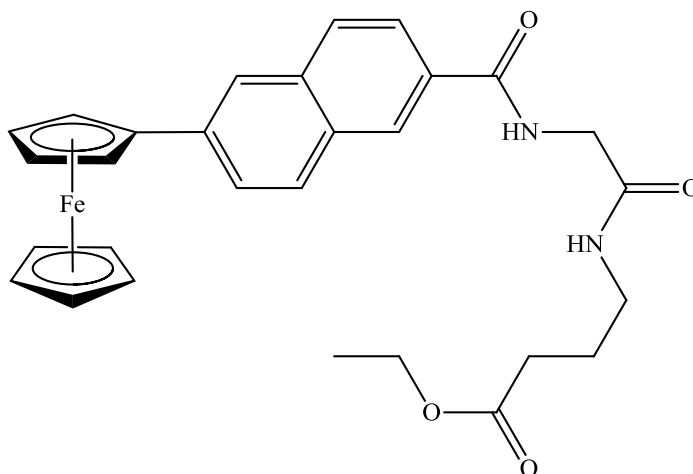
$\nu_{max}(neat)/cm^{-1}$ 3357, 3282, 3073, 1735, 1678, 1633, 1600, 1540, 1214;

δ_H (400 MHz, acetone-*d*₆): 8.28 (1H, s, ArH), 7.92 (1H, s, ArH), 7.76-7.84 (4H, m, -CONH-, ArH), 7.69 (1H, dd, *J* 1.6 and 8.8, ArH), 7.51 (1H, br. s, -CONH-), 4.78 {2H, t, *J* 1.6, *ortho* on (η^5 -C₅H₄)}, 4.29 {2H, t, *J* 1.6, *meta* on (η^5 -C₅H₄)}, 4.02 (2H, q, *J* 7.2, -OCH₂CH₃), 3.92 (5H, s, η^5 -C₅H₅), 3.84 (2H, d, *J* 5.6, -NHCH₂-), 3.59 (2H, q, *J* 6.4, -CH₂CH₂-), 2.47 (2H, t, *J* 6.4, -CH₂CH₂-), 1.09 (3H, t, *J* 7.2, -OCH₂CH₃);

δ_C (100 MHz, acetone-*d*₆): 172.4 (C=O), 170.8 (C=O), 167.3 (C=O), 140.0 (C_q), 135.9 (C_q), 132.4 (C_q), 132.2 (C_q), 129.6, 128.4, 128.1, 126.9, 125.4, 123.9, 85.5 (C_{ipso} η^5 -C₅H₄), 70.4 (η^5 -C₅H₅), 70.3 (C_{meta} η^5 -C₅H₄), 67.6 (C_{ortho} η^5 -C₅H₄), 61.4 (-OCH₂-, -ve DEPT), 41.7 (-NHCH₂-, -ve DEPT), 37.2 (-CH₂CH₂-, -ve DEPT), 36.3 (-CH₂CH₂-, -ve DEPT), 14.5 (-OCH₂CH₃).

***N*-(6-ferrocenyl-2-naphthoyl)-glycine- γ -aminobutyric acid ethyl ester 131**

The synthesis followed that of **115** using the following reagents: 6-ferrocenylnaphthalene-2-carboxylic acid (0.32 g, 0.9 mmol), 1-hydroxybenzotriazole (0.16 g, 1.2 mmol), triethylamine (5 ml), *N*-(3-dimethylaminopropyl)-*N'*-ethylcarbodiimide hydrochloride



(0.23 g, 1.2 mmol) and glycine- γ -aminobutyric acid ethyl ester trifluoroacetate salt (0.27 g, 0.9 mmol). The product was purified by column chromatography (eluant 1:1 hexane: ethyl acetate) to give the title compound as an orange solid (0.18 g, 38%), mp 140-142 °C;

$E^{0'}/\text{mV}$ 65 vs. Fc/Fc⁺;

Anal. Calc. for C₂₉H₃₀N₂O₄Fe: C, 66.2; H, 5.7; N, 5.3%. Found: C, 65.9; H, 5.9; N, 5.1;

$\lambda_{\text{max}}(\text{CH}_3\text{CN})/\text{nm}$ 375 ($\epsilon/\text{dm}^3 \text{ mol}^{-1} \text{ cm}^{-1}$ 3070), 450 (1312);

$\nu_{\text{max}}(\text{neat})/\text{cm}^{-1}$ 3374, 3246, 3082, 1704, 1672, 1638, 1566, 1538;

δ_{H} (400 MHz, acetone-*d*₆): 8.32 (1H, s, ArH), 8.01 (1H, t, *J* 5.6, -CONH-), 7.94 (1H, s, ArH), 7.78-7.86 (3H, m, ArH), 7.71 (1H, dd, *J* 1.6 and 8.4, ArH), 7.33 (1H, br. s, -CONH-), 4.78 {2H, t, *J* 2.0, *ortho* on (η^5 -C₅H₄)}, 4.30 {2H, t, *J* 2.0, *meta* on (η^5 -C₅H₄)}, 3.90-3.96 (9H, m, -OCH₂CH₃, η^5 -C₅H₅, -NHCH₂-), 3.15 (2H, q, *J* 6.8, -CH₂CH₂CH₂-), 2.22 (2H, t, *J* 7.2, -CH₂CH₂CH₂-), 1.66 (2H, qt, *J* 7.2, -CH₂CH₂CH₂-), 1.06 (3H, t, *J* 7.2, -OCH₂CH₃);

δ_{C} (100 MHz, acetone-*d*₆): 173.5 (C=O), 169.8 (C=O), 167.7 (C=O), 140.3 (C_q), 136.1 (C_q), 132.2 (C_q), 131.8 (C_q), 129.7, 128.5, 128.4, 126.9, 125.4, 123.9, 85.4 (*C*_{ipso} η^5 -C₅H₄), 70.4 (η^5 -C₅H₅), 70.3 (*C*_{meta} η^5 -C₅H₄), 67.6 (*C*_{ortho} η^5 -C₅H₄), 60.6 (-OCH₂-, -ve DEPT), 44.1 (-NHCH₂-, -ve DEPT), 39.1 (-CH₂CH₂CH₂-, -ve DEPT), 32.0 (-CH₂CH₂CH₂-, -ve DEPT), 25.8 (-CH₂CH₂CH₂-, -ve DEPT), 14.5 (-OCH₂CH₃).

***N*-(6-ferrocenyl-2-naphthoyl)- γ -aminobutyric acid-glycine ethyl ester 132**

The synthesis followed that of **115**

using the following reagents: 6-

ferrocenylnaphthalene-2-

carboxylic acid (0.36 g, 1.0

mmol), 1-hydroxybenzotriazole

(0.18 g, 1.3 mmol), triethylamine

(5 ml), *N*-(3-

dimethylaminopropyl)-*N'*-

ethylcarbodiimide hydrochloride

(0.25 g, 1.3 mmol) and γ -aminobutyric acid-glycine ethyl ester trifluoroacetate salt (0.39 g,

1.3 mmol). The product was purified by column chromatography (eluant 1:1 hexane: ethyl acetate) to give the title compound as an orange solid (0.14 g, 27%), mp 150-151 °C;

$E^{0'}$ /mV 60 vs. Fc/Fc⁺;

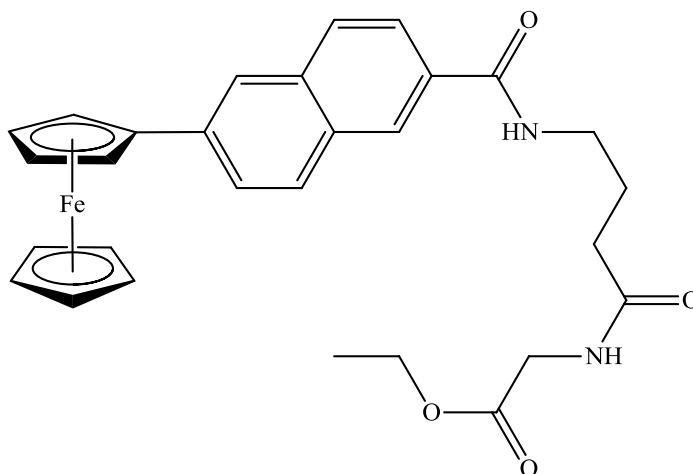
Anal. Calc. for C₂₉H₃₀N₂O₄Fe: C, 66.2; H, 5.7; N, 5.3%. Found: C, 65.9; H, 5.8; N, 5.3;

λ_{\max} (CH₃CN)/nm 370 (ϵ /dm³ mol⁻¹ cm⁻¹ 2700), 450 (1112);

ν_{\max} (neat)/cm⁻¹ 3256, 3081, 1750, 1656, 1634, 1622, 1575, 1551, 1201;

δ_{H} (400 MHz, DMSO-*d*₆): 8.67 (1H, t, *J* 5.6, -CONH-), 8.45 (1H, s, ArH), 8.38 (1H, t, *J* 6.0, -CONH-), 8.11 (1H, s, ArH), 7.94-8.01 (3H, m, ArH), 7.87 (1H, dd, *J* 1.6 and 8.4, ArH), 5.02 {2H, t, *J* 2.0, *ortho* on (η^5 -C₅H₄)}, 4.50 {2H, t, *J* 2.0, *meta* on (η^5 -C₅H₄)}, 4.08-4.17 (7H, m, -OCH₂CH₃, η^5 -C₅H₅), 3.88 (2H, d, *J* 5.6, -NHCH₂-), 3.37-3.42 (2H, m, -CH₂CH₂CH₂-), 2.30 (2H, t, *J* 7.2, -CH₂CH₂CH₂-), 1.87 (2H, qt, *J* 7.2, -CH₂CH₂CH₂-), 1.25 (3H, t, *J* 7.2, -OCH₂CH₃);

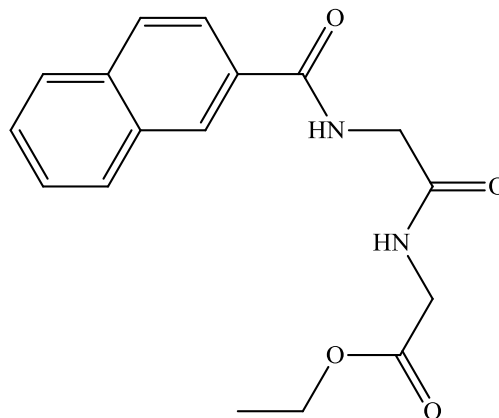
δ_{C} (100 MHz, DMSO-*d*₆): 172.5 (C=O), 170.0 (C=O), 166.2 (C=O), 138.6 (C_q), 134.4 (C_q), 131.1 (C_q), 130.7 (C_q), 128.7, 127.3, 127.2, 125.9, 124.5, 122.7, 84.1 (C_{ipso} η^5 -C₅H₄), 69.4 (η^5 -C₅H₅, C_{meta} η^5 -C₅H₄), 66.6 (C_{ortho} η^5 -C₅H₄), 60.3 (-OCH₂-, -ve DEPT), 40.6 (-NHCH₂-, -ve DEPT), 39.0 (-CH₂CH₂CH₂-, -ve DEPT), 32.7 (-CH₂CH₂CH₂-, -ve DEPT), 25.3 (-CH₂CH₂CH₂-, -ve DEPT), 14.0 (-OCH₂CH₃).



General procedure for the preparation of N-naphthoyl dipeptide derivatives.

N-(2-naphthoyl)-glycine-glycine ethyl ester 133

Glycine-glycine ethyl ester hydrochloride (0.20 g, 1.0 mmol) was added to a solution of 2-naphthoic acid (0.18 g, 1.0 mmol), 1-hydroxybenzotriazole (0.18 g, 1.3 mmol), triethylamine (0.5 ml) and *N*-(3-dimethylaminopropyl)-*N'*-ethylcarbodiimide hydrochloride (0.25 g, 1.3 mmol) in 50 ml of dichloromethane at 0 °C. After 30 minutes the solution was raised to room temperature and the



reaction was allowed to proceed for 48 h. The reaction mixture was then washed with water. The dichloromethane layer was dried over MgSO₄ and the solvent was removed *in vacuo*. The product was purified by column chromatography (eluant 1:1 hexane: ethyl acetate) to give the title compound as a white solid (0.28 g, 89%), mp 128-129 °C;

Anal. calcd. for C₁₇H₁₈N₂O₄: C, 65.0; H, 5.8; N, 8.9%. Found: C, 65.2; H, 5.9; N, 8.6;

$\nu_{\max}(\text{neat})/\text{cm}^{-1}$ 3264, 3056, 1738, 1646, 1633, 1619, 1546, 1203;

δ_{H} (400 MHz, DMSO-*d*₆): 9.05 (1H, t, *J* 5.6, -CONH-), 8.58 (1H, s, -ArH), 8.46 (1H, t, *J* 5.6, -CONH-), 8.10-8.02 (4H, m, -ArH), 7.71-7.64 (2H, m, -ArH), 4.15 (2H, q, *J* 7.2, -OCH₂CH₃), 4.04 (2H, d, *J* 5.6, -NHCH₂-), 3.92 (2H, d, *J* 5.6, -NHCH₂-), 1.25 (3H, t, *J* 7.2, -OCH₂CH₃);

δ_{C} (100 MHz, DMSO-*d*₆): 169.8 (C=O), 169.6 (C=O), 166.5 (C=O), 134.2 (C_q), 132.1 (C_q), 131.3 (C_q), 128.8, 127.8, 127.7, 127.62, 127.59, 126.7, 124.2, 60.4 (-OCH₂-, -ve DEPT), 42.5 (-NHCH₂-, -ve DEPT), 40.7 (-NHCH₂-, -ve DEPT), 14.0 (-OCH₂CH₃).

N*-(2-naphthoyl)-glycine-L-alanine ethyl ester **134*

The synthesis followed that of **133** using the following reagents: 2-naphthoic acid (0.17 g, 1.0 mmol), 1-hydroxybenzotriazole (0.18 g, 1.3 mmol), triethylamine (0.5 ml), *N*-(3-dimethylaminopropyl)-*N'*-ethylcarbodiimide hydrochloride (0.25 g, 1.3 mmol) and glycine-L-alanine ethyl ester hydrochloride (0.21 g, 1.0 mmol). The product was purified by column chromatography (eluant 1:1 hexane: ethyl acetate) to give the title compound as a white solid (0.17 g, 52%), mp 115-116 °C;

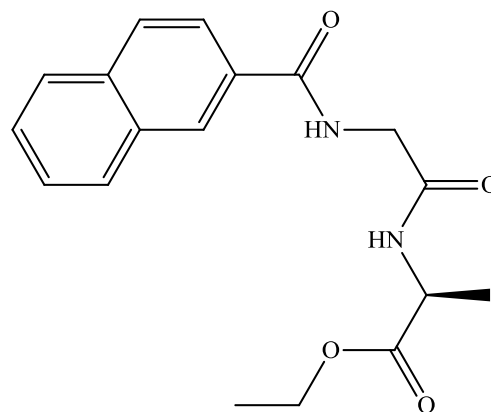
$[\alpha]_D^{20}$ -12 (*c* 0.03 in CH₃CN);

Anal. calcd. for C₁₈H₂₀N₂O₄: C, 65.8; H, 6.1; N, 8.5%. Found: C, 65.8; H, 6.2; N, 8.4;

$\nu_{\max}(\text{neat})/\text{cm}^{-1}$ 3364, 3319, 3063, 1750, 1672, 1644, 1629, 1602, 1532, 1199;

δ_{H} (400 MHz, DMSO-*d*₆): 8.88 (1H, t, *J* 6.0, -CONH-), 8.50 (1H, s, ArH), 8.40 (1H, d, *J* 7.2, -CONH-), 7.95-8.04 (4H, m, ArH), 7.58-7.65 (2H, m, ArH), 4.30 (1H, qt, *J* 7.2, -NHCH-), 4.00-4.12 (3H, m, -OCH₂CH₃, -NHCH₂-), 3.93 (1H, dd, *J* 6.0 and 16.4, -NHCH₂-), 1.31 (3H, d, *J* 7.2, -CH₃), 1.17 (3H, t, *J* 7.2, -OCH₂CH₃);

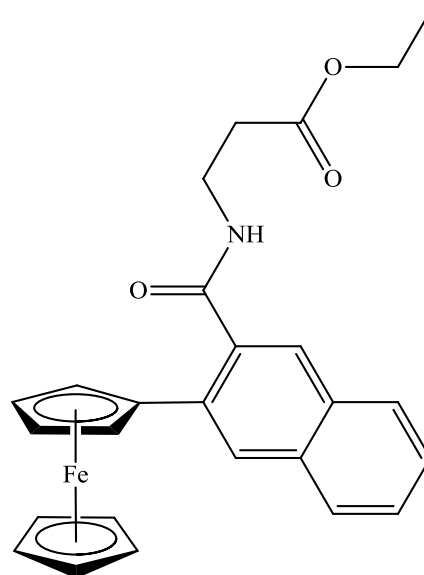
δ_{C} (100 MHz, DMSO-*d*₆): 172.5 (C=O), 168.9 (C=O), 166.4 (C=O), 134.1 (C_q), 132.1 (C_q), 131.3 (C_q), 128.8, 127.8, 127.7, 127.62, 127.59, 126.7, 124.2, 60.4 (-OCH₂-, -ve DEPT), 47.7 (α -C), 42.2 (-NHCH₂-, -ve DEPT), 17.0 (-CH₃), 14.0 (-OCH₂CH₃).



General procedure for the preparation of *N*-(ferrocenyl)naphthoyl amino acid derivatives.

***N*-(3-ferrocenyl-2-naphthoyl)- β -alanine ethyl ester 135**

β -alanine ethyl ester hydrochloride (0.15 g, 1 mmol) was added to a solution of 3-ferrocenyl-naphthalene-2-carboxylic acid (0.37 g, 1 mmol), 1-hydroxybenzotriazole (0.16 g, 1.2 mmol), triethylamine (0.5 ml) and *N*-(3-dimethylaminopropyl)-*N'*-ethylcarbodiimide hydrochloride (0.23 g, 1.2 mmol) in 50 ml of dichloromethane at 0 °C. After 30 min the solution was raised to room temperature and the reaction was allowed to proceed for 48 h. The reaction mixture was then washed with water. The dichloromethane layer was dried over MgSO₄ and the



solvent was removed *in vacuo*. The product was purified by column chromatography (eluant 1:1 hexane: ethyl acetate) to give the title compound as an orange solid (0.18 g, 40%), mp 117 °C; $E^{0'}$ /mV 24 *vs.* Fc/Fc⁺;

Anal. calcd. for C₂₆H₂₅NO₃Fe: C, 68.6; H, 5.5; N, 3.1%. Found: C, 68.1; H, 5.7; N, 3.05;

m/z (ESI) 456.1268 [M+H]⁺. C₂₆H₂₆NO₃Fe requires 456.1262;

λ_{\max} (CH₃CN)/nm 435 (ϵ /dm³ mol⁻¹ cm⁻¹ 493);

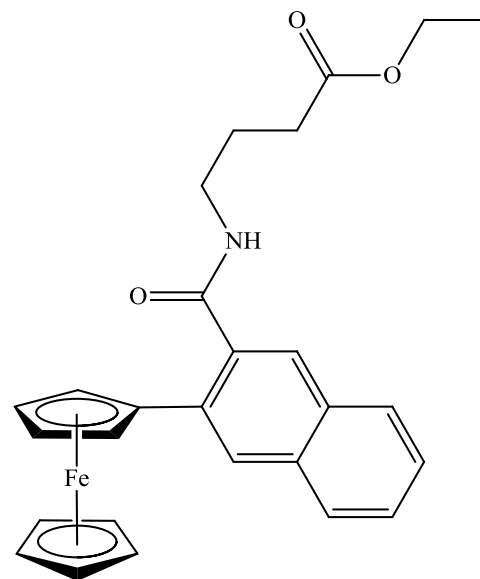
ν_{\max} (neat)/cm⁻¹ 3234, 3064, 1721, 1629, 1557, 1192;

δ_{H} (400 MHz, DMSO-*d*₆): 8.50 (1H, t, *J* 5.6, -CONH-), 8.32 (1H, s, ArH), 8.00 (1H, d, *J* 8.0, ArH), 7.89 (1H, d, *J* 8.0, ArH), 7.73 (1H, s, ArH), 7.49-7.56 (2H, m, ArH), 4.72 {2H, s, *ortho* on (η^5 -C₅H₄)}, 4.33 {2H, s, *meta* on (η^5 -C₅H₄)}, 4.09-4.13 (7H, m, -OCH₂CH₃, η^5 -C₅H₅), 3.44-3.51 (2H, m, -CH₂CH₂-), 2.57 (2H, t, *J* 6.8, -CH₂CH₂-), 1.23 (3H, t, *J* 7.2, -OCH₂CH₃);

δ_{C} (100 MHz, DMSO-*d*₆): 171.2 (C=O), 169.7 (C=O), 135.5 (C_q), 134.0 (C_q), 132.8 (C_q), 130.5 (C_q), 128.1, 127.6, 127.4, 126.9, 126.3, 126.0, 84.5 (C_{*ipso*} η^5 -C₅H₄), 69.5 (η^5 -C₅H₅), 68.8 (C_{*ortho*} η^5 -C₅H₄), 68.3 (C_{*meta*} η^5 -C₅H₄), 60.0 (-OCH₂-, -ve DEPT), 35.3 (-CH₂CH₂-, -ve DEPT), 33.5 (-CH₂CH₂-, -ve DEPT), 14.1 (-OCH₂CH₃).

***N*-(3-ferrocenyl-2-naphthoyl)- γ -aminobutyric acid ethyl ester 136**

The synthesis followed that of **135** using the following reagents: 3-ferrocenylnaphthalene-2-carboxylic acid (0.36 g, 1.0 mmol), 1-hydroxybenzotriazole (0.18 g, 1.3 mmol), triethylamine (0.5 ml), *N*-(3-dimethylaminopropyl)-*N*'-ethylcarbodiimide hydrochloride (0.25 g, 1.3 mmol) and γ -aminobutyric acid ethyl ester hydrochloride (0.17 g, 1 mmol). The product was purified by column chromatography (eluant 1:1 hexane: ethyl acetate) to give the title compound as an orange solid (0.17 g, 36%), mp 104-105 °C;



E^0/mV 29 vs. Fc/Fc^+ ;

Anal. calcd. for $C_{27}H_{27}NO_3Fe$: C, 69.1; H, 5.8; N, 3.0%. Found: C, 68.8; H, 5.8; N, 2.9;

m/z (ESI) 470.1411 $[M+H]^+$. $C_{27}H_{28}NO_3Fe$ requires 470.1419;

$\lambda_{max}(CH_3CN)/nm$ 435 ($\epsilon/dm^3 mol^{-1} cm^{-1}$ 294);

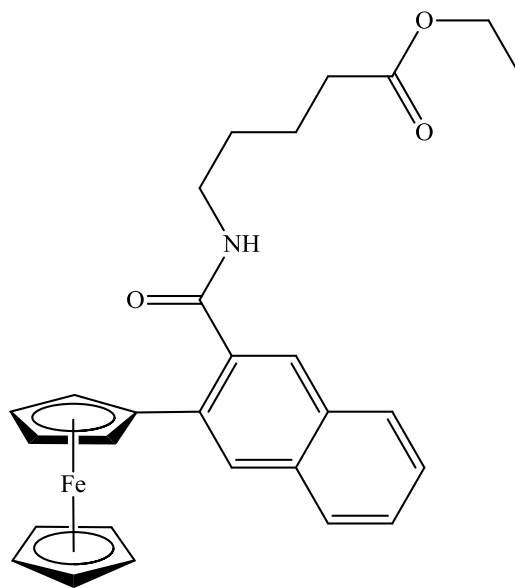
$\nu_{max}(neat)/cm^{-1}$ 3307, 3086, 1730, 1628, 1535, 1166;

δ_H (400 MHz, $DMSO-d_6$): 8.40 (1H, t, J 5.6, -CONH-), 8.33 (1H, s, ArH), 7.99 (1H, d, J 8.0, ArH), 7.92 (1H, d, J 8.0, ArH), 7.76 (1H, s, ArH), 7.48-7.56 (2H, m, ArH), 4.73 {2H, t, J 2.0, *ortho* on ($\eta^5-C_5H_4$)}, 4.32 {2H, t, J 2.0, *meta* on ($\eta^5-C_5H_4$)}, 4.06-4.11 (7H, m, -OCH₂CH₃, $\eta^5-C_5H_5$), 3.23 (2H, q, J 5.6, -CH₂CH₂CH₂-), 2.35 (2H, t, J 7.2, -CH₂CH₂CH₂-), 1.76 (2H, qt, J 7.2, -CH₂CH₂CH₂-), 1.20 (3H, t, J 7.2, -OCH₂CH₃);

δ_C (100 MHz, $DMSO-d_6$): 172.6 (C=O), 169.7 (C=O), 135.8 (C_q), 133.9 (C_q), 132.8 (C_q), 130.6 (C_q), 128.0, 127.6, 127.3, 126.9, 126.1, 126.0, 84.5 (C_{ipso} $\eta^5-C_5H_4$), 69.5 ($\eta^5-C_5H_5$), 68.8 (C_{ortho} $\eta^5-C_5H_4$), 68.2 (C_{meta} $\eta^5-C_5H_4$), 59.7 (-OCH₂-, -ve DEPT), 38.3 (-CH₂CH₂CH₂-, -ve DEPT), 31.0 (-CH₂CH₂CH₂-, -ve DEPT), 24.2 (-CH₂CH₂CH₂-, -ve DEPT), 14.1 (-OCH₂CH₃).

***N*-(3-ferrocenyl-2-naphthoyl)- δ -amino-*n*-valeric acid ethyl ester 137**

The synthesis followed that of **135** using the following reagents: 3-ferrocenylnaphthalene-2-carboxylic acid (0.36 g, 1.0 mmol), 1-hydroxybenzotriazole (0.16 g, 1.2 mmol), triethylamine (0.5 ml), *N*-(3-dimethylaminopropyl)-*N'*-ethylcarbodiimide hydrochloride (0.23 g, 1.2 mmol) and δ -amino-*n*-valeric acid ethyl ester hydrochloride (0.18 g, 1.0 mmol). The product was purified by column chromatography (eluant 1:1 hexane: ethyl acetate) to give the title compound as an orange oil (0.17 g, 35%), mp 79 °C;



$E^{0'}/\text{mV}$ 27 vs. Fc/Fc⁺;

Anal. calcd. for C₂₈H₂₉NO₃Fe: C, 69.6; H, 6.05; N, 2.9%. Found: C, 69.3; H, 6.0; N, 2.9;

m/z (ESI) 484.1566 [M+H]⁺. C₂₈H₃₀NO₃Fe requires 484.1575;

λ_{max} (CH₃CN)/nm 450 ($\epsilon/\text{dm}^3 \text{ mol}^{-1} \text{ cm}^{-1}$ 508);

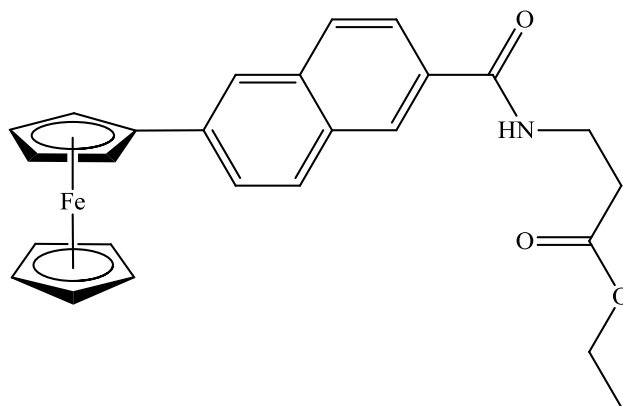
ν_{max} (neat)/cm⁻¹ 3282, 3093, 1726, 1628, 1638, 1538;

δ_{H} (400 MHz, DMSO-*d*₆): 8.38 (1H, t, *J* 5.6, -CONH-), 8.32 (1H, s, ArH), 7.99 (1H, d, *J* 8.0, ArH), 7.91 (1H, d, *J* 8.0, ArH), 7.74 (1H, s, ArH), 7.48-7.56 (2H, m, ArH), 4.74 {2H, t, *J* 1.6, *ortho* on (η^5 -C₅H₄)}, 4.33 {2H, t, *J* 1.6, *meta* on (η^5 -C₅H₄)}, 4.05-4.12 (7H, m, η^5 -C₅H₅, -OCH₂CH₃), 3.22 (2H, q, *J* 5.6, -CH₂CH₂CH₂CH₂-), 2.33 (2H, t, *J* 7.2, -CH₂CH₂CH₂CH₂-), 1.48-1.62 (4H, m, -CH₂CH₂CH₂CH₂-), 1.20 (3H, t, *J* 7.2, -OCH₂CH₃);

δ_{C} (100 MHz, DMSO-*d*₆): 172.8 (C=O), 169.6 (C=O), 135.9 (C_q), 133.9 (C_q), 132.8 (C_q), 130.6 (C_q), 127.9, 127.6, 127.3, 126.8, 126.1, 125.9, 84.5 (C_{ipso} η^5 -C₅H₄), 69.5 (η^5 -C₅H₅), 68.8 (C_{ortho} η^5 -C₅H₄), 68.2 (C_{meta} η^5 -C₅H₄), 59.7 (-OCH₂-, -ve DEPT), 38.6 (-CH₂CH₂CH₂CH₂-, -ve DEPT), 33.2 (-CH₂CH₂CH₂CH₂-, -ve DEPT), 28.2 (-CH₂CH₂CH₂CH₂-, -ve DEPT), 22.0 (-CH₂CH₂CH₂CH₂-, -ve DEPT), 14.1 (-OCH₂CH₃).

***N*-(6-ferrocenyl-2-naphthoyl)- β -alanine ethyl ester 138**

The synthesis followed that of **135** using the following reagents: 6-ferrocenylnaphthalene-2-carboxylic acid (0.36 g, 1.0 mmol), 1-hydroxybenzotriazole (0.16 g, 1.2 mmol), triethylamine (0.5 ml), *N*-(3-dimethylaminopropyl)-*N'*-ethylcarbodiimide hydrochloride (0.23



g, 1.2 mmol) and β -alanine ethyl ester hydrochloride (0.15 g, 1.0 mmol). The product was purified by column chromatography (eluant 1:1 hexane: ethyl acetate) to give the title compound as an orange solid (0.29 g, 64%), mp 123-124 °C;

E^0/mV 63 vs. Fc/Fc^+ ;

Anal. calcd. for $C_{26}H_{25}NO_3Fe$: C, 68.6; H, 5.5; N, 3.1%. Found: C, 67.8; H, 5.6; N, 3.0;

m/z (ESI) 456.1240 $[M+H]^+$. $C_{26}H_{26}NO_3Fe$ requires 456.1262;

$\lambda_{max}(CH_3CN)/nm$ 360 ($\epsilon/dm^3 mol^{-1} cm^{-1}$ 2818), 435 (1168);

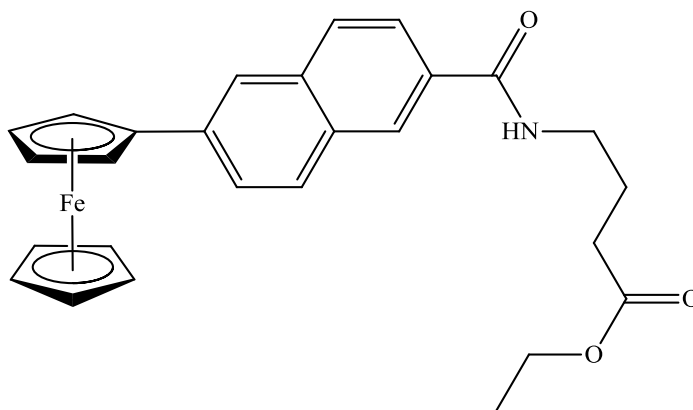
$\nu_{max}(neat)/cm^{-1}$ 3301, 3095, 1733, 1637, 1625, 1538;

δ_H (400 MHz, $DMSO-d_6$): 8.70 (1H, t, J 5.6, -CONH-), 8.38 (1H, s, ArH), 8.05 (1H, s, ArH), 7.88-7.96 (3H, m, ArH), 7.81 (1H, dd, J 1.6 and 8.4, ArH), 4.95 {2H, t, J 2.0, *ortho* on ($\eta^5-C_5H_4$)}, 4.44 {2H, t, J 2.0, *meta* on ($\eta^5-C_5H_4$)}, 4.08 (2H, q, J 7.2, -OCH₂CH₃), 4.04 (5H, s, $\eta^5-C_5H_5$), 3.56 (2H, q, J 6.8, -CH₂CH₂-), 2.63 (2H, t, J 6.8, -CH₂CH₂-), 1.19 (3H, t, J 7.2, -OCH₂CH₃);

δ_C (100 MHz, $DMSO-d_6$): 171.3 (C=O), 166.4 (C=O), 138.7 (C_q), 134.5 (C_q), 130.8 (C_q), 130.7 (C_q), 128.7, 127.3, 127.2, 125.9, 124.4, 122.7, 84.0 (C_{ipso} $\eta^5-C_5H_4$), 69.4 ($\eta^5-C_5H_5$, C_{meta} $\eta^5-C_5H_4$) 66.6 (C_{ortho} $\eta^5-C_5H_4$), 59.9 (-OCH₂-, -ve DEPT), 35.6 (-CH₂CH₂-, -ve DEPT), 33.8 (-CH₂CH₂-, -ve DEPT), 14.1 (-OCH₂CH₃).

***N*-(6-ferrocenyl-2-naphthoyl)- γ -aminobutyric acid ethyl ester 139**

The synthesis followed that of **135** using the following reagents: 6-ferrocenylnaphthalene-2-carboxylic acid (0.36 g, 1.0 mmol), 1-hydroxybenzotriazole (0.18 g, 1.3 mmol), triethylamine (0.5 ml), *N*-(3-dimethylaminopropyl)-*N'*-



ethylcarbodiimide hydrochloride (0.25 g, 1.3 mmol) and γ -aminobutyric acid ethyl ester hydrochloride (0.17 g, 1.0 mmol). The product was purified by column chromatography (eluant 1:1 hexane: ethyl acetate) to give the title compound as an orange solid (0.38 g, 81%), mp 117 °C;

$E^{0'}$ /mV 58 vs. Fc/Fc⁺;

Anal. calcd. for C₂₇H₂₇NO₃Fe: C, 69.1; H, 5.8; N, 3.0%. Found: C, 68.9; H, 5.8; N, 3.0;

m/z (ESI) 470.1417 [M+H]⁺. C₂₇H₂₈NO₃Fe requires 470.1419;

UV-Vis λ_{\max} (CH₃CN)/nm 335 (ϵ /dm³ mol⁻¹ cm⁻¹ 2532), 435 (1038);

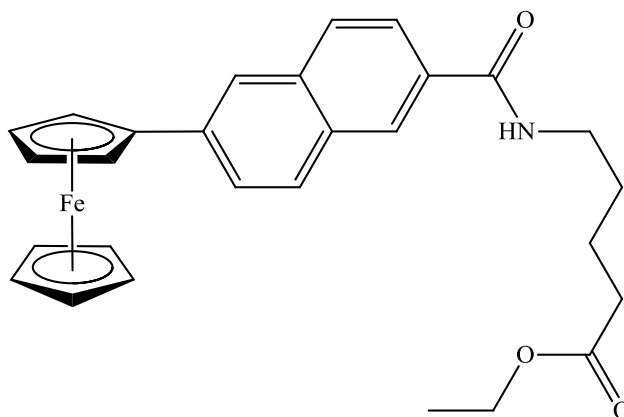
IR ν_{\max} (neat)/cm⁻¹ 3397, 3101, 1729, 1706, 1654, 1626, 1527, 1179;

δ_{H} (400 MHz, DMSO-*d*₆): 8.63 (1H, t, *J* 5.6, -CONH-), 8.39 (1H, s, ArH), 8.04 (1H, s, ArH), 7.89-7.96 (3H, m, ArH), 7.81 (1H, dd, *J* 1.6 and 8.4, ArH), 4.94 {2H, t, *J* 2.0, *ortho* on (η^5 -C₅H₄)}, 4.43 {2H, t, *J* 2.0, *meta* on (η^5 -C₅H₄)}, 4.03-4.08 (7H, m, -OCH₂CH₃, η^5 -C₅H₅), 3.34 (2H, q, *J* 5.6, -CH₂CH₂CH₂-), 2.39 (2H, t, *J* 7.2, -CH₂CH₂CH₂-), 1.83 (2H, qt, *J* 7.2, -CH₂CH₂CH₂-), 1.18 (3H, t, *J* 7.2, -OCH₂CH₃);

δ_{C} (100 MHz, DMSO-*d*₆): 172.7 (C=O), 166.3 (C=O), 138.7 (C_q), 134.4 (C_q), 131.0 (C_q), 130.7 (C_q), 128.7, 127.3, 127.2, 125.9, 124.5, 122.7, 84.1 (C_{ipso} η^5 -C₅H₄), 69.4 (η^5 -C₅H₅, C_{meta} η^5 -C₅H₄), 66.6 (C_{ortho} η^5 -C₅H₄), 59.8 (-OCH₂-, -ve DEPT), 38.6 (-CH₂CH₂CH₂-, -ve DEPT), 31.1 (-CH₂CH₂CH₂-, -ve DEPT), 24.5 (-CH₂CH₂CH₂-, -ve DEPT), 14.1 (-OCH₂CH₃).

N*-(6-ferrocenyl-2-naphthoyl)- δ -amino-*n*-valeric acid ethyl ester **140*

The synthesis followed that of **135** using the following reagents: 6-ferrocenylnaphthalene-2-carboxylic acid (0.36 g, 1.0 mmol), 1-hydroxybenzotriazole (0.18 g, 1.3 mmol), triethylamine (0.5 ml), *N*-(3-dimethylaminopropyl)-*N'*-ethylcarbodiimide hydrochloride (0.25



g, 1.3 mmol) and γ -aminobutyric acid ethyl ester hydrochloride (0.17 g, 1.0 mmol). The product was purified by column chromatography (eluant 1:1 hexane: ethyl acetate) to give the title compound as an orange solid (0.22 g, 46%), mp 65-66 °C;

E^0 /mV 58 vs. Fc/Fc⁺;

Anal. calcd. for C₂₈H₂₉NO₃Fe: C, 69.6; H, 6.05; N, 2.9%. Found: C, 69.7; H, 6.1; N, 2.9;

m/z (ESI) 484.1553 [M+H]⁺. C₂₈H₃₀NO₃Fe requires 484.1575;

λ_{\max} (CH₃CN)/nm 370 (ϵ /dm³ mol⁻¹ cm⁻¹ 3204), 450 (1304);

ν_{\max} (neat)/cm⁻¹ 3321, 3095, 1727, 1634, 1602, 1536, 1157;

δ_{H} (400 MHz, DMSO-*d*₆): 8.62 (1H, t, *J* 5.6, -CONH-), 8.38 (1H, s, -ArH), 8.05 (1H, s, -ArH), 7.86-7.96 (3H, m, -ArH), 7.81 (1H, dd, *J* 1.6 and 8.0, -ArH), 4.96 {2H, t, *J* 1.6, *ortho* on (η^5 -C₅H₄)}, 4.45 {2H, t, *J* 1.6, *meta* on (η^5 -C₅H₄)}, 4.02-4.08 (7H, m, -OCH₂CH₃, η^5 -C₅H₅), 3.31 (2H, m, -CH₂CH₂CH₂CH₂-), 2.35 (2H, t, *J* 7.2, -CH₂CH₂CH₂CH₂-), 1.56-1.62 (4H, m, -CH₂CH₂CH₂CH₂-), 1.17 (3H, t, *J* 7.2, -OCH₂CH₃);

δ_{C} (100 MHz, DMSO-*d*₆): 172.8 (C=O), 166.2 (C=O), 138.6 (C_q), 134.4 (C_q), 131.1 (C_q), 130.7 (C_q), 128.7, 127.3, 127.1, 125.9, 124.5, 122.7, 84.1 (C_{ipso} η^5 -C₅H₄), 69.4 (η^5 -C₅H₅, C_{meta} η^5 -C₅H₄), 66.6 (C_{ortho} η^5 -C₅H₄), 59.7 (-OCH₂-, -ve DEPT), 38.8 (-CH₂CH₂CH₂CH₂-, -ve DEPT), 33.2 (-CH₂CH₂CH₂CH₂-, -ve DEPT), 28.6 (-CH₂CH₂CH₂CH₂-, -ve DEPT), 22.0 (-CH₂CH₂CH₂CH₂-, -ve DEPT), 14.1 (-OCH₂CH₃).

References

1. J. Deruiter, B. E. Swearingen, V. Wandrekar and C. A. Mayfield, *Journal of Medicinal Chemistry*, 1989, **32**, 1033-1038.
2. C. G. Wermuth, *The Practice of Medicinal Chemistry*, 2nd ed., Elsevier, **2003**.
3. A. Grauer and B. Konig, *European Journal of Organic Chemistry*, 2009, 5099-5111.
4. J. Chatterjee, C. Gilon, A. Hoffman and H. Kessler, *Accounts of Chemical Research*, 2008, **41**, 1331-1342.
5. A. J. Corry, Ph.D. Thesis, Dublin City University, **2009**.
6. J. Jones, *Amino Acid and Peptide Synthesis*, Oxford University Press, **2002**.
7. J. M. Humphrey and A. R. Chamberlin, *Chemical Reviews*, 1997, **97**, 2243-2266.
8. J. C. Micheau and J. Z. Zhao, *Journal of Physical Organic Chemistry*, 2007, **20**, 810-820.
9. G. Fischer, *Chemical Society Reviews*, 2000, **29**, 119-127.
10. D. H. Williams and I. Fleming, *Spectroscopic Methods in Organic Chemistry*, McGraw-Hill, **2008**.

Chapter 5

Biological Evaluation of *N*-naphthoyl dipeptide derivatives and *N*-(ferrocenyl)naphthoyl amino acid and dipeptide derivatives which contain unusual amino acids

5.1. *In vitro* evaluation in the H1299 cell line and the Sk-Mel-28 cell line

The *in vitro* biological evaluation of *N*-naphthoyl dipeptide derivatives and *N*-(ferrocenyl)naphthoyl amino acid and dipeptide derivatives was undertaken in order to enable comparisons to be drawn with the previous group of *N*-(ferrocenyl)naphthoyl amino acid and dipeptide derivatives studied in Chapter 3. This was achieved by performing a comprehensive screen of every compound at 10 μ M and 1 μ M in the H1299 cell line, and at 10 μ M in the Sk-Mel-28 cell line, as outlined in Chapter 3 (Section 3.3). The results of the comprehensive screens are expressed as the percentage cell growth \pm standard deviation (relative to the DMSO controls). Standard deviations have been calculated using data obtained from three independent experiments.

5.1.1. *N*-(ferrocenyl)naphthoyl dipeptide derivatives

The *N*-(ferrocenyl)naphthoyl dipeptide derivatives that contain *N*-methyl amino acids were shown to inhibit cell growth in the H1299 cell line by 90% or more, when tested at the higher concentration of 10 μ M (Table 5.1). Four compounds in particular were shown to inhibit cell growth by almost 99%. A higher percentage of cell survival was observed when the H1299 cell line was treated with 1 μ M solutions of these compounds, except in the case of *N*-(6-ferrocenyl-2-naphthoyl)-sarcosine-glycine ethyl ester **120**, which was shown to be a potent inhibitor of cell growth (~95% inhibition). *N*-(3-ferrocenyl-2-naphthoyl)-sarcosine-sarcosine ethyl ester **117** and *N*-(3-ferrocenyl-2-naphthoyl)-glycine-*N*-methyl-L-alanine ethyl ester **118**, were also shown to exert a weak anti-proliferative effect (~20% inhibition) at this lower concentration.

Table 5.1 Percentage cell growth of H1299 cells in the presence of *N*-(ferrocenyl)naphthoyl dipeptide derivatives which contain *N*-methyl amino acids (**115-122**).

Compound	No.	10 μ M	1 μ M
<i>N</i> -(3-ferrocenyl-2-naphthoyl)-Gly-Sar-OEt	115	8.8 \pm 3.8	97.4 \pm 4.8
<i>N</i> -(3-ferrocenyl-2-naphthoyl)-Sar-Gly-OEt	116	4.7 \pm 1.5	86.1 \pm 15.1
<i>N</i> -(3-ferrocenyl-2-naphthoyl)-Sar-Sar-OEt	117	4.9 \pm 1.1	75.2 \pm 5.4
<i>N</i> -(3-ferrocenyl-2-naphthoyl)-Gly- <i>N</i> -Me-L-Ala-OEt	118	0.4 \pm 0.6	66.0 \pm 12.8
<i>N</i> -(6-ferrocenyl-2-naphthoyl)-Gly-Sar-OEt	119	0.5 \pm 0.7	98.1 \pm 4.4
<i>N</i> -(6-ferrocenyl-2-naphthoyl)-Sar-Gly-OEt	120	0.5 \pm 0.8	4.8 \pm 1.4
<i>N</i> -(6-ferrocenyl-2-naphthoyl)-Sar-Sar-OEt	121	0.4 \pm 0.7	102.2 \pm 16.4
<i>N</i> -(6-ferrocenyl-2-naphthoyl)-Gly- <i>N</i> -Me-L-Ala-OEt	122	4.5 \pm 2.7	97.4 \pm 12.1

The anti-proliferative effect of these *N*-methylated derivatives was shown to be weaker in the Sk-Mel-28 cell line (Table 5.2). At a concentration of 10 μ M, over half of the compounds did not exhibit any considerable inhibition of cell growth. However, *N*-(3-ferrocenyl-2-naphthoyl)-glycine-*N*-methyl-L-alanine ethyl ester **118** was found to have a reasonable anti-proliferative effect, achieving over 50% inhibition. *N*-(6-ferrocenyl-2-naphthoyl)-glycine-sarcosine ethyl ester **119** showed the strongest anti-proliferative effect, with approximately 95% inhibition, whilst *N*-(6-ferrocenyl-2-naphthoyl)-sarcosine-glycine ethyl ester **120** inhibited cell growth by approximately 80%. Despite the strong inhibitory effect of *N*-(6-ferrocenyl-2-naphthoyl)-glycine-sarcosine ethyl ester **119** in the Sk-Mel-28 cell line, this compound had no effect on proliferation in the H1299 cell line, when tested at the lower concentration of 1 μ M. *N*-(6-ferrocenyl-2-naphthoyl)-sarcosine-glycine ethyl ester **120**, on the other hand, displays a potent anti-proliferative effect in both cell lines, and therefore, further studies to determine the IC₅₀ value of this compound will be carried out.

Table 5.2 Percentage cell growth of Sk-Mel-28 cells in the presence of *N*-(ferrocenyl)naphthoyl dipeptide derivatives which contain *N*-methyl amino acids (**115-122**).

Compound	No.	10 μM
<i>N</i> -(3-ferrocenyl-2-naphthoyl)-Gly-Sar-OEt	115	61.7 \pm 27.3
<i>N</i> -(3-ferrocenyl-2-naphthoyl)-Sar-Gly-OEt	116	73.6 \pm 19.6
<i>N</i> -(3-ferrocenyl-2-naphthoyl)-Sar-Sar-OEt	117	64.0 \pm 21.5
<i>N</i> -(3-ferrocenyl-2-naphthoyl)-Gly- <i>N</i> -Me-L-Ala-OEt	118	29.3 \pm 19.6
<i>N</i> -(6-ferrocenyl-2-naphthoyl)-Gly-Sar-OEt	119	3.2 \pm 3.4
<i>N</i> -(6-ferrocenyl-2-naphthoyl)-Sar-Gly-OEt	120	15.7 \pm 9.8
<i>N</i> -(6-ferrocenyl-2-naphthoyl)-Sar-Sar-OEt	121	65.0 \pm 29.8
<i>N</i> -(6-ferrocenyl-2-naphthoyl)-Gly- <i>N</i> -Me-L-Ala-OEt	122	85.0 \pm 17

At the higher concentration of 10 μ M, the remaining *N*-(ferrocenyl)naphthoyl dipeptide derivatives were found to inhibit cell proliferation in the H1299 cell line by approximately 80% or more, except for *N*-(6-ferrocenyl-2-naphthoyl)- β -alanine-glycine ethyl ester **130**, which had no effect on cell growth (Table 5.3). Three compounds in particular were shown to inhibit cell growth by more than 96%: *N*-(6-ferrocenyl-2-naphthoyl)-glycine-D-alanine ethyl ester **124**, *N*-(6-ferrocenyl-2-naphthoyl)-glycine- β -alanine ethyl ester **129**, and *N*-(6-ferrocenyl-2-naphthoyl)- γ -aminobutyric acid-glycine ethyl ester **132**. At the lower concentration of 1 μ M, the majority of these derivatives had no effect on H1299 cell growth. *N*-(6-ferrocenyl-2-naphthoyl)-glycine- β -alanine ethyl ester **129** was shown to have a weak anti-proliferative effect (~25% inhibition), whilst *N*-(6-ferrocenyl-2-naphthoyl)-glycine-D-alanine ethyl ester **124** displayed a significant anti-proliferative effect (>50% inhibition).

Table 5.3 Percentage cell growth of H1299 cells in the presence of *N*-(ferrocenyl)naphthoyl dipeptide derivatives (**123-132**).

Compound	No.	10 μM	1 μM
<i>N</i> -(3-ferrocenyl-2-naphthoyl)-Gly-D-Ala-OEt	123	18.0 \pm 0.7	102.7 \pm 9.6
<i>N</i> -(6-ferrocenyl-2-naphthoyl)-Gly-D-Ala-OEt	124	1.9 \pm 0.7	44.8 \pm 3.0
<i>N</i> -(3-ferrocenyl-2-naphthoyl)-Gly- β -Ala-OEt	125	21.4 \pm 4.2	109.7 \pm 2.6
<i>N</i> -(3-ferrocenyl-2-naphthoyl)- β -Ala-Gly-OEt	126	21.5 \pm 2.8	116.2 \pm 11.0
<i>N</i> -(3-ferrocenyl-2-naphthoyl)-Gly-GABA-OEt	127	24.6 \pm 2.7	100.7 \pm 21.0
<i>N</i> -(3-ferrocenyl-2-naphthoyl)-GABA-Gly-OEt	128	18.9 \pm 4.5	107.0 \pm 5.4
<i>N</i> -(6-ferrocenyl-2-naphthoyl)-Gly- β -Ala-OEt	129	3.3 \pm 0.5	72.9 \pm 5.2
<i>N</i> -(6-ferrocenyl-2-naphthoyl)- β -Ala-Gly-OEt	130	87.9 \pm 9.2	87.7 \pm 8.1
<i>N</i> -(6-ferrocenyl-2-naphthoyl)-Gly-GABA-OEt	131	14.7 \pm 8.4	97.5 \pm 14.3
<i>N</i> -(6-ferrocenyl-2-naphthoyl)-GABA-Gly-OEt	132	0.2 \pm 0.6	102.8 \pm 4.6

The Sk-Mel-28 cell line was more resistant than the H1299 cell line to treatment with the remaining *N*-(ferrocenyl)naphthoyl dipeptide derivatives (Table 5.4). Only two compounds from this group were found to inhibit Sk-Mel-28 cell growth by more than 50%. *N*-(6-ferrocenyl-2-naphthoyl)-glycine-D-alanine ethyl ester **124** and *N*-(6-ferrocenyl-2-naphthoyl)-glycine- β -alanine ethyl ester **129** both had a strong anti-proliferative effect in this cell line, with approximately 85% cell growth inhibition. However, since *N*-(6-ferrocenyl-2-naphthoyl)-glycine- β -alanine ethyl ester **129** had only a weak anti-proliferative effect in the H1299 cell line at the lower concentration, only *N*-(6-ferrocenyl-2-naphthoyl)-glycine-D-alanine ethyl ester **124** will progress to further studies.

Table 5.4 Percentage cell growth of Sk-Mel-28 cells in the presence of *N*-(ferrocenyl)naphthoyl dipeptide derivatives (**123-132**).

Compound	No.	10 μM
<i>N</i> -(3-ferrocenyl-2-naphthoyl)-Gly-D-Ala-OEt	123	84.9 \pm 9.6
<i>N</i> -(6-ferrocenyl-2-naphthoyl)-Gly-D-Ala-OEt	124	15.6 \pm 4.0
<i>N</i> -(3-ferrocenyl-2-naphthoyl)-Gly- β -Ala-OEt	125	83.9 \pm 11.1
<i>N</i> -(3-ferrocenyl-2-naphthoyl)- β -Ala-Gly-OEt	126	91.7 \pm 12.8
<i>N</i> -(3-ferrocenyl-2-naphthoyl)-Gly-GABA-OEt	127	80.9 \pm 14.2
<i>N</i> -(3-ferrocenyl-2-naphthoyl)-GABA-Gly-OEt	128	82.3 \pm 16.3
<i>N</i> -(6-ferrocenyl-2-naphthoyl)-Gly- β -Ala-OEt	129	14.8 \pm 3.5
<i>N</i> -(6-ferrocenyl-2-naphthoyl)- β -Ala-Gly-OEt	130	98.4 \pm 7.6
<i>N</i> -(6-ferrocenyl-2-naphthoyl)-Gly-GABA-OEt	131	62.5 \pm 30.7
<i>N</i> -(6-ferrocenyl-2-naphthoyl)-GABA-Gly-OEt	132	89.1 \pm 17.8

5.1.2. *N*-naphthoyl dipeptide derivatives

N-naphthoyl-glycine-glycine ethyl ester **133** was found to have a slight inhibitory effect (~20% inhibition) on cell proliferation in the H1299 cell line at the higher concentration of 10 μ M, but had no effect on cell proliferation at the lower concentration of 1 μ M. At the higher concentration of 10 μ M, *N*-naphthoyl-glycine-L-alanine ethyl ester **134** had a more marked effect on cell proliferation (~70% inhibition) in the H1299 cell line, but again, H1299 cell growth was unaffected at the lower concentration of 1 μ M. The *N*-naphthoyl dipeptide derivatives did not affect cell growth in the Sk-Mel-28 cell line (Table 5.5).

Table 5.5 Percentage cell growth in the presence of *N*-naphthoyl dipeptide derivatives (**133-134**).

Compound	No.	10 μM	1 μM	10 μM
		H1299	H1299	Sk-Mel-28
<i>N</i> -(2-naphthoyl)-Gly-Gly-OEt	133	69.3 \pm 11.6	87.6 \pm 18.4	95.6 \pm 10.9
<i>N</i> -(2-naphthoyl)-Gly-L-Ala-OEt	134	28.6 \pm 4.3	107.4 \pm 9.7	96.9 \pm 8.7

5.1.3. *N*-(ferrocenyl)naphthoyl amino acid derivatives

The *N*-(3-ferrocenyl-2-naphthoyl) amino acid derivatives achieved an appreciable level of cell growth inhibition (30-60%) in the H1299 cell line, at the higher concentration of 10 μ M (Table 5.6). Of these compounds, the *N*-(3-ferrocenyl-2-naphthoyl)- γ -aminobutyric acid ethyl ester **136** showed the strongest anti-proliferative effect (~60%). Interestingly, a greater anti-proliferative effect was observed for the *N*-(3-ferrocenyl-2-naphthoyl) amino acid derivatives that contained α -amino acids (Chapter 3, Section 3.3.2.). In comparison, the *N*-(6-ferrocenyl-2-naphthoyl) amino acid derivatives were found to have a stronger anti-proliferative effect; cell growth was inhibited by at least 89%. *N*-(6-ferrocenyl-2-naphthoyl)- γ -aminobutyric acid ethyl ester **139** and *N*-(6-ferrocenyl-2-naphthoyl)- δ -amino-n-valeric acid ethyl ester **140** showed a similarly strong anti-proliferative effect (~97%). However, *N*-(6-ferrocenyl-2-naphthoyl)- γ -aminobutyric acid ethyl ester **139** was the only *N*-(ferrocenyl)naphthoyl amino acid derivative found to inhibit H1299 cell growth by more than 50% at the lower concentration of 1 μ M. At this concentration, *N*-(6-ferrocenyl-2-naphthoyl)- δ -amino-n-valeric acid ethyl ester **140** displayed only a weak anti-proliferative effect (~30% inhibition).

Table 5.6 Percentage cell growth of H1299 cells in the presence of *N*-(ferrocenyl)naphthoyl amino acid derivatives (**135-140**).

Compound	No.	10 μ M	1 μ M
<i>N</i> -(3-ferrocenyl-2-naphthoyl)- β -Ala-OEt	135	63.8 \pm 5.6	112.6 \pm 16.5
<i>N</i> -(3-ferrocenyl-2-naphthoyl)-GABA-OEt	136	39.0 \pm 5.4	105.0 \pm 24.6
<i>N</i> -(3-ferrocenyl-2-naphthoyl)- δ -Ava-OEt	137	57.0 \pm 9.7	110.3 \pm 9.2
<i>N</i> -(6-ferrocenyl-2-naphthoyl)- β -Ala-OEt	138	11.6 \pm 0.5	109.6 \pm 9.5
<i>N</i> -(6-ferrocenyl-2-naphthoyl)-GABA-OEt	139	3.0 \pm 0.6	45.7 \pm 3.6
<i>N</i> -(6-ferrocenyl-2-naphthoyl)- δ -Ava-OEt	140	3.0 \pm 0.9	62.1 \pm 6.8

In the Sk-Mel-28 cell line, only two *N*-(ferrocenyl)naphthoyl amino acid derivatives were found to have an inhibitory effect on cell growth: *N*-(6-ferrocenyl-2-naphthoyl)- δ -amino-n-valeric acid ethyl ester **140** had a significant anti-proliferative effect (~70% inhibition), whilst *N*-(6-ferrocenyl-2-naphthoyl)- γ -aminobutyric acid ethyl ester **139** displayed a strong anti-proliferative effect (~90% inhibition).

Table 5.7 Percentage cell growth of Sk-Mel-28 cells in the presence of *N*-(ferrocenyl)naphthoyl amino acid derivatives (**135-140**).

Compound	No.	10 μ M
<i>N</i> -(3-ferrocenyl-2-naphthoyl)- β -Ala-OEt	135	103.5 \pm 2.9
<i>N</i> -(3-ferrocenyl-2-naphthoyl)-GABA-OEt	136	92.3 \pm 2.7
<i>N</i> -(3-ferrocenyl-2-naphthoyl)- δ -Ava-OEt	137	98.9 \pm 5.5
<i>N</i> -(6-ferrocenyl-2-naphthoyl)- β -Ala-OEt	138	69.4 \pm 24.5
<i>N</i> -(6-ferrocenyl-2-naphthoyl)-GABA-OEt	139	9.6 \pm 1.6
<i>N</i> -(6-ferrocenyl-2-naphthoyl)- δ -Ava-OEt	140	33.1 \pm 10.5

5.1.4. IC₅₀ value determination

Further studies were conducted, as described in Chapter 3 (Section 3.3.4), to determine IC₅₀ values for *N*-(6-ferrocenyl-2-naphthoyl)-sarcosine-glycine ethyl ester **120**, *N*-(6-ferrocenyl-2-naphthoyl)-glycine-D-alanine ethyl ester **124**, and *N*-(6-ferrocenyl-2-naphthoyl)- δ -aminobutyric acid ethyl ester **139** in the H1299 cell line and the Sk-Mel-28 cell line. The IC₅₀ value for each compound was calculated using Calcsyn software, and standard deviations have been calculated using data obtained from three independent experiments. The values obtained are listed in Table 5.8.

In the H1299 cell line, a remarkable IC₅₀ value of 0.14 \pm 0.02 μ M was calculated for *N*-(6-ferrocenyl-2-naphthoyl)-sarcosine-glycine ethyl ester **120**. This value is comparable to the IC₅₀ value determined for *N*-(6-ferrocenyl-2-naphthoyl)-glycine-glycine ethyl ester **96** (0.13 \pm 0.02 μ M) in Chapter 3. Similarly, in the Sk-Mel-28 cell line an IC₅₀ value of 1.06 \pm 0.05 μ M was calculated for *N*-(6-ferrocenyl-2-naphthoyl)-sarcosine-glycine ethyl ester **120**. For

N-(6-ferrocenyl-2-naphthoyl)-glycine-D-alanine ethyl ester **124**, IC₅₀ values of 0.33 ± 0.02 μM and 1.83 ± 0.04 μM were calculated in the H1299 and Sk-Mel-28 cell lines, respectively. In comparison to *N*-(6-ferrocenyl-2-naphthoyl)-glycine-L-alanine ethyl ester **51**, this represents a four-fold improvement in anti-proliferative effect in the H1299 cell line, and a two-fold improvement in the Sk-Mel-28 cell line. *N*-(6-ferrocenyl-2-naphthoyl)-γ-aminobutyric acid ethyl ester **139** was found to have an IC₅₀ value of 0.62 ± 0.07 μM in the H1299 cell line and 1.41 ± 0.04 μM in the Sk-Mel-28 cell line.

Thus, in total, the primary and secondary SAR studies of novel ferrocenyl-peptide bioconjugates have identified five compounds that have an equivalent or more potent anti-proliferative effect in the H1299 cell line than the platinum-based anti-cancer drug, cisplatin **1** (1.4 ± 0.1 μM). Four of these compounds possess IC₅₀ values that lie in the nanomolar range. These findings represent an important progression in the study of bioorganometallic anti-cancer agents, since reported IC₅₀ values for other ferrocenyl derivatives in the A549 lung cancer cell line remain above 10 μM.¹ In addition, noteworthy IC₅₀ values that range from 1.06 ± 0.05 μM to 3.74 ± 0.37 μM have been determined for these five compounds in the Sk-Mel-28 cell line.

Table 5.8 IC₅₀ values in the H1299 and Sk-Mel-28 cell lines.

Compound	No.	H1299 (μM)	Sk-Mel-28 (μM)
<i>N</i> -(6-ferrocenyl-2-naphthoyl)-Sar-Gly-OEt	120	0.14 ± 0.02	1.06 ± 0.05
<i>N</i> -(6-ferrocenyl-2-naphthoyl)-Gly-D-Ala-OEt	124	0.33 ± 0.02	1.83 ± 0.04
<i>N</i> -(6-ferrocenyl-2-naphthoyl)-GABA-OEt	139	0.62 ± 0.07	1.41 ± 0.04

5.2. Structure-activity relationship of *N*-(ferrocenyl)naphthoyl amino acid and dipeptide derivatives

The biological data obtained from these *in vitro* studies provides more information regarding the structure-activity relationship of the *N*-(ferrocenyl)naphthoyl amino acid and dipeptide derivatives, which was established in Chapter 3 (Section 3.4). First of all, in relation to the *N*-(3-ferrocenyl-2-naphthoyl) amino acid derivatives, the anti-proliferative

effect is greatest when chiral α -amino acids with bulky side chains are employed. Extending the peptide chain length by incorporating the achiral amino acids β -alanine, γ -aminobutyric acid and δ -amino-n-valeric acid does not improve the anti-proliferative effect. In contrast, substitution at the α -carbon of the amino acid is not beneficial to the biological activity of the *N*-(6-ferrocenyl-2-naphthoyl) amino acid derivatives. The achiral amino acid derivatives (including glycine), which are devoid of steric bulk, show a greater anti-proliferative effect. The weakest anti-proliferative effect for this homologous series is observed when $n=2$, in the case of *N*-(6-ferrocenyl-2-naphthoyl)- β -alanine ethyl ester **138**, whilst the greatest anti-proliferative effect is observed when $n=3$, in the case of *N*-(6-ferrocenyl-2-naphthoyl)- γ -aminobutyric acid ethyl ester **139**. *N*-(6-ferrocenyl-2-naphthoyl)-glycine ethyl ester **92** and *N*-(6-ferrocenyl-2-naphthoyl)- δ -amino-n-valeric acid ethyl ester **140** both display an intermediate anti-proliferative effect. These results indicate that extending the length of the α -amino acid glycine by two methylene units enhances the biological activity of the *N*-(6-ferrocenyl-2-naphthoyl) amino acid derivatives. This improvement in anti-proliferative effect may be a consequence of an increase in lipophilicity or the conformational flexibility afforded by the γ -aminobutyric acid moiety. Secondly, the *N*-naphthoyl analogues of the two most potent compounds, *N*-naphthoyl-glycine-glycine ethyl ester **133** and *N*-naphthoyl-glycine-L-alanine ethyl ester **134** were found to be ineffective at inhibiting cell growth in the Sk-Mel-28 cell line and in the H1299 cell line at the lower concentration of 1 μ M. This dramatic decrease in anti-proliferative effect demonstrates conclusively that the ferrocenyl unit is essential for *in vitro* biological activity.

Finally, in relation to the *N*-(ferrocenyl)naphthoyl dipeptide derivatives, it is again evident that the *N*-(6-ferrocenyl-2-naphthoyl) dipeptide derivatives have a superior anti-proliferative effect compared to the corresponding *N*-(3-ferrocenyl-2-naphthoyl) analogues. The results of this study demonstrate that, with regard to *N*-(6-ferrocenyl-2-naphthoyl)-glycine-glycine ethyl ester **96**, *N*-methylation of the *N*-terminal glycine residue is well tolerated; the anti-proliferative effect of *N*-(6-ferrocenyl-2-naphthoyl)-sarcosine-glycine ethyl ester **120** displays a comparable anti-proliferative effect in both cell lines. However, *N*-methylation of the *C*-terminal glycine residue results in a loss of potency in the H1299

cell line, whilst *N*-methylation of both residues produces a fall in activity in both cell lines. The isosteric replacement of the *N*-terminal glycine residue with β -alanine results in a dramatic decrease in anti-proliferative effect; *N*-(6-ferrocenyl-2-naphthoyl)- β -alanine-glycine ethyl ester **130** has no effect on cell proliferation in either cell line. Similarly, isosteric replacement with γ -aminobutyric acid reduces the anti-proliferative effect. For the *C*-terminal glycine residue, replacement with the β -alanine and γ -aminobutyric acid isosteres also decreases the inhibitory effect on cell proliferation although the fall in activity is not as drastic as that observed for the *N*-terminal glycine residue.

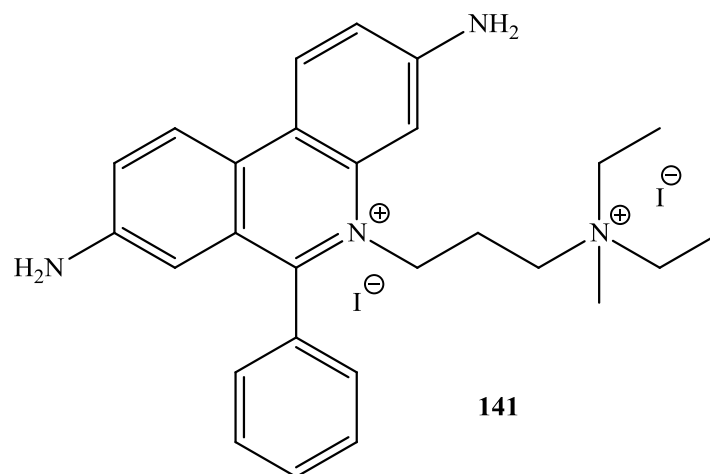
For *N*-(6-ferrocenyl-2-naphthoyl)-glycine-L-alanine ethyl ester **51**, *N*-methylation of the *C*-terminal L-alanine residue results in a loss of potency. In contrast, inverting the stereochemistry of *C*-terminal α -carbon atom enhances the anti-proliferative effect; *N*-(6-ferrocenyl-2-naphthoyl)-glycine-D-alanine ethyl ester **124** is four times more potent than *N*-(6-ferrocenyl-2-naphthoyl)-glycine-L-alanine ethyl ester **51** in the H1299 cell line, and two times more potent in the Sk-Mel-28 cell line.

5.3. Cell cycle analysis of *N*-(6-ferrocenyl-2-naphthoyl)-glycine-glycine ethyl ester (96) and *N*-(6-ferrocenyl-2-naphthoyl)-sarcosine-glycine ethyl ester (120)

The growth and division of cells proceeds *via* the cell cycle, which is typically divided into four distinct stages: the synthesis (S), mitosis (M) and two gap (G1 and G2) phases. Most normal cells, unless they have received a stimulus to proliferate or differentiate, exist in a non-dividing, quiescent state known as G0.² Cancer cells, on the other hand, are in a state of aberrant growth. The boundary between the G1 and S phases represents the main control point, or restriction point. It is at this point that the cell must decide whether to divide into two daughter cells or die, as the cell can only exist in subsequent phases for a short period. The majority of chemotherapeutic agents, *e.g.* paclitaxel **11**, function by blocking cell cycle progression after this restriction point.³

The cell cycle distribution of cells is typically analysed by flow cytometry or fluorescence activated cell sorting (FACS). Prior to analysis, the cells are stained with propidium iodide **141**, a fluorescent molecule that intercalates with the DNA present in the cell nucleus. Discrimination between the various stages of the cell cycle is possible due to changes in the

concentrations of DNA in the cells as the cycle progresses. Resting cells (G0/G1 phase) contain two copies of each chromosome. As the cells progress towards mitosis, they synthesise DNA (S phase), which allows for more intercalation and increases the fluorescence intensity. When all chromosomes have been replicated, the DNA content has doubled (G2/M phase), and thus, the cells fluoresce with twice the intensity of the G0/G1 phase. Cells in which the DNA has become fragmented or degraded (such as apoptotic cells) will exhibit a decrease in fluorescence intensity, compared to the G0/G1 phase. These cells will appear as a broad “sub-G0/G1” peak, and can represent, in addition to apoptotic cells, nuclear fragments, clumps of chromosomes, micronuclei or cells undergoing differentiation.⁴



Cell cycle analysis was performed by treating individual wells of a 24-well plate containing H1299 cells with either *N*-(6-ferrocenyl-2-naphthoyl)-glycine-glycine ethyl ester **96** or *N*-(6-ferrocenyl-2-naphthoyl)-sarcosine-glycine ethyl ester **120** at a concentration of 0.5 μM and 1.0 μM . Since DMSO can have an adverse effect on cells, a DMSO control was included in the assay, along with controls for normal (untreated) cell growth. In this case, the DMSO control wells contained a 0.2% DMSO solution. Following incubation for 48 and 72 hours, the cells were fixed in 70% ethanol, stained with propidium iodide **141** and analysed by flow cytometry.

Table 5.9 summarises the percentage of H1299 cells in each stage of the cell cycle following treatment with *N*-(6-ferrocenyl-2-naphthoyl)-glycine-glycine ethyl ester **96**, for 48 hours and 72 hours. After 48 hours, treatment of H1299 cells with 0.5 μM *N*-(6-

ferrocenyl-2-naphthoyl)-glycine-glycine ethyl ester **96** significantly increased the sub-G0/G1 population ($p = 0.006$). There is also a significant decrease in the number of cells in the S phase of the cell cycle ($p = 0.017$). The sub-G0/G1 population increases by approximately two-fold when the concentration of *N*-(6-ferrocenyl-2-naphthoyl)-glycine-glycine ethyl ester **96** is increased to 1.0 μM . At this higher concentration, the increase in the sub-G0/G1 peak is accompanied by a concomitant decrease in the G0/G1 ($p = 0.001$) and S phase ($p = 0.005$) cell populations. Similar observations were made following treatment for 72 hours; there is a significant increase in the sub-G0/G1 population of H1299 cells treated with 0.5 μM ($p = 0.032$) and 1.0 μM ($p = 0.006$) *N*-(6-ferrocenyl-2-naphthoyl)-glycine-glycine ethyl ester **96**.

Table 5.9 Cell cycle distribution of H1299 cells treated with *N*-(6-ferrocenyl-2-naphthoyl)-glycine-glycine ethyl ester **96** for 48 h or 72 h, then analysed by flow cytometry.

	Sub G0/G1	G0/G1	S	G2/M
<i>48 h</i>				
Control	4.6 \pm 1.1	40.9 \pm 0.7	44.9 \pm 1.8	9.6 \pm 1.9
0.5 μM	11.9 \pm 0.3**	39.6 \pm 2.0	39.2 \pm 0.8*	9.4 \pm 1.4
1.0 μM	21.8 \pm 1.6**	34.5 \pm 0.8**	37.1 \pm 1.2**	6.7 \pm 1.4
DMSO Control	5.3 \pm 0.9	40.8 \pm 0.9	44.4 \pm 2.9	9.6 \pm 1.3
<i>72 h</i>				
Control	2.4 \pm 0.3	46.6 \pm 0.4	41.3 \pm 0.8	9.7 \pm 1.2
0.5 μM	7.5 \pm 1.7*	44.5 \pm 2.0	39.2 \pm 1.8	8.9 \pm 2.0
1.0 μM	12.2 \pm 1.5**	41.5 \pm 3.1	37.9 \pm 1.6*	8.4 \pm 2.3
DMSO Control	2.2 \pm 0.4	47.9 \pm 3.1	40.2 \pm 3.6	9.7 \pm 0.9

Standard deviations have been calculated using data obtained from three independent experiments. Student's *t*-test was performed to determine significance: * denotes $p < 0.05$; ** denotes $p < 0.01$, when comparing treatment with control or DMSO control.

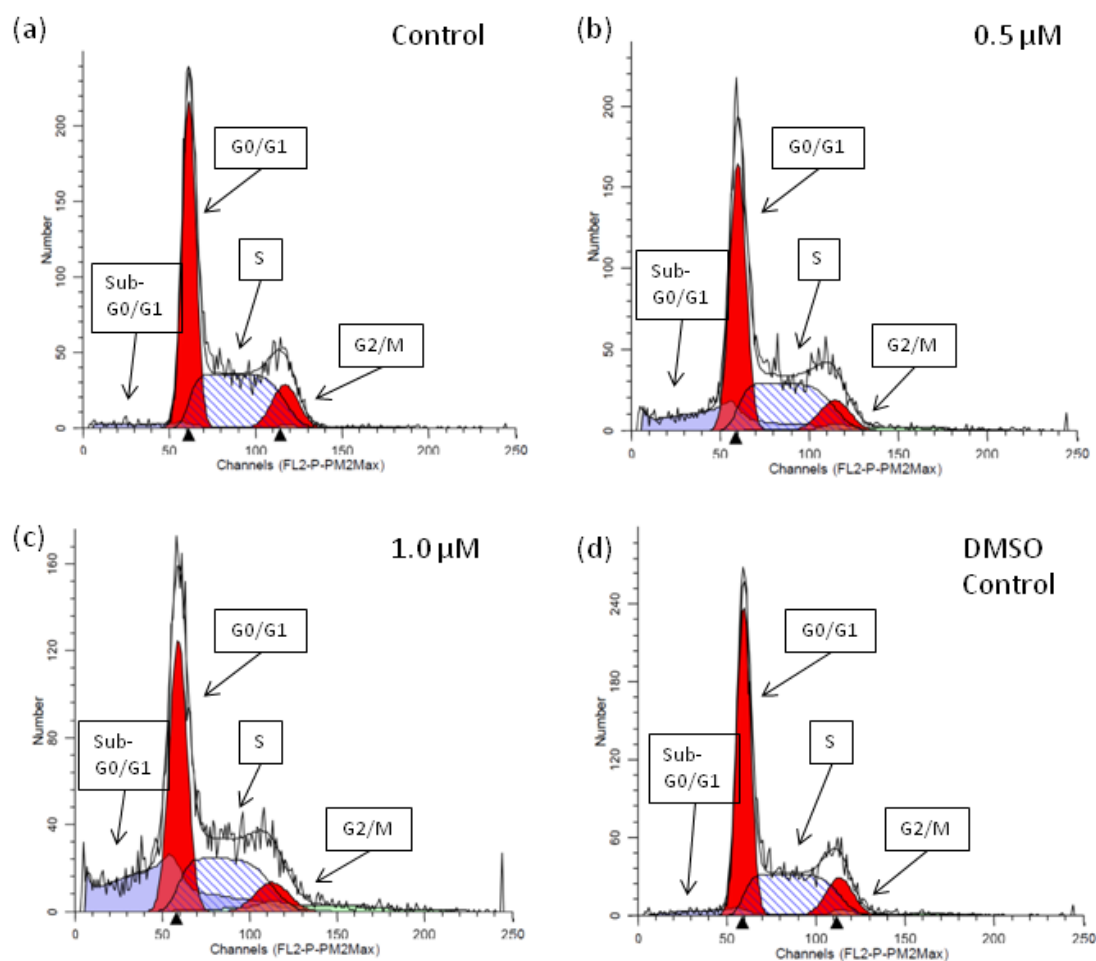


Figure 5.1 Sample graphs of H1299 cell cycle distribution after 72 hours: (a) control, (b) *N*-(6-ferrocenyl-2-naphthoyl)-glycine-glycine ethyl ester **96** (0.5 μM), (c) *N*-(6-ferrocenyl-2-naphthoyl)-glycine-glycine ethyl ester **96** (1.0 μM) and (d) DMSO control. The data obtained from the flow cytometry was analysed using ModFit software. This software calculates the number of diploid cells in G0/G1, S and G2/M phases of the cell cycle, as well as cell debris and cell aggregates. Hypodiploid cells appear as a sub-G0/G1 peak.

The cell cycle distribution of H1299 cells treated with *N*-(6-ferrocenyl-2-naphthoyl)-sarcosine-glycine ethyl ester **120** for 48 hours and 72 hours, follows a similar pattern (Table 5.10). After 48 hours, there is a significant increase in the sub-G0/G1 population ($p = 0.040$) accompanied by a decrease in the number of cells in S ($p = 0.009$) phase of the cell cycle, following treatment with the lower concentration (0.5 μM) of *N*-(6-ferrocenyl-2-

naphthoyl)-sarcosine-glycine ethyl ester **120**. Doubling the concentration of *N*-(6-ferrocenyl-2-naphthoyl)-sarcosine-glycine ethyl ester **120** to 1.0 μM , also doubles the sub-G0/G1 population. At this higher concentration, there is also a significant decrease in the number of cells in the G0/G1 ($p = 0.0004$) and S ($p = 0.002$) phases of the cell cycle. After 72 hours treatment, there is a significant increase in the sub-G0/G1 population of H1299 cells treated with 0.5 μM ($p = 0.012$) and 1.0 μM ($p = 0.015$) *N*-(6-ferrocenyl-2-naphthoyl)-sarcosine-glycine ethyl ester **120**.

Table 5.10 Cell cycle distribution of H1299 cells treated with *N*-(6-ferrocenyl-2-naphthoyl)-sarcosine-glycine ethyl ester **120** for 48 h or 72 h, then analysed by flow cytometry.

	Sub G0/G1	G0/G1	S	G2/M
<i>48 h</i>				
Control	3.6 \pm 0.4	40.5 \pm 0.6	46.4 \pm 1.3	9.6 \pm 1.0
0.5 μM	11.3 \pm 2.8*	37.2 \pm 2.0	41.3 \pm 1.3**	10.2 \pm 2.5
1.0 μM	19.5 \pm 3.0**	34.0 \pm 0.7**	38.9 \pm 1.4**	7.6 \pm 1.3
DMSO Control	4.7 \pm 1.0	39.8 \pm 1.6	45.7 \pm 2.9	9.8 \pm 2.9
<i>72 h</i>				
Control	2.9 \pm 0.2	42.4 \pm 1.1	43.9 \pm 0.1	10.8 \pm 1.0
0.5 μM	6.0 \pm 0.7*	41.1 \pm 1.0	42.0 \pm 1.0	10.8 \pm 0.6
1.0 μM	11.3 \pm 1.9*	38.4 \pm 0.4*	40.3 \pm 0.5**	10.1 \pm 1.1
DMSO Control	2.0 \pm 0.4	44.0 \pm 1.8	43.0 \pm 0.7	11.0 \pm 0.7

Standard deviations have been calculated using data obtained from three independent experiments. Student's *t*-test was performed to determine significance: * denotes $p < 0.05$; ** denotes $p < 0.01$, when comparing treatment with control.

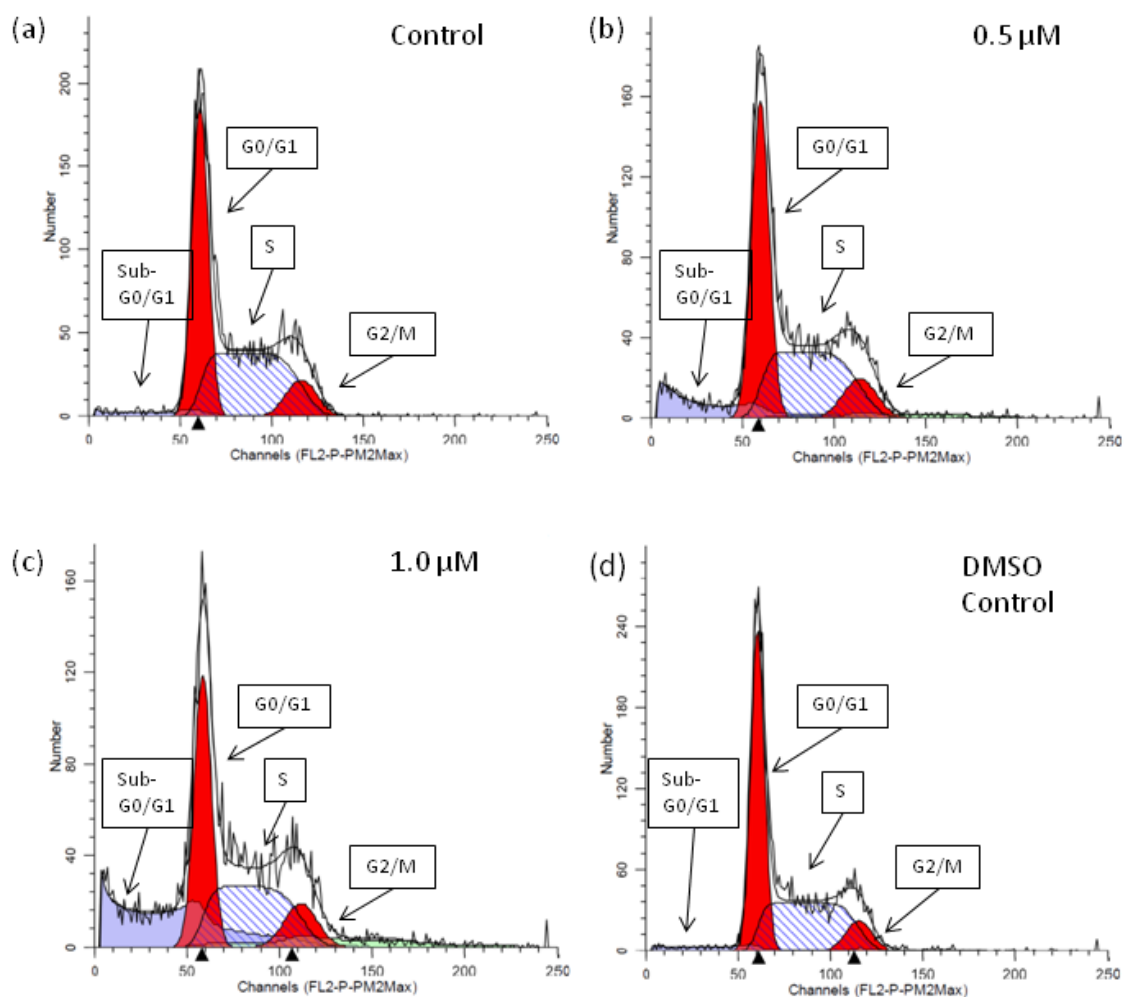


Figure 5.2 Sample graphs of H1299 cell cycle distribution after 72 hours: (a) control, (b) *N*-(6-ferrocenyl-2-naphthoyl)-sarcosine-glycine ethyl ester **120** (0.5 μ M), (c) *N*-(6-ferrocenyl-2-naphthoyl)-sarcosine-glycine ethyl ester **120** (1.0 μ M) and (d) DMSO control. The data obtained from the flow cytometry was analysed using ModFit software. This software calculates the number of diploid cells in G0/G1, S and G2/M phases of the cell cycle, as well as cell debris and cell aggregates. Hypodiploid cells appear as a sub-G0/G1 peak.

These findings suggest that the *N*-(6-ferrocenyl-2-naphthoyl) dipeptide derivatives most likely inhibit cell proliferation in the H1299 cell line by inducing apoptosis. Similar observations have been made for the ferrocenyl derivative, ferrociphenol **27** in the MCF-7

breast cancer cell line.⁵ However, further flow cytometry studies that specifically measure the levels of early and late apoptotic cells must be conducted to confirm that apoptosis is being induced by these novel ferrocenyl-peptide bioconjugates.

5.4. Conclusions

As part of a secondary SAR study, *N*-(ferrocenyl)naphthoyl amino acid and dipeptide derivatives and *N*-naphthoyl dipeptide derivatives were evaluated for *in vitro* anti-proliferative effect in lung cancer (H1299) and melanoma (Sk-Mel-28) cell lines. This study confirmed that the *N*-(6-ferrocenyl-2-naphthoyl) amino acid and dipeptide derivatives display a greater potential as anti-cancer agents than the *N*-(3-ferrocenyl-2-naphthoyl) amino acid and dipeptide derivatives. With regard to the two potential lead compounds that were identified in the primary SAR study, *N*-methylation of the C-terminal amino acid residue reduces the anti-proliferative effect. Thus, the ability of this nitrogen atom to act as a hydrogen bond donor is clearly important for biological activity. The *in vitro* biological activity of *N*-(6-ferrocenyl-2-naphthoyl)-glycine-L-alanine ethyl ester **51** was optimised by inverting the stereochemistry of the C-terminal α -carbon atom to give *N*-(6-ferrocenyl-2-naphthoyl)-glycine-D-alanine ethyl ester **124**. The replacement of either glycine residue in *N*-(6-ferrocenyl-2-naphthoyl)-glycine-glycine ethyl ester **96** with the β -alanine and γ -aminobutyric acid residues does not improve the *in vitro* biological activity, however, replacing the *N*-terminal glycine residue with sarcosine maintains the observed *in vitro* anti-proliferative effect. This could prove to be a valuable modification for future studies, since *N*-methyl derivatives are more resistant to degradation by proteases *in vivo*.⁶ It has also been clearly demonstrated in this secondary SAR study that the redox active ferrocenyl unit of these ferrocenyl-peptide bioconjugates is essential for biological activity. For the homologous series of *N*-(ferrocenyl)naphthoyl amino acid derivatives, *N*-(6-ferrocenyl-2-naphthoyl)- γ -aminobutyric acid ethyl ester **139** was identified as the most active derivative, thus extending the length of the α -amino acid glycine chain by two methylene units enhances the biological activity.

In total, these primary and secondary SAR studies have identified five ferrocenyl-peptide bioconjugates that have an equivalent or more potent anti-proliferative effect in the H1299

cell line than the platinum-based anti-cancer drug, cisplatin **1** ($1.4 \pm 0.1 \mu\text{M}$). Four of these compounds possess IC_{50} values that lie in the nanomolar range. Thus, the primary objective of this research thesis has been achieved; the anti-proliferative effect of these novel ferrocenyl-peptide bioconjugates has been enhanced by more than 30 times, compared to the most active *N*-(ferrocenyl)benzoyl peptide derivative.⁷ In addition, the *N*-(ferrocenyl)naphthoyl amino acid and dipeptide derivatives have been shown to be effective in inhibiting proliferation in the Sk-Mel-28 cell line. Significant IC_{50} values ranging from $1.06 \pm 0.05 \mu\text{M}$ to $3.74 \pm 0.37 \mu\text{M}$ have been determined for the five most potent compounds in the Sk-Mel-28 cell line. Thus, the *N*-(ferrocenyl)naphthoyl amino acid and dipeptide derivatives represent a novel class of bioorganometallic anti-cancer agents that show great promise for the treatment of lung cancer and melanoma.

Finally, cell cycle analysis in the H1299 cell line has shown the two most active ferrocenyl-peptide bioconjugates, *N*-(6-ferrocenyl-2-naphthoyl)-glycine-glycine ethyl ester **96** and *N*-(6-ferrocenyl-2-naphthoyl)-sarcosine-glycine ethyl ester **120** to cause a significant increase in the sub-G0/G1 peak, which is suggestive of apoptosis. This observation is encouraging, since the production of intracellular ROS has been shown to lead to cancer cell apoptosis.⁸ In future work, the mode of action of these novel compounds should be investigated and further studies to confirm that apoptosis is induced by these novel compounds should also be performed.

Materials and Methods

Cell cycle assays

H1299 cells were plated at a density of 2.5×10^4 cells/well in 24-well plates, in RPMI-1640 media containing 10% FCS. After 24 hours, the cells were treated with the test compound. Dimethyl sulfoxide (DMSO) control wells were included in each assay. After 48 and 72 hours, the media was collected into microcentrifuge tubes and the wells were washed with PBS, which was also collected. Cells were trypsinised and added to the media collected for each sample. The tubes were centrifuged at $300 \times g$ for 5 minutes and the media was aspirated. The cell pellets were re-suspended in PBS, and each cell suspension was transferred to a well of a round bottomed 96 well plate. The plate was centrifuged at $450 \times g$ for 5 minutes and the supernatant aspirated leaving approximately 20 μ l in each well. The remaining volume was used to re-suspend the cells and 200 μ l of ice cold 70 % ethanol was added gradually to each well. The plates were then stored at 4 °C overnight. After fixing, the cells were stained according to the protocol for the Guava Cell Cycle assay. Cells were analysed on the Guava EasyCyte (Guava Technologies) and the data was analysed using Modfit LT software (Verity).

Statistical Analysis

Analysis of the response to treatment was performed using the student's *t*-test (two-tailed with unequal variance) and p-value < 0.05 was considered statistically significant.

References

1. Y. S. Xie, X. H. Pan, B. X. Zhao, J. T. Liu, D. S. Shin, J. H. Zhang, L. W. Zheng, J. Zhao and J. Y. Miao, *Journal of Organometallic Chemistry*, 2008, **693**, 1367-1374.
2. M. Malumbres and M. Barbacid, *Nature Reviews Cancer*, 2001, **1**, 222-231.
3. M. V. R. Reddy, M. R. Mallireddigari, S. C. Cosenza, V. R. Pallela, N. M. Iqbal, K. A. Robell, A. D. Kang and E. P. Reddy, *Journal of Medicinal Chemistry*, 2008, **51**, 86-100.
4. C. Riccardi and I. Nicoletti, *Nat. Protocols*, 2006, **1**, 1458-1461.
5. A. Nguyen, V. Marsaud, C. Bouclier, S. Top, A. Vessieres, P. Pigeon, R. Gref, P. Legrand, G. Jaouen and J. M. Renoir, *International Journal of Pharmaceutics*, 2008, **347**, 128-135.
6. A. Grauer and B. Konig, *European Journal of Organic Chemistry*, 2009, 5099-5111.
7. A. J. Corry, N. O'Donovan, Á. Mooney, D. O'Sullivan, D. K. Rai and P. T. M. Kenny, *Journal of Organometallic Chemistry*, 2009, **694**, 880-885.
8. J. R. Kirshner, S. Q. He, V. Balasubramanyam, J. Kepros, C. Y. Yang, M. Zhang, Z. J. Du, J. Barsoum and J. Bertin, *Molecular Cancer Therapeutics*, 2008, **7**, 2319-2327.

Appendix I-Abbreviations and Units

Abbreviations

A

A	absorbance
ACE	angiotensin-converting enzyme
Acetone- d_6	deuterated acetone
ACN	acetonitrile
Ag AgCl	silver/silver chloride (reference electrode)
Anal.	analysis
ATCC	American Tissue Culture Centre
ATP	adenosine triphosphate
ATR	attenuated total reflection
AR	androgen receptor

B

BF_4^-	tetrafluoroborate ion
Boc	<i>tert</i> -butoxycarbonyl
BOP	benzotriazole-1-yl-oxy-tris-(dimethylamino) phosphonium hexafluorophosphate
Br	bromine
br.	broad (spectral)

C

C	carbon; concentration
Calc.	calculated
CD	cyclodextrin
CDCl_3	deuterated chloroform
CF_3	trifluoromethyl group
Cg	centroids
Cl	chlorine
CN	nitrile

Co	cobalt
CO ₂	carbon dioxide
COSY	correlation spectroscopy
Cp	cyclopentadienyl
Cq	quaternary carbon
Cu	copper
CV	cyclic voltammetry
C=O	carbonyl
D	
d	doublet (spectral)
DACH	<i>trans-R,R</i> -1,2-diaminocyclohexane
D-Ala	D-alanine
DCC	1,3-dicyclohexylcarbodiimide
DCM	dichloromethane
DCU	Dublin City University
dd	double doublets (spectral)
DEPT	distorsionless enhancement by polarisation transfer
DHT	dihydrotestosterone
DMSO	dimethylsulfoxide
DMSO- <i>d</i> ₆	deuterated dimethylsulfoxide
DNA	deoxyribonucleic acid
E	
e ⁻	electron
EAT	Ehrlich ascites tumour
EDC	<i>N</i> -(3-dimethylaminopropyl)- <i>N'</i> -ethylcarbodiimide hydrochloride
EDTA	ethylenediaminetetraacetic acid
EEDQ	2-ethoxy-1-ethoxycarbonyl-1,2-dihydroquinoline
<i>E</i> ^{0'}	formal redox potential

ER	estrogen receptor
ER(+)	estrogen receptor positive cells
ER(-)	estrogen receptor negative cells
ESI	electrospray ionisation
ESR	electron spin resonance
Et ₃ N	triethylamine
EtOH	ethanol

F

FACS	fluorescence activated cell sorting
Fc/Fc ⁺	ferrocene/ferricenium ion
FcCOOH	ferrocenecarboxylic acid
FCS	foetal calf serum
Fe	iron
Fe(II)	ferrous ion
Fe(III)	ferric ion
FT	fourier transform

G

G ₀ /G ₁ /G ₂	gap phase
Ga	gallium
GABA	γ-aminobutyric acid
Ge	germanium
Gly	glycine

H

H	hydrogen
H ₂ DCF-DA	2',7'-dichlorodihydrofluorescein diacetate
H ₂ O	water
HBr	hydrogen bromide

HBTU	<i>O</i> -(1 <i>H</i> -benzotriazol-1-yl)- <i>N,N,N',N'</i> -tetramethyluronium hexafluorophosphate
HCl	hydrochloric acid
HMBC	heteronuclear multiple bond correlation
HMPA	hexamethylphosphoramide
HMQC	heteronuclear multiple quantum coherence
HO [•]	hydroxyl radical
HOBt	1-hydroxybenzotriazole
HPβCD	hydroxypropyl-β-cyclodextrin
HPLC	high performance liquid chromatography
HPV	human papillomavirus
HRT	hormone replacement therapy
HSQC	heteronuclear single quantum coherence

I

IC ₅₀	half maximal inhibitory concentration
IMS	industrial methylated spirits
IR	infra red

J

<i>J</i>	coupling constant (spectral)
----------	------------------------------

K

KBr	potassium bromide
-----	-------------------

L

<i>l</i>	path length (in cm)
L-Ala	L-alanine
LC	liquid chromatography
L-Leu	L-leucine

L-Phe	L-phenylalanine
M	
<i>m</i>	<i>meta</i> ; mass
m	multiplet (spectral)
M	metal; mitosis phase
MALDI	matrix-assisted laser desorption/ionisation
MDR	multidrug resistance
MeOH	methanol
MgSO ₄	magnesium sulphate
MLCT	metal-ligand charge transfer
Mn	manganese
Mo	molybdenum
mp	melting point
MS	mass spectrometry
MS/MS	tandem mass spectrometry
MTIC	3-methyl-(triazen-1-yl)imidazole-4-carboxamide
MTT	3-(4,5-dimethylthiazol-2-yl)-2,5-diphenyltetrazolium bromide
<i>m/z</i>	mass to charge ratio
N	
N	nitrogen
NaNO ₂	sodium nitrite
NaOH	sodium hydroxide
NCI	National Cancer Institute
NHE	normal hydrogen electrode
Ni	nickel
NICB	National Institute for Cellular Biotechnology
Nb	niobium
<i>N</i> -Me-L-Ala	<i>N</i> -methyl-L-alanine

NMR	nuclear magnetic resonance
No.	number
NSCLC	non-small cell lung cancer
O	
O	oxygen
OD	optical density
OEt	ethoxy
OH	hydroxy
OMe	methoxy
ORTEP	oak ridge thermal ellipsoid plot
P	
<i>p</i>	<i>para</i>
P	phosphorous
PBS	phosphate buffered saline
PEG	polyethyleneglycol
PCl ₅	phosphorous pentachloride
PF ₆ ⁻	hexafluorophosphate ion
P-gp	P-glycoprotein
PLA	poly-D-lactic acid
Pt	platinum
PyBOP	benzotriazol-1-yl-oxy-tris-pyrrolidino-phosphonium hexafluorophosphate
Q	
q	quartet (spectral)
qt	quintet (spectral)
QSAR	quantitative structure-activity relationship

R

Rh	rhodium
RNA	ribonucleic acid
ROE	rotating-frame overhauser enhancement
ROESY	rotating-frame overhauser effect spectroscopy
ROS	reactive oxygen species
rpm	rotations per minute
RPMI	Roswell Park Memorial Institute
Ru	ruthenium

S

s	singlet (spectral)
S	sulfur; synthesis phase
SAR	structure-activity relationship
Sar	sarcosine
SCE	saturated calomel electrode
SCLC	small cell lung cancer
SERM	selective estrogen receptor modulator
Sn	tin
SOCl ₂	thionyl chloride

T

t	triplet (spectral); lifetime
TBAP	tetrabutylammonium perchlorate
<i>t</i> -Bu	<i>tert</i> -butyl group
<i>T_c</i>	coalescence temperature
TCD	Trinity College Dublin
TFA	trifluoroacetic acid
Ti	titanium
TMS	tetramethylsilane

TOCSY	total correlation spectroscopy
TOF	time of flight
TRIMEB	heptakis-2,3,6-tri- <i>O</i> -methyl- β -CD

U

UV	ultraviolet
----	-------------

V

V	vanadium
---	----------

Vis	visible
-----	---------

W

WHO	World Health Organisation
-----	---------------------------

Z

<i>z</i>	charge
----------	--------

Miscellaneous

(<i>E</i>)	Entegen (opposite)
(<i>Z</i>)	Zusammen (together)
2D	2-dimensional
2 <i>X</i>	2-times
8-oxo-Gua	8-oxo-7,8-dihydroguanine
α H	α -hydrogen
β -Ala	β -alanine
δ -Ava	δ -amino- <i>n</i> -valeric acid
ϵ	extinction coefficient
λ_{\max}	maximum absorbance
η^5 -C ₅ H ₄	substituted cyclopentadienyl ring
η^5 -C ₅ H ₅	unsubstituted cyclopentadienyl ring

ω	dihedral angle
\pm	plus/minus
\sim	approximately
\approx	almost equal to
$<$	less than
$>$	greater than

Units

A	ampere
Å	Ångstrom
cm	centimetre
cm ⁻¹	wavenumber(s)/per centimetre
dm	decimetre
g	gram
h	hour
Hz	hertz
l	litre
K	Kelvin
kg ⁻¹	per kilogram
M	molar
MHz	megahertz
mg	milligram
ml	millilitre
mm	millimetre
mM	millimolar
mmol	millimole
mol	mole
µl	microlitre
µm	micrometre
µM	micromolar
mV	millivolt
nm	nanometre
nM	nanomolar
°	degrees
°C	degrees Celsius
ppm	part(s) per million
s	second

V	volt
δ	chemical shift (ppm)
%	percentage

Appendix II-Publications